Improving groundwater dynamics: a key factor for successful tidal marsh restoration!

Niels Van Putte

Supervisors **Stijn Temmerman | Patrick Meire | Goedele Verreydt | Piet Seuntjens**

University of Antwerp

Improving groundwater dynamics:

a key factor for successful tidal marsh restoration!

Verbetering van de grondwaterdynamiek:

een cruciale factor voor succesvol schorherstel!

Thesis submitted for the degree of Doctor in Science: Biology at the University of Antwerp to be defended by

Niels Van Putte

promotors:

Stijn Temmerman
Patrick Meire
Goedele Verreydt
Piet Seuntjens

Faculty of Science
Department of Biology
Antwerp, 2023

University of Antwerp

Members of the doctoral committee:

Em. prof. dr. Rudy van Diggelen (chairman)	University of Antwerp
Prof. dr. Ivan Janssens	University of Antwerp
Prof. dr. Stijn Temmerman (promotor)	University of Antwerp
Prof. dr. Patrick Meire (promotor)	University of Antwerp
Dr. ing. Goedele Verreydt (promotor)	University of Antwerp
Prof. dr. ir. Piet Seuntjens (promotor)	VITO

Other jury members:

Prof. dr. Kate Spencer	Queen Mary University of London
Prof. dr. ir. Peter Herman	TU Delft

Summary

Tidal marshes are wetlands situated along coasts and estuaries that are regularly inundated by the tides. These areas consist of a vegetated marsh platform that is intersected by a network of creeks that move water, sediment and dissolved nutrients from and to the river. Tidal marshes play an important role in maintaining a good water quality in estuaries. They act as a filter by taking up certain elements from the river water and releasing other elements into the river water. This function is very relevant, especially given the deteriorated water quality in most tidal rivers worldwide.

During the past centuries, the largest area of tidal marshes worldwide has disappeared due to large scale land reclamations for urbanization, industrialization and agriculture. As a result, also their associated ecosystem services largely disappeared. In the last decades, tidal marshes are increasingly restored by reintroducing the tides in formerly embanked agricultural areas. Several studies have indicated that restored tidal marshes can deliver important ecosystem services such as coastal defense and habitat provisioning. However, the contribution of restored tidal marshes to water quality improvement remains largely unknown. This water quality improving function depends on groundwater dynamics and the interaction between the marsh soil and water that infiltrates in into the marsh platform at high tide and seeps out of the creek banks at low tide, after which it flows back to the river via these creeks.

In this thesis, we studied the effect of historical land use on the contribution of restored tidal marshes to water quality improvement in the Scheldt estuary in Belgium. We then investigated several solutions to stimulate this water quality improving function in newly restored tidal marshes.

During a comparative study, it became clear that groundwater drains deeper in a natural tidal marsh at low tide, compared to a restored tidal marsh. Here, the soil has been compacted due to the historical agricultural land use. With innovative methods such as CT-scanning of soil cores, we discovered that the organic matter content and the micro and macroporosity of the soil are significantly lower in the compacted soil of the restored marsh, compared to the soil in the natural marsh. As a result, groundwater flow is hindered in this compacted soil. After restoration, a layer of newly deposited sediment accretes on top of the old agricultural soil. The characteristics of this layer are more similar to those seen in the soil of the natural tidal marsh. In restored tidal marshes, groundwater level fluctuations are therefore limited to this layer of newly deposited sediment.

The depth of groundwater level fluctuations and the velocity at which groundwater can flow through a soil have important implications for the processes that contribute to water quality improvement, e.g. the nitrogen removal, phosphorus retention and silica cycling. The groundwater drainage depth determines how deep oxygen can penetrate into the soil. Groundwater drains deeper in the vicinity of creeks and in a more porous soil. This promotes nitrogen removal through coupled nitrification and denitrification, and

phosphorus retention on iron oxides. Increased groundwater flow leads to increased silica dissolution and transport towards tidal creeks.

The two most important factors for groundwater dynamics in tidal marshes, i.e. the soil porosity and the distance to the nearest tidal creek, were then translated into design measured to improve groundwater dynamics and associated water quality improvement in newly restored tidal marshes. Numerical modelling showed that an increase in creek density by excavation of creeks increased the volume of seepage water significantly. Artificially creating a more porous soil that is more comparable to the soil of a natural tidal marsh, e.g. by tilling and amending the soil with organic material, also enhanced groundwater dynamics. The largest gain in groundwater dynamics was observed when both measures were applied together.

To get a better understanding of the effect of soil amendments, we executed a large scale mesocosm experiment. In an embanked agricultural area we locally applied three soil treatments in which organic material (reed cuttings and woodchips, respectively) was added and/or the soil was plowed. Then, large monoliths were excavated in the three treated plots and in one untreated plot. These monoliths were then placed in a mesocosm construction and exposed to the tides to simulate tidal marsh restoration. In the treated monoliths, the groundwater drained deeper and more nitrogen was removed from the water. Additional research is required to further quantify the effects of the addition of organic matter.

This thesis provides new insights on the influence of historical land use on soil properties in restored tidal marshes, and their effect on the contribution of restored tidal marshes to water quality improvement in estuaries. For new tidal marsh restoration projects, we advise to conduct an explorative soil study. When the soil is heavily compacted, design measures, such as creek initiation and organic soil amendments can be applied to jumpstart the contribution to water quality improvement of newly restored tidal marshes.

Samenvatting

Schorren zijn de draslanden die we vinden langsheen kusten en estuaria die regelmatig overspoelen door het getij. Ze bestaan uit een begroeid schorplatform dat doorsneden is door een netwerk van kreken die water, sediment en opgeloste voedingsstoffen aan- en afvoeren. Deze gebieden spelen een belangrijke rol in het onderhouden van een goede waterkwaliteit in getijdenrivieren. Ze werken als een filter door bepaalde elementen uit het rivierwater op te nemen, en andere elementen vrij te geven aan het rivierwater. Deze functie is erg relevant, met name door de verslechterde waterkwaliteit in de meeste getijdenrivieren wereldwijd.

Gedurende de voorbije eeuwen is wereldwijd het grootste areaal aan schorren verdwenen door grootschalige landaanwinningen voor verstedelijking, industrie en landbouw. Hierdoor verdwenen ook de door schorren geleverde ecosysteemdiensten. In de laatste decennia wordt er steeds vaker aan schorherstel gedaan, waarbij ingepolderde gebieden terug onder invloed van het getij worden geplaatst. Verschillende studies hebben reeds aangetoond dat herstelde schorren belangrijke ecosysteemdiensten zoals kustbescherming en habitatvoorziening kunnen leveren. Er is echter nog veel onduidelijkheid over de rol die herstelde schorren kunnen spelen bij het verbeteren van de waterkwaliteit. Deze functie is afhankelijk van de grondwaterdynamiek en de interacties tussen de bodem van het schor en het water dat bij hoog tij in het schorplatform infiltreert en bij laag tij door kreekwanden sijpelt en zo via deze kreken terug naar de rivier stroomt.

In deze thesis onderzochten we het effect van het voormalig landgebruik op de bijdrage van herstelde schorren aan waterkwaliteitsverbetering in het Schelde-estuarium in België. Vervolgens werd naar oplossingen gezocht om deze functie te stimuleren in nieuwe schorherstelprojecten.

In een vergelijkende studie werd duidelijk dat in een natuurlijk schor het grondwater dieper wegzakt bij laag tij dan in een hersteld schor. Door het voormalig landbouwgebruik in het hersteld schor werd de bodem gecompacteerd. Via innovatieve technieken zoals CT-scanning van bodemmonsters stelden we vast dat het gehalte aan organisch materiaal in de bodem en zowel de micro- als macroporositeit significant lager zijn in de gecompacteerde bodem in het hersteld schor dan in de bodem van het natuurlijke schor. Hierdoor kan grondwater nauwelijks doorheen de bodem stromen. Na schorherstel wordt er na verloop van tijd een nieuwe laag sediment afgezet bovenop de oude landbouwbodem. De structuur van deze laag is meer gelijkend aan de bodem in een natuurlijk schor. In herstelde schorren zijn grondwaterfluctuaties dan ook beperkt tot de dikte van deze nieuw afgezette laag.

De diepte van de grondwaterfluctuaties en de snelheid waarmee grondwater doorheen de bodem kan stromen, hebben belangrijke gevolgen voor de processen die bijdragen aan verbetering van de waterkwaliteit, zoals de verwijdering van stikstof, retentie van fosfor

en cyclering van silica. De drainagediepte bepaalt tot hoe diep zuurstof in de bodem kan doordringen. Dichter bij kreken en in een meer poreuze bodem zakt het grondwater dieper weg. Dit bevordert de verwijdering van stikstof door gekoppelde nitrificatie en denitrificatie, en de binding van fosfor op ijzeroxides. Een toegenomen grondwaterstroming zorgt ervoor dat er meer silicium in het bodemwater kan oplossen en naar de kreken wordt getransporteerd.

De twee belangrijkste aspecten voor de grondwaterdynamiek in schorren, namelijk de porositeit van de bodem en de afstand tot de dichtstbijzijnde kreek, werden vertaald naar ontwerpmaatregelen die toegepast kunnen worden in nieuwe schorherstelprojecten om de grondwaterdynamiek en waterkwaliteitsverbetering te stimuleren. Via een numerieke modelstudie berekenden we dat een toename van de kreekdensiteit, door het uitgraven van kreken, de hoeveelheid grondwater die door de bodem stroomt, significant verhoogt. Ook het bewerken van de compacte bodem, bijvoorbeeld door het onderploegen van organisch materiaal, waardoor de bodem meer poreus wordt en zo meer gelijkend is aan de bodem in een natuurlijk schor, zorgt voor een toegenomen grondwaterdynamiek. De grootste winst in toename van grondwaterdynamiek wordt geboekt wanneer beide maatregelen samen worden toegepast.

Om het effect van deze bodembewerkingen verder te onderzoeken, werd een grootschalig mesocosmosexperiment uitgevoerd. Hiervoor werden in een polder met gecompacteerde bodem lokaal drie bodembewerkingen uitgevoerd waarbij de bodem werd geploegd en organisch materiaal (respectievelijk rietmaaisel en houtsnippers) al dan niet werd toegevoegd. Vervolgens werden in de bewerkte locaties en in één onbewerkte locatie grote monolieten uitgegraven die dan in een experimentele opstelling werden blootgesteld aan de getijden om zo schorherstel te simuleren. In de bewerkte monolieten draineerde het grondwater dieper en werd er meer stikstof verwijderd uit het water. Bijkomend onderzoek is nodig om de effecten van het toevoegen van organisch materiaal verder te kwantificeren.

Deze thesis verstrekt nieuwe inzichten over de invloed van historisch landgebruik op de bodemeigenschappen in herstelde schorren, en de invloed hiervan op de rol die herstelde schorren spelen in het verbeteren van de waterkwaliteit in estuaria. Voor nieuwe schorherstelprojecten wordt daarom aangeraden om steeds een verkennend bodemonderzoek uit te voeren. Bij een sterk gecompacteerde bodem kunnen ontwerpmaatregelen, zoals het uitgraven van een kreekaanzet en het bewerken van de bodem met organisch materiaal, toegepast worden om zo de bijdrage tot waterkwaliteitsverbetering sneller op gang te laten komen.

Acknowledgements

When I started this adventure long ago, I thought: "Let's study something you can't see in an place that's barely accessible". It quickly became clear that studying groundwater flow in tidal marshes fulfills both requirements with ease, and finding the answer to one question, mostly lead to even more questions. Now, it's time to wrap up the answers, and present my PhD thesis. However, this PhD would never have been successful without the help of many people, to which I owe a lot of thanks.

Let me start by thanking my four promotors. "Four promotors?" – you say? Yes, indeed, and they all played a crucial role to guide me through this PhD Journey. Thank you Stijn for coaching me and making me a better scientist. Our meetings were very constructive and I could always count on your guidance when I was lost. I would also like to express my gratitude to Patrick for the continuing support and to keep believing in the relevance of my work within the bigger picture. Thank you also for giving me the freedom to do some side projects alongside my PhD work. Although you thought these projects were "weird for a biologist", they surely kept me motivated and I learned so much by doing them. A big thank you also goes to Goedele, your curiosity and determination have been truly inspiring for me. I am convinced that we will achieve great things continuing our work together. Thanks to Piet for introducing me to the wonderful world of modelling. Although it felt like a struggle at first, it quickly became a joy to discover all the possibilities. I'm sure the skills I obtained here will be useful in my future career path. I am grateful to all jury members for their invaluable input that helped me fine-tuning the final work.

Within ECOBE, and later ECOSPHERE, the atmosphere was always nice. The positive energy and sense of humor of all my colleagues made even the most challenging experiments bearable, thank you all! In particular, thank you Ken, for introducing me into the group when I just started and for making sure a beer was never far away when we needed it, and to Steven, for our long talks when we were both working late in the office, although working mostly ended when the talking started. Talking occurred also a lot with Jonas, about one of his new crazy ideas, which often turned into even more crazy ideas after our talk. Thanks, Heleen and Ignace, for all the funny moments, and my room buddies Tom and Stefan for the countless moments of laughter that we shared in our office. Within our research group, people help each other, always! Even during a snow storm, when three tons of sand had to be carried by hand, my colleagues were eager to help. Stijn, I hope you have the feeling back in your fingers by now. Dimitri, thanks for doing all this extremely demanding physical fieldwork. I'm glad I contributed to your (probably) world record placing monitoring wells. Thank you Anne, Anke and Tom for the enormous number of samples you analyzed for me with great care.

I am grateful to all students that I supervised and their contributions to the lab- and fieldwork. In this regard, a special word of thank goes to Timothy: first my study mate and friend, then my thesis student and now my colleague. From this trajectory, it's clear that we form a good team and should continue to work together.

Also from outside our university, I owe many people. I am grateful to Ingeborg for her help and support with the numerical groundwater model, to the colleagues from the Ghent University Department of Environment for their help with the analysis of soil hydraulic properties, to DEME for the logistic help with the mesocosm experiment and of course to iFLUX, for providing the sensors and giving me the chance to present my research on many international conferences.

When I was two years into my PhD, a very special person arrived, a person that would not only enter our research group, but also my heart. Thank you Dorian for your continuous love and support, especially during the last phase of this work. Your patience and encouragement really made all the difference in keeping me going through this.

Graag wil ik ook al mijn familie en vrienden bedanken, en in het bijzonder mijn ouders, voor alle kansen en het vertrouwen dat ik van hen gekregen heb om dit hoofdstuk tot een goed einde te kunnen brengen. Ik ben jullie hiervoor enorm dankbaar!

To end, I would like to express my gratitude to the mighty Scheldt river, my constant companion throughout this journey, from wading through the mud of its marshes, to overlooking its dynamics from my apartment on the 12th floor while writing this thesis. Your ever-changing tides mirrored the highs and lows of my research. Thank you for revealing a fraction of your mysteries, yet leaving plenty for the next generation of PhD students!

Table of contents

1

Introduction

1.1 Tidal marshes deliver important ecosystem services

Tidal marshes are wetlands that are situated on the border between land and sea and are subjected to regular tidal inundations. Tidal marshes are present in both coastal zones and in estuaries and can be found in the saline, brackish, and even in the freshwater zone of these estuaries. Unlike mudflats, which are inundated every high tide and are usually bare (unvegetated), tidal marshes are only inundated during higher tides and are covered by vegetation that is adapted to these special conditions. This vegetation reduces the flow velocity of the water, giving suspended particles the chance to settle (Leonard and Luther, 1995). In this sense, the tidal marsh builds elevation by trapping of suspended sediments supplied by the river. Tidal marshes are intersected by a branching network of tidal channels or creeks (Figure 1.1). These creeks serve as flow conduits supplying and draining water, dissolved nutrients and sediments to and from the marsh platform with flood and ebb tides, respectively (e.g. Temmerman et al., 2005).

Figure 1.1: Aerial picture of the Drowned Land of Saeftinghe marsh in the Scheldt estuary in The Netherlands. The vegetated marsh platform is intersected by a branched network of creeks. ©Wouter Pattyn

Although they make up only a small proportion of the Earth's surface, estimated to cover roughly 45,000 km² (Greenberg et al., 2006) to 90,800 km² (Murray et al., 2022), tidal marshes belong to the most productive ecosystems on our planet and deliver a wide array of crucial ecosystem services (Barbier et al., 2011; Costanza et al., 2008). Tidal marshes protect shorelines from storm impacts, as they act as a buffer for water during storm surges, and marsh vegetation reduces wave heights (Möller et al., 2014; Schoutens et al., 2019; Temmerman et al., 2023). They also serve as a nursery for many fish and shellfish species (Boesch and Turner, 1984; Sheaves et al., 2015) and host vegetation that is

specifically adapted to the intertidal conditions. As such, tidal marshes largely contribute to the estuarine biodiversity. The soil of tidal marshes is an extensive pool for carbon storage (Chmura et al., 2003; Ouyang and Lee, 2014) and acts as a filter for water that inundates marshes, infiltrates into marsh soils and seeps out of creek banks to become surface water again, as such improving the water quality of estuaries (Tobias and Neubauer, 2019). This filtering function, and its relation to groundwater dynamics, is the main scope of this PhD dissertation and will be elaborated in the following paragraphs.

1.2 Tidal marsh loss and restoration

In the past centuries, a substantial part of the global tidal marsh area disappeared as a result of large scale embankments (Murray et al., 2022). As estuaries are often the center for the development of major cities, tidal marshes were mostly seen as valuable land for urbanization, development of industry and agriculture. Marshes were embanked by construction of dikes, so that the water could no longer flood the area under normal tidal conditions. This global large scale land reclamation greatly reduced the extent of the delivered ecosystem services (Wang et al., 2010) and lead to a decrease in biodiversity (e.g. Meire et al., 2005). Agricultural land use and urbanization around estuaries has put severe pressure on estuarine ecosystems. Runoff from fertilized fields loaded with nutrients ended up in the estuaries, together with untreated sewage from cities, resulting in eutrophication events. Increased industrialization often lead to large scale pollution with potentially toxic metals such as As, Co, Cr, Cu, Ni, Pb and Zn (e.g. Rodgers et al., 2020), pesticides, PCBs (polychlorinated biphenyls) (e.g. Van Ael et al., 2012), PFAS (perfluoroalkyl substances) (e.g. Allinson et al., 2019) and micro- and macro plastics (e.g. Velimirovic et al., 2022). Many of these substances can accumulate in estuarine sediments (Teuchies et al., 2013).

Given the many negative effects of land reclamation for ecosystem health and humanity, stakeholders around the world now invest a vast amount of money in tidal marsh restoration. Tidal marsh restoration aims to reverse wetland destruction in order to regain the benefits and ecosystem services provided by tidal wetlands, to increase biodiversity and to comply with conservation and environmental legislations such as the EU Habitats Directive and the EU Water Framework Directive (European Parliament and the Council of the European Union, 1992, 2000). Land managers and ecological engineers often assumed that given the right boundary conditions such as flooding regime (hydroperiod) and sediment supply, restored tidal marshes would become ecologically equivalent to their natural counterparts within a reasonable time frame (Borja et al., 2010; Spencer et al., 2017). However, the majority of recent studies indicate that this is not the case and the ecosystem functioning of restored tidal marshes is impaired compared to natural tidal marshes, even decades after restoration, in terms of vegetation composition (Brooks et al., 2015), carbon stock (Burden et al., 2019) and soil properties (Tempest et al., 2015).

Presently, tidal marsh restoration projects are predominantly executed for their contribution to mitigation of habitat loss and for storm surge attenuation, rather than their

contribution to nutrient cycling and water quality improvement. Nevertheless, nutrient cycling is essential in estuaries. Since this cycling of nutrients takes place for a large part in the soil of the tidal marsh (Whiting and Childers, 1989; Wilson and Morris, 2012), a thorough understanding of soil properties, subsurface hydrology and biogeochemistry, and how they interact and differ between natural and restored tidal wetlands, is of crucial importance to maximize the delivery of regulating ecosystem services in future tidal marsh restoration projects. In the next paragraphs, we explain the rationale for our research questions. We start by giving a short overview of the relevant aspects of groundwater flow in general. We then narrow this down to the basics of groundwater flow in tidal marshes. Next, we explain how groundwater dynamics govern several important ecosystem functions in tidal marshes. Then, we elaborate how groundwater dynamics and their associated ecosystem services can be hindered in restored tidal marshes as a result of historical land use. In the last paragraph, we combine this knowledge to formulate several research questions that will be studied in the next chapters.

1.3   Groundwater flow: a brief description

Groundwater can be defined as the water present in cavities in between soil particles. In the saturated zone, in which all these cavities are filled with water, groundwater flow follows Darcy's law (Darcy, 1856) and flows from locations where the groundwater head (i.e. the groundwater level as compared to a reference level) is higher to locations where the groundwater head is lower. In tidal marshes, these differences are caused by tidal fluctuations (see below). Within a single aquifer, the velocity at which groundwater flows through the soil is equal to the difference in groundwater head between two locations divided by the lateral distance between these locations (i.e. the hydraulic gradient), multiplied by the saturated hydraulic conductivity (K_s) of the soil, a measure for the soil's ability to conduct groundwater, which depends on the soil texture and structure. Sandy tidal marsh soils typically have a relatively high K_s compared to silty marsh sediments (Gardner, 2007). However, in the latter, the presence of macropores, such as voids created by decayed plant material and animal burrows, can vastly increase K_s (Xin et al., 2016).

During low tides, when the top of the marsh soil is not completely saturated, groundwater also flows in this unsaturated zone. Here, the Darcy equation can only be applied when the moisture content (θ) of the soil remains constant (i.e. steady state condition). In general, and especially in tidal marshes due to their dynamic environment, this is not the case, and θ varies over time as water flows through and is removed from the soil (Ursino et al., 2004). In unsaturated conditions, water flows through the soil due to capillary action, from higher matric potential to lower (i.e. more negative) matric potential (e.g. Dane and Hopmans, 2009). Groundwater can only flow through the largest pores when θ is high. As the soil becomes unsaturated, water will only be able to flow through increasingly smaller pores and the flow velocity will decrease. The Richards' equation (Richards, 1931) solves this unsaturated flow problem by expressing groundwater flow as a change in θ over time. In this equation, the hydraulic conductivity becomes a function of θ, which depends on the

distribution of pore sizes (van Genuchten, 1980). Groundwater is the main driver for the transport of dissolved elements through the subsurface of tidal wetlands (Xin et al., 2022). Dissolved elements are displaced as a result of the groundwater movement (advective transport), and as a result of the difference in concentration of the element between two locations (diffusive transport).

1.4   Soil properties and groundwater dynamics in tidal marshes

In tidal wetlands, the main driver for groundwater flow is the tidally induced fluctuation of surface water levels. When tidal marshes are flooded during high spring tides, the flooding water from the estuary typically first propagates through creeks that run from the estuary into the marsh. As soon as the flood tide reaches a water level exceeding the marsh surface elevation, the marsh is flooded by water flowing from the creeks over the marsh platform (e.g. Vandenbruwaene et al., 2015). The tidally induced movement of groundwater in the soil of tidal marshes was first described by Chapman (1938). At the start of the tidal inundation of the marsh platform, surface water infiltrates vertically into the upper part of the marsh soil and replaces air in the soil pores, resulting in a rise of the groundwater level (Figure 1.2b). When the surface water recedes during ebb tide and the surface water level in the creek declines, a subsurface hydraulic gradient emerges at the creek banks. As a result, groundwater seeps out of the creek banks, locally lowering the groundwater level (Figure 1.2c). This lowering in groundwater level continues into the marsh interior, but attenuates quickly with an increasing distance from the creek banks (Figure 1.2c) (Cao et al., 2012; Xin et al., 2022). During the next rising tide, when the surface water level in the creek exceeds the groundwater level at the creek bank, the hydraulic gradient shifts direction and water infiltrates laterally into the creek banks until the marsh platform is inundated again (Figure 1.2a). The depth and the lateral extent to which these groundwater level fluctuations occur, depends on the depth of the creek and the hydraulic properties of the soil (Gardner, 2005). Since the hydraulic conductivity is generally very low in tidal marsh soils, groundwater level fluctuations are mostly limited to the first few meters from the creek banks (Ursino et al., 2004). This also means that close to the creeks, some of the groundwater is refreshed every tidal cycle, whereas further into the marsh interior, the groundwater has a very long residence time (which may be in the order of several to tens of years) (Moffett and Gorelick, 2016). This difference in residence time has major implications for the marsh biogeochemistry, which will be discussed in the next paragraphs.
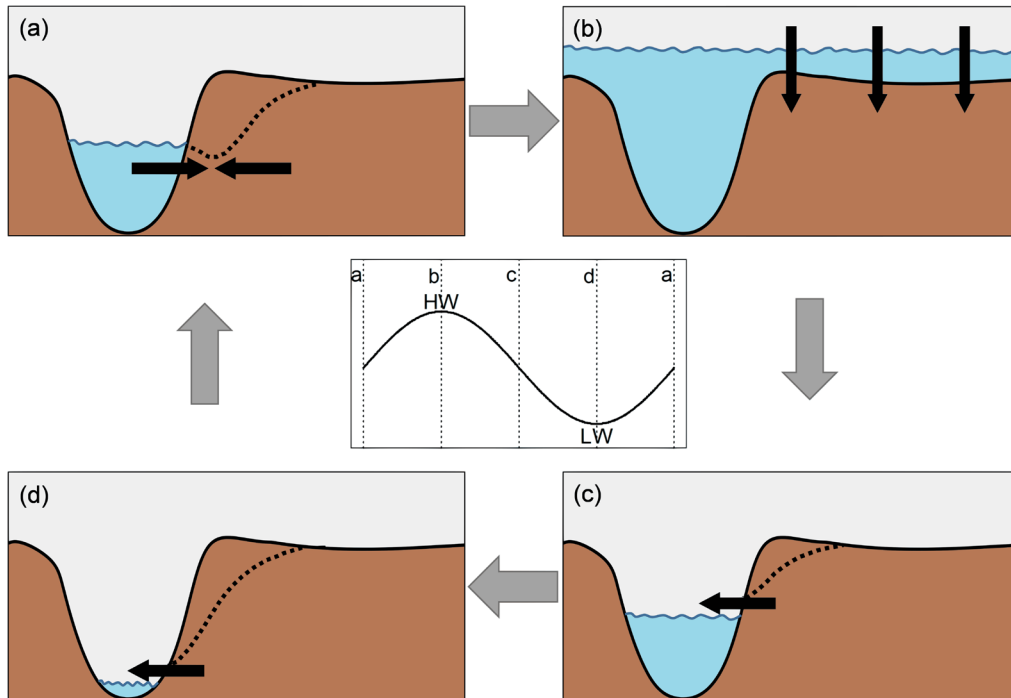
Figure 1.2: Schematic representation of a cross section of a tidal creek and the adjacent marsh platform showing the basic principles of groundwater flow in a creek-marsh system around spring tide. The middle graph represents the water level in the tidal river in function of the time and the vertical dashed lines indicate the phases that are represented in a, b, c and d. HW: high water, LW: low water. Curved dashed lines in a, c and d represent the groundwater table. (a): rising tide: water from the creek infiltrates in the creek banks while at the same time water in the marsh soil flows towards the tidal creek. (b): high water: water above the marsh platform infiltrates vertically into the marsh soil. (c): falling tide: water seeps out of the creek banks and a hydraulic gradient is formed towards the creek. (d): the process described in c continues until water enters the creek during the next rising tide. Based on text and figures in Harvey et al. (1987).

Precipitation and evapotranspiration also cause differences in water potential in the marsh soil. During the growth season, wetland plants can transpire large volumes of water, lowering the groundwater level. In the marsh interior, further away from the creeks, this is the prevailing way in which groundwater is removed from the marsh soil (Hemond and Fifield, 1982). While tidally induced groundwater infiltration and seepage also adds and removes dissolved elements, evapotranspiration only removes water. Therefore, evapotranspiration can lead to elevated solute concentrations in the groundwater (Hughes et al., 1998). However, tidal marsh vegetation can assimilate part of the solutes (Neubauer et al., 2005), partly compensating the elevated concentrations. Interactions with underlying aquifers can also induce groundwater flow in tidal marshes.

In the last decades, many studies characterized groundwater dynamics in tidal wetlands (Xin et al., 2022), and investigated the relative importance of soil hydraulic properties, e.g. the hydraulic conductivity of the soil (Gardner, 2005) and the presence of macropores (Harvey et al., 1995; Xin et al., 2009; Xin et al., 2016), vs. geomorphologic properties (e.g. marsh elevation, creek morphology and dimensions (Gardner, 2005; Harvey et al., 1987;

Xin et al., 2011)) and soil stratigraphy (Gardner, 2007; Wu et al., 2022) for groundwater seepage. Other studies focused on the effect of groundwater dynamics on soil aeration patterns (Ursino et al., 2004) and how these patterns affect vegetation zonation (Wilson et al., 2015). Despite the growing number of studies regarding subsurface hydrology in tidal marshes, nearly all these studies are conducted in natural tidal marshes, with only very few exceptions that consider groundwater dynamics in a restored tidal marsh (Tempest et al., 2015). Nevertheless, substantial differences are expected between groundwater dynamics in natural vs. restored tidal marshes, due to their different land use history, resulting in altered soil properties and the absence of creek networks. These differences are, until now, largely unexplored.

1.5 Importance of groundwater dynamics for ecosystem functioning

Roughly, the effects of groundwater dynamics on the ecosystem functioning of tidal marshes can be divided into two categories: the effect of changes in soil water content and the effect of advective and dispersive transport. When the marsh soil desaturates when the tide recedes, oxygen from the air enters some of the soil pores. These soil saturation dynamics determine where and which vegetation will establish on a given place in the marsh (Xiao et al., 2017; Xin et al., 2013). In waterlogged (completely saturated) soils, such as those often found in the interior of tidal marshes, aerobic respiration by plants is inhibited (Li et al., 2005). Some wetland species developed aerenchyma tissue to transport oxygen from their above-ground parts to their roots to overcome this problem, and hence such species have a competitive advantage to grow in waterlogged marsh interiors (Granse et al., 2022; Maricle and Lee, 2002). While other, more competitive species that are less tolerant to waterlogging, tend to thrive closer to creek banks, where soil aeration is facilitated by groundwater drainage to creeks (e.g. Wilson et al., 2015).

Changes in the oxidation state of the soil also alter the prevailing biogeochemical reactions that take place in the soil (Megonigal and Neubauer, 2019), for example the reactions that are involved in the removal of nitrogen and phosphorus from the estuarine water, and greatly contribute to the filtering function of tidal marshes. Tidally driven soil saturation dynamics induce alternating aerobic and anaerobic conditions in the upper marsh soil (Peng et al., 2022). Nitrogen in porewater is removed from the marsh system by microbially mediated coupled nitrification (aerobic) and denitrification (anaerobic). As such, nitrogen removal is partly controlled by tidally induced groundwater level fluctuations (Wolf et al., 2011). Phosphorus can be retained in the marsh soil or removed via plant uptake (Megonigal and Neubauer, 2019). In soils in which iron (Fe) is abundantly present, and that are regularly exposed to oxygen (e.g. near the marsh surface and in the vicinity of creek banks), Fe oxidizes to form iron oxyhydroxide minerals, to which phosphate can adsorb. Dissolved phosphate that is transported with groundwater flow from the marsh interior towards the tidal creeks, can be trapped in the well aerated creek bank zone in which iron oxyhydroxides are present, limiting creek bank seepage of phosphate. In this way, this so called 'iron curtain' at the creek banks mediates P retention in tidal wetland soils (Chambers and Odum, 1990; Megonigal and Neubauer, 2019).

The soil saturation state also affects the emission of greenhouse gases and the ability of the marsh to store carbon. As mineralization of organic molecules to CO_2 takes place in oxic conditions, soil aeration can result in increased organic matter decomposition. In waterlogged (saturated) conditions, on the other hand, methane (CH_4) emission is stimulated (Megonigal and Neubauer, 2019). However, the extent of CH_4 emission strongly depends on the salinity (and associated SO_4 concentrations), as SO_4 reducing bacteria compete for electron donors with methanogenic bacteria (Bartlett et al., 1987; Megonigal and Neubauer, 2019; Poffenbarger et al., 2011).

Advective transport (i.e. transport of solutes with the groundwater flow) moves solutes from the marsh soil towards tidal creeks and vice versa, and determines the residence time of solutes. In tidal marshes, advective transport governs cycling of silica, of which the cycling within the estuary is of the utmost importance for the growth of primary producers (phytoplankton) in the estuary (e.g. Lancelot, 1995). Biogenic silica in accreted plant material and dead diatoms slowly dissolves in the groundwater and is then transported towards the creeks via advection (Struyf et al., 2006). The combined effect of advection and evapotranspiration also plays an important role in regulating porewater salinity in tidal marsh sediments. Where advective transport is limited and groundwater removal is dominated by evapotranspiration, high salt concentrations can build up in the marsh soil (Cao et al., 2012).

From the previous paragraphs, it is clear that groundwater dynamics in tidal marshes control the ability of a tidal marsh to contribute to nutrient cycling and hence to water quality improvement. Knowledge on biogeochemistry in tidal marsh sediments is well established for both freshwater tidal marshes (e.g. Megonigal and Neubauer, 2019) and saltmarshes (e.g. Tobias and Neubauer, 2009). Some studies also pointed out the impaired contribution to nutrient cycling of restored tidal marshes (e.g. Burden et al., 2013; Portnoy and Giblin, 1997; Windham-Myers et al., 2013). However, the link between groundwater dynamics and biogeochemical cycling in tidal wetlands is still poorly understood. A better understanding of this link is essential, especially in restored tidal wetlands in which physicochemical soil properties and subsurface hydrology are often altered due to historical agricultural land use (Dale et al., 2018; Spencer et al., 2017; Tempest et al., 2015).

1.6   The Scheldt estuary: its past, present and future

All fieldwork for this thesis was executed in the Scheldt estuary in Belgium (Figure 1.3A). The 355 km long Scheldt river has its source in St. Quentin in the north of France and discharges into the North Sea near Vlissingen in The Netherlands. The river is mostly rain fed. Historically, the river has been subjected to large scale urbanization and industrialization, flowing through large cities such as Ghent and Antwerp, with currently about 10 million people living in its catchment area of approximately 20,000 km². The part of the river that is tidally influenced extends 160 km land inwards until the city of Ghent, where the tide is stopped by sluices. The estuary is further subdivided into the Upper Sea Scheldt (from Ghent to Antwerp), the Lower Sea Scheldt (from Antwerp to the Dutch

border and the Western Scheldt connecting to the North Sea. The Scheldt is a well-mixed and relatively turbid macro-tidal estuary. The estuary covers the entire salinity range (Figure 1.3A). Due to its funnel shaped morphology, the maximum tidal range occurs in the freshwater zone, where this average tidal range is 5.54 m (Meire et al., 2005).

The history of the Scheldt estuary as we know it today goes all the way back to the end of last glacial period, when glaciers melted due to climate change, the open landscape transformed into a forested area and the sea level rose. As a result, the braiding river system evolved into a meandering river and tides started to propagate into the river (Kiden and Verbruggen, 2001). From the 9th century on, cities such as Antwerp developed on the banks of the Scheldt river. From this period onwards, the Scheldt estuary changed drastically due to human intervention. Dikes were built and marshland was embanked for agriculture. As a result, the tides propagated increasingly more land inward. Starting from the 12th century, these large scale land reclamations often resulted in dike breaches and floodings (Missiaen et al., 2017). In the 19th and 20th century, parts of the river were straightened and the fairway was deepened, facilitating access of big ships to the port of Antwerp. Increasing urbanization, industrialization and use of artificial fertilizers for agriculture lead to a deteriorated water quality with very low oxygen concentrations in the estuary. In the winters of 1953 and 1976, large storm surges caused major material damage and casualties in the Scheldt estuary (Broekx et al., 2011). It became clear that action needed to be taken in order to mitigate and prevent further damage and to restore the ecosystem of the Scheldt estuary.
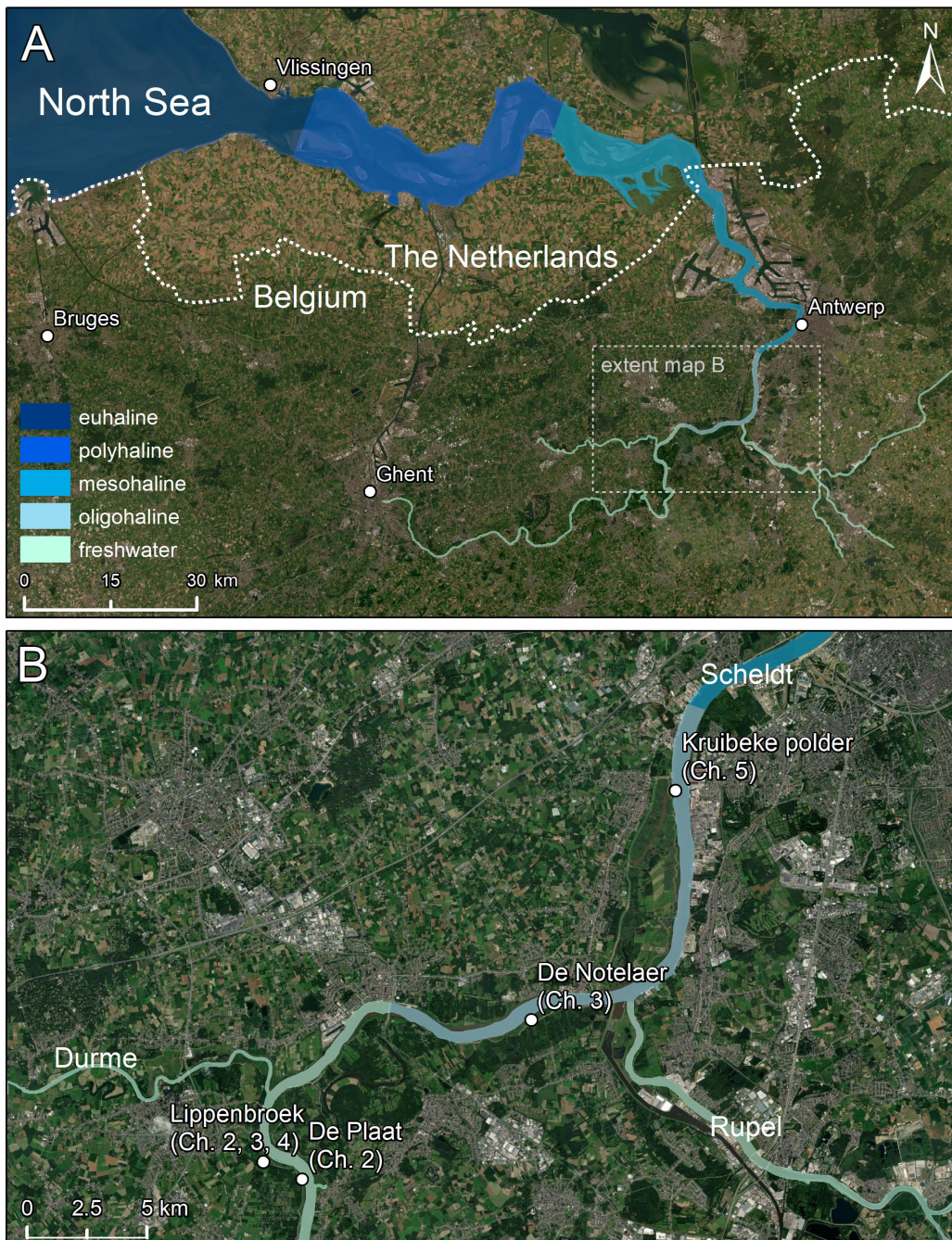
Figure 1.3: (A): Situation of the Scheldt estuary in Belgium and The Netherlands. Shaded colors drawn over the estuarine water represent the salinity category. (B): Overview map of the study areas. Detailed maps of the respective study areas follow in the next chapters. Map source: Esri, DigitalGlobe, GeoEye, Earthstar Geographics, CNES/Airbus DS, USDA, USGS, AeroGrid, IGN and the GIS User Community.

In February 1977, the Flemish government decided to carry out the 'Sigmaplan' along the Sea Scheldt, with the aim of protecting the Scheldt valley from inundations. The plan consists of strengthening existing dikes, and the construction of flood control areas (FCA's) in low lying polders bordering the estuary (Meire et al., 2014). In 2005, the plan was updated and new insights on integrated management were incorporated, aiming, apart from flood protection, also on ecological development and recreation. Increasing insights into the importance of tidal marshes for ecosystem service delivery lead to the development of flood control areas with a controlled reduced tide (FCA-CRT), in which tidal marsh development and flood protection are integrated into a single area. In these CRT areas, which are enclosed by a ring dike, a sluice system with separate inlet and outlet culvert allows for replication of the tidal regime (including spring tide – neap tide variation) in the lower elevated areas, facilitating the development of tidal nature (Maris et al., 2007). At the same time, a depression in the dike adjacent to the river (an overflow dike) allows for storage of water in the area in case of a storm surge. By the year 2030, 1600 ha of CRT areas will be constructed within the Scheldt estuary. The vegetation development and contribution to water quality improvement in these areas is carefully monitored in the OMES measuring campaigns (Maris et al., 2021). Especially the pilot restoration project Lippenbroek has been documented extensively (Beauchard et al., 2013; Cox et al., 2006; Jacobs et al., 2009; Maris et al., 2007; Oosterlee et al., 2017; Teuchies et al., 2012; Vandenbruwaene et al., 2011). Since these CRT areas are constructed on formerly embanked agricultural land and have been subjected to intensive agriculture, we can expect a compacted subsoil in these newly restored tidal marshes. Figure 1.3B gives an overview of the location of the studied marshes. A detailed description of these areas can be found in the respective chapters.

1.7   Aims, hypotheses and outline of this thesis

In this thesis, we aim to investigate the importance of groundwater dynamics for the contribution to water quality improvement of restored tidal marshes. In addition, we intend to propose design guidelines to optimize groundwater dynamics in future tidal marsh restoration projects. We start by identifying key differences in soil properties between natural and restored tidal marshes, which result in differences in groundwater flow (Chapter 2 and 3). We then relate these differences to biogeochemical cycling in tidal marshes (Chapter 3). Furthermore, we study several management practices (creek excavation and soil amendments) and to what extent they can help to improve groundwater flow and associated biogeochemical cycling in restored tidal marshes (Chapter 4 and 5).
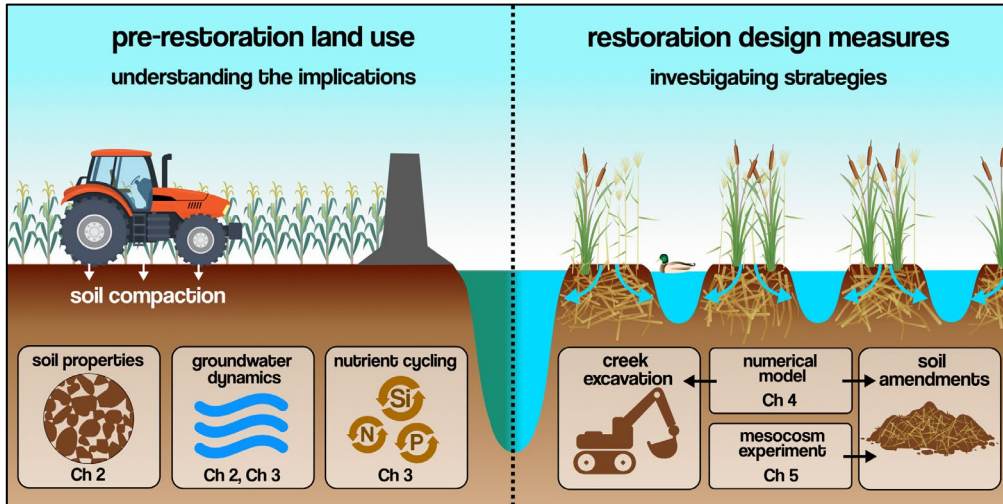
Figure 1.4: Schematic overview of the thesis outline. The left hand side shows the situation before restoration. The water quality in the estuary is bad and an embanked agricultural area is subject to soil compaction. We investigate the implications of this pre-restoration land use on soil properties (Chapter 2), groundwater dynamics (Chapter 2, Chapter 3) and nutrient cycling (Chapter 3). The right hand side depicts an artistic representation of a restored tidal marsh in which creek excavation and soil amendments were applied. Groundwater flow (represented by blue arrows) is enhanced and wetland vegetation develops. Increased nutrient cycling leads to an improved water quality in the estuary. We investigate these restoration design measures in Chapter 4 and Chapter 5.

In **Chapter 2** we aim to investigate the differences in soil physical properties and groundwater dynamics between a restored and a natural tidal marsh along the Scheldt estuary (Figure 1.4). We show that the soil in the restored tidal marsh clearly consists of a layer of newly deposited sediment, underlain by a layer of relict agricultural polder soil that has been subject to soil compaction, whereas the natural marsh soil consists only of tidally deposited sediment. Using innovative micro CT-scanning of soil cores of both layers in both a natural and a restored tidal marsh, we support the hypothesis that the soil in the natural marsh and the upper layer in the restored marsh is intersected by a dense network of macropores and organic structures, which is absent in the relict compacted layer in the restored marsh. We hypothesize that this change in physical soil structure affects the soil hydraulic properties in the restored marsh and leads to reduced groundwater dynamics as compared to a natural tidal marsh.

We elaborate this work in **Chapter 3** by studying both groundwater dynamics and porewater nutrient concentrations on multiple creek-marsh transects in both a natural and a restored tidal marsh, covering different vegetation zones and topographic locations (Figure 1.4). We investigate the relation between porewater nutrient concentrations and soil saturation dynamics, which differ in function of soil hydraulic properties and distance from the nearest tidal creek. We hypothesize that reduced groundwater dynamics, resulting from historical agricultural soil compaction, reduce the capacity of restored tidal marshes to contribute to the removal of nitrogen and phosphorus, and to cycle silica.

The ultimate goal of this doctoral thesis is to formulate guidelines to improve groundwater dynamics and associated biogeochemical cycling in newly restored tidal marshes. Given (i) the importance of the presence of a dense tidal creek network and (ii) the positive effect of organic matter content and macropores on groundwater dynamics and nutrient cycling, we hypothesize that groundwater dynamics in newly restored tidal marshes can be improved prior to restoration by (i) excavating a dense creek network and (ii) amending the soil with organic matter.

In **Chapter 4** we test these hypotheses by setting up a variably saturated groundwater flow and transport model for a creek-marsh cross section of a restored tidal marsh (Figure 1.4). The model is calibrated and evaluated using groundwater level data and soil hydraulic properties measured in Chapter 2 and 3. Here we assume that the application of organic soil amendments to a certain depth can be implemented in the model as changing the depth to the compact layer to that depth. This assumption is, however, highly simplified. Furthermore, only non-reactive transport can be considered in the numerical model. To overcome these limitations and study the effect of organic soil amendments in more detail, we set up a large scale mesocosm experiment in **Chapter 5** (Figure 1.4). Here, we hypothesize that amending the soil with organic matter (reed cuttings and wood chips), leads to improved groundwater drainage, increased removal of nitrogen and phosphorus and increased silica cycling.

In **Chapter 6** we place the results of all chapters in the broader context of tidal marsh restoration and formulate design criteria for new tidal marsh restoration projects. Furthermore, we discuss the limitations of this study and the implementation of its results, and suggest new research questions for future studies.

1.8   References

Allinson, M., Yamashita, N., Taniyasu, S., Yamazaki, E., Allinson, G., 2019. Occurrence of perfluoroalkyl substances in selected Victorian rivers and estuaries: An historical snapshot. Heliyon 5. 10.1016/j.heliyon.2019.e02472

Barbier, E.B., Hacker, S.D., Kennedy, C., Koch, E.W., Stier, A.C., Silliman, B.R., 2011. The value of estuarine and coastal ecosystem services. Ecological Monographs 81, 169-193. 10.1890/10-1510.1

Bartlett, K., Bartlett, D., Harriss, R., Sebacher, D., 1987. Methane emissions along a salt marsh salinity gradient. Biogeochemistry 4, 183-202. 10.1007/BF02187365

Beauchard, O., Jacobs, S., Ysebaert, T., Meire, P., 2013. Sediment macroinvertebrate community functioning in impacted and newly-created tidal freshwater habitats. Estuarine Coastal and Shelf Science 120, 21-32. 10.1016/j.ecss.2013.01.013

Boesch, D.F., Turner, R.E., 1984. Dependence of fishery species on salt marshes: The role of food and refuge. Estuaries 7, 460-468. 10.2307/1351627

Borja, Á., Dauer, D.M., Elliott, M., Simenstad, C.A., 2010. Medium- and Long-term Recovery of Estuarine and Coastal Ecosystems: Patterns, Rates and Restoration Effectiveness. Estuaries and Coasts 33, 1249-1260. 10.1007/s12237-010-9347-5

Broekx, S., Smets, S., Liekens, I., Bulckaen, D., De Nocker, L., 2011. Designing a long-term flood risk management plan for the Scheldt estuary using a risk-based approach. Natural Hazards 57, 245-266. 10.1007/s11069-010-9610-x

Brooks, K.L., Mossman, H.L., Chitty, J.L., Grant, A., 2015. Limited Vegetation Development on a Created Salt Marsh Associated with Over-Consolidated Sediments and Lack of Topographic Heterogeneity. Estuaries and

Coasts 38, 325-336. 10.1007/s12237-014-9824-3

Burden, A., Garbutt, A., Evans, C.D., 2019. Effect of restoration on saltmarsh carbon accumulation in Eastern England. Biology Letters 15. 10.1098/rsbl.2018.0773

Burden, A., Garbutt, R.A., Evans, C.D., Jones, D.L., Cooper, D.M., 2013. Carbon sequestration and biogeochemical cycling in a saltmarsh Subject to coastal managed realignment. Estuarine Coastal and Shelf Science 120, 12-20. 10.1016/j.ecss.2013.01.014

Cao, M., Xin, P., Jin, G.Q., Li, L., 2012. A field study on groundwater dynamics in a salt marsh - Chongming Dongtan wetland. Ecological Engineering 40, 61-69. 10.1016/j.ecoleng.2011.12.018

Chambers, R.M., Odum, W.E., 1990. Porewater Oxidation, Dissolved Phosphate and the Iron Curtain: Iron-Phosphorus Relations in Tidal Freshwater Marshes. Biogeochemistry 10, 37-52.

Chapman, V.J., 1938. Studies in Salt-Marsh Ecology Sections I to III. Journal of Ecology 26, 144-179. 10.2307/2256416

Chmura, G.L., Anisfeld, S.C., Cahoon, D.R., Lynch, J.C., 2003. Global carbon sequestration in tidal, saline wetland soils. Global Biogeochemical Cycles 17. 10.1029/2002gb001917

Costanza, R., Perez-Maqueo, O., Martinez, M.L., Sutton, P., Anderson, S.J., Mulder, K., 2008. The value of coastal wetlands for hurricane protection. Ambio 37, 241-248. 10.1579/0044-7447(2008)37[241:Tvocwf]2.0.Co;2

Cox, T.J.S., Maris, T., De Vleeschauwer, P., De Mulder, T., Soetaert, K., Meire, P., 2006. Flood control areas as an opportunity to restore estuarine habitat. Ecological Engineering 28, 55-63. 10.1016/j.ecoleng.2006.04.001

Dale, J.J., Cundy, A.B., Spencer, K.L., Carr, S.J., Croudace, I.W., Burgess, H.M., Nash, D.J., 2018. Sediment structure and physicochemical changes following tidal inundation at a large open coast managed realignment site. Science of the Total Environment. 10.1016/j.scitotenv.2018.12.323

Dane, J.H., Hopmans, J.W., 2009. Volumetric Water Content-Matric Potential Relationships, in: Silveira, L., Usunoff, E.J. (Eds.), Groundwater - Volume II. EOLSS Publications.

Darcy, H., 1856. Les fontaines publiques de la ville de Dijon: Exposition et application des principes et des formules à suivre et des formules à employer dans les questions de distribution d'eau: ouvrage terminé par un appendice relatif aux fournitures d'eau de plusieurs villes au filtrage des eaux et à la fabrication des tuyaux de fonte, de plomb, de tole et de bitume. Victor Dalmont.

European Parliament and the Council of the European Union, 1992. Directive 92/43/EEC of 21 May 1992 on the conservation of natural habitats and of wild fauna and flora. Official Journal of the European Communities L206. 22.7.1992.

European Parliament and the Council of the European Union, 2000. Directive 2000/60/EC of the European Parliament and the Council establishing a framework for the Community action in the field of water policy. Official Journal of the European Communities L327.22.12.2000.

Gardner, L.R., 2005. Role of geomorphic and hydraulic parameters in governing pore water seepage from salt marsh sediments. Water Resources Research 41. 10.1029/2004wr003671

Gardner, L.R., 2007. Role of stratigraphy in governing pore water seepage from salt marsh sediments. Water Resources Research 43. 10.1029/2006wr005338

Granse, D., Titschack, J., Ainouche, M., Jensen, K., Koop-Jakobsen, K., 2022. Subsurface aeration of tidal wetland soils: Root-system structure and aerenchyma connectivity in Spartina (Poaceae). Science of the Total Environment 802. 10.1016/j.scitotenv.2021.149771

Greenberg, R., Maldonado, J.E., Droege, S., McDonald, M.V., 2006. Tidal Marshes: A Global Perspective on the Evolution and Conservation of Their Terrestrial Vertebrates. BioScience 56, 675-685. 10.1641/0006-3568(2006)56[675:Tmagpo]2.0.Co;2

Harvey, J.W., Chambers, R.M., Hoelscher, J.R., 1995. Preferential Flow and Segregation of Porewater Solutes in Wetland Sediment. Estuaries 18, 568-578. 10.2307/1352377

Harvey, J.W., Germann, P.F., Odum, W.E., 1987. Geomorphological Control of Subsurface Hydrology in the Creek-Bank Zone of Tidal Marshes. Estuarine Coastal and Shelf Science 25, 677-691. 10.1016/0272-7714(87)90015-1

Hemond, H.F., Fifield, J.L., 1982. Subsurface Flow in Salt-Marsh Peat - a Model and Field-Study. Limnology and Oceanography 27, 126-136. 10.4319/lo.1982.27.1.0126

Hughes, C.E., Binning, P., Willgoose, G.R., 1998. Characterisation of the hydrology of an estuarine wetland. Journal of Hydrology 211, 34-49. 10.1016/S0022-1694(98)00194-2

Jacobs, S., Beauchard, O., Struyf, E., Cox, T.J.S., Maris, T., Meire, P., 2009. Restoration of tidal freshwater vegetation using controlled reduced tide (CRT) along the Schelde Estuary (Belgium). Estuarine Coastal and Shelf Science 85, 368-376. 10.1016/j.ecss.2009.09.004

Kiden, P., Verbruggen, C., 2001. Het verhaal van een rivier: de evolutie van de Schelde na de laatste ijstijd. In: Jean Bourgeois, Philippe Crombé, Guy De Mulder, Marc Rogge (Eds.): Een duik in het verleden. Schelde, Maas en Rijn in de pre- en protohistorie. Publicaties van het Provinciaal Archeologisch Museum van Zuid-Oost-Vlaanderen-Site Velzeke, Buitengewone reeks nr. 4, Provinciaal Archeologisch Museum van Zuid-Oost-Vlaanderen, Velzeke, pp.11-35, pp. 11-35.

Lancelot, C., 1995. The mucilage phenomenon in the continental coastal waters of the North Sea. Science of the Total Environment 165, 83-102. 10.1016/0048-9697(95)04545-C

Leonard, L.A., Luther, M.E., 1995. Flow hydrodynamics in tidal marsh canopies. Limnology and Oceanography 40, 1474-1484. 10.4319/lo.1995.40.8.1474

Li, H., Li, L., Lockington, D., 2005. Aeration for plant root respiration in a tidal marsh. Water Resources Research 41. 10.1029/2004WR003759

Maricle, B.R., Lee, R.W., 2002. Aerenchyma development and oxygen transport in the estuarine cordgrasses Spartina alterniflora and S. anglica. Aquatic Botany 74, 109-120. 10.1016/S0304-3770(02)00051-7

Maris, T., Baeten, S., Van den Neucker, T., van den Broeck, T., Meire, P., 2021. Onderzoek naar de gevolgen van het Sigmaplan, baggeractiviteiten en havenuitbreiding in de Zeeschelde op het milieu. Geïntegreerd eindverslag van het onderzoek verricht in 2020, deelrapport Intergetijdengebieden. ECOBE 021-R276. University of Antwerp, Antwerp.

Maris, T., Cox, T.J.S., Temmerman, S., De Vleeschauwer, P., Van Damme, S., De Mulder, T., Van den Bergh, E., Meire, P., 2007. Tuning the tide: creating ecological conditions for tidal marsh development in a flood control area. Hydrobiologia 588, 31-43. 10.1007/s10750-007-0650-5

Megonigal, J.P., Neubauer, S.C., 2019. Chapter 19 - Biogeochemistry of Tidal Freshwater Wetlands, in: Perillo, G.M.E., Wolanski, E., Cahoon, D.R., Hopkinson, C.S. (Eds.), Coastal Wetlands (Second Edition). Elsevier, pp. 641-683.

Meire, P., Dauwe, W., Maris, T., Peeters, P., Coen, L., Deschamps, M., Rutten, J., Temmerman, S., 2014. The recent "Saint Nicholas" storm surge in the Scheldt estuary: the Sigma plan proves its efficiency!, ECSA Bulletin. Estuarine and Coastal Science Association, London.

Meire, P., Ysebaert, T., Van Damme, S., Van den Bergh, E., Maris, T., Struyf, E., 2005. The Scheldt estuary: A description of a changing ecosystem. Hydrobiologia 540, 1-11. 10.1007/s10750-005-0896-8

Missiaen, T., Jongepier, I., Heirman, K., Soens, T., Gelorini, V., Verniers, J., Verhegge, J., Crombé, P., 2017. Holocene landscape evolution of an estuarine wetland in relation to its human occupation and exploitation: Waasland Scheldt polders, northern Belgium. Netherlands Journal of Geosciences 96, 35-62. 10.1017/njg.2016.24

Moffett, K.B., Gorelick, S.M., 2016. Relating salt marsh pore water geochemistry patterns to vegetation zones and hydrologic influences. Water Resources Research 52, 1729-1745. 10.1002/2015wr017406

Möller, I., Kudella, M., Rupprecht, F., Spencer, T., Paul, M., van Wesenbeeck, B.K., Wolters, G., Jensen, K., Bouma, T.J., Miranda-Lange, M., Schimmels, S., 2014. Wave attenuation over coastal salt marshes under storm surge conditions. Nature Geoscience 7, 727-731. 10.1038/ngeo2251

Murray, N.J., Worthington, T.A., Bunting, P., Duce, S., Hagger, V., Lovelock, C.E., Lucas, R., Saunders, M.I., Sheaves, M., Spalding, M., Waltham, N.J., Lyons, M.B., 2022. High-resolution mapping of losses and gains of Earth's tidal wetlands. Science 376, 744-749. 10.1126/science.abm9583

Neubauer, S.C., Anderson, I.C., Neikirk, B.B., 2005. Nitrogen cycling and ecosystem exchanges in a Virginia tidal freshwater marsh. Estuaries 28, 909-922. 10.1007/Bf02696019

Oosterlee, L., Cox, T.J.S., Vandenbruwaene, W., Maris, T., Temmerman, S., Meire, P., 2017. Tidal Marsh Restoration Design Affects Feedbacks Between Inundation and Elevation Change. Estuaries and Coasts. 10.1007/s12237-017-0314-2

Ouyang, X., Lee, S.Y., 2014. Updated estimates of carbon accumulation rates in coastal marsh sediments. Biogeosciences 11, 5057-5071. 10.5194/bg-11-5057-2014

Peng, Y., Zhou, C., Jin, Q., Ji, M., Wang, F., Lai, Q., Shi, R., Xu, X., Chen, L., Wang, G., 2022. Tidal variation and litter decomposition co-affect carbon emissions in estuarine wetlands. Science of the Total Environment 839. 10.1016/j.scitotenv.2022.156357

Poffenbarger, H.J., Needelman, B.A., Megonigal, J.P., 2011. Salinity Influence on Methane Emissions from Tidal Marshes. Wetlands 31, 831-842. 10.1007/s13157-011-0197-0

Portnoy, J.W., Giblin, A.E., 1997. Effects of historic tidal restrictions on salt marsh sediment chemistry. Biogeochemistry 36, 275-303. 10.1023/a:1005715520988

Richards, L.A., 1931. Capillary conduction of liquids through porous mediums. Journal of Applied Physics 1, 318-333.

Rodgers, K., McLellan, I., Peshkur, T., Williams, R., Tonner, R., Knapp, C.W., Henriquez, F.L., Hursthouse, A.S., 2020. The legacy of industrial pollution in estuarine sediments: spatial and temporal variability implications for ecosystem stress. Environmental Geochemistry and Health 42, 1057-1068. 10.1007/s10653-019-00316-4

Schoutens, K., Heuner, M., Minden, V., Ostermann, T.S., Silinski, A., Belliard, J.P., Temmerman, S., 2019. How effective are tidal marshes as nature-based shoreline protection throughout seasons? Limnology and Oceanography 64, 1750-1762. 10.1002/lno.11149

Sheaves, M., Baker, R., Nagelkerken, I., Connolly, R.M., 2015. True Value of Estuarine and Coastal Nurseries for Fish: Incorporating Complexity and Dynamics. Estuaries and Coasts 38, 401-414. 10.1007/s12237-014-9846-x

Spencer, K.L., Carr, S.J., Diggens, L.M., Tempest, J.A., Morris, M.A., Harvey, G.L., 2017. The impact of pre-restoration land-use and disturbance on sediment structure, hydrology and the sediment geochemical environment in restored saltmarshes.

Science of the Total Environment 587, 47-58. 10.1016/j.scitotenv.2016.11.032

Struyf, E., Dausse, A., Van Damme, S., Bal, K., Gribsholt, B., Boschker, H.T.S., Middelburg, J.J., Meire, P., 2006. Tidal marshes and biogenic silica recycling at the land-sea interface. Limnology and Oceanography 51, 838-846.

Temmerman, S., Bouma, T.J., Govers, G., Lauwaet, D., 2005. Flow paths of water and sediment in a tidal marsh: Relations with marsh developmental stage and tidal inundation height. Estuaries 28, 338-352. 10.1007/BF02693917

Temmerman, S., Horstman, E.M., Krauss, K.W., Mullarney, J.C., Pelckmans, I., Schoutens, K., 2023. Marshes and Mangroves as Nature-Based Coastal Storm Buffers. Annual review of marine science 15. 10.1146/annurev-marine-040422-092951

Tempest, J.A., Harvey, G.L., Spencer, K.L., 2015. Modified sediments and subsurface hydrology in natural and recreated salt marshes and implications for delivery of ecosystem services. Hydrological Processes 29, 2346-2357. 10.1002/hyp.10368

Teuchies, J., Beauchard, O., Jacobs, S., Meire, P., 2012. Evolution of sediment metal concentrations in a tidal marsh restoration project. Science of the Total Environment 419, 187-195. 10.1016/j.scitotenv.2012.01.016

Teuchies, J., Singh, G., Bervoets, L., Meire, P., 2013. Land use changes and metal mobility: Multi-approach study on tidal marsh restoration in a contaminated estuary. Science of the Total Environment 449, 174-183. 10.1016/j.scitotenv.2013.01.053

Tobias, C., Neubauer, S., 2009. Salt marsh biogeochemistry - An overview, pp. 445-492.

Tobias, C., Neubauer, S.C., 2019. Chapter 16 - Salt Marsh Biogeochemistry—An Overview, in: Perillo, G.M.E., Wolanski, E., Cahoon, D.R., Hopkinson, C.S. (Eds.), Coastal Wetlands (Second Edition). Elsevier, pp. 539-596.

Ursino, N., Silvestri, S., Marani, M., 2004. Subsurface flow and vegetation patterns in tidal environments. Water Resources Research 40. 10.1029/2003wr002702

Van Ael, E., Covaci, A., Blust, R., Bervoets, L., 2012. Persistent organic pollutants in the Scheldt estuary: Environmental distribution and bioaccumulation.

Environment International 48, 17-27. 10.1016/j.envint.2012.06.017

van Genuchten, M.T., 1980. A Closed-form Equation for Predicting the Hydraulic Conductivity of Unsaturated Soils. Soil Science Society of America Journal 44, 892-898. 10.2136/sssaj1980.03615995004400050002x

Vandenbruwaene, W., Maris, T., Cox, T.J.S., Cahoon, D.R., Meire, P., Temmerman, S., 2011. Sedimentation and response to sea-level rise of a restored marsh with reduced tidal exchange: Comparison with a natural tidal marsh. Geomorphology 130, 115-126. 10.1016/j.geomorph.2011.03.004

Vandenbruwaene, W., Schwarz, C., Bouma, T.J., Meire, P., Temmerman, S., 2015. Landscape-scale flow patterns over a vegetated tidal marsh and an unvegetated tidal flat: Implications for the landform properties of the intertidal floodplain. Geomorphology 231, 40-52. 10.1016/j.geomorph.2014.11.020

Velimirovic, M., Teunkens, B., Ghorbanfekr, H., Buelens, B., Hermans, T., Van Damme, S., Tirez, K., Vanhaecke, F., 2022. What can we learn from studying plastic debris in the Sea Scheldt estuary? Science of the Total Environment 851. 10.1016/j.scitotenv.2022.158226

Wang, X., Chen, W., Zhang, L., Jin, D., Lu, C., 2010. Estimating the ecosystem service losses from proposed land reclamation projects: A case study in Xiamen. Ecological Economics 69, 2549-2556. 10.1016/j.ecolecon.2010.07.031

Whiting, G.J., Childers, D.L., 1989. Subtidal advective water flux as a potentially important nutrient input to southeastern U.S.A. Saltmarsh estuaries. Estuarine, Coastal and Shelf Science 28, 417-431. 10.1016/0272-7714(89)90089-9

Wilson, A.M., Evans, T., Moore, W., Schutte, C.A., Joye, S.B., Hughes, A.H., Anderson, J.L., 2015. Groundwater controls ecological zonation of salt marsh macrophytes. Ecology 96, 840-849. 10.1890/13-2183.1

Wilson, A.M., Morris, J.T., 2012. The influence of tidal forcing on groundwater flow and nutrient exchange in a salt marsh-dominated estuary. Biogeochemistry 108, 27-38. 10.1007/s10533-010-9570-y

Windham-Myers, L., Ward, K., Marvin-DiPasquale, M., Agee, J.L., Kieu, L.H., Kakouros, E., 2013. Biogeochemical Implications of Episodic Impoundment in a Restored Tidal Marsh of San Francisco Bay, California. Restoration Ecology 21, 124-132. 10.1111/j.1526-100X.2011.00849.x

Wolf, K.L., Ahn, C., Noe, G.B., 2011. Development of Soil Properties and Nitrogen Cycling in Created Wetlands. Wetlands 31, 699-712. 10.1007/s13157-011-0185-4

Wu, X., Wang, Y., Shen, C., Zhao, Z., 2022. Variable-Density Flow and Solute Transport in Stratified Salt Marshes. Frontiers in Marine Science 8. 10.3389/fmars.2021.804526

Xiao, K., Li, H.L., Wilson, A.M., Xia, Y.Q., Wan, L., Zheng, C.M., Ma, Q., Wang, C.Y., Wang, X.S., Jiang, X.W., 2017. Tidal groundwater flow and its ecological effects in a brackish marsh at the mouth of a large sub-tropical river. Journal of Hydrology 555, 198-212. 10.1016/j.jhydrol.2017.10.025

Xin, P., Jin, G.Q., Li, L., 2009. Modelling Study on Subsurface Flows Affected by Macro-Pores in Marsh Sediments. Advances in Water Resources and Hydraulic Engineering, Vols 1-6, 1394-1400. 10.1007/978-3-540-89465-0_244

Xin, P., Kong, J., Li, L., Barry, D.A., 2013. Modelling of groundwater–vegetation interactions in a tidal marsh. Advances in Water Resources 57, 52-68. 10.1016/j.advwatres.2013.04.005

Xin, P., Wilson, A., Shen, C., Ge, Z., Moffett, K.B., Santos, I.R., Chen, X., Xu, X., Yau, Y.Y.Y., Moore, W., Li, L., Barry, D.A., 2022. Surface Water and Groundwater Interactions in Salt Marshes and Their Impact on Plant Ecology and Coastal Biogeochemistry. Reviews of Geophysics 60. 10.1029/2021RG000740

Xin, P., Yu, X.Y., Lu, C.H., Li, L., 2016. Effects of macro-pores on water flow in coastal subsurface drainage systems. Advances in Water Resources 87, 56-67. 10.1016/j.advwatres.2015.11.007

Xin, P., Yuan, L.R., Li, L., Barry, D.A., 2011. Tidally driven multiscale pore water flow in a creek-marsh system. Water Resources Research 47. 10.1029/2010wr010110

2

Groundwater dynamics in a restored tidal marsh are limited by historical agricultural soil compaction

Niels Van Putte, Stijn Temmerman, Goedele Verreydt, Piet Seuntjens, Tom Maris, Marjolein Heyndrickx, Matthieu Boone, Ingeborg Joris, Patrick Meire

2.1   Abstract

In places where tidal marshes were formerly embanked for agricultural land use, these marshes are nowadays increasingly restored with the aim to regain important ecosystem services. However, there is growing evidence that restored tidal marshes and their services develop slowly and differ from natural tidal marshes in many aspects. Here we focus on groundwater dynamics, because these affect several key ecosystem functions and services, such as nutrient cycling and vegetation development. We hypothesize that groundwater dynamics in restored tidal marshes are reduced as compared to natural marshes because of the difference in soil structure. In the macro-tidal Scheldt estuary (Belgium), in both a natural and a restored (since 2006) freshwater tidal marsh, we measured depth profiles of soil properties (grain size distribution, LOI (loss on ignition), moisture content and bulk density) and temporal dynamics of groundwater levels along a transect with increasing distance from a tidal creek. X-ray micro CT-scanning was used to quantify soil macroporosity. The restored marsh has a two-layered soil stratigraphy with a topsoil of freshly accreted sediment (ranging in depth between 10 and 60 cm, deposited since 2006) and a subsoil of compact relict agricultural soil. We found that both the soil in the natural marsh and the topsoil of the restored marsh consist of loosely packed sediment rich in macropores and organic matter, whereas the relict agricultural soil in the restored marsh is densely packed and has few macropores. Our results show that groundwater level fluctuations in the restored marsh are restricted to the top layer of newly deposited sediment (i.e. on average 0.08 m depth). Groundwater level fluctuations in the natural marsh occur over a larger depth of the soil profile (i.e. on average 0.28 m depth). As a consequence, the reduced groundwater dynamics in restored tidal marshes are expected to alter the subsurface fluxes of water and nutrients, the source-sink function and the development of marsh vegetation.

2.2   Introduction

Tidal marshes deliver many important ecosystem services: they play an important role in water quality regulation of adjacent estuaries and coastal areas (e.g. Barbier et al., 2011), carbon sequestration (e.g. Mcleod et al., 2011), mitigation of shoreline erosion and flood risks (e.g. Gedan et al., 2011) and they contribute to a large extent to the estuarine biodiversity (Costanza et al., 1997). During past centuries, however, many tidal marshes were embanked (i.e. reclaimed by building of flood defenses) and the soil was drained to gain land for agricultural, industrial or urban expansion (Bakker et al., 2002; Dijkema, 1987; Ma et al., 2014), leading to a loss of these ecosystem services. Within the framework of several legislations such as the EU Habitats and Water Framework Directive (European Parliament and the Council of the European Union, 2000), tidal marshes are increasingly restored on formerly embanked agricultural land (Blackwell et al., 2004; French, 2006; Wolters et al., 2005). The objective generally is that these restored tidal marshes develop relatively fast and deliver ecosystem services comparable to natural marshes. However, more and more studies show that restored tidal marshes and their ecosystem functions and services develop slowly (e.g. Boorman and Hazelden, 2017; Garbutt and Wolters, 2008; Garbutt et al., 2006). Recently, it has been hypothesized that this slow maturation is linked to differences in subsurface hydrology between natural and restored marshes (Tempest et al., 2015), as subsurface groundwater fluxes are determining several ecosystem processes and services such as water quality regulation through nutrient cycling (Hughes et al., 1998; Nuttle, 1988) and vegetation development (Ursino et al., 2004). A thorough understanding of groundwater dynamics in restored versus natural tidal marshes is thus indispensable to propose new solutions to mitigate this problem in future marsh restoration plans.

Groundwater flow in tidal marsh soils was first described in the early work of Chapman (1938). A more advanced knowledge of subsurface hydrology in tidal marshes was only developed in the last decades and was to a large extent based on modeling or combined field and modeling studies (e.g. Gardner, 2005; Harvey et al., 1987; Hemond and Fifield, 1982; Moffett et al., 2012; Ursino et al., 2004; Wilson and Gardner, 2006; Xia and Li, 2012; Xin et al., 2011). For example, Harvey et al. (1987) illustrated the basic movement of groundwater in a saltmarsh soil: during the rising tide, intertidal creeks gradually fill and water infiltrates in the creek banks from the moment the surface water level in the creeks exceeds the groundwater table in the surrounding marsh soil. Around spring tides, the marsh platform inundates at high tide and surface water infiltrates into the marsh soil surface. During falling tide, the groundwater flows towards the creeks and seeps out of the creek banks, creating a hydraulic gradient towards the creeks. Tidally induced groundwater level fluctuations are the largest in the close vicinity of tidal creeks and dampen further in the marsh interior (Byers and Chmura, 2014; Ursino et al., 2004), where subsurface drainage is hindered and evapotranspiration is a major contributor for groundwater abstraction (Hemond and Fifield, 1982; Nuttle, 1988). Apart from the distance to the nearest creek, drainage is controlled by the permeability or hydraulic conductivity of the marsh soil (Montalto et al., 2006). Although the topsoil of many tidal

marshes consists of fine grained, low permeable sediments, recent attention has been given to the presence of macropores (e.g. crab burrows and root channels), which might act as preferential flow paths for groundwater in marsh soils (Cao et al., 2012; Hughes et al., 1998; Susilo and Ridd, 2005; Xin et al., 2016).

Groundwater dynamics are controlling several key marsh ecosystem processes. As a result of tidally induced groundwater fluctuations, marsh sediments are intermittently saturated and unsaturated, inducing complex aeration conditions, hereby influencing plant development and the spatial distribution of marsh vegetation (Ursino et al., 2004; Xin et al., 2009; Xin et al., 2013). Impaired groundwater dynamics resulting in poor soil drainage may limit establishment and growth of marsh vegetation (Mendelssohn and Seneca, 1980). Furthermore, groundwater dynamics affect the soil redox status as more frequently saturated soils tend to exhibit more reduced conditions, which enhances the emission of methane (Byers and Chmura, 2014; Howes et al., 1981). In more aerated soils, on the other hand, microbial respiration leads to the emission of carbon dioxide (e.g. Heinsch et al., 2004). Therefore, groundwater dynamics influence the rate of carbon sequestration. Groundwater flow also induces solute exchange between the marsh soil and the surface water of adjacent estuaries or coastal areas, as pore-water seepage from creek banks exports substantial amounts of nutrients, such as dissolved silica (Struyf et al., 2007; Wilson and Gardner, 2006; Yelverton and Hackney, 1986). Especially flow in macropores enhances the advective flux of dissolved nutrients through marsh sediments (Harvey et al., 1995) and limits the diffusion and associated turnover of nutrients in the subsurface matrix.

When tidal marshes are converted to agriculture, for instance by dike building, soil drainage and associated soil aeration causes organic matter in the soil to decompose, leading to subsidence and compaction through consolidation of sediments (Brooks et al., 2015; Hazelden and Boorman, 2001; Portnoy, 1999; Spencer et al., 2008). The soil is often further compacted by the use of heavy farming equipment or trampling by cattle (Bantilan-Smith et al., 2009; Di Bella et al., 2015; Elschot et al., 2013; Nolte et al., 2013; Sloey and Hester, 2016). In saline soils, drainage can lead to soil dispersion, disintegrating the soil structure even more (Crooks and Pye, 2000). Restoring tidal marshes and their services on such historically compacted agricultural soils may therefore be hindered. Although many implications of soil compaction on developing restored tidal marshes have already been described (e.g. Sloey and Hester, 2016; Spencer et al., 2008), the link with subsurface hydrology is studied only to a limited extent.

Restored tidal marshes typically have a dual layered soil stratigraphy where the historical agricultural soil is overlain by sediment that was deposited since the reintroduction of the tidal regime, as is also the case in our restored site. Crooks and Pye (2000) suggested that compacted subsoils in tidal marshes might act as an aquaclude (i.e. an impermeable barrier for groundwater). The aim of this study is (i) to characterize both the compacted soil layer and the overlying layer of newly deposited sediment, (ii) to determine how these layers

affect groundwater level fluctuations in a restored tidal freshwater marsh and (iii) how these groundwater level fluctuations differ from those seen in a natural freshwater tidal marsh. We hypothesize that soil properties (organic matter content, bulk density and macroporosity) changed because of the former agricultural land use, leading to a reduced permeability and reduced groundwater level fluctuations in the restored marsh compared to the natural marsh.

2.3 Methods

2.3.1 Study site description

The study was conducted in the restored marsh "Lippenbroek" and the natural reference marsh "De Plaat", described in Beauchard et al. (2011) and Vandenbruwaene et al. (2011), located in the freshwater tidal zone of the macro-tidal Scheldt estuary, Hamme, Belgium (51°05' N, 4°11' E, Figure 2.1). The study sites are situated near the maximum tidal range of 4 m (neap tides) to 6 m (spring tides). Salinity varies between 0.5 and 0.75 (Jacobs et al., 2009). Meire et al. (2005) gives a more detailed description of the Scheldt estuary. The restored marsh site was, prior to the marsh restoration in 2006, an embanked agricultural area. Although the exact period of the embankment in Lippenbroek is unknown, large-scale land reclamation for agriculture in the wider area dates back from the 13th century. The elevation in the embanked site did not increase with a rising mean high water level in the river, as was the case in the natural marsh (Vandenbruwaene et al., 2011), and is therefore situated around 3 m lower than the natural marsh platform level. To obtain similar tidal conditions following restoration in the lower elevated agricultural area, the CRT (controlled reduced tide) approach was applied. In this system, the low elevated area is surrounded by a ring dike and water enters the area at high tide and leaves the area at low tide through a separate inlet and outlet sluice (Cox et al., 2006; Maris et al., 2007)(Figure 2.1), resulting in approximately 3 m lower high water levels in the CRT area compared to the estuary. During the embankment phase, parts of the site have been used for poplar (*Populus* sp.) plantations and in the last three decades before the restoration, an intensive crop rotation system with mainly maize (*Zea mays*) and potatoes (*Solanum tuberosum*) was established. During the phase of construction works needed for the restoration of tidal inundation (i.e. 2003-2006), the area was overgrown with a dense pioneer vegetation (mainly *Epilobium hirsutum* and *Urtica dioica*). Since the reintroduction of the tides in March 2006, this vegetation was outcompeted by typical low marsh vegetation (e.g. *Phragmites australis, Typha latifolia, Bolboschoenus maritimus* and *Lythrum salicaria*) and willow trees (*Salix* spp*.*) on the higher elevated parts (Jacobs et al., 2008). The natural marsh is located at the riverside of the dike approximately 1 km upstream from the inlet/outlet structures of the CRT area (Figure 2.1). At the study location, the dominant plant species are willow trees, *Impatiens glandulifera* and *Urtica dioica*.
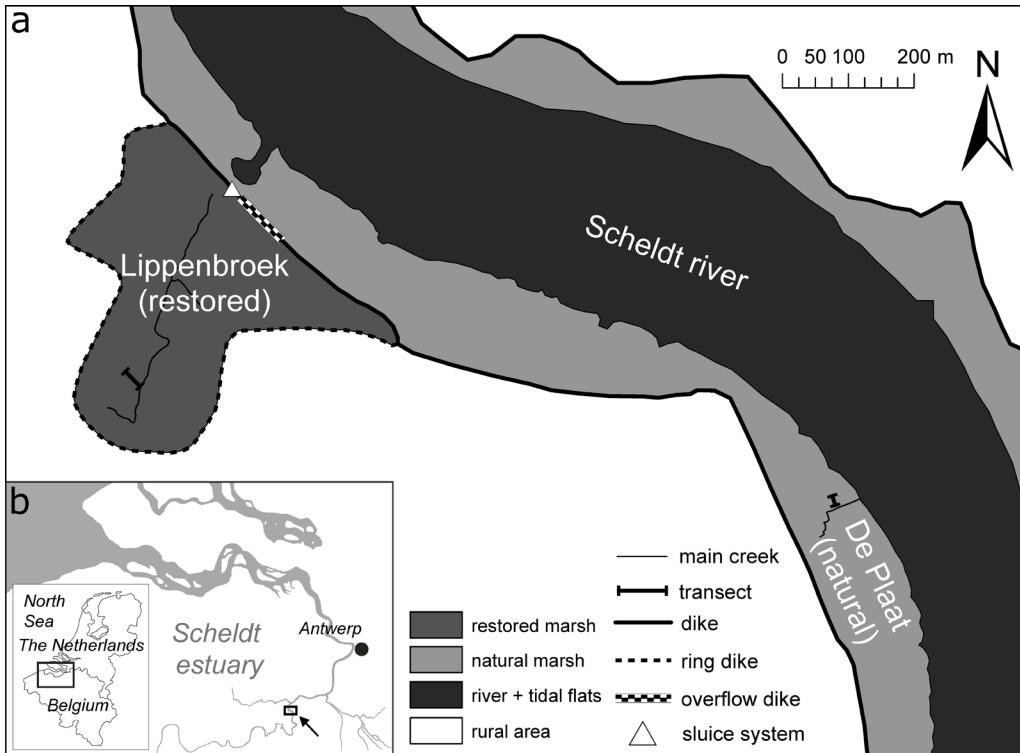
Figure 2.1: (a): Overview map of the study area, (b): situation of the study area in the Scheldt estuary (indicated with an arrow) and situation of the Scheldt estuary in Belgium and The Netherlands.
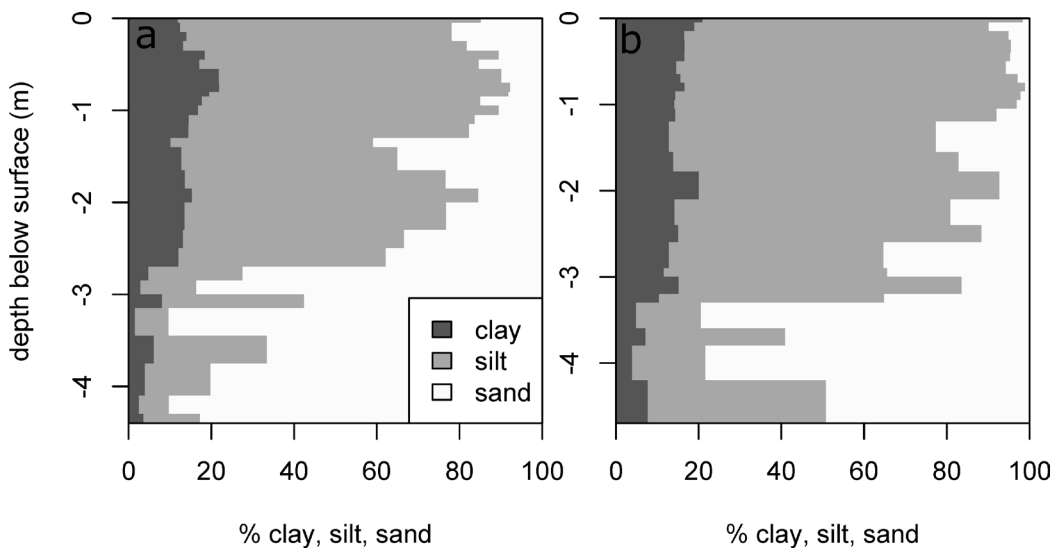

Figure 2.2: Overview of the volumetric grain size fractions (clay, silt and sand, on the scale of Wentworth (1922) and Udden (1914) for a soil profile in (a) the natural and (b) the restored marsh, respectively. Depths are expressed relative to the soil surface.

In both the natural and restored marsh sites, the top layer of the sediment is a typical marsh soil with high amounts of silt and clay (Figure 2.2). In the restored site, the sediment deposited after the reintroduction of the tides, rests on top of an approximately 2 m thick layer of relict agricultural soil, of which especially the upper part is heavily compacted. This fine grained Holocene sediment is underlain by more sandy Pleistocene sediment, including glauconite and pieces of peat. The soil stratigraphy in the natural marsh follows a typical fining upwards pattern (e.g. O'Connor and Moffett, 2015) with over 60% of sand below 3 m depth (Figure 2.2a).

2.3.2   Experimental design

All the data were collected on a transect approximately perpendicular to a tidal creek with a similar depth of approximately 1 m (see locations on Figure 2.1). This design is based on insights from literature on subsurface hydrology in tidal marshes, which state that groundwater level fluctuations and fluxes are related to the distance from tidal creeks (e.g. Gardner, 2005; Montalto et al., 2007; Ursino et al., 2004; Wilson and Gardner, 2006; Xin et al., 2013). We installed five groundwater monitoring wells with an inner diameter of 41 mm, separated 5 m and 8 m from each other in the natural and the restored marsh, respectively (Figure 2.3). A shorter transect was made in the natural marsh for the reason that any longer transect would intersect other nearby creeks. The transect in the natural marsh was located approximately 25 m inland from steep erosion cliffs that delineate the border between the marsh and the tidal flats. The first monitoring well on both transects was placed at approximately 1 m from the creek edge. The entire subsurface part of the wells was screened. Filter sand was applied in a gauze around the wells and the boreholes were sealed off from the surface with a 5 cm thick bentonite seal. In the restored marsh wells, a second bentonite seal was applied between the relict agricultural polder soil and the newly deposited sediment to prevent preferential flow between the two layers (Figure 2.3c). Pressure transducers (Mini Diver®) measured the groundwater level in the wells at an interval of 2 minutes over an almost 6 months period from October 23rd, 2015 to March 16th, 2016, covering approximately 10 spring tide – neap tide cycles. Measured groundwater level data were corrected for atmospheric pressure variations with data from a nearby weather station (www.meteomoes.be), located between 1 and 2 km from the study sites. Due to the different correction steps that are needed to obtain the absolute groundwater level, deviations of a few cm from the true value are possible. As the dataset mostly covers the winter period when the marsh platform is unvegetated, but covered with plant detritus, the effect of evapotranspiration on the groundwater level was not considered in this study. Surface water level data were obtained from the Flanders Hydraulics Research (Waterinfo, 2022). The absolute elevation of the monitoring wells and the topographic surface profile of the transects, including the creek profile, were measured with an RTK-DGPS and are presented in m TAW (the Belgian ordnance level, which at the measuring location corresponds approximately to the mean low water level). To estimate the thickness of the deposited sediment layer in the restored marsh, we took soil cores with a small gouge auger next to the monitoring wells. The soft newly deposited sediment could

easily be removed from the gouge, while the underlying relict agricultural soil is compact and therefore tightly fixed in the gouge. As such, the newly deposited sediment and underlying relict agricultural soil could be clearly distinguished and the distance between the surface level and the soil layer transition was measured with a folding rule.
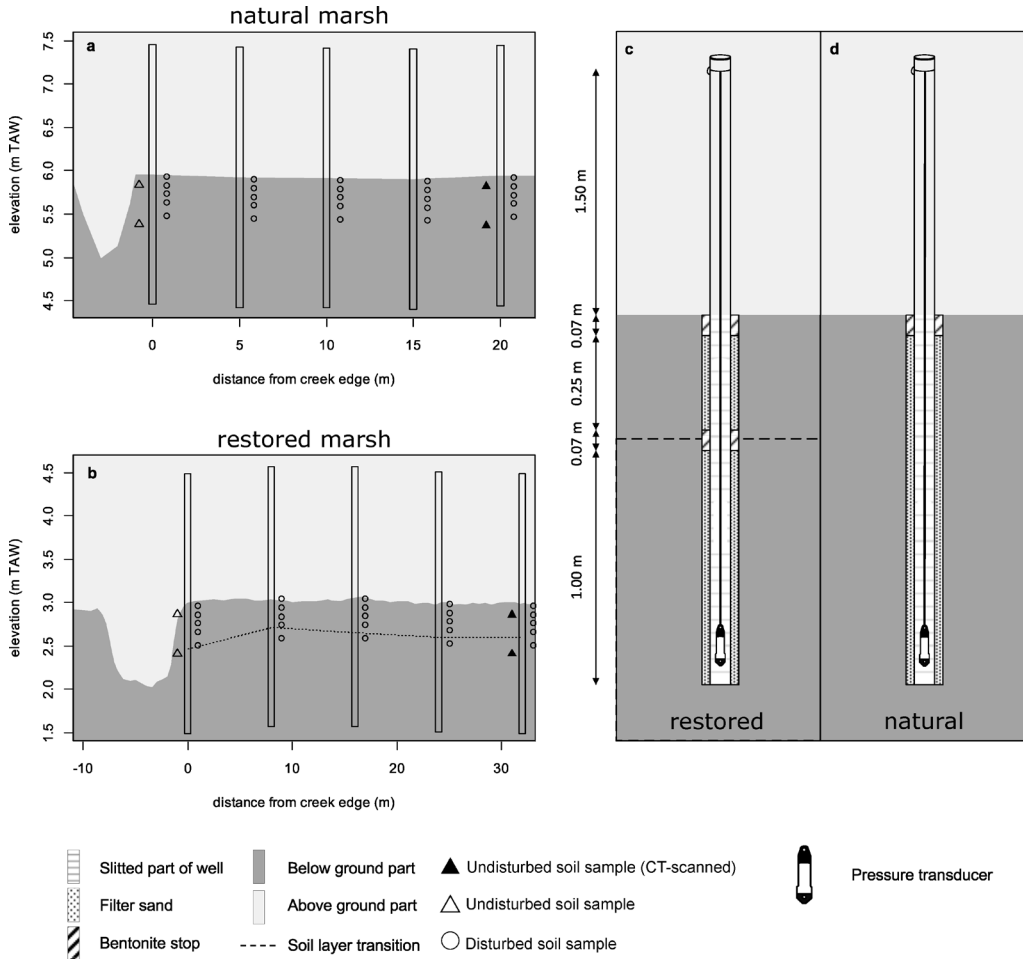

Figure 2.3: Experimental set-up and sampling locations drawn on a cross section of the creek and the marsh platform for (a) the natural marsh and (b) the restored marsh. All soil samples were taken in triplicates. Vertical bars represent the monitoring wells. The design of the monitoring wells is presented in detail in (c) for the restored marsh and (d) for the natural marsh.

Around each well on the transects, three disturbed soil cores were taken with a 5 cm wide gouge auger (Figure 2.3a,b). Each core was subsampled into five depth ranges (0 – 5 cm, 10 – 15 cm, 20 – 25 cm, 30 – 35 cm and 45 – 50 cm). Around the first and the last monitoring well on the transects (later referred to as the 'near-creek zone' and 'marsh interior', respectively), three undisturbed soil samples were taken between 10 cm and 15 cm depth (i.e. corresponding with the tidally deposited upper sediment layer in the restored marsh) and three samples between 55 cm and 60 cm depth (i.e. corresponding with the deeper former agricultural soil in the restored marsh). To minimize compaction and soil

disturbance, a borehole was made with an Edelman auger to the desired depth and the bottom of the borehole was leveled with a Riverside auger, after which the undisturbed soil sample was excavated using a sample ring kit with open ring holder. To allow analysis of these samples with computed tomography (see further), we used custom-made, sharp edged PVC sample rings with a height of 50 mm and an inner diameter of 45 mm. All samples were cooled before analyses at 4°C.

2.3.3   Micro-CT scanning of soil cores

To assess the distribution of macropores and organic matter in the marsh soil, the twelve undisturbed soil samples taken in the marsh interior in both areas were imaged using high-resolution X-ray CT scanning (μCT). This non-destructive technique allows to visualize and analyze the structure of the object in 3D (Cnudde and Boone, 2013). The scans were performed at the HECTOR system of the Ghent University Centre for X-ray Tomography (UGCT) described in Masschaele et al. (2013), using a tube voltage of 140 kV. The resulting datasets contained approximately 1 gigavoxel (1000^3) at an isotropic voxel (i.e. 3D pixel) size of 60^3 μm^3. The grey value for each voxel represents the local X-ray attenuation coefficient, which depends on both the chemical composition and density of the material. Based on the grey value histogram of the complete dataset of all scanned soil cores, threshold values were manually defined and the grey values were segmented using Octopus Analysis® (Brabant et al., 2011; Vlassenbroeck et al., 2007) in one of the following categories: air filled macropores (linear attenuation coefficients < 0.16 cm^{-1}), organic matter or water filled macropores (0.16 cm^{-1} – 0.40 cm^{-1}) and mineral sediment (> 0.40 cm^{-1}). Due to a similar X-ray attenuation, resulting in a similar grey value, water filled macropores and organic matter could not be distinguished. As a result of the partial volume effect, the grey value of each voxel is proportional to the weighted average of the linear attenuation coefficient of the different constituents present within that voxel (Barrett and Keat, 2004). Therefore, voxels containing both mineral sediment and air filled macropores have an intermediate value, which might be in the defined attenuation range of organic matter. After thresholding, voxels that were erroneously classified as a result of noise or partial volume effects were removed by applying the binary operations closing and opening (Brabant et al., 2011; Soille, 1999). The 150 first and last images (along the z-axis = depth profile) of each sample were not used in the analyses because they displayed aberrations that were due to both cone beam artefacts in the CT scans (e.g. Barrett and Keat, 2004) and disturbance of the sample edges while taking the samples (accidental smearing when removing excess sediment protruding from the sample rings). 3D renderings of the sediment, organic matter and macropore fractions were made using VGSTUDIO MAX 3.2 (www.volumegraphics.com, Figure 2.6).

2.3.4   Lab analyses

A subsample of each disturbed soil sample was used to determine the volumetric grain size distribution with a Mastersizer 2000 (Malvern Instruments Ltd.) based on laser diffraction after treatment with HCl and H_2O_2 to remove organic matter. The fraction of clay, silt and

sand in the samples was determined on the scale of Udden (1914) and Wentworth (1922) (clay: < 4 μm, silt: 4 – 63 μm, sand: 63 – 2000 μm). The remainder of the samples was dried at 70°C for at least 48 h to determine the gravimetric moisture content (weight loss/dry mass). As samples in both marshes were taken on different days, moisture content cannot be directly compared between both areas. The gravimetric organic matter content in the samples was estimated with the loss on ignition (LOI) method (e.g. Heiri et al., 2001) with a muffle furnace at a temperature of 550°C.

After CT-scanning, the vertical saturated hydraulic conductivity of the undisturbed soil samples was measured with a laboratory permeameter in which water seeps through undisturbed soil samples placed in a container filled with water (Eijkelkamp Agrisearch Equipments, 2013). We used the constant head method for samples with a saturated hydraulic conductivity higher than 1 cm/day, whereas we used the falling head method for samples with a lower hydraulic conductivity. The aim of these measurements was to test the relation between macroporosity and hydraulic conductivity for individual samples, rather than to obtain an accurate value for the field hydraulic conductivity. Bulk density was determined as dry mass (105°C, > 48 h) over total volume.

2.3.5   Data analyses

All statistical analyses were performed in R (R Development Core Team, 2022) and tidal characteristics (inundation time and frequency) were determined using the 'Tides' package (Cox and Schepers, 2018).
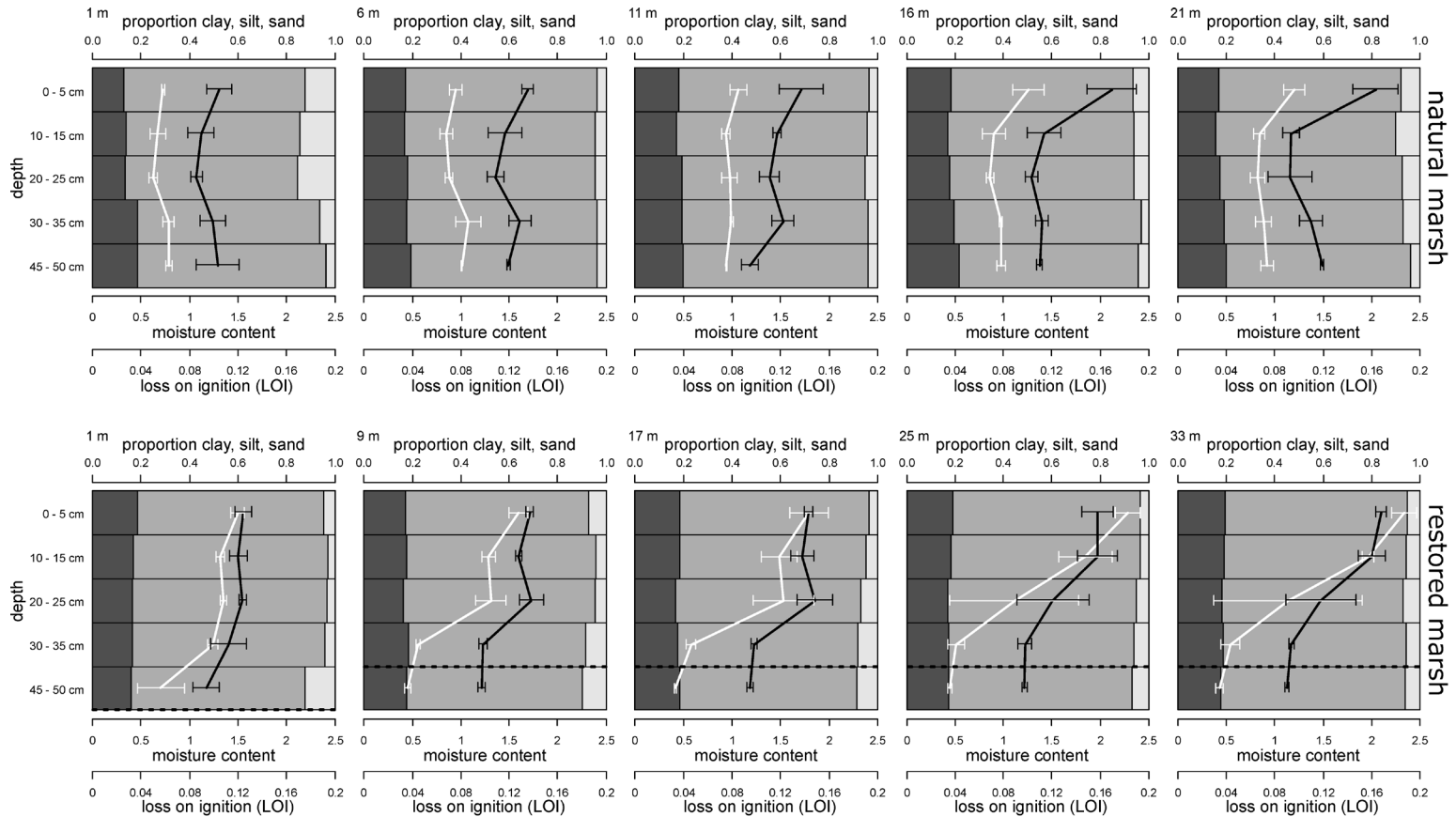
Figure 2.4: Soil properties along the transects in the natural marsh (upper panels) and the restored marsh (lower panels) as a function of the depth and distance from the creek edge (indicated in the upper left corner of each graph). Dark grey, intermediate grey and light grey bars represent the volumetric proportions of clay, silt and sand, respectively. White lines represent the gravimetric moisture content and black lines represent the loss on ignition (LOI) as a fraction. Horizontal dashed lines indicate the approximate location (rounded to the nearest sampling interval) of the transition from newly deposited sediment to compacted subsoil. Error bars indicate the standard deviation (n = 3).
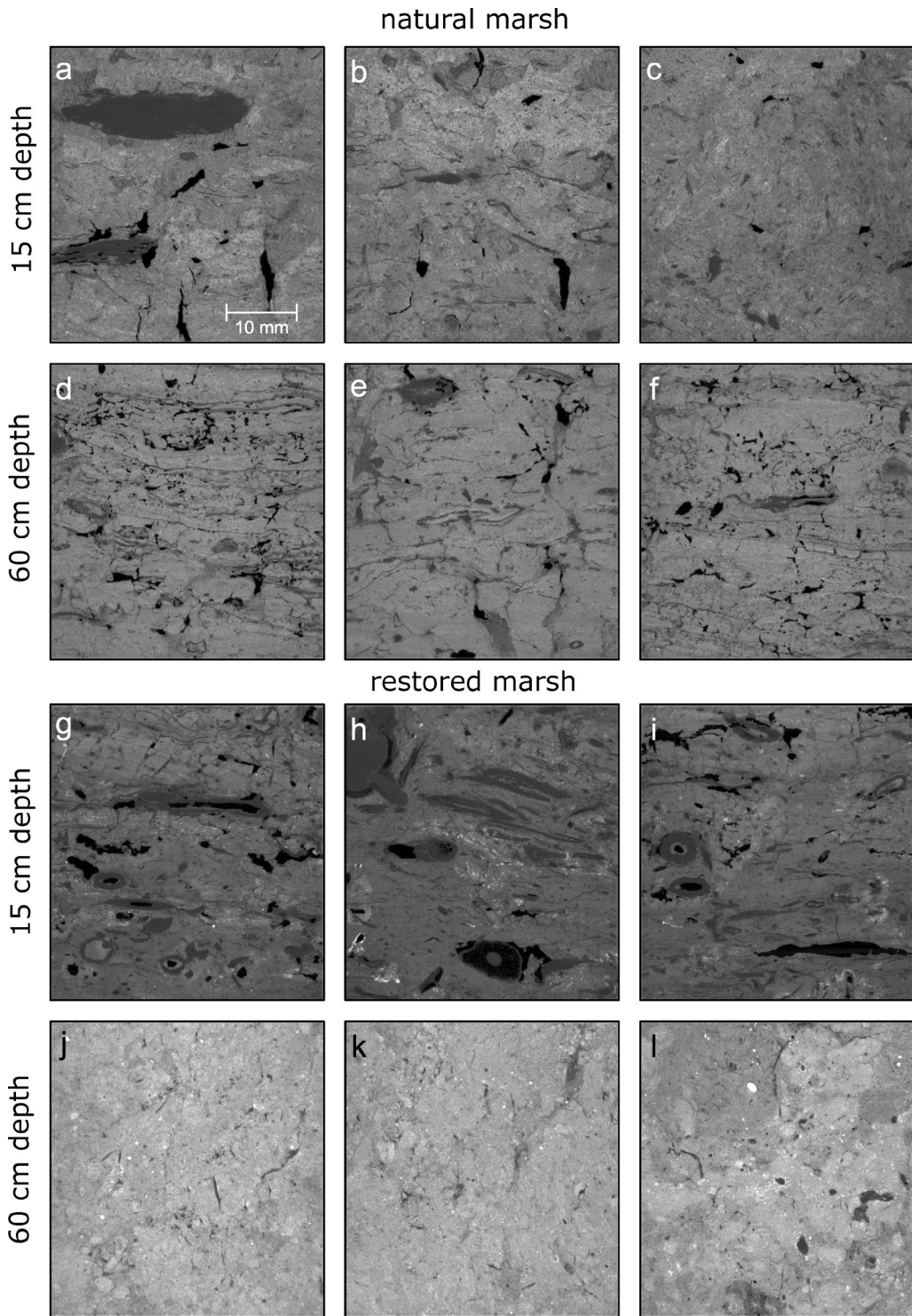
natural marsh

restored marsh

Figure 2.5: CT-scan images of all the undisturbed soil samples taken in the marsh interior. Brighter areas represent denser sediment. Dark grey areas represent organic matter or water-filled macropores, black areas represent air-filled macropores. The images show a vertical cross section through the middle of each sample.
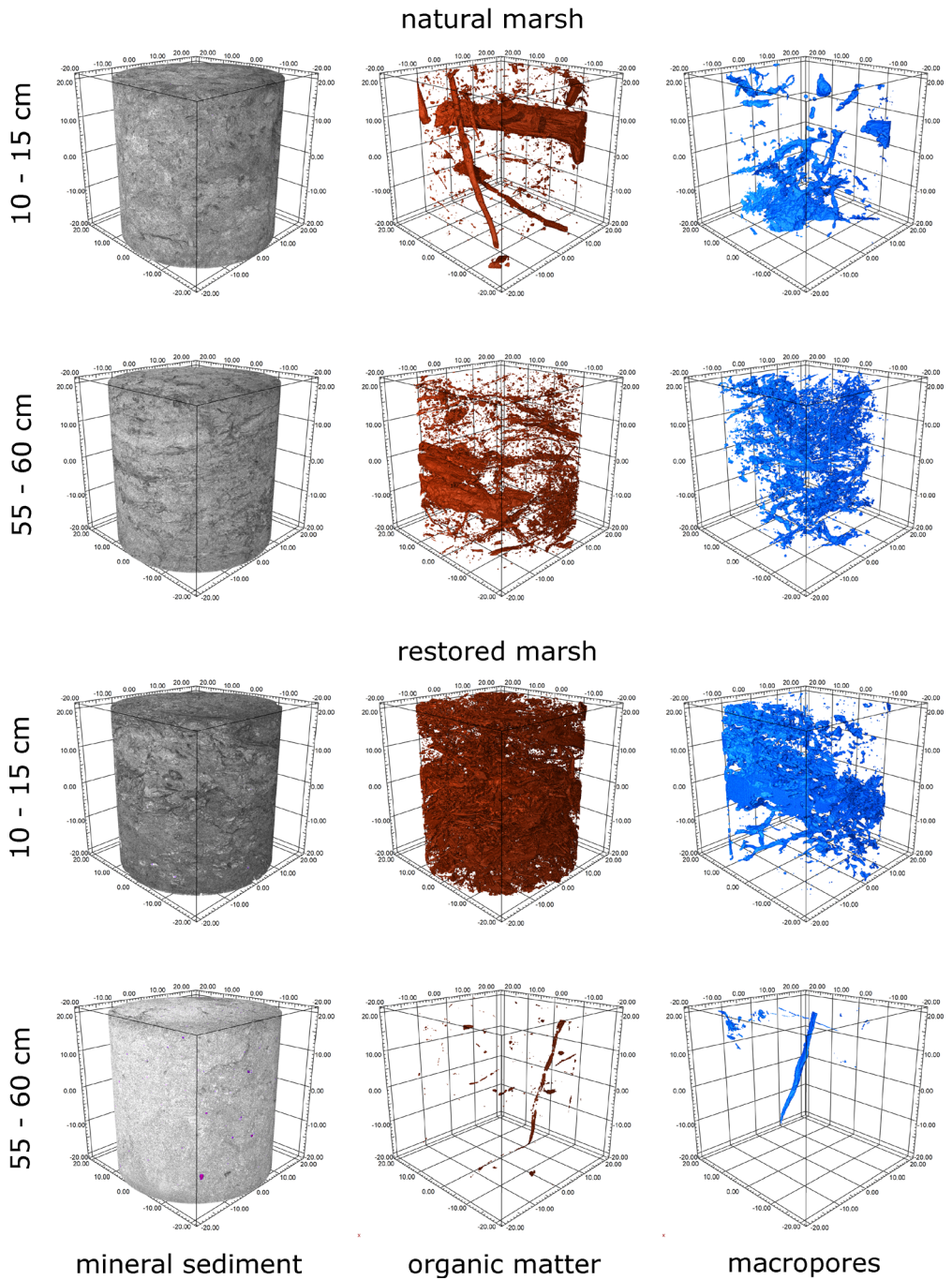
Figure 2.6: 3D renderings of the fractions of mineral sediment, organic matter and macropores for one of the triplicate samples taken in the marsh interior of both study sites. In the renderings of the mineral sediment, lighter areas represent more dense sediment. Very high density mineral inclusions are represented in purple. Labels on the axes are in mm.
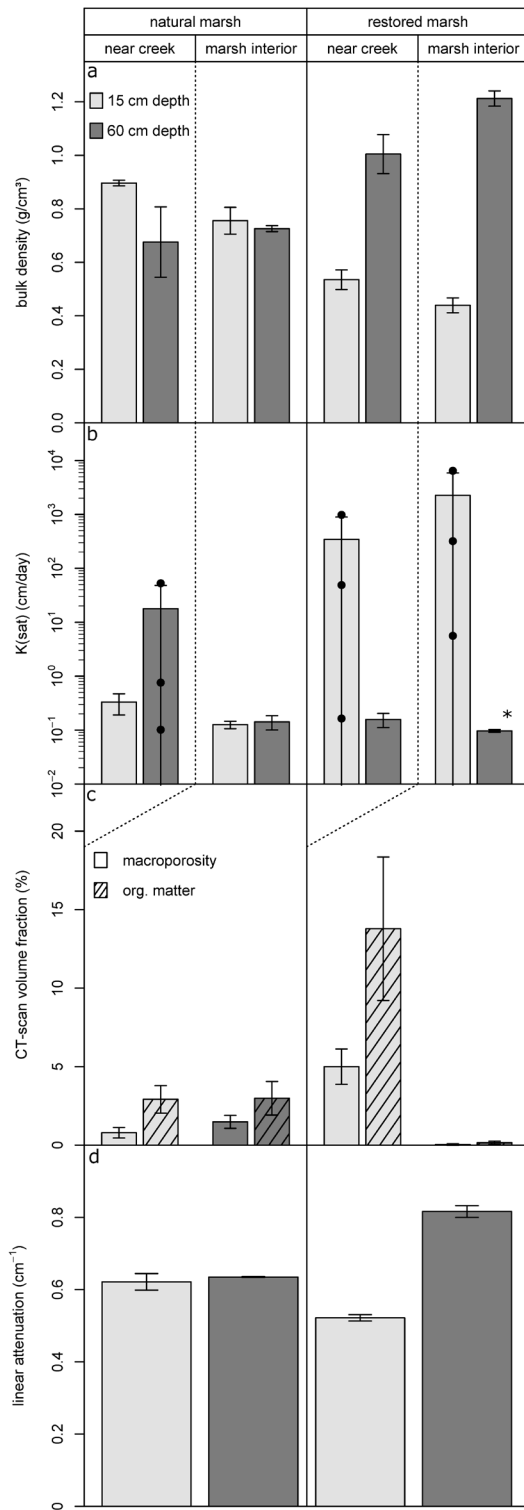
Figure 2.7: Comparison of soil properties measured on undisturbed soil samples from both the natural and the restored tidal marsh in function of depth and location in the marsh. Values are displayed as mean ± standard deviation (n = 3). (a): dry bulk density (b): saturated hydraulic conductivity. Note that the y-axis is logarithmic. Where the variation between the triplicates was several orders of magnitude, the individual measurement values are plotted as well (black bullets). *: actual value was lower than could be accurately measured with the lab permeameter. (c): volume fraction of air filled macropores and organic matter / water filled macropores. The latter could not be distinguished due to a similar X-ray attenuation. (d): Linear attenuation coefficient of the sediment phase. Note that CT-scans were only performed on samples taken in the marsh interior.

2.4 Results

2.4.1 Soil characteristics

2.4.1.1 Grain size distribution, gravimetric moisture content and organic matter content

Grain size distribution (soil texture) and organic matter content strongly control water retention in soils. In the natural marsh, a higher proportion of sand is observed close to the creek (Figure 2.4). Only in the upper 5 cm, there is an increasing soil moisture and LOI with an increasing distance from the creek. Below 5 cm, neither grain size distribution nor moisture and LOI show a clear change in function of depth or distance from the creek. In contrast, in the restored marsh, two distinct soil layers can be discerned. The upper layer consists of loosely packed sediment that was deposited since the first inundation of the marsh in 2006. Over the transect, this layer has a thickness of 39 ± 4 cm in the marsh interior and 52 ± 4 cm at 1 m from the creek. In the upper 15 cm, the organic matter and moisture content increase with an increasing distance from the creek. Below 30 cm, in the relict agricultural soil, both the LOI and moisture content are relatively constant and low.

2.4.1.2 Bulk density, macroporosity and saturated hydraulic conductivity

Figure 2.5 presents CT-scan images from soil cores in both areas. Assuming that the mineral fraction has an identical composition in both areas, which is reasonable as the sediment in both areas originates from a common source, brighter colors indicate denser packed sediment particles, i.e. a lower degree of microporosity (Cnudde and Boone, 2013; Spencer et al., 2017). Visual assessment of these images and 3D renderings of the different components (Figure 2.6), revealed that the sediment in the natural marsh is intersected by pieces of wood, roots and macropores both at 15 and at 60 cm depth. Some of these macropores have the shape of cracks or fissures, whereas others are more irregularly or tubular-shaped. In the newly deposited sediment of the restored marsh (at 15 cm depth), hollow plant structures, such as roots or stems from marsh vegetation, were clearly visible on the CT-scan images, as well as large irregular and tubular void spaces (Figure 2.5g, h, i, Figure 2.6). In the underlying relict agricultural soil (at 60 cm depth), only few small tubular and spherical macropores were present (Figure 2.5j, k, l, Figure 2.6). In both the natural and restored marsh areas, the creek banks are pierced by large holes (with diameters of several cm) that are presumably old root channels or burrows of the Chinese mitten crab (*Eriocheir sinensis*). Some of these holes have been observed to drain considerable amounts of water to the tidal creeks at low tide. Just above the compacted soil, a zone with large water filled macropores was observed. We hypothesize that this is a relic of a former ploughing layer.

For the natural marsh, an ANOVA revealed no significant difference between the volume fraction of air filled macropores nor the volume fraction of organic matter/water filled macropores for samples taken at 15 cm depth and 60 cm depth (Figure 2.7c, Table 2.1). We did find a significant difference between bulk density of the samples ($F_{1,8}$ = 9.39, p = 0.0155). A Tukey's HSD *post hoc* test indicated that bulk density at 15 cm depth is on

average 0.13 g/cm^3 higher than the bulk density at 60 cm depth (Figure 2.7a). In the restored marsh, both the volume fraction of air filled macropores and the volume fraction of organic matter/water filled macropores are significantly higher in the newly deposited sediment (15 cm depth) than in the compacted subsoil (60 cm depth, Figure 2.7, Table 2.1). Bulk density at 15 cm depth is on average 0.62 g/cm^3 lower than at 60 cm depth ($F_{1,8}$= 562.20, p < 0.001, Figure 2.7a). This is also reflected in a significantly higher linear attenuation coefficient (i.e. a lower degree of microporosity, Figure 2.7d, Table 2.1). The saturated hydraulic conductivity of the layer of newly deposited sediment in the restored marsh is very variable, and several orders of magnitude higher compared to both the compacted agricultural soil in the restored marsh, and the soil in the natural marsh (Figure 2.7b).

Table 2.1: Significance table for macroporosity, organic matter content and linear attenuation coefficient of the sediment phase based on CT-scan data that are presented in Figure 2.7. For both sites, a comparison is made between samples taken at 15 cm depth and 60 cm depth (n=3). Based on a one-way ANOVA.

	air macropores		organic matter		linear attenuation	
	$F_{1,4}$	p	$F_{1,4}$	p	$F_{1,4}$	p
natural marsh	5.149	0.086	0.007	0.938	1.050	0.3634
restored marsh	58.167	0.002	26.674	0.007	761.050	<0.001

2.4.2 Subsurface hydrology

As a result of the different elevation and the CRT design (see before), the natural and the restored marsh exhibit different inundation characteristics (Figure 2.8), as explained in Cox et al. (2006). During the measured time span, the studied region in the natural marsh was flooded in 36% of all tides and the average inundation time was 79 min, whereas the studied region in the restored marsh was flooded during 76% of all tides with an average inundation time of 276 min.

The natural and the restored marsh also showed a remarkably different pattern in groundwater dynamics. In between consecutive inundating tides (determined here as two high tides that inundate the marsh platform and are separated less than 15 h in time), the groundwater level in the natural marsh fell on average 28 cm below the marsh platform in the marsh interior and 36 cm in the near creek zone (Figure 2.9a). In the restored marsh, the decline in groundwater level in between consecutive inundating tides was on average only 8 cm below the platform in the marsh interior and 41 cm near the creek. The lowest groundwater level during neap tide was very much depending on the number of consecutive non-inundating tides (Figure 2.8). Over the measured timespan, the minimum-recorded groundwater level in the natural marsh was 72 cm below the surface averaged over the marsh interior and 94 cm near the creek. The minimum groundwater level in the restored marsh was 49 cm below the surface averaged over the marsh interior and 67 cm near the creek. In the restored marsh, the groundwater level is above the transition between the newly deposited sediment and the compact relict agricultural soil for at least

90 % of the measured time (Figure 2.9b). Thus, groundwater level fluctuations occur over a deeper soil profile in the natural marsh compared to the restored marsh.
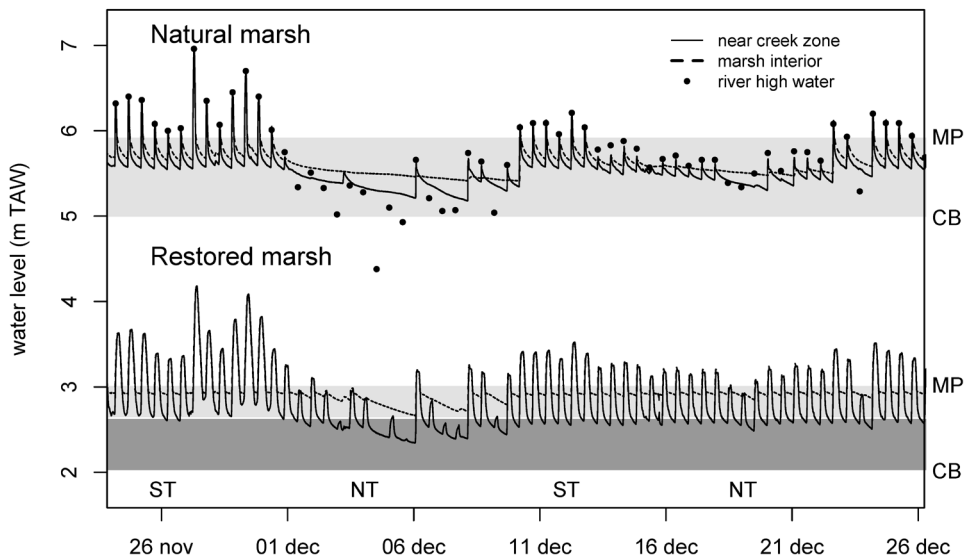

Figure 2.8: Water level measured in the monitoring wells in the natural marsh and the restored marsh for a period from November 26, 2015 to December 26, 2015 covering two spring tide (ST) – neap tide (NT) cycles. The grey shaded areas represent the elevation range between the creek bottom (CB) elevation and the average marsh platform (MP) elevation, with the dark grey part representing the old agricultural polder soil and the light grey part the deposited sediment. Note that the high water level in the restored marsh does not correspond to the high water level in the estuary as a result of the CRT design (see text).

During non-inundating tides, i.e. high tides that inundate the intertidal creeks but that do not flood the vegetated marsh platform, the groundwater table in the natural marsh rises when water fills the tidal creeks (Figure 2.8). This rise is most prominent close to the creek and less so further into the marsh interior. In the restored marsh, only the water level in the monitoring well next to the creek noticeably reacts to a rising water level in the creek. During inundating tides, the water level in all the monitoring wells in both areas rises quickly and simultaneously with the surface water level from the moment the marsh starts flooding. When the surface water recedes from the marsh platform, the water level in the wells decreases approximately logarithmic over time (Figure 2.8). The groundwater level in both the natural and the restored marsh drops faster close to the creek and slower further away from the creek, so that over time a hydraulic gradient develops towards the creek. In the natural marsh, this hydraulic gradient extends throughout the entire transect, whereas the hydraulic gradient in the restored marsh is larger and is only present in the vicinity of the creek (Figure 2.8, Figure 2.9b). After the last inundation before neap tide, the hydraulic gradient in the natural marsh becomes steeper. In the restored marsh, the decrease in groundwater level then occurs more equally along the transect. When the

groundwater table approximates the underlying relict agricultural soil in the restored marsh, the decrease in groundwater level attenuates (Figure 2.8, Figure 2.9b).
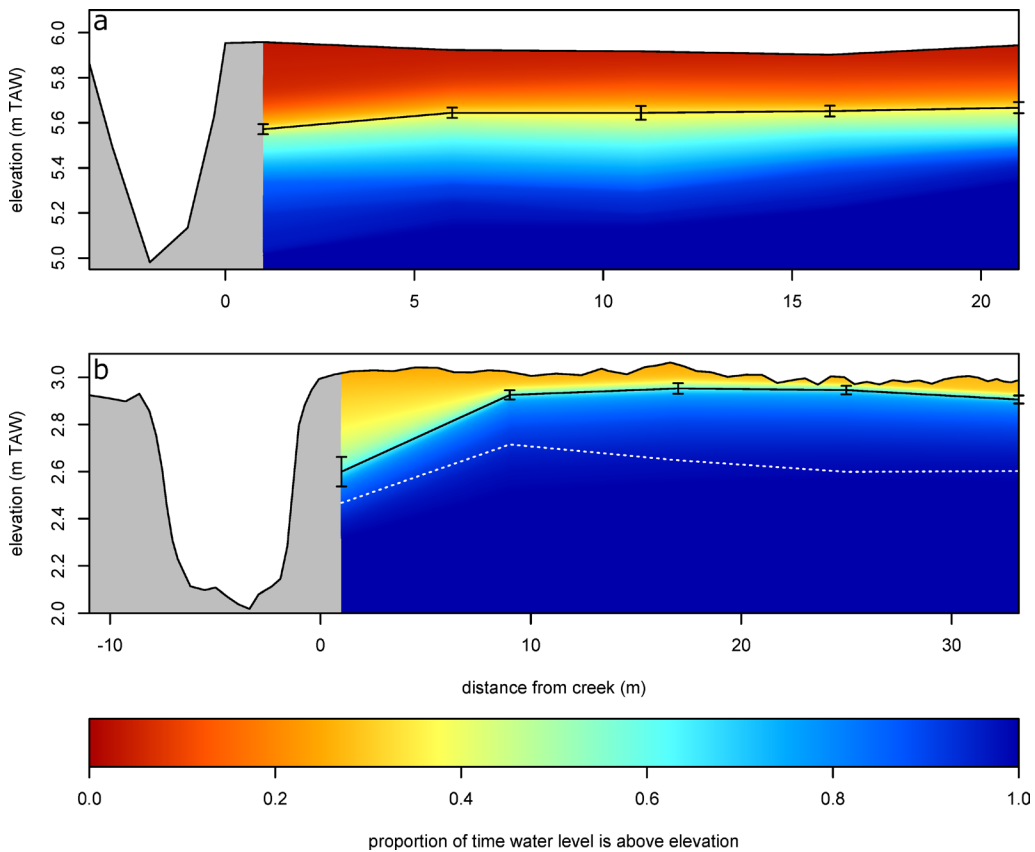

Figure 2.9: Cross section of the creek and marsh platform for (a) the natural marsh and (b) the restored marsh. Colors represent the proportion of time that the groundwater level was above the corresponding elevation on the y-axis. The colored region is restricted to the transect where the measurements took place and values are linearly interpolated between the five measuring points. Black lines represent the mean lowest groundwater level between two consecutive inundating tides. Error bars represent the standard deviation of these values. The dotted white line in the restored marsh (b) indicates the approximate location of the transition between the compact agricultural soil and the newly deposited sediment.

2.5 Discussion

Tidal marshes are increasingly restored on formerly embanked agricultural land to regain important ecosystem services, such as habitat provisioning and nutrient cycling, which are depending on groundwater dynamics and hence soil conditions. This study has shed new light on differences in physical soil properties (including macroporosity) and groundwater dynamics between a natural and a restored freshwater tidal marsh in the Scheldt estuary. Historical land-use in formerly embanked areas has often resulted in altered soil properties that may constrain the groundwater dynamics after marsh restoration. Even after decades, restored tidal marshes often differ significantly from their natural counterparts concerning e.g. vegetation composition and biogeochemical functioning (e.g.

Boorman and Hazelden, 2017; Brooks et al., 2015; Craft et al., 1991; Garbutt and Wolters, 2008; Mossman et al., 2012; Spencer et al., 2008). Although the notion that both vegetation development and nutrient cycling are strongly related to subsurface hydrology is well established for natural tidal marshes (e.g. Hughes et al., 1998; Nuttle, 1988; Wilson et al., 2015), only few papers (e.g. Montalto and Steenhuis, 2004; Tempest et al., 2015) have studied subsurface hydrology in restored tidal marshes in comparison to natural reference marshes. Our results indicate that groundwater level fluctuations occur over a deeper soil profile in the natural marsh compared to the restored marsh, where subsurface drainage is hindered by the compact relict agricultural soil, underlying the newly deposited sediment. Although the soil in the restored marsh has comparable texture in both layers, CT-scans and bulk density analyses showed that the soil in the lower agricultural soil layer is denser packed and has a significantly lower macroporosity and microporosity, a higher bulk density and lower LOI than the upper newly deposited sediment layer. Hence, both vertical and lateral groundwater fluxes are restricted to a smaller, less deep portion of the soil profile in the restored marsh.

2.5.1   Changed soil properties as a result of agricultural land use

Both the soil in the natural marsh and the upper layer of the restored marsh consist of macropores and pieces of organic matter embedded in a fine grained (mostly silt) sediment matrix. By contrast, only few small macropores are present in the relict agricultural soil. Contrary to our results, a recent study of Spencer et al. (2017) in SE England found a higher macroporosity with higher connectivity of macropores in the relict agricultural soil of a restored saltmarsh (after so-called managed realignment) compared to the layer of newly deposited sediment and the soil in a nearby natural saltmarsh. The micro-CT scans in their study contain data on a soil profile of 7.4 cm depth with the upper 4 cm being the newly deposited sediment. Hence, in that study the agricultural soil was sampled and analyzed directly beneath the newly deposited sediment, which might be in a relict macroporous ploughing layer (Spencer et al., 2017). We studied the macroporosity at 55 to 60 cm depth, which is much deeper and is considered to exist below such a ploughing layer.

Macropore networks play a very important role in marsh subsurface hydrology as they form preferential flow paths through which water can infiltrate (Hughes et al., 1998) and drain (Xin et al., 2009). As a result, macropore networks increase the hydraulic conductivity of the soil, especially in otherwise low permeable sediments (Montalto et al., 2006). In our study, this was apparent in the upper layer of the restored marsh (Table 2.1). Nevertheless, a relatively low hydraulic conductivity was measured in the samples from the natural marsh, despite the relatively high macroporosity. This observation does not correspond to the fast decline of water levels in the wells after the tide recedes (Figure 2.8). In our set-up for measuring hydraulic conductivity, only macropore networks that intersect both the top and bottom of the sample might significantly affect the hydraulic conductivity measured with a lab permeameter.

Natural freshwater tidal marshes are built up of sediment that was deposited by the tidal water over hundreds of years. Together with the mineral sediment, organic matter is deposited and gets buried within the soil (Kadiri et al., 2011). During the low water phase, the groundwater table in the marsh declines, inducing soil aeration (Xin et al., 2010). As a consequence, buried organic material is partly decomposed, resulting in the formation of macropores (Beven and Germann, 1982). Due to the increased soil aeration, more favorable conditions for plant growth (Ursino et al., 2004) and soil biota (Beauchard et al., 2013; Schmitz and Harrison, 2004) can develop, leading to a positive feedback loop (Luo et al., 2010; Tempest et al., 2015; Ursino et al., 2004; Xin et al., 2013) as decayed plant roots and burrowing invertebrates create new macropores. Harvey et al. (1995) found that the volume of macropores in the soil corresponds to the proportion of soil volume in which solute transport occurs and that nutrient concentrations can be three times higher in matrix pores compared to macropores, suggesting fast flushing of dissolved nutrients through macropore networks. Large macropores (e.g. crab burrows) in creek banks, as also observed in both of our field sites, can be responsible for faster groundwater level fluctuations near the creek banks (Montalto et al., 2006).

Tidal marshes are typically restored on low lying agricultural land that has been subjected to extended periods of drainage and subsequent subsidence and compaction of the soil, as organic matter is further mineralized (Iost et al., 2007) and, more recently, heavy farming equipment is used (Bantilan-Smith et al., 2009; Sloey and Hester, 2016), to which macropore networks are extremely vulnerable (Beven and Germann, 2013). For saltmarshes, Crooks and Pye (2000) add that in carbonate deficient soils, the soil fabric may totally collapse when clay particles disperse after drainage of the saline soil. In our freshwater study sites, this effect is expected not to play a role. Our study provides further indication that original marsh soil properties are not reversed in a reasonable time frame after the reintroduction of the tidal regime, with major implications for subsurface hydrology.

2.5.2   Reduced groundwater fluctuations in the restored tidal marsh

Tidally induced groundwater fluctuations in the restored marsh are restricted to the layer of newly deposited sediment, supporting the conclusions of Tempest et al. (2015) that the compacted soil, underlying this layer, acts as a barrier for groundwater flow. Furthermore, the groundwater level only approximates the transition of the soil layers (which is located at approximately 40 cm depth) during extended periods without inundations (i.e. around neap tides). In between consecutive inundating tides, the groundwater level in the marsh interior does not decline to more than 10 cm below the marsh platform. Close to the creek (< 1 m), the groundwater level drops deeper after the tide recedes and rises with a rising surface water level in the creek, even during non-inundating tides. We can therefore expect that, in accordance to the findings of Wilson and Gardner (2006) for numerical simulations of a natural tidal marsh, the majority of seepage to creeks originates from groundwater within the first few meters from the creek edge. This underpins the importance of a dense

creek network for the aeration and biogeochemical cycling of restored tidal marsh soils. However, compacted soil layers can hamper the incision of creek networks (Vandenbruwaene et al., 2012), possibly further reducing the capability of the marsh to increase its drainage capacity after restoration.

Groundwater level fluctuations in the natural marsh were also strongest close to the creek and weaker further in the marsh interior, but a remarkable decline in groundwater level was still observed at 21 m from the creek, which is further than described in most studies (e.g. Nuttle, 1988) who found that tidally induced groundwater drainage is negligible in a marsh soil further than 15 m from the creek. This may partly be the result of exfiltration through the steep erosion cliffs that mark the edge of the tidal marsh towards the tidal mudflats, as our transect was situated around 25 m from this approximately 1 m high cliff. As mentioned above, the observed groundwater level decrease after inundation in the natural marsh was faster than could be expected based on the measured vertical saturated hydraulic conductivity. This suggests a more complex situation where groundwater mainly flows through larger scale macropore networks that may not have been contained in our soil samples.

In this chapter, we focused on fluctuations of the groundwater table. However, in the fine grained soil of both the natural and the restored tidal marsh, a thick capillary fringe is likely to be present above the groundwater table (Kong et al., 2015). Where this groundwater table is shallow, as observed in the restored marsh, the capillary fringe can extend to the soil surface (Drabsch et al., 1999), limiting soil aeration and surface water infiltration, and promoting pore water removal by evaporation (Xin et al., 2017). In order to fully understand the subsurface hydrology of restored tidal wetlands, the capillary fringe and the overlying vadose zone should be considered as well. This requires measurements of soil water potential or water content and/or numerical simulations in a variably saturated porewater model.

2.5.3 Implications of reduced groundwater dynamics for ecosystem functioning

A slow development of soil properties and subsurface hydrology can have major implications for the ecosystem functions and services of restored wetlands, which are often targeted and expected to develop within a certain timeframe (Ballantine et al., 2015). Plant communities in restored tidal marshes have to cope with higher average groundwater levels and therefore may differ from plant communities observed in natural tidal marshes (Brooks et al., 2015; Wolters et al., 2005). These higher groundwater levels reduce the soil aeration depth. It must, however, be noted that in tidal marshes with a low hydraulic conductivity (< 8.64 cm/day = 10^{-6} m s^{-1}), an unsaturated zone can persist below the surface even during inundation (Byers and Chmura, 2014; Ursino et al., 2004). Moreover, vegetation oxidizes the sediment in the root zone (Howes et al., 1981; Kolditz et al., 2009). Besides the direct effect on groundwater levels, the compact agricultural soil can also form a barrier for plant roots (Brooks et al., 2015) and burrowing species (Tempest et al., 2015;

Xin et al., 2009), restricting the formation of macropores and thus hindering a development towards an increased soil drainage capacity. Furthermore, groundwater dynamics control several geomorphological processes. In restored tidal marshes, impaired drainage hampers consolidation of the newly deposited sediment and hence leads to a low dry bulk density of this sediment, resulting in a faster increase of the marsh platform elevation with an equal sediment mass accumulation rate. On the other hand, the less consolidated sediment has a lower bulk density and is therefore expected to have a lower shear strength and to be therefore more vulnerable to erosion (Crooks and Pye, 2000).

Despite these adverse effects that reduced groundwater drainage can have on marsh development, a fast development of a vegetation community comparable to natural freshwater tidal marshes was observed in the studied restored marsh (Jacobs et al., 2009; Oosterlee et al., 2017). This might be due to the relatively high net accretion rate of around 0.04 m yr^{-1} in the intermediate elevated parts of the marsh (Vandenbruwaene et al., 2011).

2.5.4 Implications for marsh restoration and management

Soil compaction affects subsurface hydrology in restored tidal wetlands and is therefore a widespread problem in restoration projects. To enhance surface drainage and to jumpstart further creek formation, in some marsh restoration projects, artificial creek networks are excavated in formerly embanked agricultural land before marsh restoration (e.g. Eertman et al., 2002). We expect that such creek initiation would also enhance groundwater seepage, but, according to our results, only within the first few meters from the creek edges. To increase infiltration and drainage in the marsh interior, we argue that methods should be sought to increase the hydraulic conductivity of compacted relict soil layers. One of these methods could be deep ploughing, as proposed by Brooks et al. (2015) or amending the soil with organic wastes to induce the development of macropore networks. Further research should indicate whether implementation of these methods would effectively enhance groundwater flow and biogeochemical cycling in restored tidal marshes.

2.6 Conclusions

When tidal marshes are restored on formerly embanked agricultural land that has been subjected to soil compaction, groundwater level fluctuations are restricted to the layer of newly deposited sediment. This layer has a high hydraulic conductivity, organic matter content, macroporosity and a low bulk density. However, the underlying layer of relict agricultural polder soil, which has a very low hydraulic conductivity, a low micro- and macroporosity, a low organic matter content and a high bulk density, forms an impermeable layer for groundwater. As a result, drainage in restored tidal marshes is hindered, which supposedly affects both vegetation development and nutrient cycling. Both the hydraulic conductivity (which was found to be affected by the macroporosity), and the distance from a creek are determining groundwater level fluctuations in tidal marshes. Therefore, both these factors should be considered in restoration schemes.

2.7   Acknowledgements

We would like to thank Dimitri Van Pelt and Simon De Meulenaer for field assistance. We are grateful to MeteoMoes for providing barometric data. Niels Van Putte and Marjolein Heyndrickx are SB PhD Fellow at FWO (project no. 1S17517N and 1S02016N, respectively). The Ghent University Special Research Fund (BOF-UGent) is acknowledged for the financial support to the Centre of Expertise UGCT (BOF.EXP.2017.000007). The authors have no conflict of interest to declare.

2.8   References

Bakker, J.P., Esselink, P., Dijkema, K.S., van Duin, W.E., de Jong, D.J., 2002. Restoration of salt marshes in the Netherlands. Hydrobiologia 478, 29-51. 10.1023/A:1021066311728

Ballantine, K.A., Lehmann, J., Schneider, R.L., Groffman, P.M., 2015. Trade-offs between soil-based functions in wetlands restored with soil amendments of differing lability. Ecological Applications 25, 215-225. 10.1890/13-1409.1

Bantilan-Smith, M., Bruland, G.L., MacKenzie, R.A., Henry, A.R., Ryder, C.R., 2009. A Comparison of the Vegetation and Soils of Natural, Restored, and Created Coastal Lowland Wetlands in Hawaii. Wetlands 29, 1023-1035. 10.1672/08-127.1

Barbier, E.B., Hacker, S.D., Kennedy, C., Koch, E.W., Stier, A.C., Silliman, B.R., 2011. The value of estuarine and coastal ecosystem services. Ecological Monographs 81, 169-193. 10.1890/10-1510.1

Barrett, J.F., Keat, N., 2004. Artifacts in CT: Recognition and Avoidance. RadioGraphics 24, 1679-1691. 10.1148/rg.246045065

Beauchard, O., Jacobs, S., Cox, T.J.S., Maris, T., Vrebos, D., Van Braeckel, A., Meire, P., 2011. A new technique for tidal habitat restoration: Evaluation of its hydrological potentials. Ecological Engineering 37, 1849-1858. 10.1016/j.ecoleng.2011.06.010

Beauchard, O., Jacobs, S., Ysebaert, T., Meire, P., 2013. Sediment macroinvertebrate community functioning in impacted and newly-created tidal freshwater habitats. Estuarine Coastal and Shelf Science 120, 21-32. 10.1016/j.ecss.2013.01.013

Beven, K., Germann, P., 1982. Macropores and Water-Flow in Soils. Water Resources Research 18, 1311-1325. 10.1029/WR018i005p01311

Beven, K., Germann, P., 2013. Macropores and water flow in soils revisited. Water Resources Research 49, 3071-3092. 10.1002/wrcr.20156

Blackwell, M.S.A., Hogan, D.V., Maltby, E., 2004. The short-term impact of managed realignment on soil environmental variables and hydrology. Estuarine Coastal and Shelf Science 59, 687-701. 10.1016/j.ecss.2003.11.012

Boorman, L.A., Hazelden, J., 2017. Managed re-alignment; a salt marsh dilemma? Wetlands Ecology and Management, 1-17. 10.1007/s11273-017-9556-9

Brabant, L., Vlassenbroeck, J., De Witte, Y., Cnudde, V., Boone, M.N., Dewanckele, J., Van Hoorebeke, L., 2011. Three-Dimensional Analysis of High-Resolution X-Ray Computed Tomography Data with Morpho+. Microscopy and Microanalysis 17, 252-263. 10.1017/S1431927610094389

Brooks, K.L., Mossman, H.L., Chitty, J.L., Grant, A., 2015. Limited Vegetation Development on a Created Salt Marsh Associated with Over-Consolidated Sediments and Lack of Topographic Heterogeneity. Estuaries and Coasts 38, 325-336. 10.1007/s12237-014-9824-3

Byers, S.E., Chmura, G.L., 2014. Observations on Shallow Subsurface Hydrology at Bay of Fundy Macrotidal Salt Marshes. Journal of Coastal Research 30, 1006-1016. 10.2112/Jcoastres-D-12-00167.1

Cao, M., Xin, P., Jin, G.Q., Li, L., 2012. A field study on groundwater dynamics in a salt marsh - Chongming Dongtan wetland. Ecological Engineering 40, 61-69. 10.1016/j.ecoleng.2011.12.018

Chapman, V.J., 1938. Studies in Salt-Marsh Ecology Sections I to III. Journal of Ecology 26, 144-179. 10.2307/2256416

Cnudde, V., Boone, M.N., 2013. High-resolution X-ray computed tomography in geosciences:

A review of the current technology and applications. Earth-Science Reviews 123, 1-17. 10.1016/j.earscirev.2013.04.003

Costanza, R., dArge, R., deGroot, R., Farber, S., Grasso, M., Hannon, B., Limburg, K., Naeem, S., ONeill, R.V., Paruelo, J., Raskin, R.G., Sutton, P., vandenBelt, M., 1997. The value of the world's ecosystem services and natural capital. Nature 387, 253-260. 10.1038/387253a0

Cox, T.J.S., Maris, T., De Vleeschauwer, P., De Mulder, T., Soetaert, K., Meire, P., 2006. Flood control areas as an opportunity to restore estuarine habitat. Ecological Engineering 28, 55-63. 10.1016/j.ecoleng.2006.04.001

Cox, T.J.S., Schepers, L., 2018. Tides R-package v2.1. 10.5281/zenodo.897843

Craft, C.B., Seneca, E.D., Broome, S.W., 1991. Porewater Chemistry of Natural and Created Marsh Soils. Journal of Experimental Marine Biology and Ecology 152, 187-200. 10.1016/0022-0981(91)90214-H

Crooks, S., Pye, K., 2000. Sedimentological controls on the erosion and morphology of saltmarshes: implications for flood defence and habitat recreation. Coastal and Estuarine Environments: Sedimentology, Geomorphology and Geoarchaeology 175, 207-222. 10.1144/Gsl.Sp.2000.175.01.16

Di Bella, C.E., Rodriguez, A.M., Jacobo, E., Golluscio, R.A., Taboada, M.A., 2015. Impact of cattle grazing on temperate coastal salt marsh soils. Soil Use and Management 31, 299-307. 10.1111/sum.12176

Dijkema, K.S., 1987. Changes in salt-marsh area in the Netherlands Wadden Sea after 1600, in: Huiskes, A.H.L., Blom, C.W.P.M., Rozema, J. (Eds.), Vegetation between land and sea: Structure and processes. Springer Netherlands, Dordrecht, pp. 42-51.

Drabsch, J.M., Parnell, K.E., Hume, T.M., Dolphin, T.J., 1999. The capillary fringe and the water table in an intertidal estuarine sand flat. Estuarine Coastal and Shelf Science 48, 215-222. DOI 10.1006/ecss.1998.0414

Eertman, R.H.M., Kornman, B.A., Stikvoort, E., Verbeek, H., 2002. Restoration of the Sieperda tidal marsh in the Scheldt estuary, the Netherlands. Restoration Ecology 10, 438-449. 10.1046/j.1526-100X.2002.01034.x

Eijkelkamp Agrisearch Equipments, 2013. laboratory-Permeameters: Operation instructions, Giesbeek, The Netherlands.

Elschot, K., Bouma, T.J., Temmerman, S., Bakker, J.P., 2013. Effects of long-term grazing on sediment deposition and salt-marsh accretion rates. Estuarine Coastal and Shelf Science 133, 109-115. 10.1016/j.ecss.2013.08.021

European Parliament and the Council of the European Union, 2000. Directive 2000/60/EC of the European Parliament and of the Council establishing a framework for the Community action in the field of water policy, Official Journal of the European Communities L327. 22.12.2000.

French, P.W., 2006. Managed realignment - The developing story of a comparatively new approach to soft engineering. Estuarine Coastal and Shelf Science 67, 409-423. 10.1016/j.ecss.2005.11.035

Garbutt, A., Wolters, M., 2008. The natural regeneration of salt marsh on formerly reclaimed land. Applied Vegetation Science 11, 335-344. 10.3170/2008-7-18451

Garbutt, R.A., Reading, C.J., Wolters, M., Gray, A.J., Rothery, P., 2006. Monitoring the development of intertidal habitats on former agricultural land after the managed realignment of coastal defences at Tollesbury, Essex, UK. Marine Pollution Bulletin 53, 155-164. 10.1016/j.marpolbul.2005.09.015

Gardner, L.R., 2005. Role of geomorphic and hydraulic parameters in governing pore water seepage from salt marsh sediments. Water Resources Research 41. 10.1029/2004wr003671

Gedan, K.B., Kirwan, M.L., Wolanski, E., Barbier, E.B., Silliman, B.R., 2011. The present and future role of coastal wetland vegetation in protecting shorelines: answering recent challenges to the paradigm. Climatic Change 106, 7-29. 10.1007/s10584-010-0003-7

Harvey, J.W., Chambers, R.M., Hoelscher, J.R., 1995. Preferential Flow and Segregation of Porewater Solutes in Wetland Sediment. Estuaries 18, 568-578. 10.2307/1352377

Harvey, J.W., Germann, P.F., Odum, W.E., 1987. Geomorphological Control of Subsurface Hydrology in the Creek-Bank Zone of Tidal Marshes. Estuarine Coastal and Shelf Science 25, 677-691. 10.1016/0272-7714(87)90015-1

Hazelden, J., Boorman, L.A., 2001. Soils and 'managed retreat' in South East England. Soil Use and Management 17, 150-154. 10.1079/Sum200166

Heinsch, F.A., Heilman, J.L., McInnes, K.J., Cobos, D.R., Zuberer, D.A., Roelke, D.L., 2004. Carbon dioxide exchange in a high marsh on the Texas Gulf Coast: effects of freshwater availability. Agricultural and Forest Meteorology 125, 159-172. 10.1016/j.agrformat.2004.02.007

Heiri, O., Lotter, A.F., Lemcke, G., 2001. Loss on ignition as a method for estimating organic and carbonate content in sediments: reproducibility and comparability of results. Journal of Paleolimnology 25, 101-110. 10.1023/a:1008119611481

Hemond, H.F., Fifield, J.L., 1982. Subsurface Flow in Salt-Marsh Peat - a Model and Field-Study. Limnology and Oceanography 27, 126-136. 10.4319/lo.1982.27.1.0126

Howes, B.L., Howarth, R.W., Teal, J.M., Valiela, I., 1981. Oxidation-Reduction Potentials in a Salt-Marsh - Spatial Patterns and Interactions with Primary Production. Limnology and Oceanography 26, 350-360. 10.4319/lo.1981.26.2.0350

Hughes, C.E., Binning, P., Willgoose, G.R., 1998. Characterisation of the hydrology of an estuarine wetland. Journal of Hydrology 211, 34-49. 10.1016/S0022-1694(98)00194-2

Iost, S., Landgraf, D., Makeschin, F., 2007. Chemical soil properties of reclaimed marsh soil from Zhejiang Province PR China. Geoderma 142, 245-250. 10.1016/j.geoderma.2007.08.001

Jacobs, S., Beauchard, O., Struyf, E., Cox, T.J.S., Maris, T., Meire, P., 2009. Restoration of tidal freshwater vegetation using controlled reduced tide (CRT) along the Schelde Estuary (Belgium). Estuarine Coastal and Shelf Science 85, 368-376. 10.1016/j.ecss.2009.09.004

Jacobs, S., Struyf, E., Maris, T., Meire, P., 2008. Spatiotemporal aspects of silica buffering in restored tidal marshes. Estuarine Coastal and Shelf Science 80, 42-52. 10.1016/j.ecss.2008.07.003

Kadiri, M., Spencer, K.L., Heppell, C.M., Fletcher, P., 2011. Sediment characteristics of a restored saltmarsh and mudflat in a managed realignment scheme in Southeast England. Hydrobiologia 672, 79-89. 10.1007/s10750-011-0755-8

Kolditz, K., Dellwig, O., Barkowski, J., Beck, M., Freund, H., Brumsack, H.J., 2009. Effects of De-Embankment on Pore Water Geochemistry of Salt Marsh Sediments. Journal of Coastal Research 25, 1222-1235. 10.2112/08-1053.1

Kong, J., Xin, P., Hua, G.F., Luo, Z.Y., Shen, C.J., Chen, D., Li, L., 2015. Effects of vadose zone on groundwater table fluctuations in unconfined aquifers. Journal of Hydrology 528, 397-407. 10.1016/j.jhydrol.2015.06.045

Luo, L.F., Lin, H., Li, S.C., 2010. Quantification of 3-D soil macropore networks in different soil types and land uses using computed tomography. Journal of Hydrology 393, 53-64. 10.1016/j.jhydrol.2010.03.031

Ma, Z., Melville, D.S., Liu, J., Chen, Y., Yang, H., Ren, W., Zhang, Z., Piersma, T., Li, B., 2014. Rethinking China's new great wall: Massive seawall construction in coastal wetlands threatens biodiversity. Science 346, 912-914. 10.1126/science.1257258

Maris, T., Cox, T.J.S., Temmerman, S., De Vleeschauwer, P., Van Damme, S., De Mulder, T., Van den Bergh, E., Meire, P., 2007. Tuning the tide: creating ecological conditions for tidal marsh development in a flood control area. Hydrobiologia 588, 31-43. 10.1007/s10750-007-0650-5

Masschaele, B., Dierick, M., Van Loo, D., Boone, M.N., Brabant, L., Pauwels, E., Cnudde, V., Van Hoorebeke, L., 2013. HECTOR: A 240kV micro-CT setup optimized for research. Journal of Physics: Conference Series 463. 10.1088/1742-6596/463/1/012012

Mcleod, E., Chmura, G.L., Bouillon, S., Salm, R., Bjork, M., Duarte, C.M., Lovelock, C.E., Schlesinger, W.H., Silliman, B.R., 2011. A blueprint for blue carbon: toward an improved understanding of the role of vegetated coastal habitats in sequestering CO2. Frontiers in Ecology and the Environment 9, 552-560. 10.1890/110004

Meire, P., Ysebaert, T., Van Damme, S., Van den Bergh, E., Maris, T., Struyf, E., 2005. The Scheldt estuary: A description of a changing ecosystem. Hydrobiologia 540, 1-11. 10.1007/s10750-005-0896-8

Mendelssohn, I.A., Seneca, E.D., 1980. The Influence of Soil Drainage on the Growth of Salt-Marsh Cordgrass Spartina-Alterniflora in North-Carolina. Estuarine and Coastal Marine Science 11, 27-40. 10.1016/S0302-3524(80)80027-2

Moffett, K.B., Gorelick, S.M., McLaren, R.G., Sudicky, E.A., 2012. Salt marsh ecohydrological zonation due to heterogeneous vegetation–groundwater–surface water interactions. Water Resources Research 48. 10.1029/2011WR010874

Montalto, F.A., Parlange, J.Y., Steenhuis, T.S., 2007. A simple model for predicting water table fluctuations in a tidal marsh. Water Resources Research 43. 10.1029/2004wr003913

Montalto, F.A., Steenhuis, T.S., 2004. The link between hydrology and restoration of tidal marshes in the New York New Jersey Estuary. Wetlands 24, 414-425. 10.1672/0277-5212(2004)024[0414:Tlbhar]2.0.Co;2

Montalto, F.A., Steenhuis, T.S., Parlange, J.Y., 2006. The hydrology of Piermont Marsh, a reference for tidal marsh restoration in the Hudson river estuary, New York. Journal of Hydrology 316, 108-128. 10.1016/j.jhydrol.2005.03.043

Mossman, H.L., Davy, A.J., Grant, A., 2012. Does managed coastal realignment create saltmarshes with 'equivalent biological characteristics' to natural reference sites? Journal of Applied Ecology 49, 1446-1456. 10.1111/j.1365-2664.2012.02198.x

Nolte, S., Muller, F., Schuerch, M., Wanner, A., Esselink, P., Bakker, J.P., Jensen, K., 2013. Does livestock grazing affect sediment deposition and accretion rates in salt marshes? Estuarine Coastal and Shelf Science 135, 296-305. 10.1016/j.ecss.2013.10.026

Nuttle, W.K., 1988. The Extent of Lateral Water-Movement in the Sediments of a New England Salt-Marsh. Water Resources Research 24, 2077-2085. 10.1029/WR024i012p02077

O'Connor, M.T., Moffett, K.B., 2015. Groundwater dynamics and surface water-groundwater interactions in a prograding delta island, Louisiana, USA. Journal of Hydrology 524, 15-29. 10.1016/j.jhydrol.2015.02.017

Oosterlee, L., Cox, T.J.S., Vandenbruwaene, W., Maris, T., Temmerman, S., Meire, P., 2017. Tidal Marsh Restoration Design Affects Feedbacks Between Inundation and Elevation Change. Estuaries and Coasts. 10.1007/s12237-017-0314-2

Portnoy, J.W., 1999. Salt marsh diking and restoration: Biogeochemical implications of altered wetland hydrology. Environmental Management 24, 111-120. 10.1007/s002679900219

R Development Core Team, 2022. R: A Language and Environment for Statistical Computing. R Foundation for Statistical Computing, Vienna, Austria.

Schmitz, A., Harrison, J.F., 2004. Hypoxic tolerance in air-breathing invertebrates. Respiratory Physiology & Neurobiology 141, 229-242. 10.1016/j.resp.2003.12.004

Sloey, T.M., Hester, M.W., 2016. Interactions between soil physicochemistry and belowground biomass production in a freshwater tidal marsh. Plant and Soil 401, 397-408. 10.1007/s11104-015-2760-6

Soille, P., 1999. Morphological Image Analysis. Springer-Verlag, Berlin, Heidelberg, New York.

Spencer, K.L., Carr, S.J., Diggens, L.M., Tempest, J.A., Morris, M.A., Harvey, G.L., 2017. The impact of pre-restoration land-use and disturbance on sediment structure, hydrology and the sediment geochemical environment in restored saltmarshes. Science of the Total Environment 587, 47-58. 10.1016/j.scitotenv.2016.11.032

Spencer, K.L., Cundy, A.B., Davies-Hearn, S., Hughes, R., Turner, S., MacLeod, C.L., 2008. Physicochemical changes in sediments at Orplands Farm, Essex, UK following 8 years of managed realignment. Estuarine Coastal and Shelf Science 76, 608-619. 10.1016/j.ecss.2007.07.029

Struyf, E., Temmerman, S., Meire, P., 2007. Dynamics of biogenic Si in freshwater tidal marshes: Si regeneration and retention in marsh sediments (Scheldt estuary). Biogeochemistry 82, 41-53. 10.1007/s10533-006-9051-5

Susilo, A., Ridd, P.V., 2005. The bulk hydraulic conductivity of mangrove soil perforated with animal burrows. Wetlands Ecology and Management 13, 123-133. 10.1007/s11273-004-8324-9

Tempest, J.A., Harvey, G.L., Spencer, K.L., 2015. Modified sediments and subsurface hydrology in natural and recreated salt marshes and implications for delivery of ecosystem services. Hydrological Processes 29, 2346-2357. 10.1002/hyp.10368

Udden, J.A., 1914. Mechanical composition of clastic sediments. Geological Society of America Bulletin 25, 655-744. 10.1130/GSAB-25-655

Ursino, N., Silvestri, S., Marani, M., 2004. Subsurface flow and vegetation patterns

in tidal environments. Water Resources Research 40. 10.1029/2003wr002702

Vandenbruwaene, W., Maris, T., Cox, T.J.S., Cahoon, D.R., Meire, P., Temmerman, S., 2011. Sedimentation and response to sea-level rise of a restored marsh with reduced tidal exchange: Comparison with a natural tidal marsh. Geomorphology 130, 115-126. 10.1016/j.geomorph.2011.03.004

Vandenbruwaene, W., Meire, P., Temmerman, S., 2012. Formation and evolution of a tidal channel network within a constructed tidal marsh. Geomorphology 151, 114-125. 10.1016/j.geomorph.2012.01.022

Vlassenbroeck, J., Dierick, M., Masschaele, B., Cnudde, V., Hoorebeke, L., Jacobs, P., 2007. Software tools for quantification of X-ray microtomography. Nuclear Instruments & Methods in Physics Research Section a-Accelerators Spectrometers Detectors and Associated Equipment 580, 442-445. 10.1016/j.nima.2007.05.073

Waterinfo, 2022. Neerslag, droogte, getijden en overstromingen, Vlaamse Milieumaatschappij, Waterbouwkundig Laboratorium, Maritieme Dienstverlening & Kust, De Vlaamse Waterweg.

Wentworth, C.K., 1922. A scale of grade and class terms for clastic sediments. The Journal of Geology 30, 377-392. 10.1086/622910

Wilson, A.M., Evans, T., Moore, W., Schutte, C.A., Joye, S.B., Hughes, A.H., Anderson, J.L., 2015. Groundwater controls ecological zonation of salt marsh macrophytes. Ecology 96, 840-849. 10.1890/13-2183.1

Wilson, A.M., Gardner, L.R., 2006. Tidally driven groundwater flow and solute exchange in a marsh: Numerical simulations. Water Resources Research 42. 10.1029/2005wr004302

Wolters, M., Garbutt, A., Bakker, J.P., 2005. Salt-marsh restoration: evaluating the success of de-embankments in north-west Europe. Biological Conservation 123, 249-268. 10.1016/j.biocon.2004.11.013

Xia, Y.Q., Li, H.L., 2012. A combined field and modeling study of groundwater flow in a tidal marsh. Hydrology and Earth System Sciences 16, 741-759. 10.5194/hess-16-741-2012

Xin, P., Gibbes, B., Li, L., Song, Z.Y., Lockington, D., 2010. Soil saturation index of salt marshes subjected to spring-neap tides: a new variable for describing marsh soil aeration condition. Hydrological Processes 24, 2564-2577. 10.1002/hyp.7670

Xin, P., Jin, G.Q., Li, L., Barry, D.A., 2009. Effects of crab burrows on pore water flows in salt marshes. Advances in Water Resources 32, 439-449. 10.1016/j.advwatres.2008.12.008

Xin, P., Kong, J., Li, L., Barry, D.A., 2013. Modelling of groundwater-vegetation interactions in a tidal marsh. Advances in Water Resources 57, 52-68. 10.1016/j.advwatres.2013.04.005

Xin, P., Yu, X.Y., Lu, C.H., Li, L., 2016. Effects of macro-pores on water flow in coastal subsurface drainage systems. Advances in Water Resources 87, 56-67. 10.1016/j.advwatres.2015.11.007

Xin, P., Yuan, L.R., Li, L., Barry, D.A., 2011. Tidally driven multiscale pore water flow in a creek-marsh system. Water Resources Research 47. 10.1029/2010wr010110

Xin, P., Zhou, T.Z., Lu, C.H., Shen, C.J., Zhang, C.M., D'Alpaos, A., Li, L., 2017. Combined effects of tides, evaporation and rainfall on the soil conditions in an intertidal creek-marsh system. Advances in Water Resources 103, 1-15. 10.1016/j.advwatres.2017.02.014

Yelverton, G.F., Hackney, C.T., 1986. Flux of Dissolved Organic-Carbon and Pore Water through the Substrate of a *Spartina alterniflora* Marsh in North-Carolina. Estuarine Coastal and Shelf Science 22, 255-267. 10.1016/0272-7714(86)90116-2

3

Historical soil compaction impairs biogeochemical cycling in restored tidal marshes through reduced groundwater dynamics

Niels Van Putte, Stijn Temmerman, Piet Seuntjens, Goedele Verreydt, Timothy De Kleyn, Dimitri Van Pelt, Patrick Meire

3.1 Abstract

Tidal marshes are generally restored on formerly embanked agricultural land where historical soil compaction often impairs the extent of tidally induced groundwater dynamics and soil aeration patterns after restoration. Since groundwater dynamics are crucial for biogeochemical cycling (e.g. removal of nitrogen, retention of phosphorus and delivery of dissolved silica), we hypothesized that soil aeration patterns can be linked to porewater nutrient concentrations and that these differ between natural and restored tidal marshes.

We studied soil hydraulic properties and groundwater dynamics in function of depth and distance from the nearest tidal creek in a natural and a restored freshwater tidal marsh in the Scheldt estuary, Belgium. We measured monthly porewater nutrient concentrations over a depth profile during one year using porewater equilibrators and linked these concentrations to the calculated soil saturation index (the proportion of time the soil is saturated at a certain depth).

The aerated zone generally extended over a deeper soil profile in the natural marsh compared to the restored marsh. The soil saturation index was negatively correlated with nitrate and positively correlated with ammonium concentrations. Concentrations of phosphate and dissolved iron were significantly positively correlated to the soil saturation index, suggesting retention of phosphate on iron oxides in well aerated zones, which are more abundant in the natural marsh compared to the restored marsh. Dissolved silica porewater concentrations were not correlated to the soil saturation index. Both the depth profile of soil hydraulic properties and soil saturation were found to be very site specific, even within the same marsh, suggesting the need for a pre-restoration assessment of soil hydraulic properties and stratigraphy to determine where and which design measures are required to optimize nutrient cycling in newly restored tidal marshes.

3.2   Introduction

Tidal marshes, which naturally occur along estuaries, are highly valued for the delivery of ecosystem services, such as the regulation of water quality through filtering, especially in anthropogenically impacted estuaries with excessive loads of nutrients such as nitrogen and phosphorous (e.g. Barbier et al., 2011). Soil-groundwater interactions in tidal marshes play a crucial role in this water quality regulation service (e.g. Barbier et al., 2011; Chmura et al., 2003; Teuchies et al., 2013). In tidal wetlands, groundwater dynamics are mostly tidally driven (Caetano et al., 2012; Wilson and Morris, 2012; Xin et al., 2022). During high tide, a part of the flooding water infiltrates into the soil surface, raising the groundwater level. During ebb tide, the infiltrated groundwater flows through the subsurface in the direction of tidal creeks, which typically occur in tidal marshes (e.g. Gardner, 2005b). When groundwater levels decline during ebb tides, air enters the larger soil pores an aerates the soil, creating oxic conditions as opposed to the reduced conditions that continue to prevail deeper down the soil profile (Howes et al., 1981). This depth-dependent difference in redox conditions, and especially the alternating aerated and saturated state in the vertical soil compartment in which groundwater level fluctuations occur, give rise to profound impacts on biogeochemical reactions (e.g. Caetano et al., 2012; Megonigal and Neubauer, 2019; Wolf et al., 2011).

In the past centuries, natural tidal marsh area drastically declined throughout the world, due to large scale land reclamation for urbanization, industry and agriculture, by building of dikes to prevent tidal flooding and by soil drainage (Gedan et al., 2009). More recently, however, there is an increasing demand for tidal marsh restoration for biodiversity conservation and delivery of ecosystem services in the framework of several legislations such as the EU Habitats Directive and Water Framework Directive (European Parliament and the Council of the European Union, 1992, 2000). Tidal marsh restoration is mostly executed on formerly reclaimed agricultural land. The former agricultural land use is often paired with negative ecological effects. The use of artificial fertilizers caused an excessive input of nutrients in estuaries (Peng et al., 2016; Xin et al., 2022). The excavation of artificial ditches caused excessive soil drainage, resulting in mineralization of organic matter, soil consolidation and reduction of soil porosity. In addition, trampling by cattle and/or the use of heavy farming equipment often lead to further soil compaction and reduction of soil porosity (Sloey and Hester, 2016; Spencer et al., 2017; Van Putte et al., 2020 (Chapter 2)).

Tidal marsh restoration can be achieved using several methods, such as managed realignment (e.g. Esteves, 2014) or controlled reduced tide (CRT) systems (e.g. Oosterlee et al., 2017). In both methods, a new dike is built further landward and an opening is made in the original dike, so that the area is again subjected to the tides. Although many marsh restoration projects can be considered successful, it often requires decades of sediment accretion and ecosystem development before the delivery of ecosystem services approaches levels as observed in natural tidal marshes (Ballantine et al., 2012; Brooks et al., 2015; Mossman et al., 2012; Spencer et al., 2017). The altered soil structure resulting from the historical wetland reclamation and agricultural practices has several implications

for the new tidal marsh development. In this study, we focus on effects of the altered soil structure on groundwater level fluctuations and the interaction with nutrient cycling. Since nutrient cycling in tidal marsh soils is governed by groundwater dynamics, impaired groundwater flow is expected to negatively impact the contribution of newly restored tidal marshes to water quality improvement.

The depth to which groundwater level fluctuations occur is inherently depending on (i) the time in between consecutive high tides that flood the marsh, (ii) the distance to and the depth of nearby tidal channels and (iii) the soil structure and soil hydraulic properties, in particular the saturated hydraulic conductivity (K_s), which depends on the porosity and pore size distribution of the soil (Dlapa et al., 2020). In natural tidal marshes, the soil consists of sediment that is accreted by deposition of suspended sediments supplied by water flooding the marshes at high tides, intermixed with both allochthonous and autochthonous organic matter such as plant debris (Van de Broek et al., 2018). When this organic matter decomposes, it creates void spaces (macropores) that greatly increase the hydraulic conductivity of the soil (Tempest et al., 2015; Van Putte et al., 2020 (Chapter 2); Xin et al., 2016). In addition, tidal marshes are typically intersected by a dense creek network that forms a flow conduit for both surface and subsurface drainage (e.g. Kearney and Fagherazzi, 2016). As a result, both high (macro)porosity of the soil and high creek density promote soil-groundwater interactions and enhance nutrient cycling.

The contribution of tidal marshes to nutrient cycling is crucial for maintaining a good water quality in estuaries and coastal zones, as these are often impacted by anthropogenic nutrient loads. Here, we focus on the effect of groundwater level fluctuations and associated soil aeration on porewater concentrations of nitrogen (N), phosphorus (P) and dissolved silica (DSi). We focus on these three nutrients as their ratio is crucial to sustain healthy phytoplankton communities, which are major primary producers at the base of estuarine food webs (Lancelot, 1995; Struyf et al., 2005b). In estuaries with high anthropogenic inputs of N and P, limitation of DSi can cause a shift from diatom dominated phytoplankton communities to other phytoplankton communities, often resulting in eutrophication problems. When groundwater flows through a tidal marsh soil before seeping out of creek banks, tidal marsh soils can remove nitrogen from the groundwater by coupled nitrification and denitrification (Peng et al., 2016). These processes take place under aerobic and anaerobic conditions, respectively (Thompson et al., 1995). Therefore, we expect that the alternating presence and extent of both anoxic and oxic zones, which is governed by groundwater dynamics, controls the capacity of a tidal marsh to remove nitrogen. Soil aeration also affects P retention in marsh soils, as dissolved phosphate sorbs to iron oxides under aerobic conditions, as opposed to anaerobic conditions where P remains in solution (Chambers and Odum, 1990; Megonigal and Neubauer, 2019). Tidal marsh soils also play an important role in the recycling of silica as particulate biogenic silica (BSi) from plant debris and dead diatoms dissolves in porewater and seeps out of the creek banks through advective transport governed by groundwater flow (Struyf et al., 2006). As

such, it becomes again available as dissolved silica (DSi) for estuarine primary production by planktonic diatoms.

Although many studies described porewater nutrient concentration profiles in tidal wetlands (e.g. Caetano et al., 2012; Neubauer et al., 2005; Thompson et al., 1995; Williams et al., 2014), our contribution is to link measured nutrient concentration profiles to soil aeration patterns governed by groundwater dynamics. We hypothesize that soil aeration patterns differ between a natural and a restored tidal marsh due to altered groundwater dynamics as a result of historical agricultural soil compaction in the restored marsh (Tempest et al., 2015; Van Putte et al., 2020 (Chapter 2)). Furthermore, we hypothesize that these aeration patterns can be linked to porewater nutrient concentrations, and we determine at which depth along the soil profile (i) the main form of dissolved nitrogen (nitrate vs. ammonium) will occur in the porewater, (ii) phosphate is retained and (iii) dissolved silica concentrations are highest. These insights are helpful in the design of new tidal marsh restoration projects to assess the effects of certain design measures (e.g. creek excavation or soil amendments) that alter soil aeration patterns, on biogeochemical cycling.

3.3   Methods

3.3.1   Study sites

Field data was acquired in the natural marsh 'De Notelaer' (51° 07' 08" N, 4° 16' 21" E) and the restored marsh 'Lippenbroek' (51° 05' 06" N, 4° 10' 17" E), both located along the freshwater part of the Scheldt estuary in Belgium (Figure 3.1a). The marsh sites are experiencing a semidiurnal tide with an average tidal range of 5.40 m (Meire et al., 2005). The natural marsh (Figure 3.1c) is characterized by two distinct zones. The older zone of the marsh was used as pasture until at least the 1950's. By 1965, willow trees (*Salix* sp.) were planted for the cultivation of willow withies (Temmerman et al., 2003). Currently, the old marsh is still covered by willow vegetation, which is also the natural climax successional stage of the freshwater tidal marshes along the Scheldt estuary. The younger zones (developed from tidal mudflat to marsh since the 1940's) are mostly covered with reed (*Phragmites australis*).

The restored marsh (Figure 3.1b) has been an embanked agricultural area since large scale land reclamations in the 13th century. In the last decades before marsh restoration, the area was mainly used as farmland, pastures and poplar (*Populus* x *canadensis*) plantations. It was converted to a tidal wetland in 2006 using the CRT (controlled reduced tide) principle through which water from the estuary enters and leaves the area through a separate inlet – and outlet sluice (Cox et al., 2006; Oosterlee et al., 2017). The resulting tidal inundation regime in the restored marsh is similar to adjacent natural marshes in terms of inundation depth and frequency, but has an increased inundation time with a stagnant phase of approximately 2 hours. During its agricultural phase, the soil on which the restored marsh developed, was heavily compacted. Since the restoration in 2006, between 0 cm and 100

cm (depending on the location) of tidally deposited sediment has accreted on top of this compact agricultural soil.
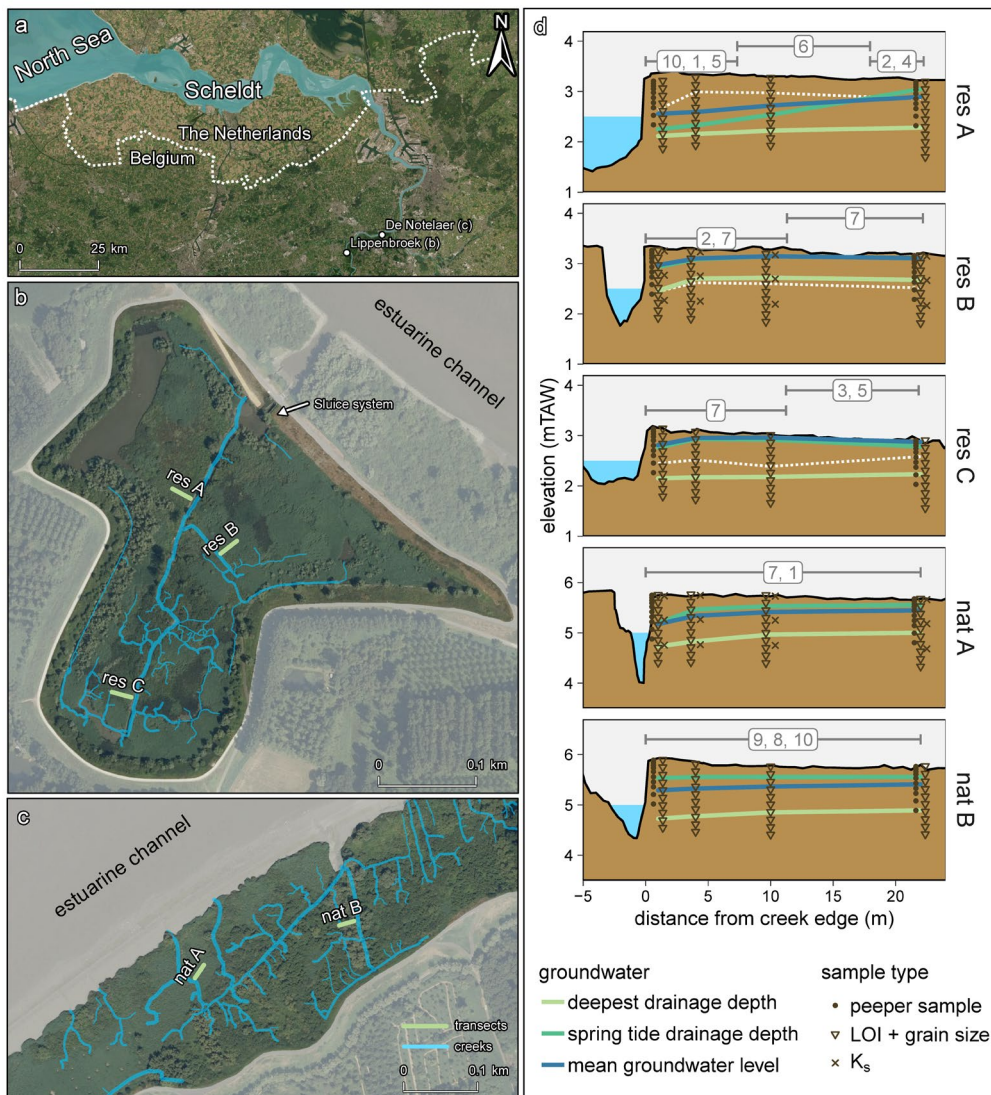

Figure 3.1: (a): Overview of the location of the study areas within the Scheldt estuary. The estuary is shaded in blue. (b): Location of the study transects in the restored marsh Lippenbroek. (c): Location of the study transects in the natural marsh De Notelaer. Tidal marshes are shown in bright colors, whereas the estuarine channel, mudflats and terrestrial habitats are shown in faded colors. (d): Cross-sectional view of the study transects indicated in b and c. White dotted lines in the restored marsh transects indicate the depth of the transition between the relict compact agricultural soil and the layer of newly deposited sediment. Spring tide drainage depth is defined as the average groundwater drainage depth in between successive high tides flooding the marshes (see text for further explanation). Grey horizontal bars denote the extent of plant species on the transects with the number corresponding to the respective species in the label: (1): *Convolvulus sepium*, (2): *Glyceria maxima*, (3): *Lythrum salicaria*, (4): *Mentha aquatica*, (5): *Persicaria hydropiper*, (6): *Phalaris arundinacea*, (7): *Phragmites australis*, (8): *Poa trivialis*, (9): *Salix* sp., (10): *Urtica dioica.* Map source for a: Esri, DigitalGlobe, GeoEye, Earthstar Geographics, CNES/Airbus DS, USDA, USGS, AeroGrid, IGN and the GIS User Community; map source for b and c: GDI-Vlaanderen.

3.3.2   Transects

In both sites, we established 22 m long transects perpendicular to a main tidal creek (2 transects in the natural marsh and 3 transects in the restored marsh, Figure 3.1d). We assume that groundwater mainly flows towards the nearest tidal creek along such transects perpendicular to a tidal creek (Gardner, 2005a), although some deviation from this flow direction may not be excluded (Xin et al., 2011). The locations of the transects were selected to obtain variation across the transects in vegetation type, marsh platform elevation and thickness of the newly deposited sediment layer in the restored marsh (Figure 3.1d). As elaborated in more detail in the next paragraphs, measurements of groundwater dynamics, basic soil properties (gravimetric soil moisture content, median grain size, loss on ignition (LOI)) and porewater nutrient concentrations were performed on all transects, on sampling locations as indicated in Figure 3.1d. A detailed study of the soil hydraulic properties (bulk density and saturated hydraulic conductivity (K_s)) was only performed on one transect in each marsh, further referred to as 'focus transects'. Transects nat A and res B (Figure 3.1) were chosen as focus transects due to their resemblance in dominant vegetation type (*Phragmites australis*) and creek dimensions.

On each transect, a measuring location was defined at 1 m, 4 m, 10 m and 22 m from the creek edge. The distance between subsequent measuring locations increases because larger differences in groundwater dynamics and soil properties are expected in the close vicinity of the creeks as compared to the marsh interior (Gardner, 2005a; Van Putte et al., 2020 (Chapter 2)). We always used a wooden bench to access the measuring locations in order to prevent soil disturbance by trampling.

3.3.3   Groundwater dynamics

We placed a 41 mm inner diameter PVC (polyvinylchloride) groundwater monitoring well at each measuring location. These wells were installed up to a depth of 1.50 m below the soil surface and were slotted over the entire subsurface part except from the upper 5 – 10 cm just below the surface, where a bentonite plug was installed to prevent surface water infiltration. The wells emerged 1.70 m above the soil surface to prevent surface water from entering the wells from the top. The pressure head in the monitoring wells was logged every minute with a pressure transducer (Rugged Troll 100, In Situ Inc.). In both study areas, an extra pressure transducer was installed above the surface to log the atmospheric pressure. During every field visit, a manual measurement of the groundwater level was taken as a control for the logged data.

3.3.4   Transect mapping and soil sampling

The elevation profile of the transects and creeks, and the elevation of the wells was measured with a total station (SET510k, Sokkia Co. Ltd) where reference points were available, and with an RTK-dGPS (Trimble R8s, Trimble Inc.) in the other case. At each measuring location, three soil cores were taken with a gouge auger until 1.4 m depth. By feeling manually where the soil structure changed over the depth, we estimated the depth of the transition between the newly deposited sediment (which was easy to deform by

hand) and the compact agricultural soil (very difficult to deform) in the restored marsh. The soil cores were then subdivided into subsamples in 5 cm intervals. These samples were later analyzed for grain size distribution, gravimetric moisture content and loss on ignition (LOI). On the focus transects (Figure 3.1d) undisturbed triplicate soil samples were taken at three depths (2 – 7 cm, 50 – 55 cm and 100 – 105 cm) at every measurement location. A borehole was made to the desired depth with an Edelman auger and the bottom of the hole was leveled using a Riverside auger. An undisturbed soil sample of 100 cm^3 was then taken using a sample ring kit with open ring holder. These samples were later used to determine the saturated hydraulic conductivity (K_s). Samples were taken at 2 m from the monitoring wells (but at the same distance from the creek) to avoid disturbance of groundwater dynamics measured in the wells. For the same reason, boreholes were refilled with bentonite clay afterwards. For reference, additional soil samples were taken to determine the P, N, C and Si content in the soil at different depths. These results and the respective methods are presented in Supplement S3.1 and Figure S3.1.

3.3.5 Porewater chemistry sampling

At 1 m (near creek zone) and 22 m (marsh interior) from the creek edge, we installed a porewater equilibrator based on dialysis sampling (also known as and further referred to as 'peeper'). The working of these peepers is based on the principle first described by Hesslein (1976) and the design was modified to be reusable by Jacobs (2002). The peepers consist of an 8 cm diameter PVC (polyvinylchloride) pipe containing 10 open compartments placed at depths up to 0.90 m with increasing intervals at increasing depths below the soil surface (Figure 3.1d). The compartments are separated from the surrounding soil by a PVDF (polyvinylidene fluoride) microfiltration membrane with a maze size of 0.2 µm (NADIR® MV020 T, MICRODYN-NADIR) that was attached to the PVC pipe with a solvent free two-component adhesive. The principle of this peeper is that dissolved nutrients (listed below) in the soil pore water surrounding the peeper are exchanged through the membrane until the water in the peeper compartments is in osmotic equilibrium with the surrounding soil pore water. Every compartment of the peepers is connected to two thin tubes that both extend above the soil surface and are closed by a plastic valve with luer-lock connection. Via one of the tubes, the compartments were filled with demineralized deoxygenated (by means of purging with dinitrogen gas (N_2)) water. After one month, water was removed from the compartments by injecting N_2 in one of the tubes with a syringe, and simultaneously sucking water from the compartment through the second tube with another syringe. There is no general consensus about the needed equilibration time for porewater equilibrators. Values in literature vary from 3 days to 1 month (Bally et al., 2005). Therefore, an equilibration time of 1 month was deemed sufficient in our study. The first 5 mL of water was discarded as this water was in the tubing and not in contact with the soil. A maximum of 60 mL of water was extracted from the compartments. Although the small pore size of the membrane does not allow suspended solids to enter the compartments, some samples contained small flakes of unknown precipitate; in such case, water samples were filtered through 0.45 µm

CHROMAFIL® PET filters. Samples were transferred into clean 30 mL vials, pre-acidified with 1.5 mL 69% HNO_3 for analyses of PO_4, SO_4, Ca, K, Mg, Na, Fe, Zn, Mn and Si and 3 mL H_2SO_4 for analyses of NH_4, NO_2, NO_3 and Cl, respectively. Samples were stored cool until analysis. After the extraction, the compartments were refilled and this process was repeated every month for 13 months from February 2019 to March 2020. We always performed the sampling around spring tide. In compartments located in the variably saturated zone, there was sometimes insufficient water to extract 60 mL. In that case, the amount of water that could be extracted was equally divided over the vials.

3.3.6 Lab analyses

3.3.6.1 Soil physicochemical properties

1 g of the soil samples was transferred to an Erlenmeyer flask. After treatment with HCl and H_2O_2 to remove organic matter, the median grain size was assessed with a Mastersizer 2000 (Malvern Panalytical) based on laser diffraction. The gravimetric moisture content was determined after drying the samples at 105 °C. The loss on ignition (LOI) was used as a proxy for the organic matter content. We followed the protocol of Heiri et al. (2001) with a muffle furnace temperature of 550 °C during at least 4 hours.

3.3.6.2 Soil hydraulic properties

The saturated hydraulic conductivity (K_s) is the most important soil hydraulic parameter determining groundwater flow. To measure K_s, soil samples were fully saturated and then placed in a laboratory permeameter. Most samples were measured using the constant head method (Eijkelkamp Agrisearch Equipments, 2013). Samples with a K_s that was too low to accurately measure using the constant head method, were measured using the falling head method. For the latter, a burette inside a rubber stop cock was inserted in a sample holder. A positive pressure head was applied on the samples by filling the burette with water. While the water seeped through the samples, we noted the decline in pressure head over time. K_s was then calculated using Darcy's law (Darcy, 1856) and exponential regression of the pressure head in function of time. After these analyses, the samples were dried and their dry bulk density was determined.

3.3.6.3 Analyses of nutrient concentrations

Analyses of NH_4, NO_2, NO_3 and Cl were performed on a colorimetric segmented flow analyzer (SAN++, Skalar, Breda, The Netherlands). PO_4, SO_4, Ca, K, Mg, Na, Fe, Zn, Mn and Si were analyzed on an ICP-OES spectrometer (iCAP 6000 series, thermos Scientific, Camebridge, UK). Monthly river water concentrations of NO_3, NH_4, PO_4, Fe, Si and SO_4 were provided by the OMES monitoring program (Maris et al., 2020) and analyzed using the same methods as for the pore water samples. In this study, we focus on porewater nutrient concentrations of NO_3, NH_4, PO_4, Fe and DSi. Other measured elements are not discussed but are presented in Figure S3.3 to Figure S3.11.

3.3.7   Data analyses

Groundwater level data from February 2019 to March 2020 were used to calculate the soil saturation index (SSI) for every measuring location over a depth profile to 1 m depth. The SSI is defined as the proportion of a tidal period that the groundwater level is above a respective depth (i.e. the proportion of time that the soil is saturated). This index was defined by Xin et al. (2010) to describe the soil aeration conditions providing more information than the commonly used 'hydroperiod', i.e. the proportion of a tidal period the marsh is inundated, which only takes into account tidal inundation characteristics and ignores subsurface drainage. For every measuring location, we also determined the lowest groundwater level that occurred in between consecutive tides that flood the marsh platform (which occur around spring tide). The average of these values (for the entire measuring timespan) is defined as the 'spring tide drainage depth'.

Nutrient concentrations were compared with the SSI using a Spearman correlation test in R (R Core Team, 2021). Since we were not primarily interested in seasonal variation, but rather in the overall effect of SSI on nutrient concentrations, the temporal effect was removed separately for every sampling location with a cubic spline regression, using the residual values of this regression in the correlation test.

3.4   Results

Physical soil properties are a main factor in determining the extent of groundwater dynamics and soil aeration. In Figure 3.2, we give an overview of the soil properties as a function of depth for the focus transects in both areas. In the nat A transect, physical soil properties vary with an increasing distance from the creek. The median grain size and bulk density decrease with an increasing distance from the creek edge, whereas the LOI and gravimetric moisture content increase. The difference in soil properties in function of the distance from the creek mostly decreases with an increasing depth beneath the soil surface. K_s is highly variable, but without a consistent relation with depth or distance from the creek.

On transect res B in the restored marsh, the soil properties in the upper layer of tidally deposited sediment (above the dotted line in Figure 3.2) are similar to the natural marsh. At the transition to the historically compacted subsoil, however, a sharp transition is visible. Here, the LOI and the gravimetric moisture content are lower compared to the upper layer, and the bulk density is more than double that of the upper layer. Compared to the upper layer, the K_s of the compacted subsoil is several orders of magnitude lower. The res C transect shows a comparable pattern, but with a shallower depth to the compact subsoil (Figure S3.2). The res A transect shows a remarkably different soil stratigraphy. Here the transition between the soil layers is less pronounced. Starting at around 1 m below the soil surface, a sharp increase in median grain size is apparent (Figure S3.2). Below 1 m depth, we found a layer of almost pure sand below the compact agricultural soil, which we did not find in the other transects at those depths.
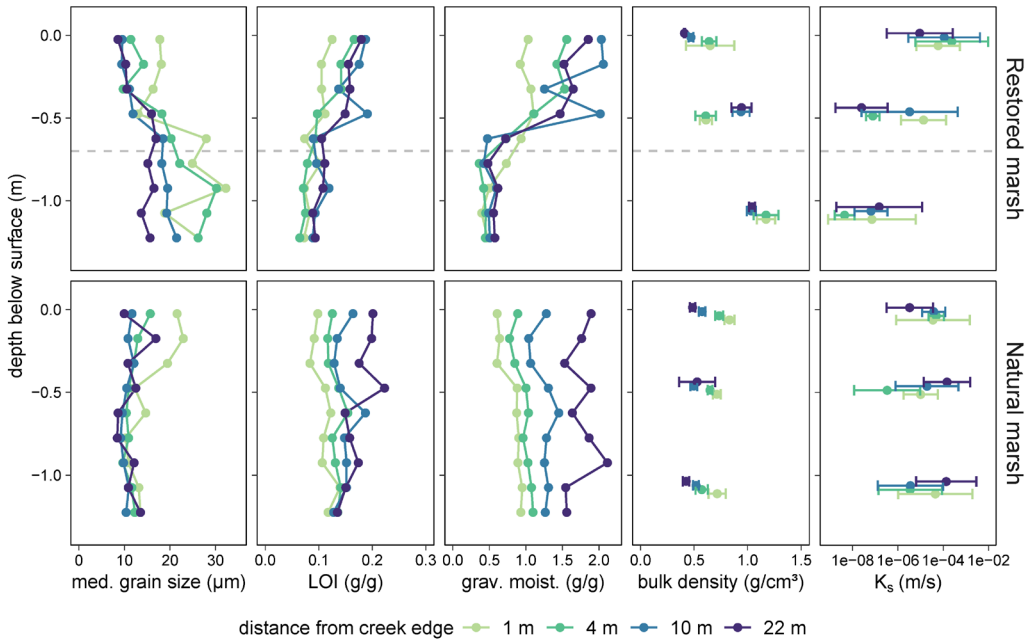
Figure 3.2: Soil properties as a function of the depth below the soil surface for the focus transects (res B and nat A) in the restored marsh (upper panels) and the natural marsh (lower panels), respectively. Different colors refer to different measuring locations with increasing distance from the creek edge. For the restored marsh, the dotted grey horizontal line indicates the depth of the transition between the layer of newly deposited sediment on top of the historical agricultural compact soil. Bulk density values are presented as mean ± standard deviation (n = 4). Values for saturated hydraulic conductivity (K_s) are given as the geometric mean with the error bars denoting the distance between the geometric mean divided by and multiplied by the geometric standard deviation, respectively. Note the log scale in the x-axis of the K_s plot.

3.4.1   Groundwater dynamics and soil saturation index (SSI)

The SSI is calculated based on groundwater level fluctuations. At the soil surface, the SSI is higher in the restored marsh as compared to the natural marsh at all locations. At every transect in both areas, the variably saturated zone (where SSI < 1) extends to a larger depth close to the creek compared to the marsh interior (Figure 3.3). This difference with distance from the creek is most apparent in the restored marsh at the lower elevated transects res B and res C, where a very distinct transition between the upper deposited layer and the compact relict soil is present (Figure S3.2). On the res A transect, the deepest drainage depth (and thus the extent of the variably saturated zone) is much larger, also in the marsh interior. At this location, groundwater level fluctuations extend much further into the marsh interior, even during non-inundating tides. In the natural tidal marsh, the top soil has a very low SSI due to the low hydroperiod (Figure 3.3). Because the transects in the natural marsh also have a (slightly) lower inundation frequency, the period around neap tide when the marsh platform is not inundated is longer. Therefore, groundwater levels decline towards a larger depth beneath the soil surface. As a result, in the natural tidal marsh, the mean groundwater level is deeper than the spring tide drainage depth (i.e. the mean drainage depth in between consecutive tides that flood the marsh platform

around spring tide), whereas in the restored marsh, the mean groundwater level mostly coincides or even exceeds the spring tide drainage depth (Figure 3.1d).
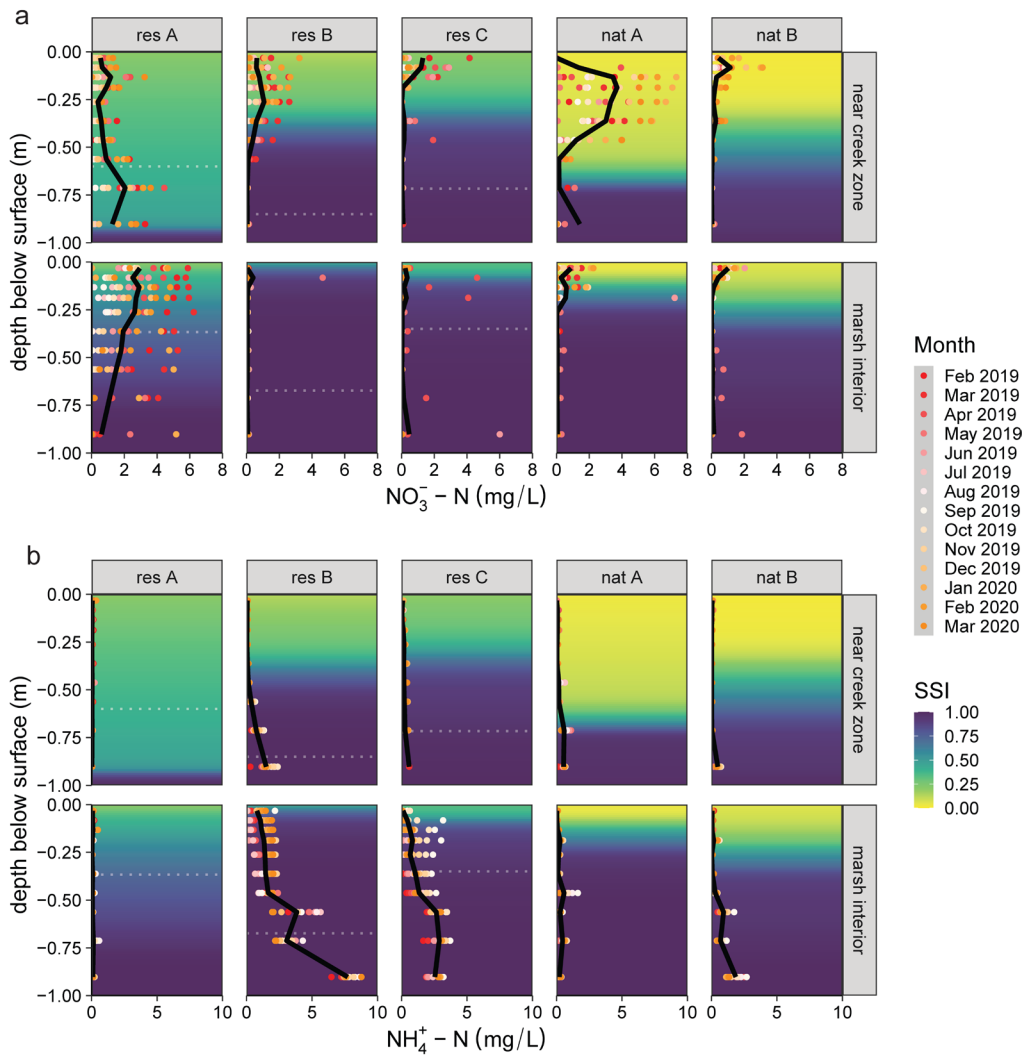

Figure 3.3: Porewater concentrations of (a) nitrate and (b) ammonium. Bullets indicate the individual monthly results and the black line represents the mean concentration. Background colors indicate the soil saturation index (SSI). Grey dotted lines represent the transition between the tidally deposited sediment layer and the underlying compact relict soil in the restored marsh. Near creek zone and marsh interior are 1 m and 22 m from the creek edge, respectively.

3.4.2   Porewater chemistry

3.4.2.1   Nitrogen

In the marsh porewater, nitrate concentrations are negatively correlated to the SSI (ρ = -0.21, p < 0.001). In the well aerated upper zone, NO_3 concentrations are in the same order of magnitude as the river water NO_3 concentrations and follow a similar pattern of higher concentrations in winter months compared to summer months (Figure 3.4, Figure 3.3a). In the marsh interior at transects res B and res C, the poorly drained soil is depleted of nitrate. Here, dissolved nitrogen is mostly present as ammonium, as concentrations of nitrite were always very low (on average $1.90 \cdot 10^{-3}$ mg/L, Figure S3.3). NH_4 concentrations are positively correlated with the SSI (ρ = 0.32, p < 0.001). In the compact subsoil of the res B and res C transects, concentrations of NH_4 greatly exceed the river water NH_4 concentrations (Figure 3.4, Figure 3.3b). In the marsh interior of the res B transect, high NH_4 concentrations occur even in the top soil several cm below the soil surface (Figure 3.3b). The highest concentration of NH_4 occurs at 90 cm depth in the marsh interior of the res B transect, where also the highest concentration of dissolved iron was observed (Figure 3.3b, Figure 3.5b).
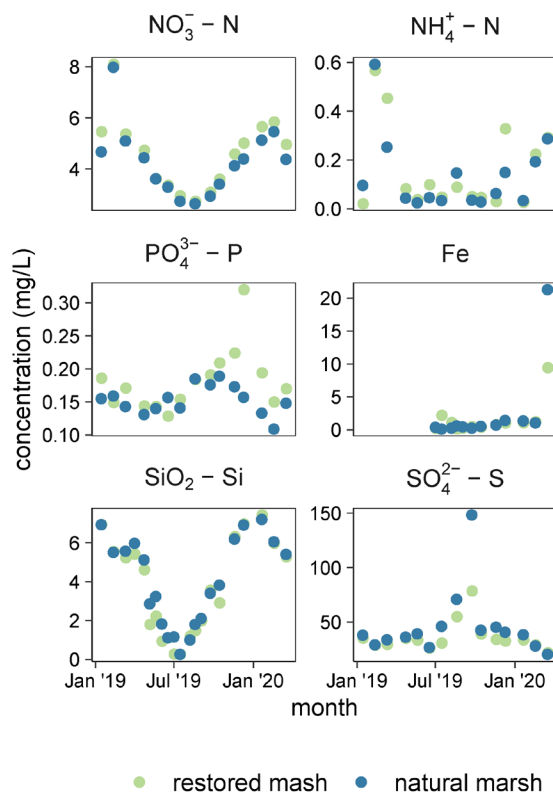

Figure 3.4: Concentration of nitrate, ammonium, phosphate, iron, silica and sulphate in the estuarine water near the natural and the restored marsh during the measuring period from January 2019 to March 2020. Data source: OMES (Maris et al., 2020)
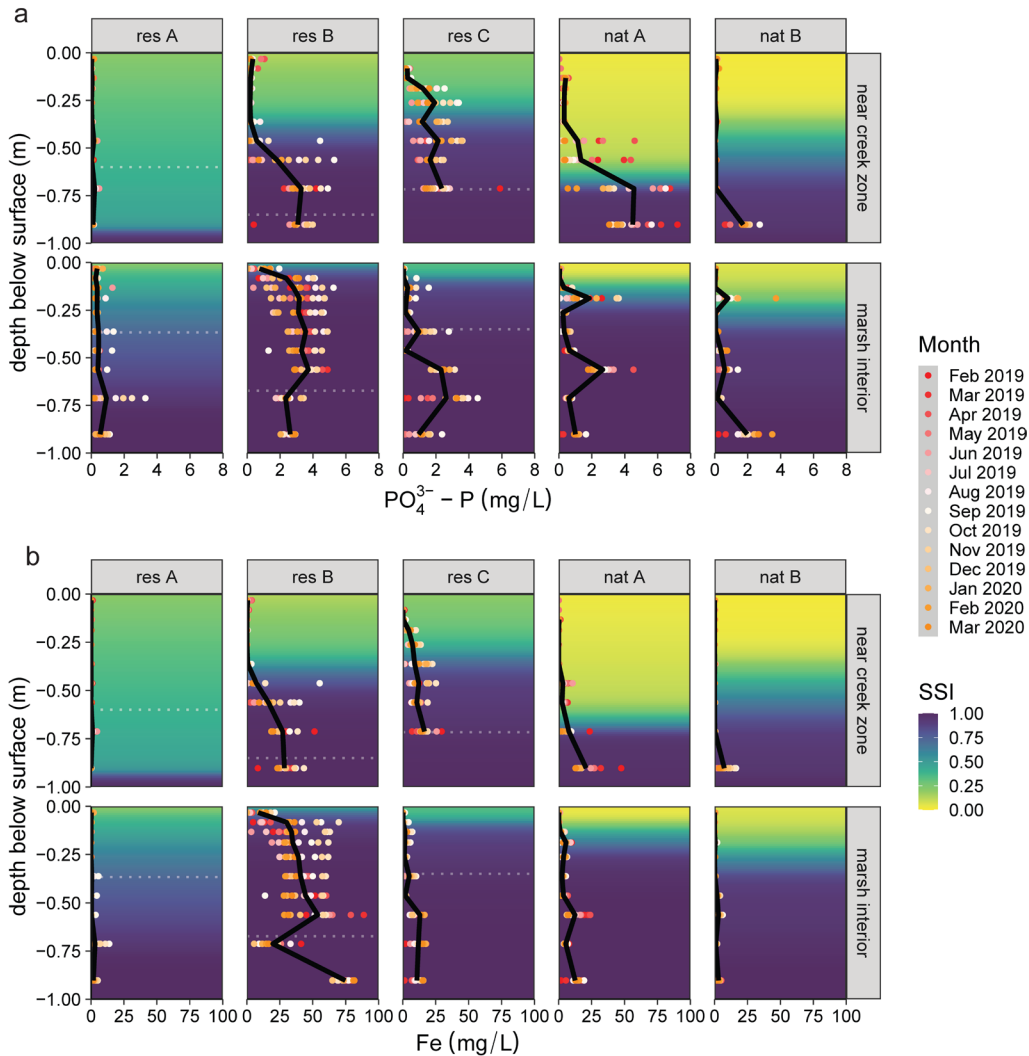
Figure 3.5: Porewater concentrations of (a) phosphate and (b) dissolved iron. Bullets indicate the individual monthly results and the black line represents the mean concentration. Background colors indicate the soil saturation index (SSI). Grey dotted lines represent the transition between the tidally deposited sediment layer and the underlying compact relict soil in the restored marsh. Near creek zone and marsh interior are 1 m and 22 m from the creek edge, respectively.

3.4.2.2   *Phosphorus*

The concentration of dissolved phosphate is strongly correlated with the SSI ($\rho = 0.43$, $p <$ 0.001). In the reduced, poorly aerated soil in both the natural and the restored marsh, concentrations of phosphate reach a multiple of river water concentrations, whereas concentrations in the well aerated top layer with a low SSI are lower (Figure 3.4, Figure 3.5a). The same applies to the concentration of dissolved iron, which is also strongly positively correlated to the SSI ($\rho = 0.44$, $p <$ 0.001). Fe concentrations in the saturated zone (where SSI = 1) display a mean value of 31.82 mg/L in the restored marsh and 8.34

mg/L in the natural marsh, whereas river water Fe concentrations are mostly below 2 mg/L (except for March 2020, Figure 3.4)

3.4.2.3 Dissolved silica

No significant correlation was found between the SSI and the concentration of dissolved silica in the porewater, when tested for all data points in general ($p = 0.439$). In the natural marsh, however, DSi concentrations are highest in the well aerated topsoil, which does not apply to the restored marsh (Figure 3.6). In the latter case, an increasing DSi concentration with an increasing depth is observed, irrespective of the SSI profile. Concerning soil biogenic silica (BSi) concentrations, no relationship with depth was observed (Table S3.1). Porewater DSi concentrations are on average higher in summer months compared to winter months, as opposed to the river water in which dissolved silica concentrations are always higher in winter months.
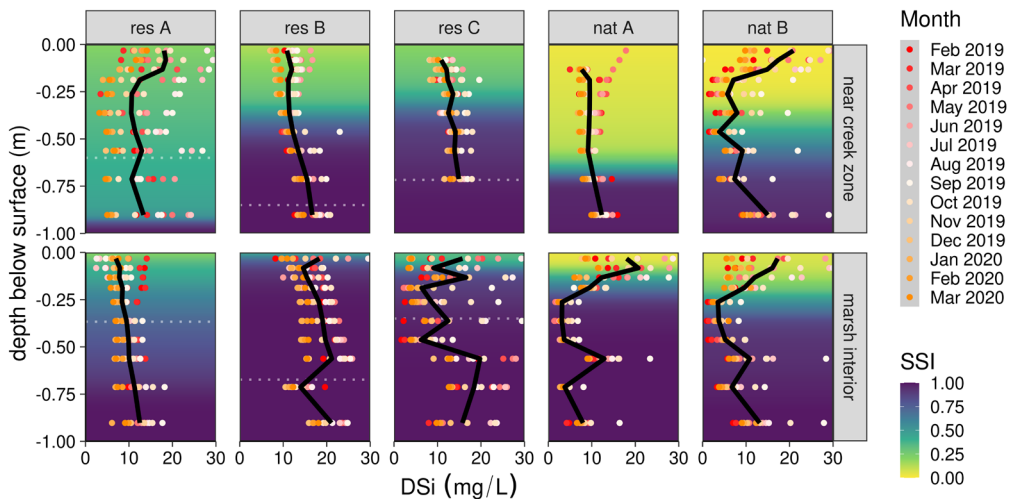

Figure 3.6: Porewater concentrations of dissolved silica. Bullets indicate the individual monthly results and the black line represents the mean concentration. Background colors indicate the soil saturation index (SSI). Grey dotted lines represent the transition between the tidally deposited sediment layer and the underlying compact relict soil in the restored marsh. Near creek zone and marsh interior are 1 m and 22 m from the creek edge, respectively.

3.5 Discussion

When tidal marshes are restored on formerly embanked agricultural land, groundwater dynamics in these newly restored tidal marshes are often restricted to a smaller portion of the soil depth profile as compared to natural tidal marshes, due to historical agricultural soil compaction (Spencer et al., 2017; Van Putte et al., 2020 (Chapter 2)) and the absence of a dense creek network in restored marshes (Chirol et al., 2015). Here we investigated the effect of these reduced groundwater dynamics on depth profiles of soil porewater concentrations of dissolved nutrients in a restored versus a natural tidal marsh. In this way, we gained insights into the effects of historical agricultural soil compaction on porewater nutrient dynamics and we discuss the implications for the associated water quality

improving function of restored tidal wetlands. In Figure 3.7, we present a conceptual schematic overview of our main findings with respect to the current literature. The insights gained in our study can be used to elaborate mitigation strategies for soil compaction (e.g. soil amendments) and to optimize the delivery of regulating ecosystem services (here water quality regulation) in future tidal marsh restoration projects.
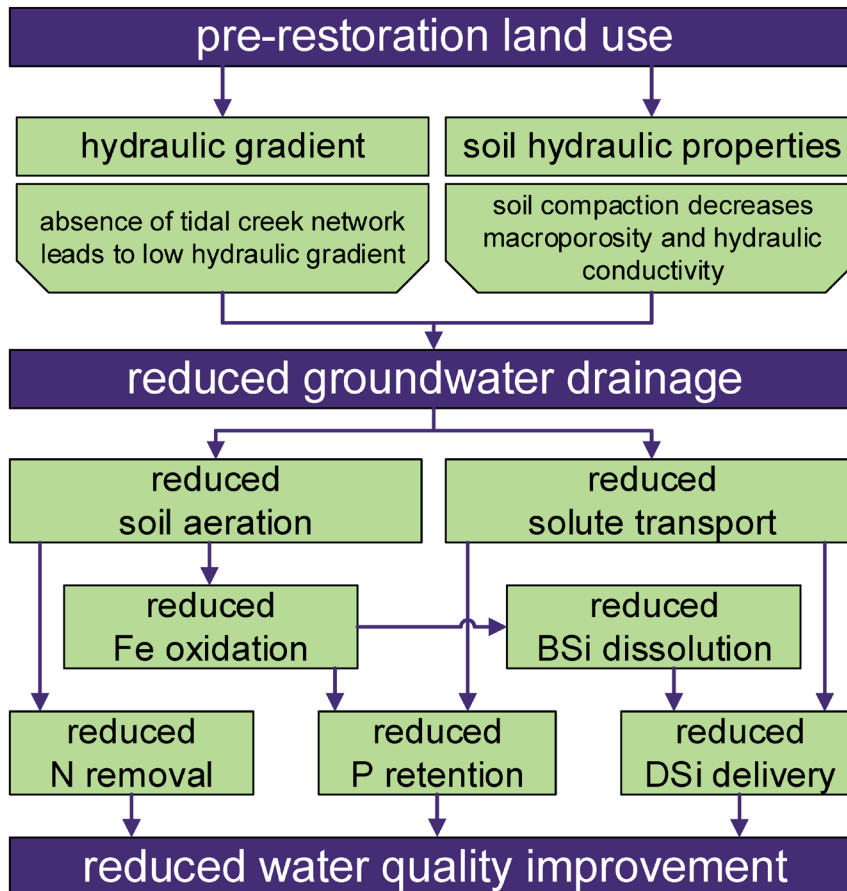

Figure 3.7: Schematic overview of the effects of pre restoration land use on the water quality improvement function of restored tidal marshes.

When tidal marshes are restored on formerly embanked agricultural land, a layer of tidally deposited sediment accumulates on top of the relict agricultural soil. This relict soil layer has often been subjected to compaction and consolidation by the use of heavy farming machinery, cattle grazing and excessive soil drainage, leading to mineralization of organic matter, removal of soil pore water and collapse of soil pores (Crooks and Pye, 2000; Keshta et al., 2020; Spencer et al., 2017; Van Putte et al., 2020 (Chapter 2)). Although the layer of newly deposited sediment has physical and chemical characteristics comparable to the soil of natural tidal marshes (Figure 3.2), the presence of a compact subsoil underneath can

hamper tidally induced groundwater level fluctuations and limit the depth of soil aeration (Tempest et al., 2015; Van Putte et al., 2020 (Chapter 2)). These soil conditions may alter the prevailing biogeochemical reactions that are crucial for water quality improvement (Xin et al., 2022).

In this study we quantified the soil aeration status by calculating the soil saturation index (SSI) introduced by Xin et al. (2010). Although the SSI provided to be a useful indicator for soil aeration status and associated biogeochemistry, there are some limitations to its use. Since the SSI is calculated based on the proportion of time the soil is either saturated or not saturated, it ignores partial saturation of soils. However, Van Putte et al. (2022)(Chapter 4) found that a large fraction of the soil pores above the groundwater level remains saturated even at highly negative matric potential. This is especially true in macroporous soils with fine sediments, as tidal marshes often are (Spencer et al., 2017; Van Putte et al., 2020 (Chapter 2); Xu et al., 2021). Secondly, as the SSI is calculated from the groundwater level (as opposed to the pressure head), it reflects anomalies caused by the presence of perched groundwater tables that might occur in tidal marshes when unsaturated zones persist in the marsh soil even during inundations (Ursino et al., 2004). Furthermore, many wetland plants, which are adapted to rooting in waterlogged conditions, can bring oxygen into the soil trough diffusive transport in aerenchyma (Takahashi et al., 2014). Although this only changes oxygenation conditions locally, the dense network of plant roots in wetland soils can effectively affect the soil aeration status and prevailing biogeochemical reactions (Sorrell and Brix, 2013). Despite these limitations, strong correlations between the calculated SSI and porewater nutrient concentrations indicate the validity of the SSI as an indicator for the water quality improving function of tidal wetlands.

The vertical profile of the SSI depends on several factors. First of all, the SSI at the soil surface is primarily affected by the marsh's inundation regime: directly, due to inundation time and indirectly due to the inundation frequency, as longer non-inundated periods occur around neap tides at higher elevated sites. At the soil surface in the restored marsh, lower SSI values were found compared to the natural marsh. This is because the inundation time in the restored marsh is higher due to the stagnant phase as a result of the CRT design. Secondly, lower SSI values occur where groundwater drains fast after tidal inundation. In the natural tidal marsh, where the distribution of physical soil properties is mostly uniform along the soil profile (Figure 3.2), the drainage rate depends on the hydraulic properties of the soil, in particular the K_s, the porosity, and the hydraulic gradient towards creeks (Gardner, 2005b). A steep hydraulic gradient arises near the creek banks at low tide, forcing groundwater to flow towards the creeks and to seep out of the creek banks, lowering the soil saturation in the vicinity of the creeks (Xin et al., 2013). Where the tidally deposited sediment is underlain by a relict compact soil, as is the case in the restored marsh, the establishment of a hydraulic gradient is impaired and drainage and decrease of the soil saturation is limited. This corresponds to our observation in the res B and res C transects, where the soil layer transition is most obvious (Figure 3.2, Figure S3.2). However, at the res A transect, very fast drainage and a steep hydraulic gradient, lowering

the SSI up to a substantial depth, was observed. We suspect that this is due to a hydrological connection of the upper layer with a highly permeable sandy layer underneath the relict agricultural soil, since soil stratigraphy is a major governing factor in groundwater dynamics in tidal marshes (Gardner, 2007). This is, however, only possible when the relict agricultural soil itself connects these layers through macropore networks. This might be possible as a result of spatially varying soil hydraulic properties of the relict agricultural soil, as different parts of the restored marsh area previously experienced different alternating cultivation types, including cultivation of vegetables, maize (*Zea mays*) and poplar (*Populus* x *canadensis*) plantations (Jacobs et al., 2009), which might result in different soil hydraulic properties. Therefore, we suggest that different pre-restoration land use practices may result in different development trajectories after marsh restoration, indicating the need for our research, including assessments of soil properties and stratigraphy before restoration.

Our study showed that depth profiles of nutrient concentrations are related to the depth of groundwater level fluctuations and soil aeration. In zones with a high SSI, such as the marsh interior, especially in the restored marsh, nitrogen accumulates in the porewater in the form of ammonium (NH_4) reaching concentrations multiple times higher compared to the river water (Figure 3.4, Figure 3.3b). Here, anoxic conditions prevent nitrification and promote ammonification (e.g. Wolf et al., 2011). In the compact agricultural soil, which has a lower organic matter content (Figure 3.2), ammonium stays in solution as the CEC (cation exchange capacity) is lower and less binding sites for NH_4 are present (Reddy and DeLaune, 2008). In addition, the abundant presence of other cations such as Ca^{2+} in the compact soil (Figure S3.4) can result in the displacement of NH_4 from exchange complexes which enhances diffusive fluxes from the anaerobic to the aerobic zones, promoting nitrification (Reddy and DeLaune, 2008). In the upper zones where the SSI is lower, nitrogen is mainly present as NO_3. Porewater NO_3 concentrations were generally higher closer to the creek (except for transect res A). Here, the residence time of the porewater is shorter (Van Putte et al., 2022 (Chapter 4)) resulting in porewater nitrate concentrations that are more similar to estuarine water nitrate concentrations. In addition, the very fast groundwater drainage close to tidal creeks might actually limit the denitrification potential, as a shallow depth to the anaerobic zone promotes denitrification (Megonigal and Neubauer, 2019). In the marsh interior, where the residence time is longer, nitrate concentrations are lower as NO_3 is removed by denitrification and the porewater is less often refreshed. Since coupled nitrification – denitrification is enhanced by fluctuation of groundwater levels and consequent alternating aerobic and anaerobic conditions (Zheng et al., 2016), impaired removal of nitrogen from the estuarine water by the marsh soil is expected where groundwater dynamics are reduced, as is the case in the res B and res C transects in the restored marsh, especially in the marsh interior, where aerobic conditions prevail only in the topmost soil.

Contrary to nitrogen, phosphorus is not removed from the marsh system but mostly retained in marsh soils. As is apparent in Figure 3.5, both dissolved phosphate and

dissolved iron concentrations significantly correlate with SSI and are higher in anoxic zones. In well aerated zones, dissolved ferrous compounds oxidize and form iron oxyhydroxides that precipitate from solution, to which phosphate can sorb. In this way, iron oxidation through soil aeration controls phosphorus solubility (Chambers and Odum, 1990; Reddy and DeLaune, 2008). Groundwater flow plays a very important role in phosphorus retention in tidal marshes. Dissolved phosphate moves from the more anoxic marsh interior towards the well aerated creek zone through porewater advection. Here, the dissolved phosphate sorbs to iron oxides resulting in decreased phosphate concentrations in the groundwater seeping from the creek banks (Chambers and Odum, 1990; Megonigal and Neubauer, 2019), forming an 'iron curtain' that traps dissolved phosphorus. Chambers and Odum (1990) found that, although the sorption sites on iron oxyhydroxide molecules in the creek bank zone are quickly saturated, lowering the potential for phosphate retention, this is compensated by the advective transport of dissolved iron towards the well aerated creek bank zone. Here, the oxidation of this iron forms new sorption sites for phosphate retention. Since the compact subsoil in the restored marsh reduces the extent of the aerated zone, this trapping of phosphate ions is expected to be impaired as less sorption sites for phosphate are available. Tidal marsh soils contain a wide range of iron oxyhydroxides (Yu et al., 2021). The presence of different species of iron oxyhydroxides results in a large phosphate sorption heterogeneity, as these iron oxyhydroxides differ in number and type of sorption sites (Warrinnier et al., 2018).

Under anoxic conditions, PO_4 ions are released from Fe and Al oxyhydroxides (Lauryssen et al., 2022). Therefore, we argue that PO_4 can be released to the surface water when reintroduced tidal inundations lead to anoxic soil conditions in newly restored tidal marshes with a compact, poorly drained soil. Indeed, long term monitoring of nutrient mass balances in the restored site revealed a shift from mostly net P release, in the first three years after marsh restoration, towards mostly net P later on (Maris et al., 2020). In the poorly aerated interior of the restored marsh, PO_4 concentrations greatly exceed the PO_4 concentration in the surface water in the adjacent estuary, even in the top 10 cm, promoting diffusive flux of PO_4 from the porewater to the surface water (van Raaphorst and Kloosterhuis, 1994). Based on the information in this paragraph, we suggest that P retention in newly restored tidal marshes can be enhanced by amplification of groundwater dynamics (e.g. through creek excavation or topsoil amendments (Van Putte et al., 2022 (Chapter 4))), providing more sorption sites for P and enhanced advective transport of dissolved P from anaerobic to aerobic zones.

Tidal wetlands are known to play an important role as 'silica recyclers'. Biogenic silica (BSi) in accreted plant litter dissolves into porewater and is advectively transported to creeks via groundwater (Struyf et al., 2005a). DSi concentrations in both studied marshes mostly exceeded the river water concentration by a great amount. In fact, highest porewater concentrations occurred at low river water concentrations during late summer. This can be explained as silica dissolution is enhanced at higher temperatures (Struyf et al., 2005b). In addition, during summer, BSi in plant litter and dead diatoms that accreted during the

preceding autumn and winter dissolve into the porewater (Struyf et al., 2007). We did not find an indication that the concentration of DSi is correlated to the SSI. In the natural marsh, however, we found a strong contrast of higher DSi concentrations in the upper aerated zone compared to the lower zone. A recent study by Huang et al. (2022) showed that BSi dissolution in freshwater soils is strongly enhanced when Fe^{2+} concentrations are lower than 20 µM (1.12 mg/L). In our study areas, this condition is only fulfilled in the well aerated top zone (Figure 3.5b). In this zone, and especially near tidal creeks, groundwater has a shorter residence time, facilitating faster flushing of infiltrated water through the soil (Van Putte et al., 2022 (Chapter 4)). Since BSi dissolution rates increase at lower DSi concentrations (Huang et al., 2022), increased advective transport is expected to enhance Si recycling rates in tidal wetlands, especially when concentrations in the estuarine water are low.

We discussed the depth profile of nutrient concentrations in function of soil aeration and saturation. However, a multitude of factors determine the prevailing biogeochemical reactions that result in the observed concentration profiles. Denitrification, for example, is favored by the availability of soil organic matter (i.e. mainly plant debris and microbial necromass)(Megonigal and Neubauer, 2019). The presence of soil organic matter increases the cation exchange capacity of the soil, promoting accumulation of nutrients (e.g. Ballantine and Schneider, 2009). The cation exchange capacity is also affected by the soil texture. Especially the abundance of clay particles increases the cation exchange capacity (e.g. Ellis and Atherton, 2003). In addition, nutrient uptake by plants also regulates porewater nutrient concentrations (Negrin et al., 2011). To fully understand nutrient concentration profiles, all these factors should be taken into account.

Based on our results, we expect the ability of a restored tidal marsh to contribute to water quality improvement to largely depend on the marsh accretion rate. Given a sufficient sediment supply, tidal marsh soils quickly trap organic material, forming a highly organic, macroporous soil. The thickness of this soil layer above the relict agricultural soil determines the vertical extent of soil aeration (Van Putte et al., 2022 (Chapter 4)). Organic soils with temporally variable saturated and unsaturated conditions facilitate nitrogen removal through coupled nitrification and denitrification (Thompson et al., 1995). Furthermore, these soils stimulate the oxidation of Fe ions, forming ferric oxyhydroxides to which PO_4 can adsorb, which helps removing P from the surface water (Chambers and Odum, 1990) and promotes BSi dissolution into DSi, which is then exported from the marsh soil through advective transport (Struyf et al., 2006). Therefore, we suggest that, the faster the accretion rate of tidally deposited sediment is, the faster its contribution to water quality improvement will develop. In marshes where suspended sediment supply is limited, we propose that several pre-restoration design measures may be applied in order to (i) increase the organic matter content and macroporosity of the compact topsoil, through e.g. organic matter amendments and soil tillage (e.g. Havens et al., 2002) and (ii) to increase the creek drainage density, e.g. through creek excavation (e.g. Chirol et al., 2015), in order to establish hydraulic gradients towards creeks at low tides. In a model

study, Van Putte et al. (2022)(Chapter 4) showed a substantial increase in soil aeration and advective transport when these design measures are applied prior to restoration. Additional research is required to investigate the effect of these design measures on biogeochemical cycling and the potential for water quality improvement in newly restored tidal marshes.

3.6 Conclusions

In this study, we compared the biogeochemical functioning of a natural and a restored tidal marsh by measuring porewater nutrient concentrations over a vertical soil profile and linking these to the soil saturation index (SSI) calculated from groundwater level fluctuations. We found that the SSI profile is strongly related to depth dependent variations in soil hydraulic properties, especially in relation to the difference between the compact relict agricultural soil beneath the tidally deposited marsh sediments. The SSI is an easy to calculate proxy for soil aeration and, although there are some limitations, it strongly correlates with the vertical distribution of several porewater nutrient concentrations. Where the presence of a historically compacted subsoil hampers groundwater drainage, nitrification is impaired and dissolved nitrogen is mainly present as ammonium. In well drained zones, such as near creeks in the natural tidal marsh, denitrification is impaired and high nitrate concentrations build up, suggesting the benefit of the co-existence of both saturated and unsaturated zones in the marsh soil to maximize nitrogen removal. Furthermore, we found the presence of dissolved phosphate to be highly positively correlated to the SSI, with very high concentrations in the compacted soil in the restored marsh, implying the importance of soil aeration for improved P retention. DSi concentrations were always higher in the porewater compared to the river water, indicating augmented DSi delivery through advective transport with increased groundwater dynamics. In general, we conclude that soil aeration patterns and associated biogeochemical cycling is highly depending on pre-restoration land use and post-restoration subsurface hydrology.

3.7 Acknowledgements.

3.8 References

Ballantine, K., Schneider, R., 2009. Fifty-five years of soil development in restored freshwater depressional wetlands. Ecological Applications 19, 1467-1480. 10.1890/07-0588.1

Ballantine, K., Schneider, R., Groffman, P., Lehmann, J., 2012. Soil Properties and Vegetative Development in Four Restored Freshwater Depressional Wetlands. Soil Science Society of America Journal 76, 1482-1495. 10.2136/sssaj2011.0362

Bally, G., Mesnage, V., Verney, R., Clarisse, O., Dupont, J.P., Ouddanne, B., Lafite, R., 2005. Dialysis porewater sampler: a strategy for time equilibration optimisation. Phosphates in Sediments, Proceedings, 9-20.

Barbier, E.B., Hacker, S.D., Kennedy, C., Koch, E.W., Stier, A.C., Silliman, B.R., 2011. The value of estuarine and coastal ecosystem services. Ecological Monographs 81, 169-193. 10.1890/10-1510.1

Brooks, K.L., Mossman, H.L., Chitty, J.L., Grant, A., 2015. Limited Vegetation Development on a Created Salt Marsh Associated with Over-Consolidated Sediments and Lack of Topographic Heterogeneity. Estuaries and Coasts 38, 325-336. 10.1007/s12237-014-9824-3

Caetano, M., Bernardez, P., Santos-Echeandia, J., Prego, R., Vale, C., 2012. Tidally driven N, P, Fe and Mn exchanges in salt marsh sediments of Tagus estuary (SW Europe). Environmental Monitoring and Assessment 184, 6541-6552. 10.1007/s10661-011-2439-2

Chambers, R.M., Odum, W.E., 1990. Porewater Oxidation, Dissolved Phosphate and the Iron Curtain: Iron-Phosphorus Relations in Tidal Freshwater Marshes. Biogeochemistry 10, 37-52.

Chirol, C., Gallop, S., Pontee, N., Haigh, I., Thompson, C., 2015. Creek networks: natural evolution and design choices for intertidal habitat recreation, Proceedings of Sea Lines of Communication: Construction.

Chmura, G.L., Anisfeld, S.C., Cahoon, D.R., Lynch, J.C., 2003. Global carbon sequestration in tidal, saline wetland soils. Global Biogeochemical Cycles 17. 10.1029/2002gb001917

Cox, T.J.S., Maris, T., De Vleeschauwer, P., De Mulder, T., Soetaert, K., Meire, P., 2006. Flood control areas as an opportunity to restore estuarine habitat. Ecological Engineering 28, 55-63. 10.1016/j.ecoleng.2006.04.001

Crooks, S., Pye, K., 2000. Sedimentological controls on the erosion and morphology of saltmarshes: implications for flood defence and habitat recreation. Coastal and Estuarine Environments: Sedimentology, Geomorphology and Geoarchaeology 175, 207-222. 10.1144/Gsl.Sp.2000.175.01.16

Darcy, H., 1856. Les fontaines publiques de la ville de Dijon: exposition et application. Victor Dalmont.

Dlapa, P., Hriník, D., Hrabovský, A., Šimkovic, I., Žarnovičan, H., Sekucia, F., Kollár, J., 2020. The Impact of Land-Use on the Hierarchical Pore Size Distribution and Water Retention Properties in Loamy Soils. Water 12, 339.

Eijkelkamp Agrisearch Equipments, 2013. laboratory-Permeameters: Operation instructions, Giesbeek, The Netherlands.

Ellis, S., Atherton, J.K., 2003. Properties and development of soils on reclaimed alluvial sediments of the Humber estuary, eastern England. Catena 52, 129-147. 10.1016/S0341-8162(02)00179-0

Esteves, L.S., 2014. What is managed realignment?, Managed Realignment: A Viable Long-Term Coastal Management Strategy? Springer, pp. 19-31.

European Parliament and the Council of the European Union, 1992. Directive 92/43/EEC of 21 May 1992 on the conservation of natural habitats and of wild fauna and flora. Official Journal of the European Communities L206. 22.7.1992.

European Parliament and the Council of the European Union, 2000. Directive 2000/60/EC of the European Parliament and of the Council establishing a framework for the Community action in the field of water policy, Official Journal of the European Communities L327. 22.12.2000.

Gardner, L.R., 2005a. A modeling study of the dynamics of pore water seepage from intertidal marsh sediments. Estuarine Coastal and Shelf Science 62, 691-698. 10.1016/j.ecss.2004.10.005

Gardner, L.R., 2005b. Role of geomorphic and hydraulic parameters in governing pore water seepage from salt marsh sediments.

Water Resources Research 41. 10.1029/2004wr003671

Gardner, L.R., 2007. Role of stratigraphy in governing pore water seepage from salt marsh sediments. Water Resources Research 43. 10.1029/2006wr005338

Gedan, K.B., Silliman, B.R., Bertness, M.D., 2009. Centuries of human-driven change in salt marsh ecosystems. Annual review of marine science 1, 117-141.

Havens, K.J., Varnell, L.M., Watts, B.D., 2002. Maturation of a constructed tidal marsh relative to two natural reference tidal marshes over 12 years. Ecological Engineering 18, 305-315. 10.1016/S0925-8574(01)00089-1

Heiri, O., Lotter, A.F., Lemcke, G., 2001. Loss on ignition as a method for estimating organic and carbonate content in sediments: reproducibility and comparability of results. Journal of Paleolimnology 25, 101-110. 10.1023/a:1008119611481

Hesslein, R.H., 1976. An in situ sampler for close interval pore water studies1. Limnology and Oceanography 21, 912-914. 10.4319/lo.1976.21.6.0912

Howes, B.L., Howarth, R.W., Teal, J.M., Valiela, I., 1981. Oxidation-Reduction Potentials in a Salt-Marsh - Spatial Patterns and Interactions with Primary Production. Limnology and Oceanography 26, 350-360. 10.4319/lo.1981.26.2.0350

Huang, L., Parsons, C.T., Slowinski, S., Van Cappellen, P., 2022. Amorphous silica dissolution kinetics in freshwater environments: Effects of Fe2+ and other solution compositional controls. Science of the Total Environment 851. 10.1016/j.scitotenv.2022.158239

Jacobs, P.H., 2002. A new rechargeable dialysis pore water sampler for monitoring sub-aqueous in-situ sediment caps. Water Research 36, 3121-3129. 10.1016/S0043-1354(01)00542-5

Jacobs, S., Beauchard, O., Struyf, E., Cox, T.J.S., Maris, T., Meire, P., 2009. Restoration of tidal freshwater vegetation using controlled reduced tide (CRT) along the Schelde Estuary (Belgium). Estuarine Coastal and Shelf Science 85, 368-376. 10.1016/j.ecss.2009.09.004

Kearney, W.S., Fagherazzi, S., 2016. Salt marsh vegetation promotes efficient tidal channel networks. Nature Communications 7, 12287. 10.1038/ncomms12287

Keshta, A., Koop-Jakobsen, K., Titschack, J., Mueller, P., Jensen, K., Baldwin, A., Nolte, S., 2020. Ungrazed salt marsh has well connected soil pores and less dense sediment compared with grazed salt marsh: a CT scanning study. Estuarine, Coastal and Shelf Science 245. 10.1016/j.ecss.2020.106987

Lancelot, C., 1995. The mucilage phenomenon in the continental coastal waters of the North Sea. Science of the Total Environment 165, 83-102. 10.1016/0048-9697(95)04545-C

Lauryssen, F., Crombé, P., Maris, T., Van Maldegem, E., Van de Broek, M., Temmerman, S., Smolders, E., 2022. Estimation of the natural background of phosphate in a lowland river using tidal marsh sediment cores. Biogeosciences 19, 763-776. 10.5194/bg-19-763-2022

Maris, T., Gelsomini, P., Horemans, D., Meire, P., 2020. OMES rapport 2019: Onderzoek naar de gevolgen van het Sigmaplan, baggeractiviteiten en havenuitbreiding in de Zeeschelde op het milieu. Universiteit Antwerpen, Antwerpen.

Megonigal, J.P., Neubauer, S.C., 2019. Chapter 19 - Biogeochemistry of Tidal Freshwater Wetlands, in: Perillo, G.M.E., Wolanski, E., Cahoon, D.R., Hopkinson, C.S. (Eds.), Coastal Wetlands (Second Edition). Elsevier, pp. 641-683.

Meire, P., Ysebaert, T., Van Damme, S., Van den Bergh, E., Maris, T., Struyf, E., 2005. The Scheldt estuary: A description of a changing ecosystem. Hydrobiologia 540, 1-11. 10.1007/s10750-005-0896-8

Mossman, H.L., Brown, M.J.H., Davy, A.J., Grant, A., 2012. Constraints on Salt Marsh Development Following Managed Coastal Realignment: Dispersal Limitation or Environmental Tolerance? Restoration Ecology 20, 65-75. 10.1111/j.1526-100X.2010.00745.x

Negrin, V.L., Spetter, C.V., Asteasuain, R.O., Perillo, G.M.E., Marcovecchio, J.E., 2011. Influence of flooding and vegetation on carbon, nitrogen, and phosphorus dynamics in the pore water of a Spartina alterniflora salt marsh. Journal of Environmental Sciences 23, 212-221. 10.1016/S1001-0742(10)60395-6

Neubauer, S.C., Anderson, I.C., Neikirk, B.B., 2005. Nitrogen cycling and ecosystem exchanges in a Virginia tidal freshwater marsh. Estuaries 28, 909-922. 10.1007/Bf02696019

Oosterlee, L., Cox, T.J.S., Vandenbruwaene, W., Maris, T., Temmerman, S., Meire, P., 2017. Tidal Marsh Restoration Design Affects Feedbacks Between Inundation and Elevation Change. Estuaries and Coasts. 10.1007/s12237-017-0314-2

Peng, X., Ji, Q., Angell, J.H., Kearns, P.J., Yang, H.J., Bowen, J.L., Ward, B.B., 2016. Long-term fertilization alters the relative importance of nitrate reduction pathways in salt marsh sediments. Journal of Geophysical Research: Biogeosciences 121, 2082-2095. 10.1002/2016JG003484

R Core Team, 2021. R: A Language and Environment for Statistical Computing, Vienna, Austria.

Reddy, K.R., DeLaune, R.D., 2008. Biogeochemistry of Wetlands: Science and Applications. CRC Press.

Sloey, T.M., Hester, M.W., 2016. Interactions between soil physicochemistry and belowground biomass production in a freshwater tidal marsh. Plant and Soil 401, 397-408. 10.1007/s11104-015-2760-6

Sorrell, B.K., Brix, H., 2013. Gas Transport and Exchange through Wetland Plant Aerenchyma, Methods in Biogeochemistry of Wetlands, pp. 177-196.

Spencer, K.L., Carr, S.J., Diggens, L.M., Tempest, J.A., Morris, M.A., Harvey, G.L., 2017. The impact of pre-restoration land-use and disturbance on sediment structure, hydrology and the sediment geochemical environment in restored saltmarshes. Science of the Total Environment 587, 47-58. 10.1016/j.scitotenv.2016.11.032

Struyf, E., Dausse, A., Van Damme, S., Bal, K., Gribsholt, B., Boschker, H.T.S., Middelburg, J.J., Meire, P., 2006. Tidal marshes and biogenic silica recycling at the land-sea interface. Limnology and Oceanography 51, 838-846.

Struyf, E., Temmerman, S., Meire, P., 2007. Dynamics of biogenic Si in freshwater tidal marshes: Si regeneration and retention in marsh sediments (Scheldt estuary). Biogeochemistry 82, 41-53. 10.1007/s10533-006-9051-5

Struyf, E., Van Damme, S., Gribsholt, B., Meire, P., 2005a. Freshwater marshes as dissolved silica recyclers in an estuarine environment (Schelde estuary, Belgium). Hydrobiologia 540, 69-77. 10.1007/s10750-004-7104-0

Struyf, E., Van Damme, S., Gribsholt, B., Middelburg, J.J., Meire, P., 2005b. Biogenic silica in tidal freshwater marsh sediments and vegetation (Schelde estuary, Belgium). Marine Ecology Progress Series 303, 51-60. 10.3354/meps303051

Takahashi, H., Yamauchi, T., Colmer, T.D., Nakazono, M., 2014. Aerenchyma Formation in Plants, in: van Dongen, J.T., Licausi, F. (Eds.), Low-Oxygen Stress in Plants: Oxygen Sensing and Adaptive Responses to Hypoxia. Springer Vienna, Vienna, pp. 247-265.

Temmerman, S., Govers, G., Meire, P., Wartel, S., 2003. Modelling long-term tidal marsh growth under changing tidal conditions and suspended sediment concentrations, Scheldt estuary, Belgium. Marine Geology 193, 151-169. 10.1016/S0025-3227(02)00642-4

Tempest, J.A., Harvey, G.L., Spencer, K.L., 2015. Modified sediments and subsurface hydrology in natural and recreated salt marshes and implications for delivery of ecosystem services. Hydrological Processes 29, 2346-2357. 10.1002/hyp.10368

Teuchies, J., Vandenbruwaene, W., Carpentier, R., Bervoets, L., Temmerman, S., Wang, C., Maris, T., Cox, T.J.S., Van Braeckel, A., Meire, P., 2013. Estuaries as Filters: The Role of Tidal Marshes in Trace Metal Removal. Plos One 8. 10.1371/journal.pone.0070381

Thompson, S.P., Paerl, H.W., Go, M.C., 1995. Seasonal Patterns of Nitrification and Denitrification in a Natural and a Restored Salt-Marsh. Estuaries 18, 399-408. Doi 10.2307/1352322

Ursino, N., Silvestri, S., Marani, M., 2004. Subsurface flow and vegetation patterns in tidal environments. Water Resources Research 40. 10.1029/2003wr002702

Van de Broek, M., Vandendriessche, C., Poppelmonde, D., Merckx, R., Temmerman, S., Govers, G., 2018. Long-term organic carbon sequestration in tidal marsh sediments is dominated by old-aged allochthonous inputs in a macrotidal estuary. Global Change Biology 24, 2498-2512. 10.1111/gcb.14089

Van Putte, N., Meire, P., Seuntjens, P., Joris, I., Verreydt, G., Hambsch, L., Temmerman, S., 2022. Solving hindered groundwater dynamics in restored tidal marshes by creek excavation and soil amendments: A model study. Ecological Engineering 178. 10.1016/j.ecoleng.2022.106583

Van Putte, N., Temmerman, S., Verreydt, G., Seuntjens, P., Maris, T., Heyndrickx, M., Boone, M., Joris, I., Meire, P., 2020. Groundwater dynamics in a restored tidal marsh are limited by historical soil compaction. Estuarine, Coastal and Shelf Science 244. 10.1016/j.ecss.2019.02.006

van Raaphorst, W., Kloosterhuis, H.T., 1994. Phosphate sorption in superficial intertidal sediments. Marine Chemistry 48, 1-16. 10.1016/0304-4203(94)90058-2

Warrinnier, R., Goossens, T., Braun, S., Gustafsson, J.P., Smolders, E., 2018. Modelling heterogeneous phosphate sorption kinetics on iron oxyhydroxides and soil with a continuous distribution approach. European Journal of Soil Science 69, 475-487. 10.1111/ejss.12549

Williams, A.A., Lauer, N.T., Hackney, C.T., 2014. Soil Phosphorus Dynamics and Saltwater Intrusion in a Florida Estuary. Wetlands 34, 535-544. 10.1007/s13157-014-0520-7

Wilson, A.M., Morris, J.T., 2012. The influence of tidal forcing on groundwater flow and nutrient exchange in a salt marsh-dominated estuary. Biogeochemistry 108, 27-38. 10.1007/s10533-010-9570-y

Wolf, K.L., Ahn, C., Noe, G.B., 2011. Development of Soil Properties and Nitrogen Cycling in Created Wetlands. Wetlands 31, 699-712. 10.1007/s13157-011-0185-4

Xin, P., Gibbes, B., Li, L., Song, Z.Y., Lockington, D., 2010. Soil saturation index of salt marshes subjected to spring-neap tides: a new variable for describing marsh soil aeration condition. Hydrological Processes 24, 2564-2577. 10.1002/hyp.7670

Xin, P., Li, L., Barry, D.A., 2013. Tidal influence on soil conditions in an intertidal creek-marsh system. Water Resources Research 49, 137-150. 10.1029/2012wr012290

Xin, P., Wilson, A., Shen, C., Ge, Z., Moffett, K.B., Santos, I.R., Chen, X., Xu, X., Yau, Y.Y.Y., Moore, W., Li, L., Barry, D.A., 2022. Surface Water and Groundwater Interactions in Salt Marshes and Their Impact on Plant Ecology and Coastal Biogeochemistry. Reviews of Geophysics 60. 10.1029/2021RG000740

Xin, P., Yu, X.Y., Lu, C.H., Li, L., 2016. Effects of macro-pores on water flow in coastal subsurface drainage systems. Advances in Water Resources 87, 56-67. 10.1016/j.advwatres.2015.11.007

Xin, P., Yuan, L.R., Li, L., Barry, D.A., 2011. Tidally driven multiscale pore water flow in a creek-marsh system. Water Resources Research 47. 10.1029/2010wr010110

Xu, X., Xin, P., Zhou, T., Xiao, K., 2021. Effect of macropores on pore-water flow and soil conditions in salt marshes subject to evaporation and tides. Estuarine, Coastal and Shelf Science 261. 10.1016/j.ecss.2021.107558

Yu, C., Xie, S., Song, Z., Xia, S., Åström, M.E., 2021. Biogeochemical cycling of iron (hydr-)oxides and its impact on organic carbon turnover in coastal wetlands: A global synthesis and perspective. Earth-Science Reviews 218. 10.1016/j.earscirev.2021.103658

Zheng, Y., Hou, L., Liu, M., Liu, Z., Li, X., Lin, X., Yin, G., Gao, J., Yu, C., Wang, R., Jiang, X., 2016. Tidal pumping facilitates dissimilatory nitrate reduction in intertidal marshes. Scientific Reports 6. 10.1038/srep21338

4

Solving hindered groundwater dynamics in restored tidal marshes by creek excavation and soil amendments: a model study

Niels Van Putte, Patrick Meire, Piet Seuntjens, Ingeborg Joris, Goedele Verreydt, Lorenz Hambsch, Stijn Temmerman

4.1   Abstract

Groundwater fluxes in tidal marshes largely control key ecosystem functions and services, such as vegetation growth, soil carbon sequestration, and nutrient cycling. In tidal marshes restored on formerly embanked agricultural land, groundwater fluxes are often limited as compared to nearby natural marshes, as a result of historical agricultural soil compaction. To improve the functioning of restored tidal marshes, knowledge is needed on how much certain design options can optimize soil-groundwater interactions in future restoration projects. Based on measured data on soil properties and tidally induced groundwater dynamics, we calibrated and evaluated a 2D vertical model of a creek-marsh cross-section, accounting for both saturated and unsaturated groundwater flow and solute transport in a variably saturated groundwater flow model. We found that model simulations of common restoration practices such as soil amendments (increasing the depth of porous soil on top of the compact layer) and creek excavation (increasing the creek density) increase the soil aeration depth and time, the drainage depth and the solute flux, and decrease the residence time of solutes in the porewater. Our simulations indicate that increasing the depth to the compact layer from 20 cm to 40 cm, or increasing the creek density from 1 creek to 2 creeks along a 50 m marsh transect (while maintaining the total creek cross-sectional area), in both cases more than doubles the volume of water processed by the marsh soil. We discuss that this may stimulate nutrient cycling. As such, our study demonstrates that groundwater modelling can support the design of marsh restoration measures aiming to optimize groundwater fluxes and related ecosystem services.

4.2   Introduction

The flow of shallow groundwater is a key process in the ecohydrological functioning of tidal marsh ecosystems. When tidal marshes are inundated at high tide, part of the flooding water infiltrates into the marsh surface. At low tide, part of this water seeps out of the creek banks, lowering the groundwater level especially in the vicinity of tidal creeks (e.g. Chapman, 1938; Harvey et al., 1987). These tidally induced temporal and spatial variations in groundwater level control the soil aeration conditions (Li et al., 2005; Ursino et al., 2004), which further affect key ecosystem functions such as soil organic carbon storage or decomposition (Guimond et al., 2020) and vegetation zonation patterns (Wilson et al., 2015; Xie et al., 2020; Xin et al., 2013). Groundwater flow also regulates the cycling rate of nutrients in the marsh (Wang et al., 2011; Wilson and Gardner, 2006). As such, interactions between the groundwater and the soil are of high importance for the filtering capacity of tidal wetlands and their contribution to water quality improvement in the adjacent estuary. From the above, it is clear that groundwater dynamics are key for the delivery of regulating ecosystem services of tidal marsh ecosystems. Nevertheless, groundwater dynamics are rarely considered in the design of tidal marsh restoration schemes.

Along estuaries and coasts worldwide, there is an increasing demand for restoration of tidal marshes that have formerly been embanked, drained and converted to agricultural land. Marsh restoration is seen as a viable management strategy to counteract the loss of their ecosystem services due to large scale land reclamations in the past (Wolters et al., 2005). However, years after restoration, many restored tidal marshes still exhibit an impaired delivery of soil related ecosystem services compared to their natural counterparts. Their soil is often structurally different from the soil in natural tidal marshes (e.g. Burden et al., 2013; Craft et al., 2002; Van Putte et al., 2020 (Chapter 2)). In natural tidal marshes, the soil consists of tidally deposited sediment, intermixed with plant debris and large void spaces, creating a macroporous soil. In the embanked areas, agricultural practices such as drainage of the soil and the use of heavy farming equipment often lead to mineralization of organic matter, compaction and consolidation of the soil, reducing its porosity and hydraulic conductivity. When a tidal marsh is restored on such an embanked land, this compact soil may act as an impermeable barrier for soil-water interactions (Crooks and Pye, 2000; Spencer et al., 2017; Van Putte et al., 2020 (Chapter 2)). Groundwater level fluctuations and hence nutrient cycling are restricted to the layer of tidally deposited sediment that accumulates on top of the compact soil over time, whereas in natural marsh systems, groundwater and nutrient flow may occur over much deeper portions of the soil profile (Tempest et al., 2015; Van Putte et al., 2020 (Chapter 2)). Given the above, there is an urgent need to counteract the restrictions of the compact soil and to optimize soil-groundwater interactions in future tidal marsh restoration projects.

Since the 1980's, many efforts were made to simulate groundwater dynamics in natural tidal marshes. The complexity of these models increased over time (Marois and Stecher, 2020). Moffett et al. (2012) give an extended overview of the earliest models. These first models are restricted to simulating flow in the saturated zone (Harvey et al., 1987; Nuttle,

1988), while later developed models use the Richards' equation to simulate both saturated and unsaturated flow (Ursino et al., 2004; Wilson and Gardner, 2006; Xin et al., 2009b). Several modelling studies consider a dual layered soil stratigraphy (Gardner, 2007; Xin et al., 2012) and some models also incorporate the effects of evapotranspiration (Hemond and Fifield, 1982; Ursino et al., 2004; Xin et al., 2017) and/or soil compressibility (Gardner and Wilson, 2006; Xin et al., 2009a). Only in a limited number of model studies, groundwater flow is coupled to solute transport (Chassagne et al., 2012; Wilson and Gardner, 2006). Recently, much attention is given to the presence of macropores, for instance created by burrowing invertebrate species, and their effect on groundwater flow in tidal marshes (Cao et al., 2012; Xin et al., 2009b; Xin et al., 2016; Xu et al., 2021). Until now, however, groundwater models have not yet been applied for modelling hindered groundwater flow and solute transport in restored tidal marshes with a historically compacted subsoil. Given the increasing number of marsh restoration projects in which this historical soil compaction hampers ecological development, improved scientific insights are needed on the impact of different restoration design options on groundwater flow and transport.

In this modelling study, we simulate the effect of several design options on the ecohydrological functioning of newly restored tidal marshes. Therefore, we apply a numerical groundwater model to a 2D marsh-creek cross section, using parameter values based on field measurements in a restored tidal marsh. In the marsh design scenarios, we vary **(a)** the creek density and **(b)** the depth of the compact layer. The rationale behind these design options is explained below.

(a) Groundwater level fluctuations are typically strongest in the vicinity of tidal creeks. The majority of the seepage water originates from only a few meters from a tidal creek (Gardner, 2005a; Hughes et al., 1998; Xin et al., 2010). With this in mind, we hypothesize that initial excavation of a denser creek network in restored marshes will also increase the total seepage flux and increase the volume of the marsh soil that interacts with the groundwater. The excavation of an initial creek network prior to restoration is a common practice to enhance surface water drainage and vegetation establishment in restoration projects in which natural creek formation is inhibited or strongly slowed down by the relict compact soil (Liu et al., 2020; O'Brien and Zedler, 2006; Tovey et al., 2009; Vanlede et al., 2015).

(b) As groundwater dynamics are inhibited by the compact soil layer, we hypothesize that the depth of this compact layer determines the depth of the soil profile over which soil-water interactions take place. To reverse the effect of historical agricultural soil compaction, organic soil amendments (e.g. ploughing and mixing wood chips with soil) prior to reflooding have been proposed as a management strategy to 'decompact" the soil and to obtain a soil structure comparable to that found in natural tidal marshes (Callaway et al., 1997; Havens et al., 2002; Kadiri et al., 2011). Still, practical implementation of soil amendments in tidal marshes are rare (except Gibson et al., 1994; Ott et al., 2020; Zedler, 2000). For non-tidal

wetland soils, however, several studies indicate the success of soil amendments in ameliorating soil structure (Fei et al., 2019; Scott et al., 2020; Wolf et al., 2019).

We determine the effect of these tidal marsh restoration design options on (i) groundwater drainage depth, (ii) soil saturation index (i.e. the proportion of the spring tide – neap tide cycle that a specific location in the marsh soil is saturated (Xin et al., 2010)) and (iii) the total seepage flux of both water and solutes. Lastly, we also estimate (iv) the residence time of the groundwater.

4.3 Methods

4.3.1 Field data

4.3.1.1 Study site

The study site is situated in the restored marsh 'Lippenbroek', located along the freshwater tidal part of the Scheldt estuary in Belgium (51°05'06.8" N 4°10'19.3"E, Figure 4.1b). The estuary has a semidiurnal tide with an average tidal range of approximately 6 m near the studied tidal marsh. This marsh experiences an inundation frequency (percentage of flooding high tides) of 56% at the study location. The marsh is restored on land that has been under agricultural practice since large scale land reclamation in the 13th century, by building of dikes and drainage of the original wetlands. It was restored to a tidal wetland in 2006 using the CRT (controlled reduced tide) principle described in Maris et al. (2007). Since the restoration, the mean elevation of the site increased with 2.35 cm year^{-1} on average due to accretion of tidal sediment (Oosterlee et al., 2017). On the study transect, 60 cm has been deposited on top of the compact agricultural soil. The vegetation consists of wetland plants, mainly reed (*Phragmites australis)* and cattail (*Typha latifolia*) in the lower elevated parts where the transect is located, and mainly willow trees (*Salix* sp.) and stinging nettle (*Urtica dioica*) in the higher elevated parts (Jacobs et al., 2009). Since the marsh restoration, a tidal channel network initially developed relatively rapidly, but the development slowed down after approximately 3 years, resulting in an estimated, approximate average distance of 27.4 m to the nearest tidal creek (Vandenbruwaene et al., 2012).

4.3.1.2 Transects and wells

A 22 m long cross-sectional transect from a tidal creek over the marsh platform was established in the field (Figure 4.1c). On the transect, we placed one monitoring well in the creek to measure surface water level fluctuations and four monitoring wells in the marsh soil to study groundwater level fluctuations. These wells were placed at increasing distances form the creek (1 m, 4 m, 10 m and 22 m) as the groundwater level fluctuations were expected to decrease with an increasing distance from the creek (Van Putte et al., 2020 (Chapter 2)). The monitoring wells were slotted over the entire below-ground part and placed up to a depth of 1.75 m below the soil surface. The pressure head in the wells was measured every minute with pressure transducers (Rugged Troll 100, In-Situ Inc.) and corrected for variations in atmospheric pressure. The surface topography of the transect

and the absolute elevation of the wells was measured with a total station (Sokkia SET510k) and recorded in m relative to TAW (the Belgian ordnance datum). Approximately one month of groundwater level measurements (from the 24th of January to the 21st of February 2019, i.e. two spring tide-neap tide cycles) was selected for our analyses.
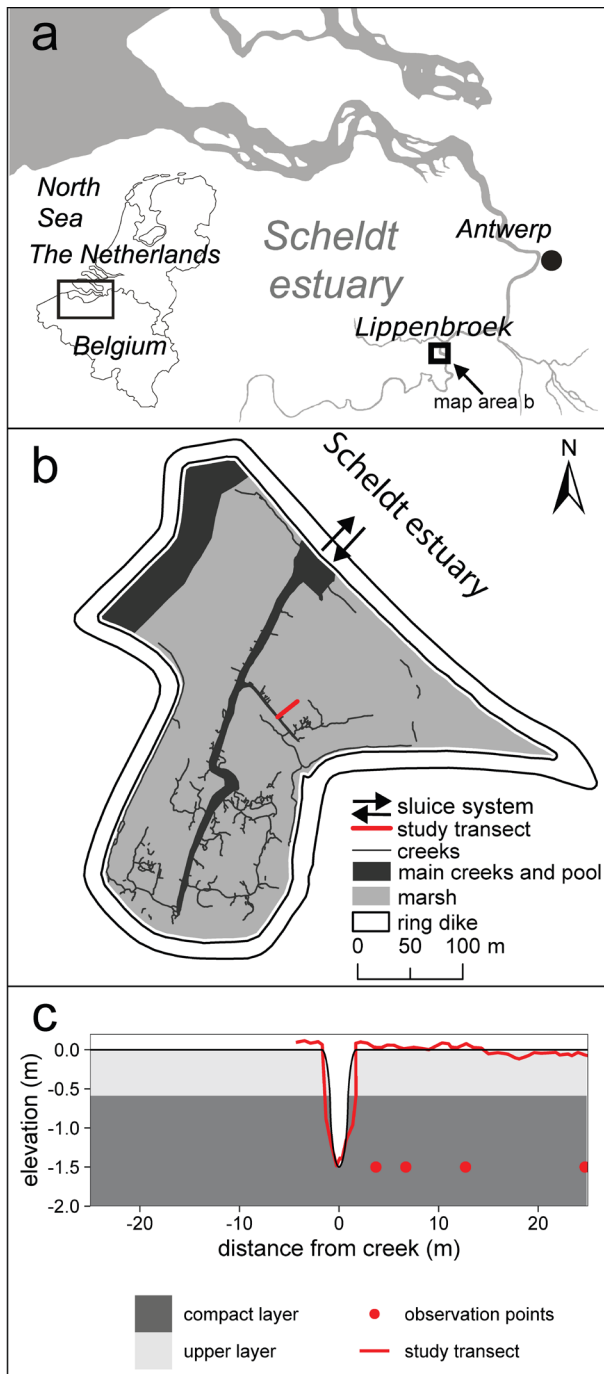

Figure 4.1 (a): Situation of the study area within the Scheldt estuary. (b): Overview map of the study area (Lippenbroek) with indication of the study transect, (c): model domain based on the measured transect elevation profile (in red).

4.3.1.3   Soil profiles and soil samples

Along the transect, the soil profile was described to determine the depth of the compacted agricultural soil relative to the soil surface. This was done with a gouge auger, sampling the soil profile near every monitoring well along the transect, and allowing easy distinction between the compact layer and the loose sediment layer on top of it. In addition, undisturbed soil samples of 100 cm^3 were taken at 2 – 7 cm depth (i.e. in the newly deposited sediment) and 100 – 105 cm depth (i.e. in the compact relict agricultural soil) in six replicates at each of the locations of the wells.

4.3.1.4   Soil hydraulic properties

Four out of six replicates of the soil samples were used to measure the dry bulk density (ρ_b) and the saturated hydraulic conductivity (K$_s$). These samples were fully saturated and K$_s$ was measured using either the constant head method (Eijkelkamp Agrisearch Equipments, 2013) for high permeable soil samples and the falling head method for low permeable soils. For the latter, a burette inside a rubber stop cock was inserted in the sample holder. A positive pressure head was applied on the samples by filling the burette with water. While the water seeped through the samples, we noted the decline in pressure head over time. K$_s$ was calculated using Darcy's law (Darcy, 1856) and exponential regression of the pressure head in function of time.

The remaining replicates were used to determine the SWRC (Soil Water Retention Curve) and were placed in a sandbox (Eijkelkamp Soil & Water, 2019). Suctions of 10 cm, 30 cm, 50 cm, 70 cm and 100 cm were applied. Samples were weighed after each pressure step after reaching equilibrium states to determine the volumetric water content (θ). The water retention at suctions of 340 cm, 1020 cm and 15300 cm was determined on a smaller subsample using ceramic plate extractors (Cresswell et al., 2008). The obtained volumetric soil moisture data in function of applied pressure were averaged over the two replicates. The SWRC was fitted with the retention/conductivity model of van Genuchten-Mualem (van Genuchten, 1980) with the RETC (RETention Curve) code formula described in Van Genuchten et al. (1991):

$$\theta(h) = \begin{cases} \theta_r + \dfrac{\theta_s - \theta_r}{[1 + |\alpha h|^n]^{1-1/n}} & h < 0 \\ \theta_s & h \geq 0 \end{cases} \qquad \text{Equation 4.1}$$

In Equation 4.1, $\theta(h)$ [-] is the volumetric soil water content in function of the pressure head h [L] expressed as the pressure exerted by a water column with height h, θ_r [-] is the residual water content and θ_s [-] is the saturated water content; n is an index for the pore size distribution and α is a shape factor that relates to the inverse of the air entry value.

4.3.2 model development

4.3.2.1 Domain properties

We set up a two-dimensional variably saturated groundwater model using the HYDRUS 2D/3D software (Senja et al., 2017). The model domain geometry is a creek-marsh cross section with an idealized topography that is approximating the measured average marsh platform elevation and the creek depth and width on the studied transect (Figure 4.1). The domain has a total length of 50 m. The domain bottom was chosen arbitrarily at 2 m below the marsh platform elevation. Deepest measured groundwater levels were never deeper than 0.5 m, and the creek depth was 1.5 m. No exchange with aquifers underneath was assumed due to the presence of the compact subsoil. The domain was divided into two layers: an upper layer of recently deposited sediment and a lower layer of compact relict agricultural soil. Based on field measurements, the soil layer transition was set at 0.60 m below the marsh platform elevation. For these two layers, the measured values for the soil hydraulic properties, averaged for the different locations on the transect, were attributed to the respective soil layer.

A finite element mesh (FEM) was generated for the model domain and consists of approximately 20000 nodes. Mesh refinements were made around the creek banks and the transition between soil layers where higher spatial differences in pressure head and water content were expected. Observation nodes were inserted in the mesh at the location and depth where monitoring wells were installed in the marsh (Figure 4.1c) to compare the measured and simulated groundwater levels.

4.3.2.2 Boundary and initial conditions

Fluctuations of the surface water level that were measured in the creek were imposed as a time variable pressure head boundary condition to the creek banks and the marsh platform. This boundary was allowed to develop into a seepage face where the nodal pressure became negative, i.e. at the border of the saturated flow field and the atmosphere. A no-flux boundary was applied at the sides and the bottom of the domain as no water was expected to enter or leave the domain via the bottom through the presence of the compact agricultural soil.

4.3.2.3 Governing equations

4.3.2.3.1 Water flow

To describe variably saturated water flow, the Richards' equation is solved (Richards, 1931). For a planar 2D vertical domain, this equation is given by Equation 4.2,

$$\frac{\partial \theta}{\partial t} = \frac{\partial}{\partial x}\left[K(h)\left(\frac{\partial h}{\partial x} + 1\right)\right] + \frac{\partial}{\partial z}\left[K(h)\left(\frac{\partial h}{\partial z} + 1\right)\right] \qquad \text{Equation 4.2}$$

in which θ [-] is the volumetric water content, h [L] is the pressure head and x [L] and z [L] are the spatial coordinates in the horizontal and vertical dimensions, t [T] is the time and

K(h) [LT^{-1}] is the hydraulic conductivity of the soil as a function of the pressure head, given by Equation 4.3 (van Genuchten, 1980).

$$K(h) = K_s S_e^l \left[1 - \left(1 - S_e^{\frac{n}{n-1}} \right)^{1-\frac{1}{n}} \right]^2 \qquad \text{Equation 4.3}$$

Here, *n* [-] is an index for the pore-size distribution, *l* [-] is the pore connectivity parameter taken as 0.5 (Mualem, 1976) and S_e [-] is the effective degree of saturation, which is given by Equation 4.4 (van Genuchten, 1980),

$$S_e = \frac{\theta - \theta_r}{\theta_s - \theta_r} \qquad \text{Equation 4.4}$$

where θ_r [-] is the residual water content and θ_s [-] is the saturated water content. Groundwater flow in tidal marsh sediments is known to occur mainly through macropores intersecting the sediment matrix (Harvey and Nuttle, 1995; Xiao et al., 2019; Xin et al., 2016). Therefore, our model was set up as a dual porosity model with a mobile (macropores) and an immobile (matrix) region. This model assumes that groundwater flow is restricted to the mobile region. The relative distribution of the matrix- and macropore space was estimated based on the results of micro-CT scans of soil cores from the same field site, described in Van Putte et al. (2020)(Chapter 2) in which macropores are defined as pores > 60 μm. The Richards equation (Equation 4.2) can be rewritten for both regions and a simple mass balance equation to describe a change in soil water moisture (Equation 4.5),

$$\frac{\partial \theta_m}{\partial t} = \frac{\partial}{\partial x}\left[K(h)\left(\frac{\partial h}{\partial x} + 1 \right) \right] + \frac{\partial}{\partial z}\left[K(h)\left(\frac{\partial h}{\partial z} + 1 \right) \right] - \Gamma_w \qquad \text{and} \qquad \frac{\partial \theta_{im}}{\partial t} = \Gamma_w \qquad \text{Equation 4.5}$$

with θ_m [-] and θ_{im} [-] being the volumetric soil moisture content in the mobile and the immobile region, respectively and Γ_w [T^{-1}] being the mass transfer rate from the mobile to the immobile region (Gerke and van Genuchten, 1993). This mass transfer rate is assumed to be proportional to the difference in effective saturation between the mobile and the immobile regions (Equation 4.6),

$$\Gamma_w = \frac{\partial \theta_{im}}{\partial t} = \omega[S_e^m - S_e^{im}] \qquad \text{Equation 4.6}$$

where S_e^m [-] and S_e^{im} [-] are the effective saturation of the mobile and the immobile region, respectively, and ω [T^{-1}] is a first order rate coefficient (Simunek et al., 2003). As ω depends on many unknown soil properties, the model was calibrated to find the best corresponding simulation for the measured pressure heads.

4.3.2.3.2   Residence time and solute transport

We estimated the residence time of the porewater in the marsh soil to determine the locations where water is replaced on a short time scale. For this purpose, the transport of a non-reactive solute was implemented in the model and we calculated for each location in the domain the half-life, i.e. the time it takes to remove half of the solute mass in that location. The initial tracer concentration in the pore water in the domain was set to 1 whereas the concentration in the flooding water was set to 0. As such, during the simulation, porewater seeps out of the creek banks and is replaced with flooding water. Since the residence time is essentially simulated as a 'tracer', this method takes into account dispersion and diffusion, in contrast to more traditional groundwater age determination methods such as particle tracking (Goode, 1996; Suckow, 2014; Turnadge and Smerdon, 2014; Wilson and Gardner, 2006).

For the dual porosity model, the solute flux equations for the mobile and immobile region are given by Equation 4.7 (advection dispersion equation) and Equation 4.8, respectively (van Genuchten and Wierenga, 1976).

$$\theta_m \frac{\partial c_m}{\partial t} = \frac{\partial}{\partial x}\left(\theta_m D_m \frac{\partial c_m}{\partial x}\right) - \frac{\partial q_x c_m}{\partial x} + \frac{\partial}{\partial z}\left(\theta_m D_m \frac{\partial c_m}{\partial z}\right) - \frac{\partial q_z c_m}{\partial z} - \Gamma_s \qquad \text{Equation 4.7}$$

$$\Gamma_s = \theta_{im} \frac{\partial c_{im}}{\partial t} = \omega_s (c - c_{im}) + \Gamma_w c^* \qquad \text{With} \quad c^* = \begin{cases} c_m & \Gamma_w > 0 \\ c_{im} & \Gamma_w < 0 \end{cases} \qquad \text{Equation 4.8}$$

In these equations, c_m and c_{im} [ML^{-3}] are the concentrations of the solute in the mobile and immobile region, respectively. q_x and q_z [LT^{-1}] are the volumetric flux densities in the x and z dimension. Γ_s [MT^{-1}] is the solute exchange rate between the two regions and ω_s [T^{-1}] is the solute exchange rate coefficient. D_m [L] is the dispersion coefficient of the mobile region, which is defined as Equation 4.9,

$$D_m = \frac{\theta}{\theta_m} D \qquad \text{Equation 4.9}$$

where D [L] is the effective dispersion coefficient. Dispersion rates differ in the x and z direction. The dispersion for a vertical two-dimensional domain can be written as Equation 4.10 (Bear, 1972),

$$\begin{cases} \theta D_{xx} = D_L \dfrac{q_x^2}{|q|} + D_T \dfrac{q_z^2}{|q|} + \theta D_w \tau_w \\[2mm] \theta D_{zz} = D_L \dfrac{q_z^2}{|q|} + D_T \dfrac{q_z^2}{|q|} + \theta D_w \tau_w \\[2mm] \theta D_{xz} = (D_L - D_T) \dfrac{q_x q_z}{|q|} \end{cases} \qquad \text{Equation 4.10}$$

where D_L and D_T [L] are the longitudinal and transversal dispersivities, respectively, D_w [L] is the molecular diffusion coefficient and τ_w [-] is the tortuosity factor, which was estimated as Equation 4.11 by Millington and Quirk (1961).

$$\tau_w = \frac{\theta^{7/3}}{\theta_s^2}$$

Equation 4.11

In our simulations, we assumed that the solute concentration in the immobile region is initially in equilibrium with the mobile region. Table 4.1 gives an overview of the values of the model input parameters and how they were defined.

Table 4.1: Model input parameters

Soil layer	Upper layer	compact layer
ρ_b [g/cm^3]	0.54 [a]	1.10 [a]
K_s [m/s]	3.50·10^{-5} [a,b]	4.16·10^{-8} [a]
$\theta_{s,m}$ [-]	0.05 [a,c]	0.55 [a,c]
$\theta_{s,im}$ [-]	0.71 [a,c]	0.01 [a,c]
$\theta_{r,m}$ [-]	0.00 [a,c]	0.00 [a,c]
$\theta_{r,im}$ [-]	0.09 [a,c]	0.01 [a,c]
α [m^{-1}]	3.45 [a]	0.37 [a]
n [-]	1.19 [a]	1.18 [a]
ω [-]	5.00·10^{-3} [b]	5.00·10^{-3} [b]
D_L [m]	0.10 [d]	0.10 [d]
D_T [m]	0.01 [d]	0.01 [d]
D_w [m^2/s]	1.00·10-9 [e]	1.00·10-9 [e]
ω_s [s^{-1}]	8.33·10^{-7} [f]	8.33·10^{-7} [f]

[a] lab measurements on soil samples and parameter estimation with RETC
[b] model calibration
[c] based on micro-CT scans in Van Putte et al. (2020)(Chapter 2)
[d] based on Wilson and Gardner (2006)
[e] based on Holz et al. (2000)
[f] based on Jaynes and Horton (1998)

4.3.2.3.3   Drainage depth

We analyzed groundwater drainage depth on two time scales that are relevant in context of a tidal system, and we refer to these two time scales by introducing the terms "spring tide drainage depth" and "neap tide drainage depth". During about 10 days around the occurrence of spring tide, the marsh surface is flooded by most semi-diurnal high tides, and emerges during every semi-diurnal low tide (Figure 4.2). The spring tide drainage depth is then defined as the average groundwater drainage depth below the soil surface in between tides that flood the marsh platform (i.e. the lowest groundwater level reached during the low water phase in between two high water phases that both inundate the marsh platform). The spring tide drainage depth relates to the zone which desaturates nearly every tide. The neap tide drainage depth is defined as the maximum drainage depth that

occurred during the measured timespan. This drainage occurs during neap tide when the marsh platform is not inundated for several days (Figure 4.2). Underneath the neap tide drainage depth, the soil remains always saturated. Drainage depths were calculated using the Tides package for R (Cox and Schepers, 2018).
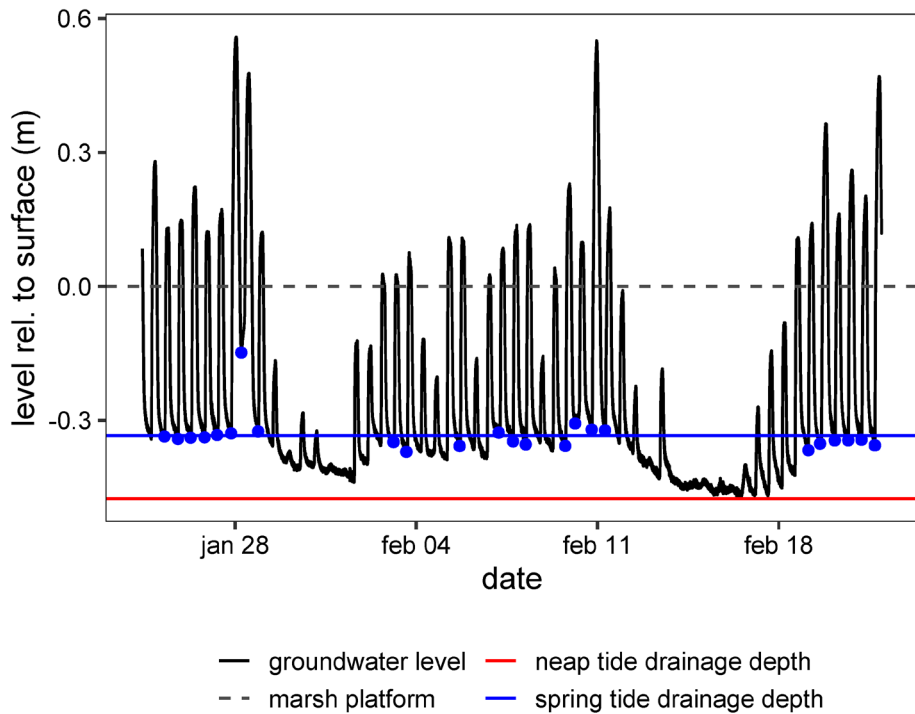

Figure 4.2: Clarification of the newly introduced terms 'spring tide drainage depth' and 'neap tide drainage depth'. This figure represents the measured groundwater level at 1 m from the creek edge during two spring tide - neap tide cycles. The blue bullets indicate the drainage depth between consecutive flooding tides. The spring tide drainage depth is defined as the average of these values.

4.3.2.4   Sensitivity analysis

The model was tested for its sensitivity to values for the parameters K_s, α and the mass transfer coefficient ω. The saturated hydraulic conductivity K_s is the most important hydraulic parameter governing groundwater flow and seepage (Gardner, 2005b; Xin et al., 2012) and laboratory measurements revealed a wide variation on the data spanning multiple orders of magnitude (Figure 4.3). The α parameter is a shape parameter of the SWRC and is roughly related to the inverse of the air entry value, the matric potential which corresponds to the beginning of desaturation (Van Genuchten et al., 1991). The ω value had to be calibrated because it could not be estimated from the measured hydraulic properties. A value of 0.05 resulted in the best model performance. The model performance

was evaluated with the Nash-Sutcliffe model efficiency coefficient (Equation 4.12) (Nash and Sutcliffe, 1970) by comparing the simulated and measured pressure heads,

$$ME = 1 - \frac{\sum(OBS - SIM)^2}{\sum(OBS - MEAN)^2}$$
<div align="right">Equation 4.12</div>

where *ME* is the model efficiency coefficient, *OBS* are the observed pressure heads, *SIM* are the simulated pressure heads and *MEAN* is the mean of the observed pressure heads. Observed and simulated pressure heads during flooding of the marsh platform were not included in the evaluation since this would lead to overestimation of the model efficiency as the pressure head at the top boundary of the domain was set equal to the measured pressure head during inundation.

4.3.3   Scenario analyses

In total, we ran 25 different scenarios in which the depth (relative to the soil surface) of the compact layer and the number of creeks in the domain were varied. The depth of the compact layer was varied as 20 cm, 40 cm, 60 cm, 80 cm and 100 cm below the soil surface. A transition depth of 60 cm is the reference situation. A scenario with a deeper or less deep soil transition can represent either a difference in sedimentation rate of the marsh, or the depth to which soil amendments (e.g. tillage with addition of organic matter to increase soil porosity) are applied in a newly restored tidal marsh.

Model domains with 1, 2, 3, 4 and 5 creeks along the 50 m long transect were considered. As a result, the distance between the creeks varies from 50 m (1 creek in domain) to 10 m (5 creeks in domain). These distances are within the range of the average distance to the nearest tidal creek generally observed in tidal marshes (Chirol et al., 2018). When increasing the creek density, the creek width to depth ratio of all the creeks in the domain was conserved. This was done to approximate realistic scenarios, for which excavating of the creeks would result in creek dimensions that are expected to be close to morphodynamic equilibrium. At equilibrium, the total cross sectional area of creeks in a tidal marsh is proportional to the tidal prism, i.e. the total flood and ebb water volumes flooding onto and draining from the surrounding marsh platform surface area (D'Alpaos et al., 2010; Lawrence et al., 2004; Vandenbruwaene et al., 2013). Following this reasoning, in the different scenarios with increasing number of creeks over our cross-section, we made sure that the total creek cross-sectional area remained constant, as the tidal prism is not changing in between the different scenarios. Where the statistical significance of differences between the outcome of different scenarios was tested, we used a two-way ANOVA.

4.4   Results

4.4.1   Field data and model input

4.4.1.1   Measured soil properties

An analysis of the soil properties reveals the distinct characteristics of the relict compact soil (lower layer) and the newly deposited sediment (upper layer). The bulk density in the lower layer is more than twice the bulk density in the upper layer (Figure 4.3a). This difference is also reflected in the K_s values (Figure 4.3b).
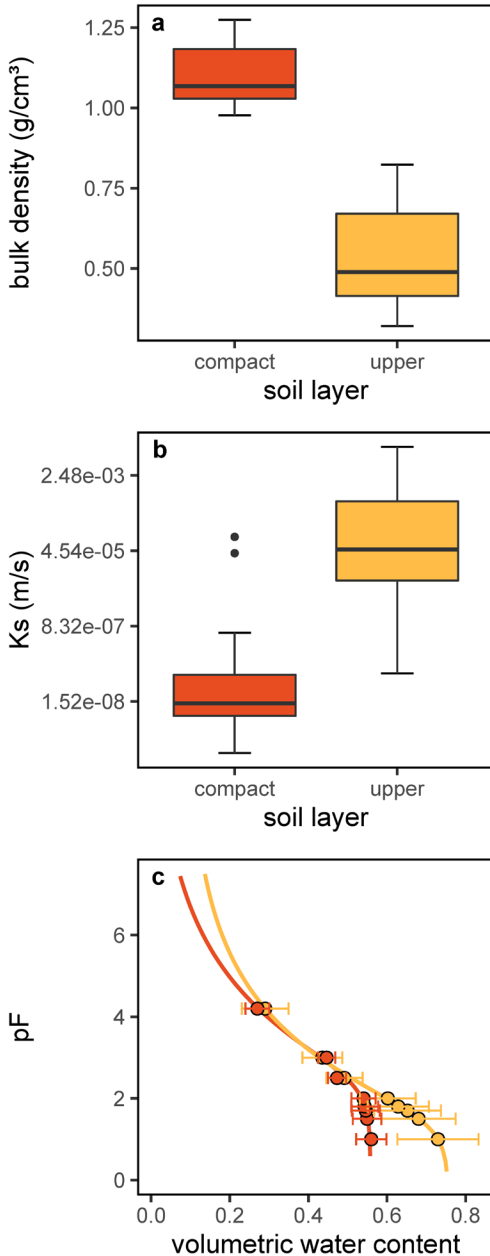

Figure 4.3: Soil hydraulic properties for the compact soil layer (orange) and the layer of newly deposited sediment (yellow). (a): boxplot of the bulk density (n=16) (b): boxplot of the saturated hydraulic conductivity (n=16) (note the logarithmic y-axis), (c): soil water retention curves. bullets indicate the measured water contents to the corresponding applied suction and error bars represent the standard deviation on these values (n=8). Lines depict the regression curves using the van Genuchten – Mualem model (Mualem, 1976).

The hydraulic conductivity of the upper layer shows values ranging over several orders of magnitude, denoting a large spatial heterogeneity of soil physical properties and the presence of macropores. The hydraulic conductivity of the lower layer is on average 1476 times lower and less variable than in the upper layer (Figure 4.3b). Figure 4.3c shows the soil water retention curve for both soil layers. The upper soil layer has a higher porosity (Table 4.1). In the low pressure range (10 – 100 cm), the soil water content decreases more with an increasing suction in the upper layer compared to the lower layer, indicating the presence of larger pores in the upper layer. At higher suctions, the soil water retention curves for both layers converge.

4.4.1.2   Measured subsurface hydrology

The subsurface hydrology measured at the transect follows a distinctive pattern. During flooding of the marsh platform, the water level in the wells approximates the surface water level (Figure 4.4). In all wells, but especially in the well at 4 m from the creek, a time lag is observed. When the tide recedes towards low tide, the groundwater level declines until the next flooding high tide. This decline is more profound close to the creek and attenuated further away from the creek.
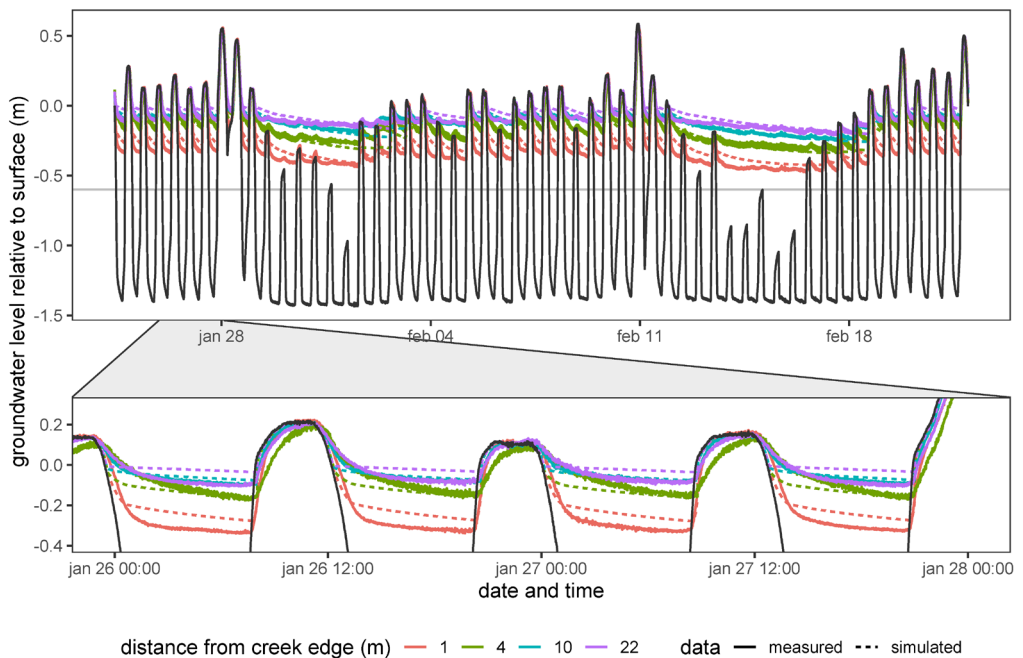

Figure 4.4: Comparison of the measured and simulated groundwater level fluctuations on a transect perpendicular to a tidal creek in the restored marsh covering two spring tide - neap tide cycles in the winter of 2019. The solid black line represents the creek surface water level that was used as a time variable boundary condition in the model. The grey horizontal line indicates the approximate depth of the transition between the tidally deposited sediment and the underlying compact soil.

During neap tides, the groundwater level in the marsh soil declines further. Tides that only flood the creeks but not the marsh platform affect the groundwater level only in the close vicinity of the tidal creek. The groundwater level never falls below the transition between the newly deposited sediment and the compact soil, which remains always saturated.

4.4.2 Model performance

The model was run with the parameters indicated in Table 4.1. The model input parameters Ks, α and ω were calibrated to obtain the best simulated pressure heads. For these parameters, a sensitivity analysis was performed, which is summarized in Supplement S4.1 and Figure S4.1. The drainage depth was simulated with good accuracy (ME > 0.55) up till 10 m from the creek (Table 4.2).

Table 4.2: Nash-Sutcliffe model efficiency coefficient for simulated and measured pressure heads along the transect.

Distance from creek edge	ME coefficient
1 m	0.57
4 m	0.68
10 m	0.66
22 m	-0.14

At 1 m from the creek, the model underestimated the spring tide drainage depth, which may be because of the steeper creek edge on the field transect vs. the modeled transect (Figure 4.1). Our model always underestimated the drainage depth at 22 m from the creek. The latter may be because further away from the transect creek, other (smaller) creeks may also influence the local groundwater level in the field, while this is not represented in the model. Because in the scenario analysis we focus on scenarios with smaller distances between creeks, we decided to calibrate the unknown model parameters for best model performance on the results up to 10 m from the creek.

4.4.3 Impact of the compact layer on subsurface hydrology

We quantify the effect of the presence of the compact layer by making a comparison between the base scenario (compact layer at 60 cm depth) and a scenario without a compact layer (i.e. the entire soil profile consists of tidally deposited sediment). For the latter scenario, the lower layer was attributed the same hydraulic properties as the upper layer.
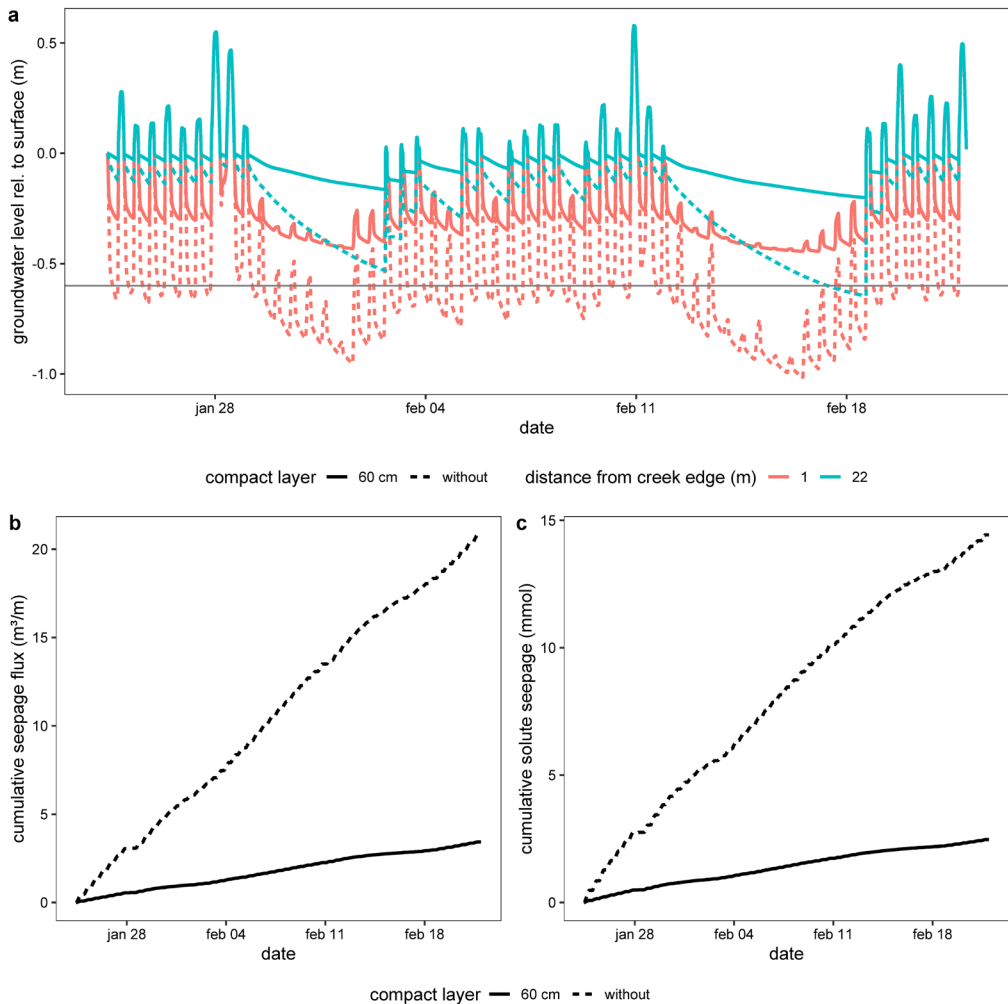
Figure 4.5: Comparison of a simulation in the absence of a compact layer and with a compact layer at a depth of 0.60 m. (a): groundwater level fluctuations during 2 spring tide – neap tide cycles near the creek and in the marsh interior. The grey horizontal line indicates the depth of the compact layer if present. (b): cumulative seepage flux per meter creek length. (c): cumulative solute seepage flux per meter creek length.

In between tides that flood the marsh platform, the spring tide drainage depth at 1 m from the creek is 0.28 m in the base scenario and 0.45 m in the scenario without a compact layer. In the marsh interior at 22 m from the creek, the difference in the spring tide drainage depth between the base scenario and the scenario without a compact layer is smaller (Figure 4.5). Here, the effect of the compact layer is more pronounced in the neap tide drainage depth (0.04 m vs. 0.15 m). From Figure 4.5a, it is apparent that in the marsh interior, the drainage depth depends mainly on the elapsed time since the last inundation of the marsh platform. Figure 4.5b represents the cumulative seepage flux over the time. This is the total volume of water that passed through the marsh soil and seeped out of the creek banks during the simulated time. Without a compact soil layer, 6.06 times more

water passes through the marsh soil compared to the current situation. The cumulative solute seepage flux (Figure 4.5c), shows a similar pattern. The solute mass removed from the domain after two spring tide – neap tide cycles is 5.84 times higher without the presence of the compact layer. Especially in the run without the compact layer, the solute seepage rate slightly decreases near the end of the simulation. This indicates the start of depletion of solute in the zone near the creek.
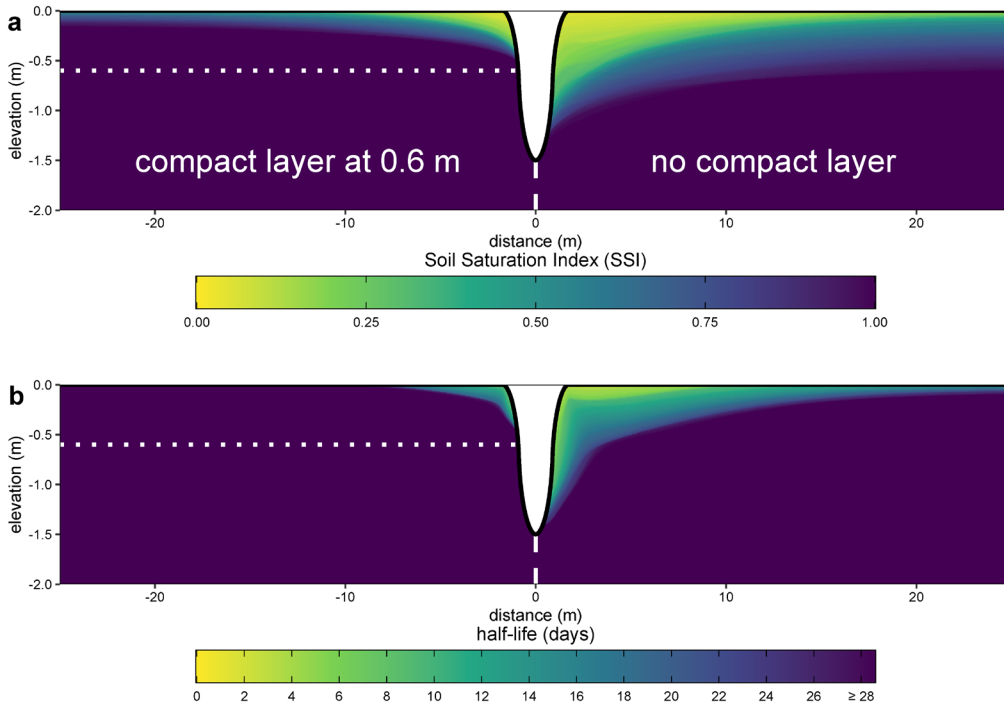

Figure 4.6: (a): Spatial distribution of the soil saturation index (SSI) for the simulation in the absence of a compact layer (right) and the simulation with a compact layer at 0.60 m (left). A value of 1 indicates that the soil at that location is saturated for 100% of the time. Saturated soil is defined as soil where $\theta \geq \theta_s - 0.01$. (b): Spatial distribution of the solute half-life (i.e. the time it takes to remove half of the solute mass at a given location). A half-life of > 28 days means that no solute was removed in that location of the domain during the simulated timespan (2 spring tide – neap tide cycles). The dotted horizontal line represents the transition between the compact soil and the tidally deposited sediment.

The presence of the compact layer strongly affects the spatial distribution of the SSI (soil saturation index). The proportion of the domain in which the soil is unsaturated for at least half of a spring tide – neap tide cycle is 4.70 times higher without the presence of a compact layer compared to the base situation. In this base situation, the variably saturated zone (i.e. zone at least unsaturated for some of the time), is limited to only 0.38 m below the soil surface near the creek (at 1 m) and 0.15 m in the marsh interior (at 22 m from the creek edge, Figure 4.6a). In the simulation without a compact layer, this zone extends to a depth of 1.06 m near the creek and 0.60 m in the marsh interior.

The effect of the compact layer is also clearly present in the retention times of a non-reactive solute in the domain. Figure 4.6b shows the half-life (time it takes to remove half of the mass of the solute) for the domain. In the base simulation, the soil further away than ca. 7 m from the creek edge never loses half of its solute mass over the simulated 28-days period. Here, solute is only removed in the vicinity of the creeks. In the scenario without a compact layer, solute is partly removed up to a depth of 0.09 m, even in the marsh interior (22 m from the creek edge).

4.4.4   Scenario analyses for tidal marsh restoration design options

Model scenarios were run to simulate (i) creek excavation and (ii) soil amendments as possible restoration design options to optimize groundwater dynamics in newly restored tidal marshes. Therefore, 25 different model domains were made with all possible combinations of (i) transition depth between the upper loose sediment layer and bottom compact layer at 0.20, 0.40, 0.60, 0.80 and 1 m depth and (ii) 1, 2, 3, 4 and 5 creeks over the 50-m cross-section.

Close to the creeks, we see a large significant effect ($p < 0.001$) of the transition depth on the spring tide drainage depth as well as on the neap tide drainage depth (Figure 4.7a). However, as the transition of the soil layers gets deeper, the effect decreases. At 1 m from the creek edge, the number of creeks in the domain does not significantly alter the spring tide drainage depth ($p = 0.18$). The neap tide drainage depth, however, is significantly affected by the number of creeks ($p = 0.01$) . Until a transition depth of 60 cm, the drainage depth increases with the number of creeks. For transition depths larger than 80 cm, however, the drainage depth decreases when the number of creeks becomes larger than 3 (Figure 4.7c). This effect can be attributed to the reduction in creek depth with an increasing number of creeks, as we applied a constant total creek cross-sectional area (see methods for reasoning). Further away from the creeks, the spring tide drainage depth is significantly affected by both the soil layer transition depth and the number of creeks ($p < 0.001$). Here also, at deeper soil layer transition depths, over 5 creeks in the domain do not increase the drainage depth anymore. Over the entire marsh domain, both the number of creeks and the soil layer transition depth affect the depth of the variably saturated zone, whereas closer to the creek the soil layer transition has a more profound effect.
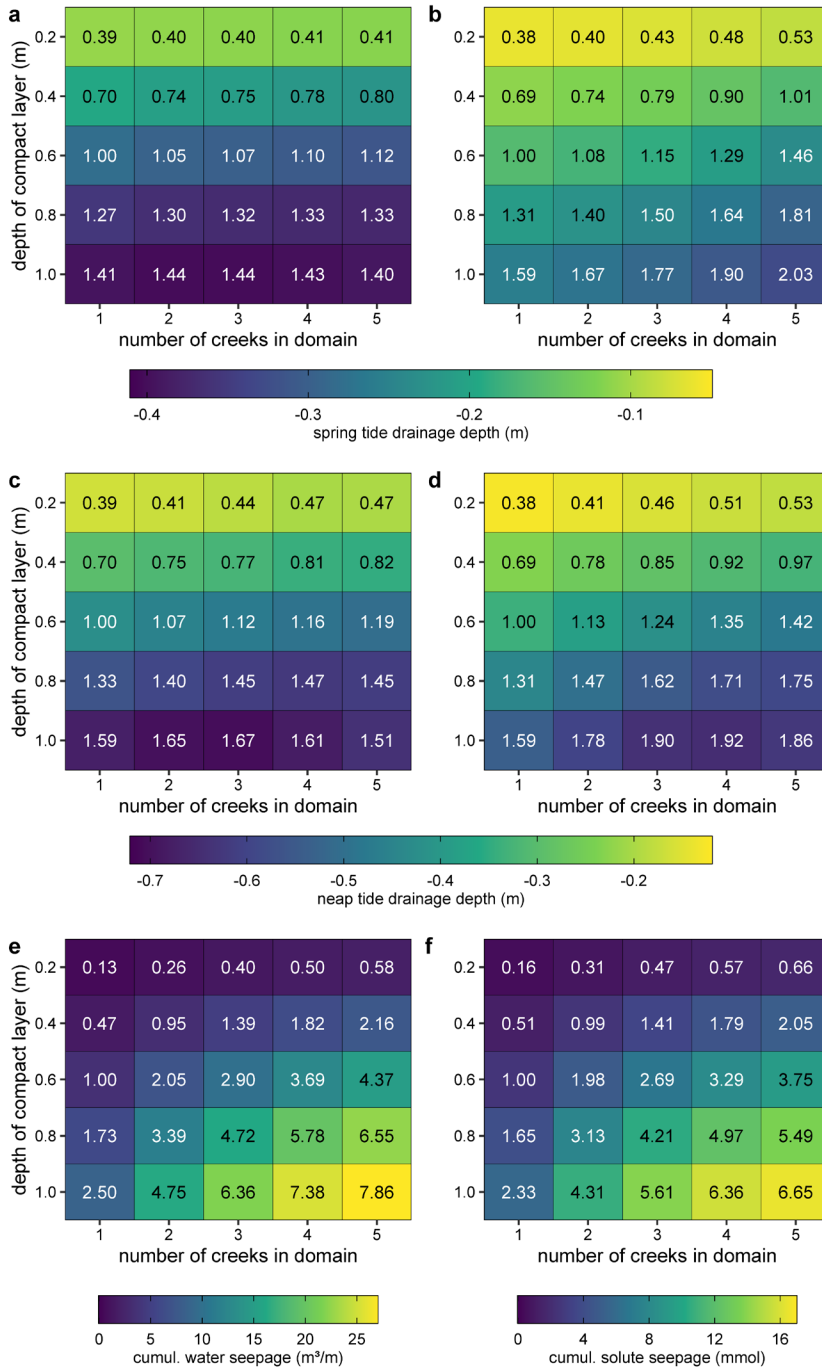
Figure 4.7: (a,b): Spring tide drainage depth relative to the soil surface at 1 m and 4 m from the creek edge, respectively; (c,d): neap tide drainage depth relative to the soil surface at 1 m and 4 m from the creek, respectively; (e): cumulative water seepage volume after two spring tide – neap tide cycles (expressed in volume per meter creek length); (f): cumulative solute seepage after two spring tide – neap tide cycles. Labels in the plots represent the value of the respective scenario relative to the base scenario (with 1 creek in the domain and transition depth at 0.60 m below the soil surface).

Both the number of creeks in the domain and the soil layer transition depth positively affect the volume of water that effectively flows through the marsh soil over a given timespan (Figure 4.7e). Compared to the base scenario, multiplying the number of creeks with a factor of 2, leads to more than a doubling of the cumulative water seepage flux. The effects on the cumulative solute flux are similar (Figure 4.7f), although, as mentioned earlier, the cumulative solute flux on a longer time span is expected to congregate for the different scenarios, as it is ultimately limited by depletion of solute in the domain.

The proportion of the time that the soil is saturated (the soil saturation index, SSI) is affected by both the number of creeks in the domain and the depth of the soil transition. Here, we assume that a specific location in the soil is unsaturated when the local soil moisture content is 1% lower than the soil moisture content at saturation. We compare the extent of the zone where the SSI is under 95% between the different scenarios.
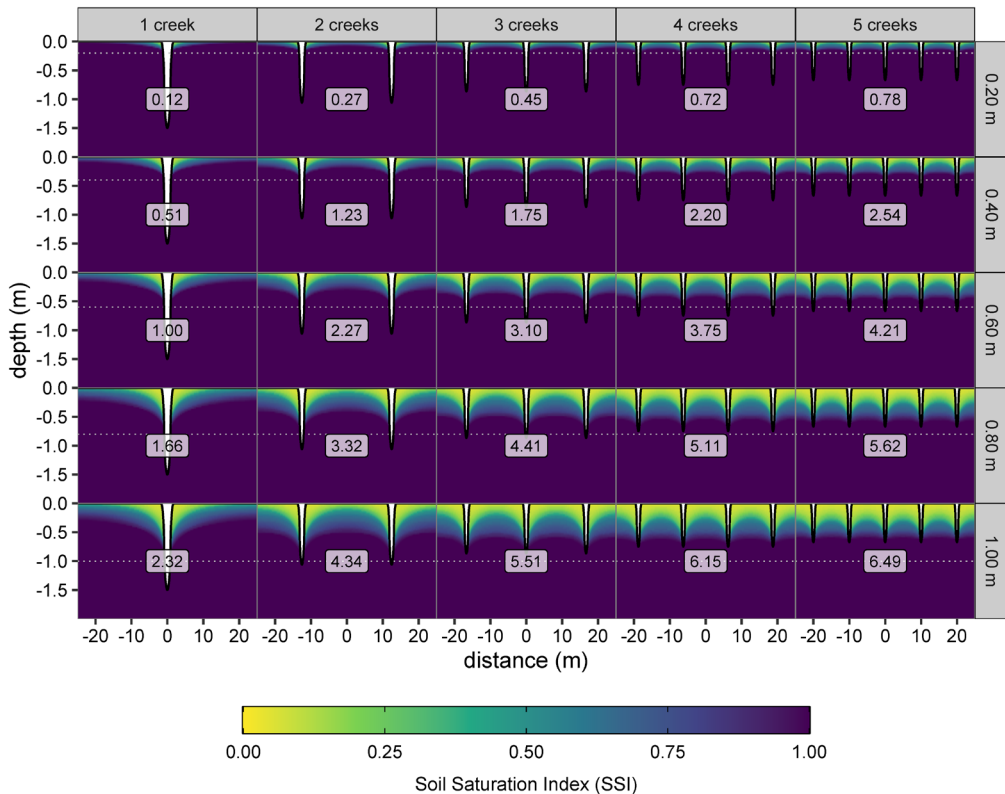

Figure 4.8: Spatial distribution of the Soil Saturation Index for all the scenarios during two spring tide – neap tide cycles. An SSI of 1 means that the soil is always saturated. Saturated soil is defined as soil where $\theta \geq \theta_s - 0.01$. The labels indicate the proportion of the domain that is unsaturated for at least 50% of the simulated timespan, relative to the reference scenario (with 1 creek and transition depth at 0.60 m), where this proportion is 0.025. Dashed horizontal lines indicate the soil layer transition.

Both the number of creeks in the domain and the soil layer transition depth affect the SSI. In all scenarios, the extent of the variably saturated zone is limited to the layer of newly deposited/amended soil. A larger number of creeks increases the extent of the variably saturated zone (Figure 4.8). Although the marsh platform is inundated for 17% of the time, the SSI near the surface is lower than this value. This indicates that the soil can remain (slightly) unsaturated, even during inundation.
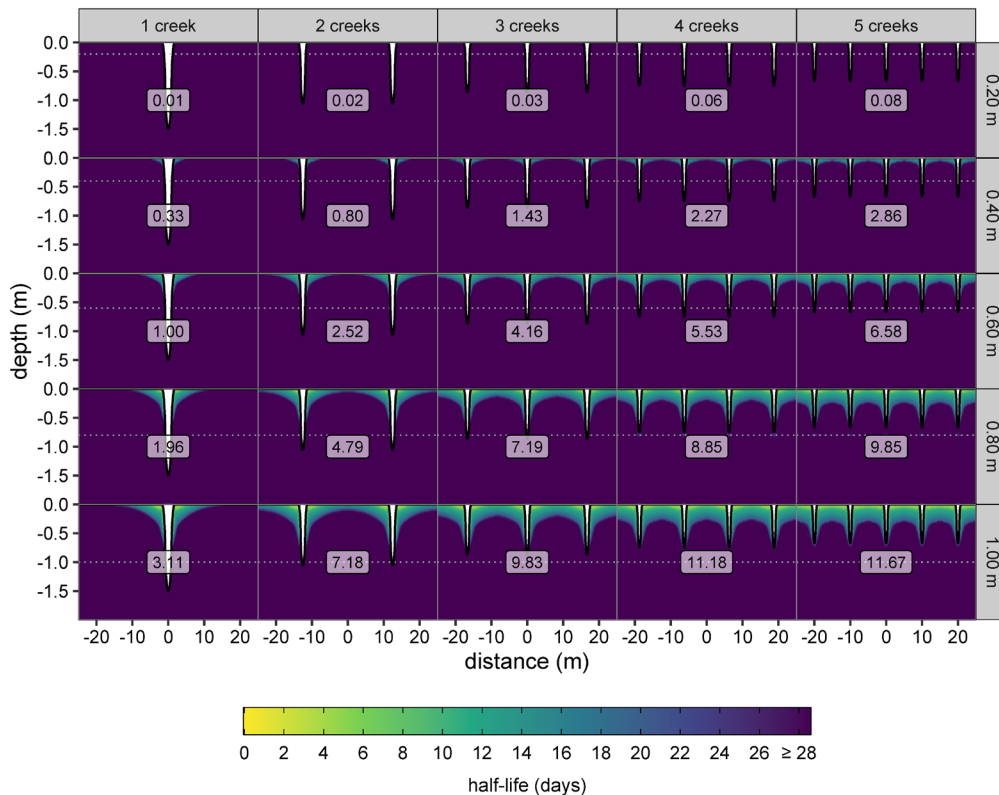

Figure 4.9: Spatial distribution of the time it takes to remove half of the solute mass (half-life) for all the scenarios. Half-lives of over 28 days indicate that the solute mass remained larger than 50% of the initial mass during the entire simulation time (two spring tide-neap tide cycles). Labels indicate the proportion of the domain in which at least 50% of the solute mass was removed within the simulation time, relative to the base scenario (1 creek and transition depth at 0.60 m), in which this proportion is 0.017. The dotted white lines indicate the transition between the soil layers.

We further investigated the removal of a conservative tracer in the domain in which the porewater has an initial concentration of 1 and the concentration in the flooding water is 0. We calculated for every node in the domain the time it takes to remove half of the solute mass in that node. Close to the creek edges, this 'half-life' time is short, as the solute is transported by advection to the creek during the falling tide and the porewater is replaced by infiltrating surface water during the rising tide (Figure 4.9). The concentration near the creek edges increases again when porewater from the marsh interior flows towards the

creeks during the next falling tide. Hence, the concentration near the creek edges follows an oscillating pattern (not shown).

In the marsh interior, where the soil is mostly saturated, solute is predominantly removed by diffusive processes. Initially, the tracer is rapidly removed but the removal rate declines as the most active zone gets depleted in tracer mass. We can expect that in the compact soil in the marsh interior, it can take decades to centuries for all the solute tracer to be removed from the porewater.

4.5   Discussion

Agricultural soil compaction alters the structure of the soil in formerly embanked and drained wetlands. When tidal marshes are restored on such compact agricultural land, their subsurface hydrology is impaired compared to natural tidal marshes, which may result in reduced vegetation growth and altered biogeochemical cycling. The compact agricultural soil layer typically persists long after restoration and forms a barrier for groundwater dynamics and associated ecosystem functioning (Crooks and Pye, 2000; Tempest et al., 2015; Van Putte et al., 2020 (Chapter 2)). Regarding the latter, there is a critical need for understanding of subsurface ecohydrology in restored tidal marshes to optimize delivery of ecosystem services in future tidal marsh restoration projects. In this chapter, we use a vertical 2D variably saturated dual porosity groundwater model to simulate groundwater flow in a restored tidal marsh with a compact subsoil. For the first time for tidal marshes, we also solve the solute transport problem using the advection dispersion equation. This enables us to calculate the residence time and half-life of a non-reactive tracer, which is not possible by solving only the flow problem. With this coupled model, we are able to accurately predict the pressure head distribution in the marsh up to 10 m from the creek edges. Our model results clearly show that the compact layer limits tidally induced porewater circulation in the marsh soil.

The model is focused on tidally induced groundwater dynamics and solute transport and does not consider porewater extraction by evapotranspiration by vegetation and porewater recharge by precipitation. In this study, we only considered porewater circulation during winter, when the effects of evapotranspiration are negligible. Nevertheless, evapotranspiration has a major effect on porewater removal in the growth season, especially in the marsh interior where porewater drainage towards creeks is limited (Hemond and Fifield, 1982; Nuttle, 1988). We observed that during the growth season, neap tide drainage depths in the marsh interior are deeper compared to the winter season (data not shown). Near the creek, tidally induced porewater circulation prevails, also in the summer growing season. While our calculations therefore might overestimate the soil saturation index, especially for marsh interior locations farther away from creeks, we argue that seepage fluxes, residence times and associated effects on biogeochemical cycling are much more affected by tidally induced porewater circulation. After all, we showed, in accordance with Harvey et al. (1987), that the majority of the seepage and solute transport originates from the soil in the vicinity of tidal creeks. Our model also does

not consider shrinking and swelling and compression of the soil matrix during tidal inundation. According to Wilson and Morris (2012) and Gardner and Wilson (2006), omitting soil compressibility effects from the model can result in overestimation of seepage fluxes. However, Xin et al. (2009b) point out that the effect of soil compressibility is minimal and can be ignored for soils with a hydraulic conductivity larger than 10^{-6} m/s, which is the case for the tidally deposited sediment in our model ($3.50\cdot10^{-5}$ m/s). Variably saturated pore water flow in our model is governed by the single phase (only water flow) form of the Richards' equation (Richards, 1931) and therefore does not explicitly consider the flow of air in soil pores, which can have a significant effect on the estimation of soil aeration. Not incorporating the entrapment of air may lead to a persistent unsaturated zone and an overestimation of infiltration volumes during inundation (Li et al., 2005). However, Xin et al. (2009b) argue that it is unlikely that such a persistent unsaturated zone would exist in the presence of large macropores (e.g. crab burrows) as is the case in the restored tidal marsh considered in our study.

Decomposition of large organic matter parts (e.g. plant stems and roots) leads to void spaces that act as preferential flow channels and, in this way, further enhances porewater circulation in the marsh soil. Previous studies have shown that groundwater flow in tidal marshes is often dominated by preferential flow through macropores (Van Putte et al., 2020 (Chapter 2); Xin et al., 2009b; Xin et al., 2016). Therefore, we constructed a model domain consisting of a micropore region and a macropore region that can exchange porewater based on the respective volumetric soil moisture content in both regions. In this way, we accounted for the fast initial drainage trough the macropores and a slower drainage during neap tides when water from the micropore region is transferred to the macropore region and drains towards the creeks (Figure 4.4). In general, our model was able to simulate the pressure head distribution with good accuracy up to 10 m from the creek edge. Further away from the creek edge, our model systematically overestimated the groundwater level compared to field measurements. We hypothesize that this is due to the choice of boundary conditions. To generalize our model results, we applied a flat surface topography to our model, whereas in the field the marsh elevation decreases further away from the creek (Figure 4.1c), increasing the hydraulic gradient. Furthermore, our model considers only groundwater flow along a one-dimensional transect and in relation to one creek. The farther away from that one considered creek, the larger the chance that the observed groundwater dynamics are related to more complex flow patterns. This may also contribute to the increasing deviation of model simulations and observations with increasing distance from the considered creek. In our simulations we did not consider evapotranspiration, soil compressibility and air entrapment. As a result, our model has fewer input parameters and is therefore easier to apply and modify by other scientists aiming to support stakeholders in decision making concerning optimal marsh restoration design.

Based on scenario analyses, we identify and evaluate design measures for marsh restoration, which can alleviate the effects of the compact layer on the hindered groundwater circulation.

Even a decade after the marsh restoration, the compact soil layer forms a barrier for soil-groundwater interactions. Our model results suggest that approximately 6 times more water would pass through the marsh soil during a spring tide – neap cycle in the absence of the compact layer, compared to the present situation (Figure 4.4). The median hydraulic conductivity in the compact layer in our study area is $4.16·10^{-8}$ m/s, and is therefore classified as nearly impermeable following the classification of Bear (1972). The presence of the compact layer decreases the drainage depth and increases the soil saturation index in tidal marshes, leading to more frequent waterlogged soils and reduced aeration depth (Figure 4.6a). This soil aeration is, however, crucial for the establishment and zonation of tidal wetland plants; waterlogged soils can inhibit the growth of several plant species (Hou et al., 2020). The soil saturation index of the upper marsh soil correlates with spatial plant zonation in tidal wetlands (Ursino et al., 2004; Xin et al., 2013). Tidal marsh habitats adjacent to tidal creeks are less prone to vegetation die-off and provide better plant growth conditions. The absence of a developed creek network may therefore lead to the formation of pools and waterlogged soils (Schepers et al., 2017). Thus, an extended creek network is beneficial for both surface and subsurface drainage.

Tidal marshes restored on formerly embanked agricultural land often exhibit a lower creek density compared to natural tidal marshes. The presence of the compact agricultural soil inhibits or slows down natural creek incision and creek network development (Liu et al., 2020; Vandenbruwaene et al., 2012). Hence initial excavation of creeks may be advised to stimulate porewater seepage and soil aeration. We found that compared to the reference situation (1 creek in a 50 m transect and the compact layer at a depth of 60 cm), doubling the creek density more than doubles the proportion of the marsh soil with an SSI smaller than 50 % (Figure 4.8) and the volume of water that flows through the marsh soil. However, as more creeks are added to the domain, their depth decreases to conserve the total creek cross sectional area. As a consequence, the effect of excavating more creeks on groundwater flow decreases with an increasing number of creeks already present. A creek density of more than 3 creeks in 50 m even reduces the drainage depth (Figure 4.7c), highlighting the effect of creek depth on drainage depths. When the compact layer is shallow (i.e. in the early stage after the restoration), however, the reduction in drainage depth with an increasing creek density was not observed. We conclude that especially the interaction between the creek density and the depth of the soil transition determines soil aeration, drainage depths and seepage fluxes. Soil amendments (by tilling the soil and/or mixing it with organic matter) increase the hydraulic conductivity of the soil (Kuncoro et al., 2014) and increase the depth from the soil surface to the compact layer. Based on the results of the scenario analyses, we can state that increasing the depth to the compact layer promotes soil aeration, seepage fluxes and soil-groundwater interactions, which are

crucial for biogeochemical cycling in tidal marshes. A combination of both creek excavation and soil amendments is therefore suggested for new tidal marsh restoration projects.

Porewater drainage is the main driver for silica recycling in tidal marshes, which plays a major role in estuarine primary production by diatoms (Struyf et al., 2005). Dissolved silica, resulting from the dissolution of biogenic silica from marsh vegetation, for example, is advectively transported with the porewater draining towards the creeks (Struyf et al., 2006). Our model simulations indicate that the residence time of the porewater in the marsh soil decreases when soil amendments and/or creek excavation are applied. In the compact subsoil, the half-life of the solute tracer exceeds the simulation time (28 days). This suggests that dissolved nutrients in the compact layer reside months or even years before seeping out of the creek banks, which is consistent with Xin et al. (2011). As the availability of biogenic silica (BSi) in most tidal marshes is constantly high and dissolution occurs fast (Struyf et al., 2007), we expect an increased delivery of dissolved silica (DSi) to the estuary when residence times are shorter. With a shallow compact layer and high residence times, further dissolution of BSi might be hampered due to high concentrations of DSi already present in the porewater. According to our model results, silica delivery could be enhanced by ensuring a sufficient creek density and an upper porous soil layer. Both the number of creeks in the domain and the depth to the compact layer affect the residence time and turnover rate of nutrients in the marsh porewater.

Increased soil aeration by creek excavation and soil amendments is expected to increase nitrification processes as those processes are aerobic, and subsequent denitrification which is primarily limited by the availability of nitrate and the presence of organic carbon (Martin and Reddy, 1997; Wolf et al., 2011). Soil amendments in which organic matter is added can thus promote denitrification. On the other hand, faster drainage and increased soil aeration facilitates organic matter mineralization and can therefore decrease the contribution of the marsh to carbon sequestration (e.g. Guimond et al., 2020), although further research is needed to investigate the impact of soil aeration on carbon sequestration in restored tidal marshes.

Excavating a denser creek network does not only alter subsurface flow, soil aeration and nutrient cycling, but will also affect surface flow hydrodynamics and sedimentation – erosion processes, and as such influence the bio-geomorphic development of the restored marsh (Gourgue et al., 2021). Although this is beyond the scope of this paper, it is clear that marsh design options can have different effects on the various functions and ecosystem services of restored marshes. With this chapter, we contribute to the knowledge on the effect of different design options on ecosystem functioning, so that stakeholders of a marsh restoration project can make a design based on prioritizing the delivery of certain ecosystem services.

4.6   Conclusions

- Using a dual porosity groundwater model, we were able to accurately simulate pressure head dynamics in a restored tidal marsh up to 10 m from the creek edge, indicating the importance of macropore flow in tidal marsh soils.
- The compact agricultural subsoil is 1476 times less permeable compared to the overlying layer of tidally deposited sediment and therefore forms a barrier for groundwater – soil interactions.
- According to our model simulations, 6.06 times less water passes through the marsh soil and 5.84 times less solute was removed in the reference situation compared to a scenario in which the compact subsoil is absent.
- A scenario analysis revealed that doubling the creek density or increasing the depth to the compact layer by 20 cm both more than doubles the volume of groundwater processed by the marsh soil.
- Initial creek initiation and soil amendments are therefore recommended to improve groundwater – soil interactions in newly restored tidal marshes.
- While increased seepage flows are expected to be beneficial for some ecosystem services such as the delivery of DSi to the estuary and removal of nitrogen from the surface water, other ecosystem services such as carbon sequestration might be negatively affected by increased soil aeration.

4.7   Acknowledgements

4.8   References

Bear, J., 1972. Dynamics of Fluids in Porous Media. American Elsevier Publishing Company.

Burden, A., Garbutt, R.A., Evans, C.D., Jones, D.L., Cooper, D.M., 2013. Carbon sequestration and biogeochemical cycling in a saltmarsh Subject to coastal managed realignment. Estuarine Coastal and Shelf Science 120, 12-20. 10.1016/j.ecss.2013.01.014

Callaway, J.C., Zedler, J.B., Ross, D.L., 1997. Using tidal salt marsh mesocosms to aid wetland restoration. Restoration Ecology 5, 135-146. 10.1046/j.1526-100X.1997.09716.x

Cao, M., Xin, P., Jin, G.Q., Li, L., 2012. A field study on groundwater dynamics in a salt marsh - Chongming Dongtan wetland. Ecological Engineering 40, 61-69. 10.1016/j.ecoleng.2011.12.018

Chapman, V.J., 1938. Studies in Salt-Marsh Ecology Sections I to III. Journal of Ecology 26, 144-179. 10.2307/2256416

Chassagne, R.L., Lecroart, P., Beaugendre, H., Capo, S., Parisot, J.P., Anschutz, P., 2012. Silicic acid flux to the ocean from tidal permeable sediments: A modeling study. Computers & Geosciences 43, 52-62. 10.1016/j.cageo.2012.02.014

Chirol, C., Haigh, I.D., Pontee, N., Thompson, C.E., Gallop, S.L., 2018. Parametrizing tidal creek morphology in mature saltmarshes using semi-automated extraction from lidar. Remote Sensing of Environment 209, 291-311. 10.1016/j.rse.2017.11.012

Cox, T.J.S., Schepers, L., 2018. Tides R-package v2.1. 10.5281/zenodo.897843

Craft, C., Broome, S., Campbell, C., 2002. Fifteen years of vegetation and soil development after brackish-water marsh creation. Restoration Ecology 10, 248-258. 10.1046/j.1526-100X.2002.01020.x

Cresswell, H.P., Green, T.W., McKenzie, N.J., 2008. The Adequacy of Pressure Plate Apparatus

for Determining Soil Water Retention. Soil Science Society of America Journal 72, 41-49. 10.2136/sssaj2006.0182

Crooks, S., Pye, K., 2000. Sedimentological controls on the erosion and morphology of saltmarshes: implications for flood defence and habitat recreation. Coastal and Estuarine Environments: Sedimentology, Geomorphology and Geoarchaeology 175, 207-222. 10.1144/Gsl.Sp.2000.175.01.16

D'Alpaos, A., Lanzoni, S., Marani, M., Rinaldo, A., 2010. On the tidal prism - channel area relations. Journal of Geophysical Research-Earth Surface 115. 10.1029/2008jf001243

Darcy, H., 1856. Les fontaines publiques de la ville de Dijon: exposition et application. Victor Dalmont.

Eijkelkamp Agrisearch Equipments, 2013. laboratory-Permeameters: Operation instructions, Giesbeek, The Netherlands.

Eijkelkamp Soil & Water, 2019. Sandbox for pF-determination: User manual, Giesbeek, The Netherlands.

Fei, Y.H., She, D.L., Gao, L., Xin, P., 2019. Micro-CT assessment on the soil structure and hydraulic characteristics of saline/sodic soils subjected to short-term amendment. Soil & Tillage Research 193, 59-70. 10.1016/j.still.2019.05.024

Gardner, L.R., 2005a. A modeling study of the dynamics of pore water seepage from intertidal marsh sediments. Estuarine Coastal and Shelf Science 62, 691-698. 10.1016/j.ecss.2004.10.005

Gardner, L.R., 2005b. Role of geomorphic and hydraulic parameters in governing pore water seepage from salt marsh sediments. Water Resources Research 41. 10.1029/2004wr003671

Gardner, L.R., 2007. Role of stratigraphy in governing pore water seepage from salt marsh sediments. Water Resources Research 43. 10.1029/2006wr005338

Gardner, L.R., Wilson, A.M., 2006. Comparison of four numerical models for simulating seepage from salt marsh sediments. Estuarine Coastal and Shelf Science 69, 427-437. 10.1016/j.ecss.2006.05.009

Gerke, H.H., van Genuchten, M.T., 1993. Evaluation of a 1st-Order Water Transfer Term for Variably Saturated Dual-Porosity Flow Models. Water Resources Research 29, 1225-1238. 10.1029/92wr02467

Gibson, K.D., Zedler, J.B., Langis, R., 1994. Limited Response of Cordgrass (Spartina-Foliosa) to Soil Amendments in a Constructed Marsh. Ecological Applications 4, 757-767. 10.2307/1942006

Goode, D.J., 1996. Direct Simulation of Groundwater Age. Water Resources Research 32, 289-296. 10.1029/95wr03401

Gourgue, O., van Belzen, J., Schwarz, C., Vandenbruwaene, W., Vanlede, J., Belliard, J.P., Fagherazzi, S., Bouma, T.J., van de Koppel, J., Temmerman, S., 2021. Biogeomorphic modeling to assess resilience of tidal marsh restoration to sea level rise and sediment supply. Earth Surface Dynamics 2021, 1-38. 10.5194/esurf-2021-66

Guimond, J.A., Yu, X., Seyfferth, A.L., Michael, H.A., 2020. Using Hydrological-Biogeochemical Linkages to Elucidate Carbon Dynamics in Coastal Marshes Subject to Relative Sea Level Rise. Water Resources Research 56. 10.1029/2019WR026302

Harvey, J.W., Germann, P.F., Odum, W.E., 1987. Geomorphological Control of Subsurface Hydrology in the Creek-Bank Zone of Tidal Marshes. Estuarine Coastal and Shelf Science 25, 677-691. 10.1016/0272-7714(87)90015-1

Harvey, J.W., Nuttle, W.K., 1995. Fluxes of Water and Solute in a Coastal Wetland Sediment .2. Effect of Macropores on Solute Exchange with Surface-Water. Journal of Hydrology 164, 109-125. 10.1016/0022-1694(94)02562-P

Havens, K.J., Varnell, L.M., Watts, B.D., 2002. Maturation of a constructed tidal marsh relative to two natural reference tidal marshes over 12 years. Ecological Engineering 18, 305-315. 10.1016/S0925-8574(01)00089-1

Hemond, H.F., Fifield, J.L., 1982. Subsurface Flow in Salt-Marsh Peat - a Model and Field-Study. Limnology and Oceanography 27, 126-136. 10.4319/lo.1982.27.1.0126

Holz, M., Heil, S.R., Sacco, A., 2000. Temperature-dependent self-diffusion coefficients of water and six selected molecular liquids for calibration in accurate H-1 NMR PFG measurements. Physical Chemistry Chemical Physics 2, 4740-4742. DOI 10.1039/b005319h

Hou, W., Zhang, R., Xi, Y., Liang, S., Sun, Z., 2020. The role of waterlogging stress on the distribution of salt marsh plants in the Liao River estuary wetland. Global

Ecology and Conservation 23. 10.1016/j.gecco.2020.e01100

Hughes, C.E., Binning, P., Willgoose, G.R., 1998. Characterisation of the hydrology of an estuarine wetland. Journal of Hydrology 211, 34-49. 10.1016/S0022-1694(98)00194-2

Jacobs, S., Beauchard, O., Struyf, E., Cox, T.J.S., Maris, T., Meire, P., 2009. Restoration of tidal freshwater vegetation using controlled reduced tide (CRT) along the Schelde Estuary (Belgium). Estuarine Coastal and Shelf Science 85, 368-376. 10.1016/j.ecss.2009.09.004

Jaynes, D.B., Horton, R., 1998. Field parameterization of the mobile/immobile domain model., in: Selim, H.M., Ma, L. (Eds.), Physical Nonequilibrium in Soils: Modeling and Application. Ann Arbor Press, Chelsea, MI, pp. 297-310.

Kadiri, M., Spencer, K.L., Heppell, C.M., Fletcher, P., 2011. Sediment characteristics of a restored saltmarsh and mudflat in a managed realignment scheme in Southeast England. Hydrobiologia 672, 79-89. 10.1007/s10750-011-0755-8

Kuncoro, P.H., Koga, K., Satta, N., Muto, Y., 2014. A study on the effect of compaction on transport properties of soil gas and water I: Relative gas diffusivity, air permeability, and saturated hydraulic conductivity. Soil and Tillage Research 143, 172-179. 10.1016/j.still.2014.02.006

Lawrence, D.S.L., Allen, J.R.L., Havelock, G.M., 2004. Salt Marsh Morphodynamics: An Investigation of Tidal Flows and Marsh Channel Equilibrium. Journal of Coastal Research 20, 301-316.

Li, H.L., Li, L., Lockington, D., 2005. Aeration for plant root respiration in a tidal marsh. Water Resources Research 41. 10.1029/2004wr003759

Liu, Z., Fagherazzi, S., She, X., Ma, X., Xie, C., Cui, B., 2020. Efficient tidal channel networks alleviate the drought-induced die-off of salt marshes: Implications for coastal restoration and management. Science of the Total Environment 749. 10.1016/j.scitotenv.2020.141493

Maris, T., Cox, T.J.S., Temmerman, S., De Vleeschauwer, P., Van Damme, S., De Mulder, T., Van den Bergh, E., Meire, P., 2007. Tuning the tide: creating ecological conditions for tidal marsh development in a flood control area. Hydrobiologia 588, 31-43. 10.1007/s10750-007-0650-5

Marois, D.E., Stecher, H.A., 2020. A simple, dynamic, hydrological model for mesotidal salt marshes. Estuarine Coastal and Shelf Science 233. 10.1016/j.ecss.2019.106486

Martin, J.F., Reddy, K.R., 1997. Interaction and spatial distribution of wetland nitrogen processes. Ecological Modelling 105, 1-21. 10.1016/S0304-3800(97)00122-1

Millington, R., Quirk, J.P., 1961. Permeability of Porous Solids. Transactions of the Faraday Society 57. 10.1039/tf9615701200

Moffett, K.B., Gorelick, S.M., McLaren, R.G., Sudicky, E.A., 2012. Salt marsh ecohydrological zonation due to heterogeneous vegetation–groundwater–surface water interactions. Water Resources Research 48. 10.1029/2011WR010874

Mualem, Y., 1976. A new model for predicting the hydraulic conductivity of unsaturated porous media. Water Resources Research 12, 513-522. 10.1029/WR012i003p00513

Nash, J.E., Sutcliffe, J.V., 1970. River flow forecasting through conceptual models part I — A discussion of principles. Journal of Hydrology 10, 282-290. 10.1016/0022-1694(70)90255-6

Nuttle, W.K., 1988. The Extent of Lateral Water-Movement in the Sediments of a New England Salt-Marsh. Water Resources Research 24, 2077-2085. 10.1029/WR024i012p02077

O'Brien, E.L., Zedler, J.B., 2006. Accelerating the restoration of vegetation in a southern California salt marsh. Wetlands Ecology and Management 14, 269-286.

Oosterlee, L., Cox, T.J.S., Vandenbruwaene, W., Maris, T., Temmerman, S., Meire, P., 2017. Tidal Marsh Restoration Design Affects Feedbacks Between Inundation and Elevation Change. Estuaries and Coasts. 10.1007/s12237-017-0314-2

Ott, E.T., Galbraith, J.M., Daniels, W.L., Aust, W.M., 2020. Effects of amendments and microtopography on created tidal freshwater wetland soil morphology and carbon. Soil Science Society of America Journal 84, 638-652. 10.1002/saj2.20057

Richards, L.A., 1931. Capillary conduction of liquids through porous mediums. Journal of Applied Physics 1, 318-333.

Schepers, L., Kirwan, M., Guntenspergen, G., Temmerman, S., 2017. Spatio-temporal development of vegetation die-off in a submerging coastal marsh. Limnology and

Oceanography 62, 137-150.
10.1002/lno.10381

Scott, B., Baldwin, A., Ballantine, K., Palmer, M., Yarwood, S., 2020. The role of organic amendments in wetland restorations: Organic Amendments Wetland Restoration. Restoration Ecology. 10.1111/rec.13179

Senja, M., Simunek, J., van Genuchten, M.T., 2017. HYDRUS 2D/3D, version 2.05.0240 ed. PC-Progress s.r.o., Prague, Czech Republic.

Simunek, J., Jarvis, N.J., van Genuchten, M.T., Gardenas, A., 2003. Review and comparison of models for describing non-equilibrium and preferential flow and transport in the vadose zone. Journal of Hydrology 272, 14-35.

Spencer, K.L., Carr, S.J., Diggens, L.M., Tempest, J.A., Morris, M.A., Harvey, G.L., 2017. The impact of pre-restoration land-use and disturbance on sediment structure, hydrology and the sediment geochemical environment in restored saltmarshes. Science of the Total Environment 587, 47-58. 10.1016/j.scitotenv.2016.11.032

Struyf, E., Dausse, A., Van Damme, S., Bal, K., Gribsholt, B., Boschker, H.T.S., Middelburg, J.J., Meire, P., 2006. Tidal marshes and biogenic silica recycling at the land-sea interface. Limnology and Oceanography 51, 838-846.

Struyf, E., Van Damme, S., Gribsholt, B., Bal, K., Beauchard, O., Middelburg, J.J., Meire, P., 2007. Phragmites australis and silica cycling in tidal wetlands. Aquatic Botany 87, 134-140. 10.1016/j.aquabot.2007.05.002

Struyf, E., Van Damme, S., Gribsholt, B., Middelburg, J.J., Meire, P., 2005. Biogenic silica in tidal freshwater marsh sediments and vegetation (Schelde estuary, Belgium). Marine Ecology Progress Series 303, 51-60. 10.3354/meps303051

Suckow, A., 2014. The age of groundwater – Definitions, models and why we do not need this term. Applied Geochemistry 50, 222-230. 10.1016/j.apgeochem.2014.04.016

Tempest, J.A., Harvey, G.L., Spencer, K.L., 2015. Modified sediments and subsurface hydrology in natural and recreated salt marshes and implications for delivery of ecosystem services. Hydrological Processes 29, 2346-2357. 10.1002/hyp.10368

Tovey, E.L., Pontee, N.I., Harvey, R., 2009. Managed Realignment at Hesketh Out Marsh West. Proceedings of the Institution of Civil Engineers - Engineering Sustainability 162, 223-228. 10.1680/ensu.2009.162.4.223

Turnadge, C., Smerdon, B.D., 2014. A review of methods for modelling environmental tracers in groundwater: Advantages of tracer concentration simulation. Journal of Hydrology 519, 3674-3689. 10.1016/j.jhydrol.2014.10.056

Ursino, N., Silvestri, S., Marani, M., 2004. Subsurface flow and vegetation patterns in tidal environments. Water Resources Research 40. 10.1029/2003wr002702

Van Genuchten, M., Leij, F., Yates, S., Williams, J., 1991. The RETC Code for Quantifying Hydraulic Functions of Unsaturated Soils. EPA/600/2-91/065, R.S. 83.

van Genuchten, M.T., 1980. A Closed-form Equation for Predicting the Hydraulic Conductivity of Unsaturated Soils. Soil Science Society of America Journal 44, 892-898. 10.2136/sssaj1980.03615995004400050002x

van Genuchten, M.T., Wierenga, P.J., 1976. Mass-Transfer Studies in Sorbing Porous-Media .1. Analytical Solutions. Soil Science Society of America Journal 40, 473-480. 10.2136/sssaj1976.03615995004000040011x

Van Putte, N., Temmerman, S., Verreydt, G., Seuntjens, P., Maris, T., Heyndrickx, M., Boone, M., Joris, I., Meire, P., 2020. Groundwater dynamics in a restored tidal marsh are limited by historical soil compaction. Estuarine, Coastal and Shelf Science 244. 10.1016/j.ecss.2019.02.006

Vandenbruwaene, W., Bouma, T.J., Meire, P., Temmerman, S., 2013. Bio-geomorphic effects on tidal channel evolution: impact of vegetation establishment and tidal prism change. Earth Surface Processes and Landforms 38, 122-132. 10.1002/esp.3265

Vandenbruwaene, W., Meire, P., Temmerman, S., 2012. Formation and evolution of a tidal channel network within a constructed tidal marsh. Geomorphology 151, 114-125. 10.1016/j.geomorph.2012.01.022

Vanlede, J., Maximova, T., Vandenbruwaene, W., Plancke, Y., Verwaest, T., Mostaert, F., 2015. Inrichtingsplan Hedwige-Prosperpolder: Deelrapport 2 – Resultaten van het hydrodynamisch

model. Versie 6.0., Waterbouwkundig Laboratorium: Antwerpen, België.

Wang, W.W., Li, D.J., Zhou, J.L., Gao, L., 2011. Nutrient dynamics in pore water of tidal marshes near the Yangtze Estuary and Hangzhou Bay, China. Environmental Earth Sciences 63, 1067-1077. 10.1007/s12665-010-0782-1

Wilson, A.M., Evans, T., Moore, W., Schutte, C.A., Joye, S.B., Hughes, A.H., Anderson, J.L., 2015. Groundwater controls ecological zonation of salt marsh macrophytes. Ecology 96, 840-849. 10.1890/13-2183.1

Wilson, A.M., Gardner, L.R., 2006. Tidally driven groundwater flow and solute exchange in a marsh: Numerical simulations. Water Resources Research 42. 10.1029/2005wr004302

Wilson, A.M., Morris, J.T., 2012. The influence of tidal forcing on groundwater flow and nutrient exchange in a salt marsh-dominated estuary. Biogeochemistry 108, 27-38. 10.1007/s10533-010-9570-y

Wolf, E.C., Rejmankova, E., Cooper, D.J., 2019. Wood chip soil amendments in restored wetlands affect plant growth by reducing compaction and increasing dissolved phenolics. Restoration Ecology 27, 1128-1136. 10.1111/rec.12942

Wolf, K.L., Ahn, C., Noe, G.B., 2011. Development of Soil Properties and Nitrogen Cycling in Created Wetlands. Wetlands 31, 699-712. 10.1007/s13157-011-0185-4

Wolters, M., Garbutt, A., Bakker, J.P., 2005. Salt-marsh restoration: evaluating the success of de-embankments in north-west Europe. Biological Conservation 123, 249-268. 10.1016/j.biocon.2004.11.013

Xiao, K., Wilson, A.M., Li, H., Ryan, C., 2019. Crab burrows as preferential flow conduits for groundwater flow and transport in salt marshes: A modeling study. Advances in Water Resources 132. 10.1016/j.advwatres.2019.103408

Xie, H., Yi, Y., Hou, C., Yang, Z., 2020. In situ experiment on groundwater control of the ecological zonation of salt marsh macrophytes in an estuarine area. Journal of Hydrology 585. 10.1016/j.jhydrol.2020.124844

Xin, P., Gibbes, B., Li, L., Song, Z.Y., Lockington, D., 2010. Soil saturation index of salt marshes subjected to spring-neap tides: a new variable for describing marsh soil aeration condition. Hydrological Processes 24, 2564-2577. 10.1002/hyp.7670

Xin, P., Jin, G.Q., Li, L., 2009a. Modelling Study on Subsurface Flows Affected by Macro-Pores in Marsh Sediments. Advances in Water Resources and Hydraulic Engineering, Vols 1-6, 1394-1400. 10.1007/978-3-540-89465-0_244

Xin, P., Jin, G.Q., Li, L., Barry, D.A., 2009b. Effects of crab burrows on pore water flows in salt marshes. Advances in Water Resources 32, 439-449. 10.1016/j.advwatres.2008.12.008

Xin, P., Kong, J., Li, L., Barry, D.A., 2012. Effects of soil stratigraphy on pore-water flow in a creek-marsh system. Journal of Hydrology 475, 175-187. 10.1016/j.jhydrol.2012.09.047

Xin, P., Kong, J., Li, L., Barry, D.A., 2013. Modelling of groundwater-vegetation interactions in a tidal marsh. Advances in Water Resources 57, 52-68. 10.1016/j.advwatres.2013.04.005

Xin, P., Yu, X.Y., Lu, C.H., Li, L., 2016. Effects of macro-pores on water flow in coastal subsurface drainage systems. Advances in Water Resources 87, 56-67. 10.1016/j.advwatres.2015.11.007

Xin, P., Yuan, L.R., Li, L., Barry, D.A., 2011. Tidally driven multiscale pore water flow in a creek-marsh system. Water Resources Research 47. 10.1029/2010wr010110

Xin, P., Zhou, T.Z., Lu, C.H., Shen, C.J., Zhang, C.M., D'Alpaos, A., Li, L., 2017. Combined effects of tides, evaporation and rainfall on the soil conditions in an intertidal creek-marsh system. Advances in Water Resources 103, 1-15. 10.1016/j.advwatres.2017.02.014

Xu, X., Xin, P., Zhou, T., Xiao, K., 2021. Effect of macropores on pore-water flow and soil conditions in salt marshes subject to evaporation and tides. Estuarine, Coastal and Shelf Science 261. 10.1016/j.ecss.2021.107558

Zedler, J.B., 2000. Handbook for Restoring Tidal Wetlands. CRC Press.

5

Organic soil amendments improve groundwater dynamics and nutrient cycling in a restored tidal marsh mesocosm

Niels Van Putte, Stijn Temmerman, Goedele Verreydt, Piet Seuntjens, Dimitri Van Pelt, Patrick Meire

5.1 Abstract

Tidal marsh soil properties play a major role in water quality regulation through nutrient cycling in adjacent tidal rivers, as surface water infiltrates and drains through the tidal marsh soil back to tidal channels. This filter function may be a reason for tidal marsh restoration on areas that were formerly converted to agricultural land, but is often impaired due to historical agricultural soil compaction and artificial drainage. Here, we investigated whether organic soil amendments can improve groundwater dynamics and the filter function of restored tidal marshes, through an in situ field mesocosm experiment in the Scheldt estuary, Belgium. We locally applied four soil treatments (tilling, tilling + amendment with reed cuttings, tilling + amendment with wood chips and a control treatment) on a historically compacted agricultural soil where tidal marsh restoration was planned. In each treated plot, a 1.69 m^3 soil monolith was excavated and inserted in a field mesocosm construction where it was subjected to the tides. Soil properties (except for bulk density) did not significantly differ before and after application of the organic soil amendments. Nevertheless, the groundwater drainage depth was significantly deeper in the treated monoliths. The amended soils contributed significantly more to nitrogen removal from the water as compared to the control treatment. All monoliths acted as a sink for phosphate and a source for dissolved silica. Therefore, our results support the effectiveness of organic soil amendments to improve the water quality regulation function in tidal marsh restoration projects.

5.2 Introduction

Tidal marshes along estuaries and coasts, located on the transition zone between water and land, provide a wide array of valuable ecosystem services such as storm surge defense (Costanza et al., 2008; Narayan et al., 2016), habitat provisioning (Barbier et al., 2011), carbon sequestration (Mcleod et al., 2011) and water quality improvement (Mitsch and Gosselink, 2000; Wolf et al., 2011). In the past centuries, many of these tidal wetlands were embanked by the construction of dikes and drainage of the former wetlands, as such cutting them off from the tidal influence and converting them to urban, industrial or agricultural areas, the latter becoming so called 'polders'. These large-scale embankments lead to a dramatic decrease in global tidal marsh area. Recent insights indicate that not only the valuable habitats have disappeared, but also their many associated ecosystem services (e.g. Barbier et al., 2011).

During the last decades, tidal marshes are increasingly restored on formerly embanked agricultural land to reach biodiversity goals such as the EU Habitats Directive (European Parliament and the Council of the European Union, 1992) and to regain the delivery of their ecosystem services (Boerema and Meire, 2017). This can be accomplished e.g. through managed realignment, in which a part of the dike is breached (French, 2006) or by the construction of flood control areas with a controlled reduced tide (FCA-CRT) (Maris et al., 2007). In both cases, the embanked land is brought again under tidal influence. It is generally assumed that these so-called 'restored tidal marshes' show a fast development of marsh vegetation and delivery of their ecosystem services. However, an increasing number of studies shows an impaired delivery of soil related ecosystem services in restored tidal marshes as compared to natural tidal marshes (Burden et al., 2013).

In embanked land used for agricultural purposes, the physical structure and chemical composition of the soil often changed significantly (Portnoy and Giblin, 1997; Tempest et al., 2015; Van Putte et al., 2020 (Chapter 2)). Grazing by cattle and the use of heavy farming equipment lead to compaction of the soil and a reduction of the soil porosity (Bantilan-Smith et al., 2009; Keshta et al., 2020; Spencer et al., 2017). Furthermore, the construction of artificial drainage ditches and the absence of regular tidal inundations often caused excessive soil aeration and organic matter mineralization (e.g. Iost et al., 2007), promoting further soil compaction. In addition, leaching of artificial fertilizers from embanked areas lead to elevated concentrations of nitrogen and phosphorus in the soil and in estuarine waters (Kennish, 2002).

When tidal marshes are restored on formerly embanked agricultural land, the relict compact agricultural soil hampers soil – groundwater interactions and groundwater flow due to a reduced porosity and hydraulic conductivity (Tempest et al., 2015; Van Putte et al., 2020 (Chapter 2)). The compact soil also hinders marsh vegetation development as plant roots have difficulties penetrating compacted soils (Shierlaw and Alston, 1984) and as many species cannot cope with water ponding that may occur on top of the impermeable compacted soil (Mossman et al., 2020). In addition, the compact soil slows down the

geomorphological development of an extended tidal creek network, which is crucial for both surface and subsurface drainage and associated soil aeration in natural marshes (Liu et al., 2020; Vandenbruwaene et al., 2012). Therefore, in restored tidal marshes, groundwater flow and soil-groundwater interactions are largely restricted to the top layer of tidally deposited sediment that has, in comparison to the compacted soil below it, a lower bulk density and higher porosity due to the burial and partial decomposition of organic matter (Tempest et al., 2015; Van Putte et al., 2020 (Chapter 2)).

Groundwater dynamics control the water quality improving function of tidal wetlands. For example, dissolved silica (DSi) resulting from the dissolution of biogenic silica (BSi) present in buried plant litter and dead diatoms, is advectively transported from the marsh soil to the estuary driven by groundwater flow (Struyf et al., 2006). Tidally induced groundwater level fluctuations mediate nitrification when the soil is aerated and denitrification when the soil is saturated, removing nitrogen from the estuary (Gutknecht et al., 2006). Phosphate is retained in tidal marsh soils through sorption to iron oxides, which are abundant in aerated tidal marsh soils in the vicinity of tidal creeks (Chambers and Odum, 1990). Recent studies suggest that impaired groundwater dynamics resulting from historical agricultural soil compaction in restored tidal marshes, can limit the contribution to water quality improvement of these marshes (Spencer et al., 2017; Tempest et al., 2015; Van Putte et al., 2022 (Chapter 4)). Given the importance of the water quality regulation function to comply with legislations such as the EU Water Framework Directive (European Parliament and the Council of the European Union, 2000) and the increasing number of tidal marsh restoration projects, there is a growing demand for methods to improve groundwater dynamics and associated water quality improvement in newly restored tidal marshes.

Organic soil amendments (i.e. mixing the topsoil with organic waste material) have been widely used in non-tidal wetland restoration projects to improve soil physical properties and nutrient cycling (Scott et al., 2020). These soil amendments have also been proposed as a measure to improve soil physical and chemical properties in newly restored tidal wetlands and to jumpstart their development (Callaway et al., 1997; Havens et al., 2002). However, only a few field studies were conducted to test the effect of soil amendments on several ecosystem functions in tidal wetlands. Foster-Martinez and Variano (2018) found that application of biosolids as soil amendments in tidal marsh creation projects promotes vegetation development in marshes created with dredged sediments. However, Gibson et al. (1994) argue that although organic amendments temporarily increase soil nutrient contents, high decomposition rates quickly deplete these nutrient pool. Similarly, Ott et al. (2020) found no increased organic carbon and nitrogen content in amended restored marsh soils 12 years after the amendments. Maietta et al. (2020), however, discovered a strongly altered soil microbial community after application of plant litter amendments.

At present, the effect of organic soil amendments on the water quality improving function of restored tidal marshes remains largely unknown. Biogeochemical water quality

improvement depends on (i) groundwater dynamics that are inherently related to soil physical properties and (ii) microbially mediated biochemical processes. Both these factors are expected to alter by the application of soil amendments. In this study, we use an in situ mesocosm set-up to test the potential of organic soil amendments to 'decompact' the relict agricultural soil and to promote soil – groundwater interactions and associated biogeochemical cycling in newly restored tidal wetlands. We hypothesize that:

(i)   application of soil amendments decreases the bulk density and increases the porosity the soil

(ii)   as a result, groundwater can drain faster in amended marsh soil, promoting soil aeration

(iii)   application of soil amendments increases soil – groundwater interactions and hereby stimulates biogeochemical cycling, including nitrogen (N) and phosphorus (P) removal and delivery of dissolved silica (DSi)

5.3   Methods

5.3.1   Study location

We executed the study in a large (12 by 13 m) mesocosm construction (see further) located near the Kruibeke polder in the Scheldt estuary in Flanders, Belgium (Figure 5.1b), further described in Meire et al. (2005). The construction is located in the brackish part where the estuary is macrotidal with an average tidal range of 5.40 m. The electrical conductivity of the estuarine water is highly variable and ranges from 0.5 mS/cm in winter to 20 mS/cm in late summer (Waterinfo, 2022). We used soil excavated from formerly embanked agricultural land in the Kruibeke polder for the experiment (see further). This soil was formed on alluvial river sediments accumulated after the end of the last ice age. During most of the Holocene, when there was a fluvial regime in the river and no tides yet, a layer of peat was formed in the river valley. Several centuries after the start of the common era, when the tides started to propagate to the region of the Kruibeke polder, the peat formation transitioned into deposition of a 50 – 100 cm layer of clay and silt (Mys et al., 1983). The soil excavated for our experiment was from this top layer of clay and silt (see further). The polder was embanked in the twelfth to thirteenth century when large-scale land reclamation for agriculture was common in the valley of the Scheldt river. Since the embankment, the largest part of the polder was used as crop fields, grasslands and forestry (De Haan and Verboven, 2008). Recently, an area of 135 ha in the polder was converted to a flood control area with a controlled reduced tide (CRT) in the framework of the Flemish Sigmaplan to protect the hinterland from floods and restore tidal marshes that largely disappeared after the large scale embankments (Cox et al., 2006; Oosterlee et al., 2017). Since June 2017, tidal water flows in and out of the area through separate inlet- and outlet sluices.
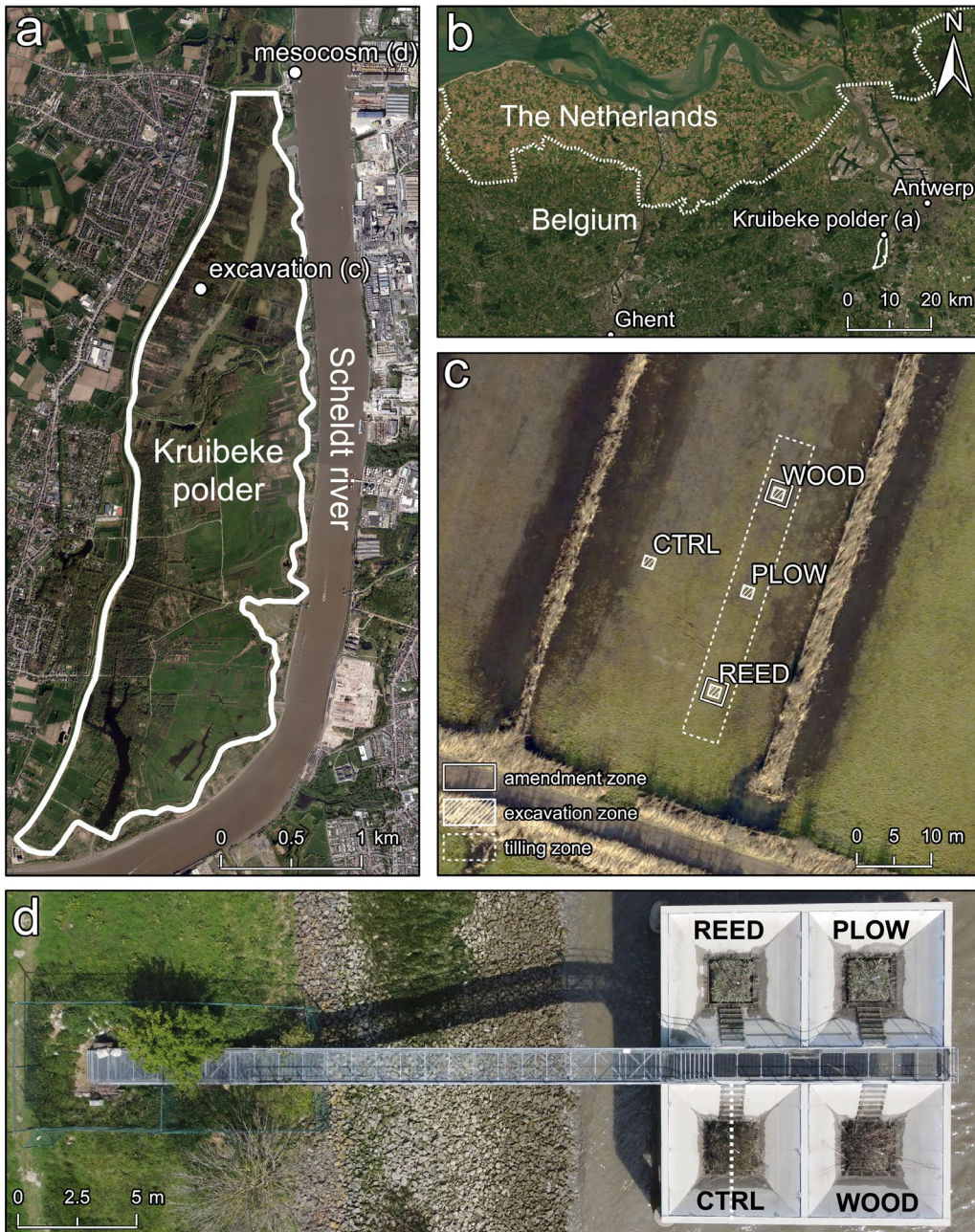
Figure 5.1: (a): Situation of the excavation site and mesocosm location within the Kruibeke polder. (b): Situation of the Kruibeke polder in the Scheldt estuary. (c): Aerial view of the excavation site; the tilling zone refers to the zone that was plowed and rototilled, the amendment zone refers to the zone in which organic matter was applied before tilling; the excavation zone refers to the location where the soil was excavated. (d): Aerial view of the mesocosm set-up located in the Scheldt river; the dashed white line indicates the cross-section drawn in Figure 5.2. The black labels refer to the treatment that was applied to the monolith in the respective mesocosm unit: PLOW: tillage and no amendments, REED: tillage and amendment with reed cuttings, WOOD: tillage and amendment with wood chips and CTRL: control treatment, no tillage and no amendments. Image source for a, b and c: GDI-Vlaanderen.

5.3.2 Experiment preparation

The Kruibeke polder (Figure 5.1a) was chosen for this experiment as it exhibits a compact upper soil layer that is typical for agricultural embanked polder areas. We conducted a survey throughout the area to find a field with the most compacted soil profile. On the chosen field (Figure 5.1c, latitude 51°9'45"N longitude 4°18'56"E), four 3 by 3-m plots were selected where we applied the soil amendments. The present vegetation (mainly *Agrostis stolonifera*) was mown and cuttings were removed from the field to minimize the effect of the present vegetation on soil amendments.

Four treatments were applied on the respective plots. In the first treatment (further referred to as REED), the soil was mixed with approximately 9 kg/m² of freshly mown reed (*Phragmites australis*) cuttings from within the Kruibeke polder. Reed cuttings are easily available as a cheap organic waste product from reed mowing in tidal wetlands for nature management with the aim of slowing down vegetation succession to *Salix* sp. In the second treatment (WOOD), the soil was mixed with approximately 22 kg/m² of wood chips from smaller twigs including leaves from mainly poplar trees (*Populus* sp.), which are abundantly available in the wider study area. In the REED and WOOD plots, the respective organic matter was spread out equally over the plot. Afterwards, the soil in these plots was plowed, so that the organic matter ended up approximately 30 cm below the soil surface. To ensure the presence of organic matter also in the upper 30 cm, a second layer of organic amendments was spread out on the surface of the plots. The plots were then rototilled. The same plowing and rototilling treatments were applied on the PLOW plot, but without adding organic matter. In the CTRL plot, no treatments were applied and the soil was left undisturbed. It must be noted that in the REED, WOOD and PLOW treatments, although the vegetation was mown, the remaining grass present on the plots was also mixed with the soil, adding to the organic matter content.

Metal containers of 1.50 by 1.50 m in surface area and 0.75 m depth were inserted in the soil with a crane (Figure S5.1a). The soil around the monoliths was then excavated and a base plate was inserted underneath the monoliths and welded onto the metal container (Figure S5.1b). The monoliths were then transferred to stainless steel containers that were entirely perforated with 3 cm diameter holes through the four vertical side walls of the containers (Figure S5.1c). Subsequently, the monoliths were transported to the mesocosm construction (Figure S5.1e, see next paragraph) by a boat on the river and lowered into their respective mesocosm unit by a crane on a pontoon (Figure S5.1d).

5.3.3 Mesocosm construction

The mesocosm set-up is located in the Scheldt river (Figure 5.1d, latitude 51°10'35.5"N longitude 4°19'30.5"E) and consists of four funnel shaped units each measuring 5.57 by 5.57 m in surface area (Figure 5.2, Figure 5.3). These funnels protect the monoliths from waves and currents and create a sheltered marsh environment. The monoliths were placed in the construction so that the top of the monolith soil was located at 4.85 m TAW (the Belgian ordnance level), experiencing a tidal inundation frequency of 0.85 (i.e. being

inundated by 85% of high tides) and an average inundation time of 120 minutes. The four mesocosm units consist of an inner container of 1.60 by 1.60 m in surface area and 0.80 m in depth in which the soil monoliths were placed. The 5 cm space in between the inner container and the monoliths was filled with filter sand (1 – 2 mm grain size) and capped by a filter gauze filled with bentonite clay on the top to prevent clogging of this space with estuarine sediment (Figure 5.2D, F). The inner container is located inside an outer container of 2 by 2 m. This outer container is directly connected to the river by an opening (Figure 5.2I) through which river water can flow both in and out the mesocosm units. Water can flow between the inner and outer container through a permeable filter sponge (Figure 5.2G) to prevent fine suspended sediment from clogging soil pores and the filter sand. The void space between the inner and the outer container (Figure 5.2E) silted up rapidly and was therefore cleaned every month on the day before the drainage measurements (see further) were conducted. Vegetation that started growing naturally on the soil monoliths was left undisturbed, but roots and stems protruding into the outer container were removed and vegetation was mown in autumn after all above-ground plant material died off. The evolution of vegetation composition during the course of the experiment is presented in Table S5.4.
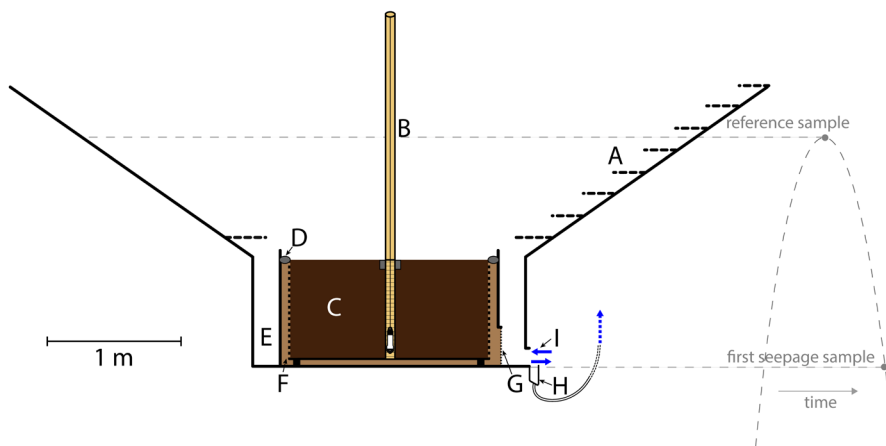

Figure 5.2: Cross-section of one of the mesocosm units indicated in Figure 5.1d. (A): stairs to reach the monoliths (B): groundwater monitoring well (C): soil monolith (D): filter gauze filled with bentonite (E): space between inner and outer container (F): space between inner container and soil monoliths filled with filter sand (G): filter sponge (H): drainage water collection basin (I): opening in the outer container through which the river water can enter and leave the mesocosm unit. The grey dashed curve on the right side represents the water level in the river around high tide in function of time. A reference sample from the river water is taken around high tide. The first soil drainage water sample is taken when the water level in the river drops below the bottom of the mesocosm unit.

5.3.4 Soil samples

Undisturbed soil samples were taken at different depths (5, 15, 35 and 75 cm) in the four selected plots (but outside the excavation area, see Figure 5.1c) before and after application of the treatments to measure the loss on ignition (LOI) and bulk density. In

addition, we took soil samples in the mesocosm monoliths after 29 months since the start of the experiment on which we determined the saturated hydraulic conductivity and soil water retention curve. These results and their respective methods are presented in Supplement S5.2 and Figure S5.4. All undisturbed soil samples were taken in 100-cm^3 sample rings.

Figure 5.3: Picture of the mesocosm set-up at low tide taken 3.5 years after the start of the experiment showing the four units containing the soil monoliths with different treatments. From left to right and top to bottom: CTRL: control treatment, no tillage and no amendments, REED: tillage and amendment with reed cuttings, WOOD: tillage and amendment with wood chips and PLOW: tillage and no amendments. Photo taken by Tim van den Broeck.

5.3.5 Groundwater measurements

We installed a 41-mm diameter HDPE monitoring well in the center of every soil monolith with the bottom of the well located at the bottom of the soil monoliths (Figure 5.2B). The wells protruded 1.77 m from the soil surface to prevent surface water from entering the top of the wells at high tide. The wells were horizontally slotted over their entire subsurface part except for the upper 5 cm and were sealed off with a bentonite plug to prevent surface water infiltration in the borehole. A filter gauze was applied around the well screen. The groundwater level was recorded inside the four wells with an interval of 1 minute using pressure transducers (Rugged Troll 100, In-Situ Inc.). The data were corrected for atmospheric pressure variations with data from a barometric pressure transducer located in the Kruibeke polder. The elevation of the well tops was measured with an RTK-GPS.

5.3.6 Drainage water sampling and analysis

Sampling of the drainage water, draining from the soil monoliths after tides receded, was performed monthly from February 2019 to April 2020, in order to measure the drainage volume and nutrient concentrations. Sampling always took place when the high water phase occurred early in the morning (i.e. in between spring tide and neap tide), and always after a high tide that inundated the surface of all four soil monoliths. A reference sample of the river water was taken at the moment of high tide in every mesocosm unit (Figure 5.2). Sampling of the drainage water started during the ebb phase when the water level in the river dropped below the bottom of the mesocosm units (Figure 5.2). This means that we were not able to capture the draining water from the soil monoliths when the water level in the river was in between the top and the bottom of the soil monolith, because this drainage water was inherently mixed with surface water in the outer container. Drainage water from the mesocosm units was collected in a small collector basin mounted below the outer container (Figure 5.2H). We used a four channel peristaltic pump to pump the water from the four collector basins into 5-L measuring beakers located on the upper platform. The drainage volume from all monoliths was recorded every 30 minutes during the first 5 hours and then every 60 minutes during the last 2 hours. At the same sampling intervals, a 250-mL sample was taken and divided over two 30-mL vials (pre-treated with 3 mL 69% H_2SO_4 for TDIN (total dissolved inorganic nitrogen) and 1.5 mL 69% HNO_3 for PO_4 and DSi, respectively) by passing them through 0.45-µm syringe filters. Samples were stored cool up to the analyses. We stopped the sampling when unexpected rain occurred (this happened in April 2019 and March 2020) as the drainage water would else be contaminated with rainwater collected in the mesocosm funnels. For March 2019, no data on drainage volumes are available due to pump failure during the measurements and no samples were taken in June 2019. Analysis for TDIN was done using continuous flow analysis (CFA) on a colorimetric segmented flow analyzer (SAN++, Skalar, Breda, The Netherlands). Concentrations of PO_4, and DSi were analyzed on an ICP-OES (inductively coupled plasma – optical emission spectrometry) spectrometer (iCAP 6000 series, Thermo Scientific, Camebridge, UK). Concentrations of Cl, SO_4, Ca, K, Mg, Na, Fe, Zn, Mn and DOC were also measured. The respective analysis methods and results for these elements are presented Table S5.1 and Figure S5.5.

5.3.7 Nutrient content in organic amendments

Samples from the organic amendments and the vegetation present on the polder were taken to determine the content of total N and total P. Therefore, 0.3 g of dried (70 °C) grinded plant material was transferred to a digestion tube containing H_2SO_4-salicylic acid-H_2O_2 following the method of Novozamsky et al. (1983). In addition, we determined the BSi content by incubating 0.03 g subsamples in 25 mL 0.5 M NaOH at 80 °C for 5h following DeMaster (1981). After extraction, analysis of N, P and Si was measured using CFA (see above).

5.3.8   Analysis of soil properties

We hypothesized that the bulk density and organic matter content would not differ between the plots before the application of the treatments, but would significantly differ between the plots after the application of the treatments. We therefore determined the dry bulk density and the proportion loss on ignition (LOI) on the undisturbed soil samples taken before the monolith excavation. The proportion LOI was determined following the protocol in Heiri et al. (2001) with a muffle furnace temperature of 550°C during 4 hours.

5.3.9   Data analyses

Differences in soil nutrient concentrations before application of the treatments were investigated using an ANOVA and consequent Tukey post hoc test. The depth at which the samples were taken was used as a random factor in the statistical model. Nutrient concentrations were log-transformed in case of heteroscedasticity. Using a log-transformation is only useful when larger variances coincide with larger observations. This was not the case regarding the observed bulk density and LOI before and after application of the treatments. To take this into account, we used inverse weighting (Pinheiro and Bates, 2009) with the "varIdent" function in R (R Development Core Team, 2022), after which a two-way ANOVA was executed. Values for bulk density and LOI in the CTRL plot were set equal before and after, since no soil treatment was applied in the CTRL plot, and therefore no change in soil properties was expected.

Differences in groundwater dynamics were assessed by calculating the tidal drainage depth (i.e. the groundwater drainage depth in between consecutive overtopping tides) with the Tides package in R (Cox and Schepers, 2018). These depths were then compared between the amended monoliths and the CTRL monolith using an ANOVA with time as covariate, followed by a Dunnett post hoc test.

To estimate the net import or export of nutrients from the soil monoliths, we calculated a mass balance under the assumption that all the volume of drainage water during one tidal cycle was equal to the volume of water that infiltrated into the soil monolith during the preceding high water phase (i.e. a conservative mass balance), following Equation 5.1.

$$m = \sum (\Delta V) \cdot c_i - \sum (\Delta V \cdot c_d) \qquad \text{Equation 5.1}$$

Here, m is the mass balance, ΔV is the increase in drainage volume during the time interval between taking consecutive samples, c_d is the concentration in the respective drainage water sample and c_i is the concentration in the inundation water at high tide.

The mass balance was divided by the surface area of the soil monoliths (2.25 m²) to estimate the mass balance per area. For statistical analyses, the data were grouped per season (winter = Jan and Feb 2020, spring = May 2019 and Apr 2020, summer = Jul , Aug and Sep 2019 and autumn = Oct, Nov and Dec 2019) and analyzed using a two-way ANOVA and Tukey post hoc test.
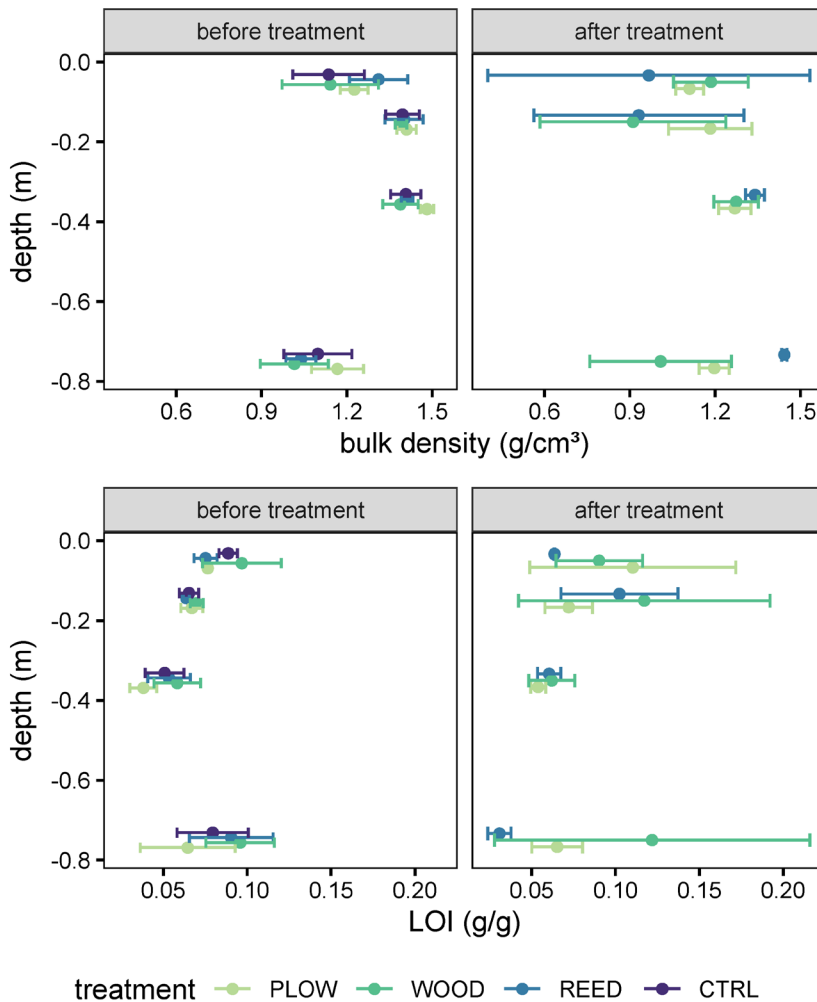
Figure 5.4: Comparison of bulk density and LOI (loss on ignition) before and after application of the soil treatments (n = 3). Error bars denote the standard deviation. Note that no data is available for CTRL after treatment, as no treatment was applied here.

5.4 Results

5.4.1 Nutrient concentrations in organic soil amendments

In the REED amendment, both the concentration of N and BSi were higher as compared to the WOOD amendment. The grass present on the polder (*Agrostis stolonifera*) contained the highest concentrations of P, N and BSi (Table 5.1). This grass was mown before application of the treatments, but grass stubbles and roots were not removed.

Table 5.1: Nutrient stoichiometry in the organic amendments (n = 3). 'Grass' refers to the vegetation (*Agrostis stolonifera*) that was present in the field.

	P (mg/g)	N (mg/g)	BSi (mg/g)
reed	1.10 ± 0.04	9.08 ± 0.34	14.51 ± 0.18
wood	1.12 ± 0.02	6.70 ± 0.02	0.89 ± 0.05
grass	2.77 ± 0.13	17.41 ± 1.09	12.68 ± 0.37

5.4.2   Soil properties before and after organic soil amendments

Before the application of the treatments, soil samples were taken in the selected plots at different depths and analyzed for their NH_4^+, NO_3^- and PO_4^{3-} content and grain size distribution. Since these analyses were performed merely to assure an equal pre-treatment condition in the four selected plots, these results and the used methods are presented in Supplement S5.1, Figure S5.2 and Figure S5.3. Overall, there was no reason to assume unequal conditions among the selected plots before the treatments.

Before the application of the treatments, the soil in the selected plot did not significantly differ between the plots concerning bulk density (p = 0.08), the LOI only differed significantly between the WOOD and PLOW treatments (p = 0.01), with a small difference of 0.02 g/g LOI (Figure 5.4). After application of the treatments, a higher heterogeneity of soil properties within the plots was observed (Figure 5.4). Nevertheless, the LOI did not differ significantly before and after application of the treatments (p = 0.23). Overall, the bulk density was significantly lower after application of the treatments (p = 0.02), on average 0.10 g/cm^3 lower than before the treatments.

5.4.3   Groundwater dynamics

Groundwater level fluctuations in the PLOW treatment followed a distinctively different pattern compared to the other treatments (Figure 5.5). Here, the groundwater level declined fast when the tide receded and dropped until the bottom of the soil monolith was reached.

In the WOOD and REED treatments, the groundwater level initially declined fast after the tide receded, but then stabilized and reached an average level of 0.47 m (REED) and 0.43 m (WOOD) below the soil surface. In the CTRL treatment, the initial groundwater drainage rate was slower, but this rate was sustained for a longer time compared to the REED and WOOD treatments (Figure 5.5). During neap tides, the groundwater level in the PLOW, REED and WOOD responded to high tide levels that did not approximate the soil surface level of the monolith, indicating lateral infiltration through pore networks. This was not the case for the CTRL monolith. Over the years of the experiment, groundwater level fluctuations in the CTRL treatment attenuated (Figure 5.5), possibly indicating clogging of the pore network or the monitoring well filter. The spring tide drainage depth in all three treated plots was significantly deeper (p < 0.001) compared to the CTRL plot (Table S5.2).
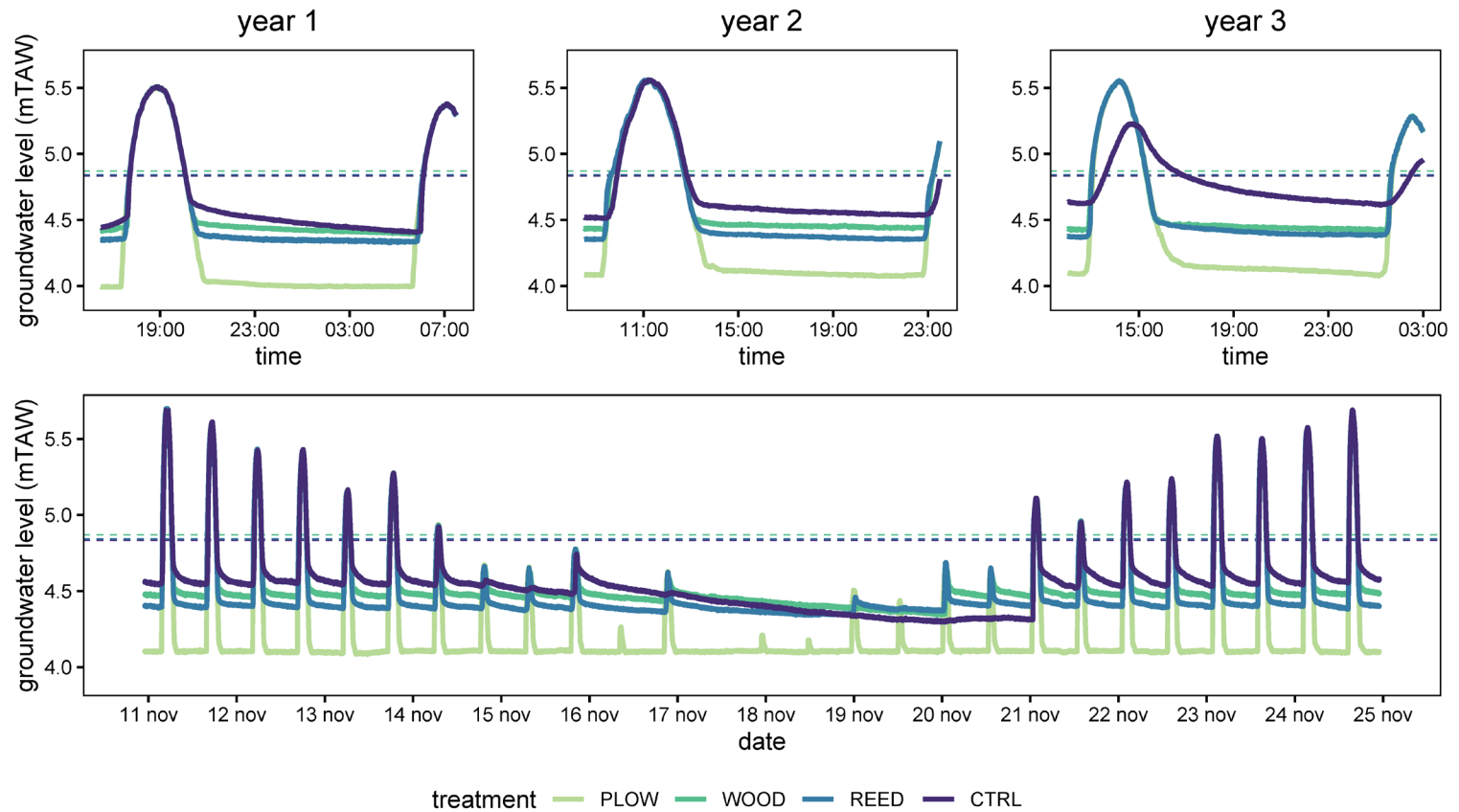
Figure 5.5: Groundwater dynamics in the four soil monoliths during spring tide after one, two and three years since the start of the experiment (upper panels). Groundwater dynamics in the first year of the experiment during a complete spring tide – neap tide cycle (lower panel). Dashed horizontal lines represent the soil surface elevation of the respective soil monolith.
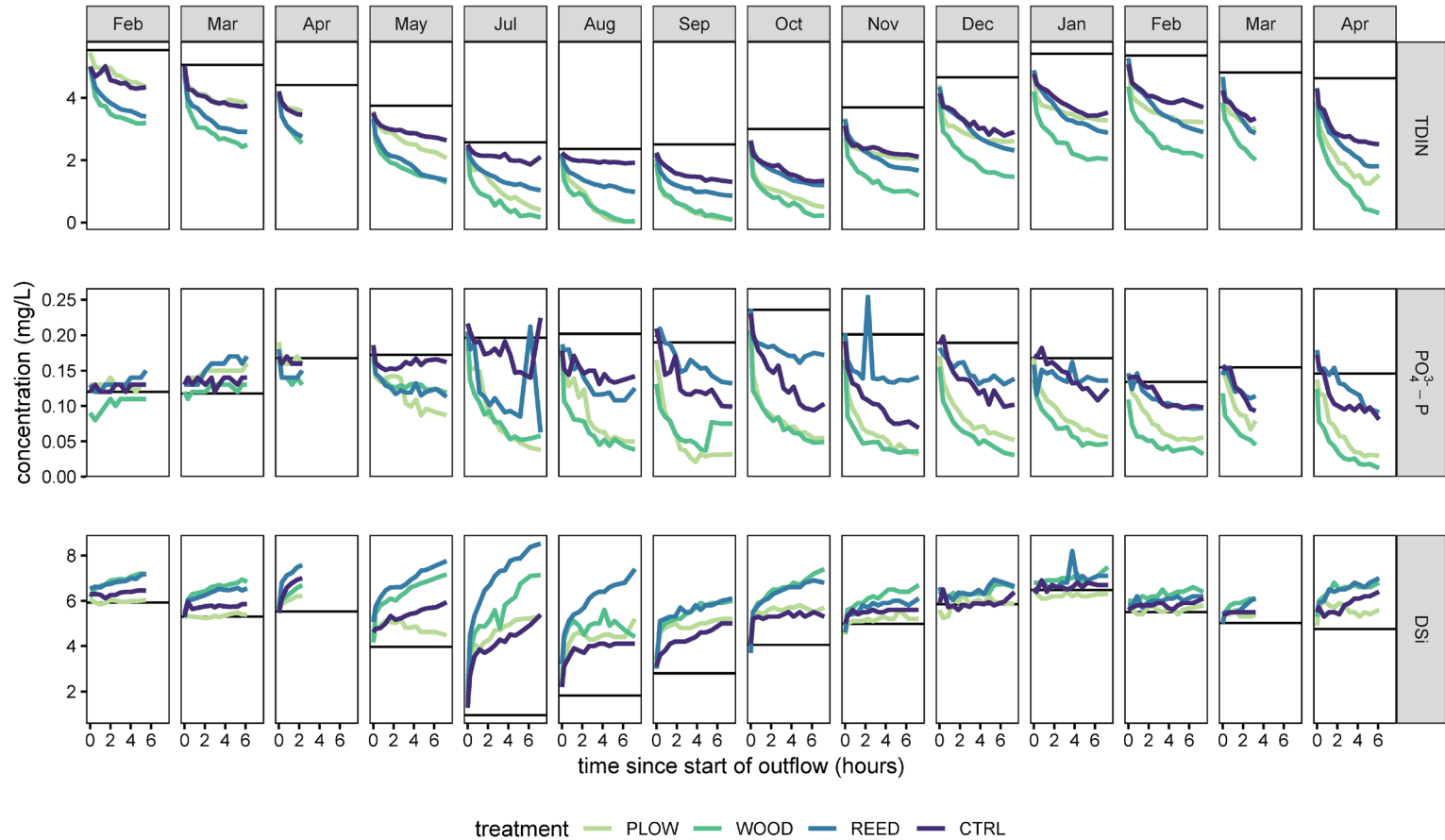
Figure 5.6: Evolution of nutrient concentrations in the soil drainage water during the outflow phase measured monthly during individual tides from February 2019 until April 2020. Black horizontal lines indicate the concentration of the respective nutrient in the river surface water at high tide.
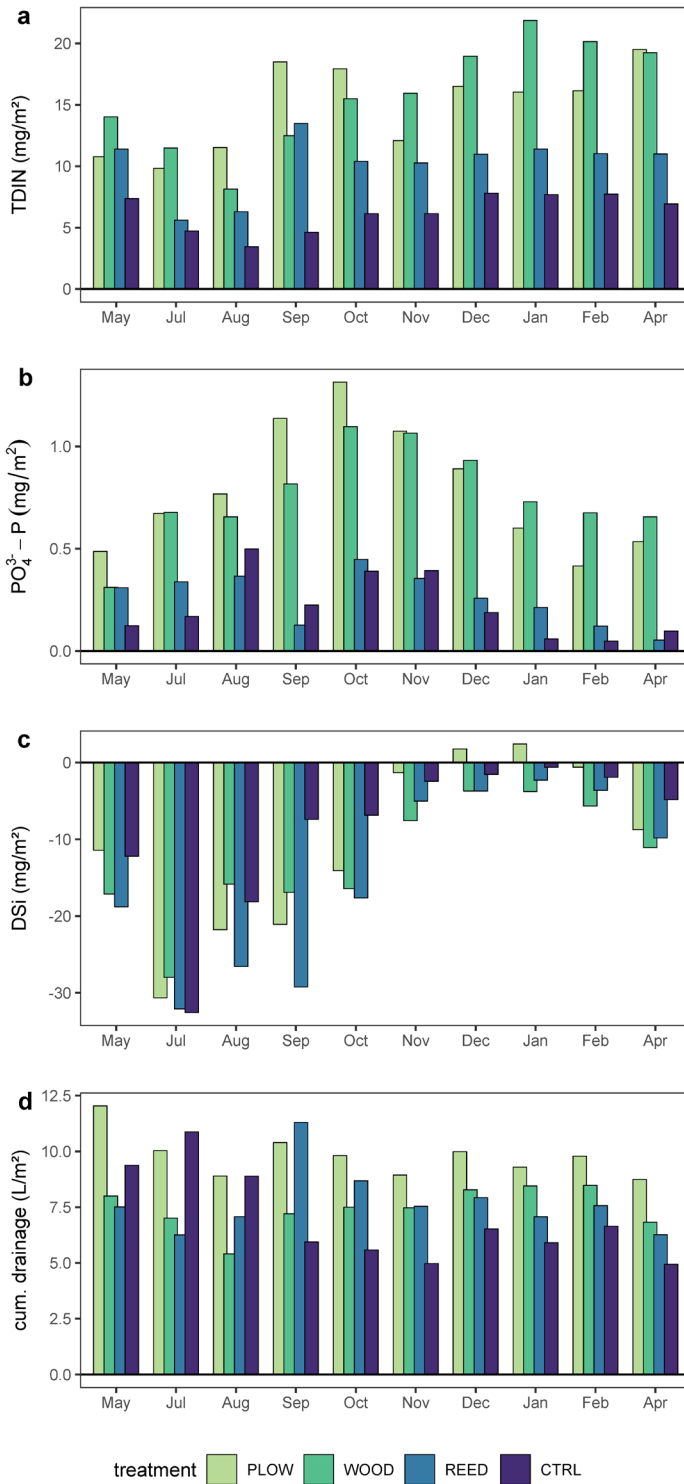
Figure 5.7: Mass balance per tidal cycle per unit of area for TDIN (a), PO$_4$ (b) and DSi (c) and cumulative drainage volume (d). A positive mass balance indicates a net import of the respective element into the soil. Data from May 2019 to April 2020. Mass balances of other measured elements are presented in Figure S5.5.

5.4.4   Drainage water biogeochemistry

Nutrient concentrations in the soil drainage water at the start of the outflow phase were similar among the four treatments and also similar to the concentrations in the inundation water (Figure 5.6). The concentration in the four treatments then deviated and followed an approximately logarithmic pattern over time. At the start of the outflow, the TDIN concentration in the drainage water in all the treatments was similar to the concentration in the estuary. During the outflow phase, the concentration in the drainage water decreased. This was the case for all treatments, although the decrease was generally higher in the treated plots compared to the CTRL treatment. The concentration of TDIN in the estuary was lower around summer (Figure 5.6). The mass balance per tidal cycle (Figure 5.7a), which accounts for the drainage volume, shows that there was always a net import of TDIN into the soil monoliths, with a significantly larger import in the treated monoliths compared to the CTRL monolith, and a significantly larger import outside of the summer season (Table S5.3).

During the outflow phase, the PO_4 concentration decreased over time, except for the winter months in 2019 (Figure 5.6). The decrease in PO_4 concentration was more profound when concentrations of PO_4 in the estuary were higher, which was during autumn. At the end of the drainage phase, PO_4 concentrations in the PLOW and WOOD treatments were lower compared to the REED and CTRL treatments. Those first treatments also showed a significantly higher contribution to PO_4 removal from the water column (Table S5.3).

The concentration of DSi in the drainage water mostly increased during the outflow phase for all treatments (Figure 5.6). This increase in DSi concentration was remarkably higher when the concentration in the estuary was low, which was the case in early summer. The increase was more profound in the organic treatments (REED and WOOD) compared to the PLOW and CTRL treatments. Overall, all the soil monoliths were a net source of DSi, except for the PLOW treatment during winter, when there was a slight import of DSi into the soil (Figure 5.7c). The export of DSi was not significantly different between the treatments, but was significantly higher in summer compared to winter (Table S5.3).

5.5   Discussion

In restored tidal marshes, groundwater seepage and nutrient cycling are often limited as compared to natural tidal marshes due to historical agricultural soil compaction and subsequent alteration of soil physical properties (Crooks and Pye, 2000; Tempest et al., 2015; Van Putte et al., 2020 (Chapter 2)). As such, there is a pressing need to gain insights in several restoration practices to alleviate this problem in future tidal marsh restoration projects. Here, we set up a mesocosm experiment in which we applied organic amendments to 'decompact' the soil and to stimulate soil-groundwater interactions and groundwater drainage.

In our experiments, we used a combination of plowing and subsequent rototilling to amend the soil with organic matter. Although long term repeated plowing is one of the main causes

of subsoil compaction due to pressure applied by agricultural equipment (e.g. Verbist et al., 2007), plowing can effectively be used to apply a layer of organic matter amendments up to a depth of around 30 cm. We then used rototilling to mix the soil with the organic amendments. We found a significantly lower bulk density in the amended soils compared to the CTRL plot. The higher variance we found for both bulk density and LOI after application of the treatments may result from an increased soil heterogeneity that is difficult to sample in the 100-cm^3 sample rings we used.

The groundwater drainage depth in between inundating tides was significantly deeper in the treated soils. This depth denotes the bottom of the zone that is intermittently saturated and unsaturated. This alternating soil aeration status enhances the removal of nitrogen from the system. In addition, soil aeration controls plant growth and development (Moffett et al., 2012; Ursino et al., 2004). This suggests that tilling and/or organic soil amendments can promote faster vegetation establishment in newly restored tidal marshes.

By calculating the nutrient mass balance, we were able to assess the impact of organic soil amendments on the exchange of N, P and Si with the tidal river. The ratio of these elements in the estuarine water has a direct impact on the primary production in the estuary (Garnier et al., 2010). Surprisingly, we found that the soil is on average a net source of DSi throughout the year (with only a small net import of DSi in the PLOW treatment during winter), in contrary to Carey and Fulweiler (2014) who found a salt marsh in Rhode Island, USA, to be a net sink for both DSi and BSi. However, freshwater and brackish tidal marshes have been found to be net DSi sources (Struyf et al., 2005). The soil of many freshwater and brackish tidal marshes consists for a large part of wetland plant debris (e.g. Temmerman et al., 2003), of which a substantial amount is reed. Reed contains high concentrations of BSi that can dissolve in the pore water and can be transported to the tidal river (Jacobs et al., 2008; Struyf et al., 2006). Struyf et al. (2007) state that in reed dominated tidal marshes, 40% of DSi export can be attributed to decomposition of *Phragmites australis*. Incorporating reed cuttings in newly restored tidal marsh soils is therefore a viable way to mimic the soil of natural tidal marshes. In the REED treatment, the DSi concentrations at the end of the drainage phase were the highest, especially during summer months, when concentrations in the tidal river were lower, which is in agreement with the findings of Van Damme et al. (2009). Tidal marshes play a crucial role in Si transformation and cycling, which is an essential regulating ecosystem service (Carey and Fulweiler, 2014; Jacobs et al., 2013; Struyf et al., 2005). Therefore, we argue that increasing DSi export through organic amendments can enhance the delivery of regulating ecosystem services of newly restored tidal marshes.

In tidal wetlands, nitrogen is removed from the marsh soil through coupled nitrification and denitrification (e.g. Wolf et al., 2011). Although denitrification in wetlands is more profound at higher temperatures (Hernandez and Mitsch, 2007), we found a higher removal of TDIN during winter months, when the concentration of TDIN in the river was higher. During these winter months, we observed the highest N removal in the plot

amended with woodchips. Woodchips contain high amounts of active ion exchange compounds (e.g. lignin and cellulose) to which sorption of NH_4-N is promoted (Dumont et al., 2014; Meffe et al., 2016). The beneficial use of poplar woodchips (*Populus* sp.) in soil amendments for water quality improvement has been stated previously. Poplar woodchips enhance the microbial activity, hereby reducing the redox status and promoting ammonium sorption, nitrification and denitrification (Meffe et al., 2016). Several studies found significantly higher denitrification rates in wetland soils amended with organic matter (e.g. Sutton-Grier et al., 2009; Yao et al., 2018). Remarkably, the PLOW treatment (in which no organic matter was added) also induced a high N removal compared to the CTRL monolith. Although we did not add additional organic matter to the PLOW plot, the grass that was present on the site was mixed with the soil during the treatments, which adds to the soil organic matter content. In addition, the PLOW monolith often showed the largest drainage volumes. Therefore, more nitrogen depleted water seeped out of the PLOW monolith at low tide compared to the other treatments. All treatments show a significantly higher N removal compared to the CTRL monolith and our results suggest the benefit of tilling and amending the soil with organic matter for enhanced denitrification.

Only in the WOOD and PLOW treatments, significantly more phosphate (PO_4) was removed from the drainage water compared to the CTRL treatment. The outcome of studies investigating PO_4 removal through organic soil amendments in wetlands is highly variable. While some papers indicate a positive effect of organic amendments on P removal (Bruland and Richardson, 2004), other studies found no effect (Meffe et al., 2016) or even a lower P removal with increased organic matter additions (Walker and Shannon, 2006). Meffe et al. (2016) state that PO_4 is removed from the water by sorption to calcium. Indeed, we found a higher Ca export in the PLOW and WOOD treatments (results shown in Figure S5.5), but we cannot state whether this results from the addition of organic amendments, since we did not measure Ca in either the soil nor in the organic matter used for the amendments.

The first water that seeps out of the soil monoliths has a similar chemical composition to the inundation water. The nutrient concentrations then increase (DSi) or decrease (TDIN and PO_4) rapidly and this increase or decrease diminishes over the course of the drainage phase. Howes and Goehringer (1994) explain this pattern as follows: water that laterally infiltrated into the soil during the last high tide, and therefore has a chemical composition similar to the inundation water, seeps out of the soil first, followed by water that comes from the more interior part of the soil and consists of water that infiltrated through the soil surface. This latter part of the drainage water takes a longer pathway through the soil pore network, resulting in a higher residence time, increased contact with the soil matrix and therefore an altered chemical composition.

This pilot study presents the first results of the effect of organic soil amendments on water quality improvement in restored tidal marshes. However, the design of the mesocosm construction presents two main limitations. Firstly, only four mesocosm units were available, excluding the possibility to replicate soil treatments. We limited the risk of this

shortcoming by using large (1.5 m x 1.5 m x 0.75 m) monoliths and repeated sampling. Secondly, we were only able to sample the drainage water after the surface water level in the river dropped below the bottom of the soil monoliths. However, since this first outflow water is similar in chemical composition to the inundation water, we are confident that our calculated mass balances still provide a good estimate of the nutrient exchange between the flooding water and the marsh soil near a tidal creek.

In tidal marsh ecosystems, pore water seepage is governed by the interaction of creek network density and soil hydraulic properties (Van Putte et al., 2022 (Chapter 4)). Therefore, our results might overestimate the per area mass balance since the water could seep from the four sides of the soil monoliths in the experiment and might therefore be more representative for nutrient exchange near tidal creeks. We argue that the application of soil amendments to stimulate groundwater drainage and nutrient removal is most efficient when applied where a dense creek network is present, which can be achieved through creek initiation (Liu et al., 2020; Tovey et al., 2009).

The results of our study support the benefits of organic amendments to ameliorate the water quality improving function of newly restored tidal marshes. Despite the large benefits of organic soil amendments for wetland restoration supported by our study, soil amendments also present several risks. Increased soil organic matter content promotes microbial activity and, as a result, increases the methane emission of the wetland (Ballantine et al., 2015; Scott et al., 2022). Management strategies should therefore be based on the desired provision of ecosystem services.

5.6   Acknowledgements

5.7   References

Ballantine, K.A., Lehmann, J., Schneider, R.L., Groffman, P.M., 2015. Trade-offs between soil-based functions in wetlands restored with soil amendments of differing lability. Ecological Applications 25, 215-225. 10.1890/13-1409.1

Bantilan-Smith, M., Bruland, G.L., MacKenzie, R.A., Henry, A.R., Ryder, C.R., 2009. A comparison of the vegetation and soils of natural, restored, and created coastal lowland wetlands in Hawai'i. Wetlands 29, 1023-1035. 10.1672/08-127.1

Barbier, E.B., Hacker, S.D., Kennedy, C., Koch, E.W., Stier, A.C., Silliman, B.R., 2011. The value of estuarine and coastal ecosystem services. Ecological Monographs 81, 169-193. 10.1890/10-1510.1

Boerema, A., Meire, P., 2017. Management for estuarine ecosystem services: A review. Ecological Engineering 98, 172-182. 10.1016/j.ecoleng.2016.10.051

Bruland, G.L., Richardson, C.J., 2004. Hydrologic Gradients and Topsoil Additions Affect Soil Properties of Virginia Created Wetlands. Soil Science Society of America Journal 68, 2069-2077. 10.2136/sssaj2004.2069

Burden, A., Garbutt, R.A., Evans, C.D., Jones, D.L., Cooper, D.M., 2013. Carbon sequestration and biogeochemical cycling in a saltmarsh Subject to coastal managed realignment. Estuarine Coastal and Shelf Science 120, 12-20. 10.1016/j.ecss.2013.01.014

Callaway, J.C., Zedler, J.B., Ross, D.L., 1997. Using tidal salt marsh mesocosms to aid wetland restoration. Restoration Ecology 5, 135-146. 10.1046/j.1526-100X.1997.09716.x

Carey, J.C., Fulweiler, R.W., 2014. Salt marsh tidal exchange increases residence time of silica in estuaries. Limnology and Oceanography 59, 1203-1212. 10.4319/lo.2014.59.4.1203

Chambers, R.M., Odum, W.E., 1990. Porewater Oxidation, Dissolved Phosphate and the Iron Curtain: Iron-Phosphorus Relations in Tidal Freshwater Marshes. Biogeochemistry 10, 37-52.

Costanza, R., Perez-Maqueo, O., Martinez, M.L., Sutton, P., Anderson, S.J., Mulder, K., 2008. The value of coastal wetlands for hurricane protection. Ambio 37, 241-248. 10.1579/0044-7447(2008)37[241:Tvocwf]2.0.Co;2

Cox, T.J.S., Maris, T., De Vleeschauwer, P., De Mulder, T., Soetaert, K., Meire, P., 2006. Flood control areas as an opportunity to restore estuarine habitat. Ecological Engineering 28, 55-63. 10.1016/j.ecoleng.2006.04.001

Cox, T.J.S., Schepers, L., 2018. Tides R-package v2.1. 10.5281/zenodo.897843

Crooks, S., Pye, K., 2000. Sedimentological controls on the erosion and morphology of saltmarshes: implications for flood defence and habitat recreation. Coastal and Estuarine Environments: Sedimentology, Geomorphology and Geoarchaeology 175, 207-222. 10.1144/Gsl.Sp.2000.175.01.16

De Haan, A., Verboven, H., 2008. Polder van Kruibeke, Bazel en Rupelmonde. Agentschap Onroerend Erfgoed.

DeMaster, D.J., 1981. The supply and accumulation of silica in the marine environment. Geochimica Et Cosmochimica Acta 45, 1715-1732. 10.1016/0016-7037(81)90006-5

Dumont, P., Chadwick, D., Robinson, S., 2014. Nutrient removal capacity of wood residues for the Agro-environmental safety of ground and surface waters. Sustainability, Agri, Food and Environmental Research 2. 10.7770/safer-V2N2-art758

European Parliament and the Council of the European Union, 1992. Directive 92/43/EEC of 21 May 1992 on the conservation of natural habitats and of wild fauna and flora. Official Journal of the European Communities L206. 22.7.1992.

European Parliament and the Council of the European Union, 2000. Directive 2000/60/EC of the European Parliament and the Council establishing a framework for the Community action in the field of water policy. Official Journal of the European Communities L327.22.12.2000.

Foster-Martinez, M.R., Variano, E.A., 2018. Biosolids as a marsh restoration amendment. Ecological Engineering 117, 165-173. 10.1016/j.ecoleng.2018.02.012

French, P.W., 2006. Managed realignment - The developing story of a comparatively new approach to soft engineering. Estuarine Coastal and Shelf Science 67, 409-423. 10.1016/j.ecss.2005.11.035

Garnier, J., Beusen, A., Thieu, V., Billen, G., Bouwman, L., 2010. N:P:Si nutrient export ratios and ecological consequences in coastal seas evaluated by the ICEP

approach. Global Biogeochemical Cycles 24. 10.1029/2009GB003583

Gibson, K.D., Zedler, J.B., Langis, R., 1994. Limited Response of Cordgrass (Spartina-Foliosa) to Soil Amendments in a Constructed Marsh. Ecological Applications 4, 757-767. 10.2307/1942006

Gutknecht, J.L.M., Goodman, R.M., Balser, T.C., 2006. Linking soil process and microbial ecology in freshwater wetland ecosystems. Plant and Soil 289, 17-34. 10.1007/s11104-006-9105-4

Havens, K.J., Varnell, L.M., Watts, B.D., 2002. Maturation of a constructed tidal marsh relative to two natural reference tidal marshes over 12 years. Ecological Engineering 18, 305-315. 10.1016/S0925-8574(01)00089-1

Heiri, O., Lotter, A.F., Lemcke, G., 2001. Loss on ignition as a method for estimating organic and carbonate content in sediments: reproducibility and comparability of results. Journal of Paleolimnology 25, 101-110. 10.1023/a:1008119611481

Hernandez, M.E., Mitsch, W.J., 2007. Denitrification in created riverine wetlands: Influence of hydrology and season. Ecological Engineering 30, 78-88. 10.1016/j.ecoleng.2007.01.015

Howes, B.L., Goehringer, D.D., 1994. Porewater Drainage and Dissolved Organic-Carbon and Nutrient Losses through the Intertidal Creekbanks of a New-England Salt-Marsh. Marine Ecology Progress Series 114, 289-301. 10.3354/meps114289

Iost, S., Landgraf, D., Makeschin, F., 2007. Chemical soil properties of reclaimed marsh soil from Zhejiang Province PR China. Geoderma 142, 245-250. 10.1016/j.geoderma.2007.08.001

Jacobs, S., Muller, F., Teuchies, J., Oosterlee, L., Struyf, E., Meire, P., 2013. The Vegetation Silica Pool in a Developing Tidal Freshwater Marsh. Silicon 5, 91-100. 10.1007/s12633-012-9136-9

Jacobs, S., Struyf, E., Maris, T., Meire, P., 2008. Spatiotemporal aspects of silica buffering in restored tidal marshes. Estuarine Coastal and Shelf Science 80, 42-52. 10.1016/j.ecss.2008.07.003

Kennish, M.J., 2002. Environmental threats and environmental future of estuaries. Environmental Conservation 29, 78-107. 10.1017/S0376892902000061

Keshta, A., Koop-Jakobsen, K., Titschack, J., Mueller, P., Jensen, K., Baldwin, A., Nolte, S., 2020. Ungrazed salt marsh has well connected soil pores and less dense sediment compared with grazed salt marsh: a CT scanning study. Estuarine, Coastal and Shelf Science 245. 10.1016/j.ecss.2020.106987

Liu, Z., Fagherazzi, S., She, X., Ma, X., Xie, C., Cui, B., 2020. Efficient tidal channel networks alleviate the drought-induced die-off of salt marshes: Implications for coastal restoration and management. Science of the Total Environment 749. 10.1016/j.scitotenv.2020.141493

Maietta, C.E., Monsaint-Queeney, V., Wood, L., Baldwin, A.H., Yarwood, S.A., 2020. Plant litter amendments in restored wetland soils altered microbial communities more than clay additions. Soil Biology and Biochemistry 147. 10.1016/j.soilbio.2020.107846

Maris, T., Cox, T.J.S., Temmerman, S., De Vleeschauwer, P., Van Damme, S., De Mulder, T., Van den Bergh, E., Meire, P., 2007. Tuning the tide: creating ecological conditions for tidal marsh development in a flood control area. Hydrobiologia 588, 31-43. 10.1007/s10750-007-0650-5

Mcleod, E., Chmura, G.L., Bouillon, S., Salm, R., Björk, M., Duarte, C.M., Lovelock, C.E., Schlesinger, W.H., Silliman, B.R., 2011. A blueprint for blue carbon: toward an improved understanding of the role of vegetated coastal habitats in sequestering CO2. Frontiers in Ecology and the Environment 9, 552-560. 10.1890/110004

Meffe, R., de Miguel, Á., Martínez Hernández, V., Lillo, J., de Bustamante, I., 2016. Soil amendment using poplar woodchips to enhance the treatment of wastewater-originated nutrients. Journal of Environmental Management 180, 517-525. 10.1016/j.jenvman.2016.05.083

Meire, P., Ysebaert, T., Van Damme, S., Van den Bergh, E., Maris, T., Struyf, E., 2005. The Scheldt estuary: A description of a changing ecosystem. Hydrobiologia 540, 1-11. 10.1007/s10750-005-0896-8

Mitsch, W.J., Gosselink, J.G., 2000. The value of wetlands: importance of scale and landscape setting. Ecological Economics 35, 25-33. 10.1016/S0921-8009(00)00165-8

Moffett, K.B., Gorelick, S.M., McLaren, R.G., Sudicky, E.A., 2012. Salt marsh ecohydrological zonation due to heterogeneous

vegetation–groundwater–surface water interactions. Water Resources Research 48. 10.1029/2011WR010874

Mossman, H.L., Grant, A., Davy, A.J., 2020. Manipulating saltmarsh microtopography modulates the effects of elevation on sediment redox potential and halophyte distribution. Journal of Ecology 108, 94-106. 10.1111/1365-2745.13229

Mys, M., Gullentops, F., Janssens, P., Wuytack, M.J., Stinissen, H., 1983. De holocene evolutie van de alluviale vlakte van de Beneden-Schelde. Tijdschrift van de Belgische Vereniging voor Aardrijkskundige Studies 30, 217-255.

Narayan, S., Beck, M.W., Reguero, B.G., Losada, I.J., van Wesenbeeck, B., Pontee, N., Sanchirico, J.N., Ingram, J.C., Lange, G.M., Burks-Copes, K.A., 2016. The Effectiveness, Costs and Coastal Protection Benefits of Natural and Nature-Based Defences. Plos One 11.

Novozamsky, I., Houba, V.J.G., van Eck, R., van Vark, W., 1983. A novel digestion technique for multi-element plant analysis. Communications in Soil Science and Plant Analysis 14, 239-248. 10.1080/00103628309367359

Oosterlee, L., Cox, T.J.S., Vandenbruwaene, W., Maris, T., Temmerman, S., Meire, P., 2017. Tidal Marsh Restoration Design Affects Feedbacks Between Inundation and Elevation Change. Estuaries and Coasts. 10.1007/s12237-017-0314-2

Ott, E.T., Galbraith, J.M., Daniels, W.L., Aust, W.M., 2020. Effects of amendments and microtopography on created tidal freshwater wetland soil morphology and carbon. Soil Science Society of America Journal 84, 638-652. 10.1002/saj2.20057

Pinheiro, J.C., Bates, D., 2009. Mixed-Effects Models in S and S-PLUS. Springer.

Portnoy, J.W., Giblin, A.E., 1997. Effects of historic tidal restrictions on salt marsh sediment chemistry. Biogeochemistry 36, 275-303. 10.1023/A:1005715520988

R Development Core Team, 2022. R: A Language and Environment for Statistical Computing. R Foundation for Statistical Computing, Vienna, Austria.

Scott, B., Baldwin, A., Ballantine, K., Palmer, M., Yarwood, S., 2020. The role of organic amendments in wetland restorations: Organic Amendments Wetland Restoration. Restoration Ecology. 10.1111/rec.13179

Scott, B., Baldwin, A.H., Yarwood, S.A., 2022. Quantification of potential methane emissions associated with organic matter amendments following oxic-soil inundation. Biogeosciences 19, 1151-1164. 10.5194/bg-19-1151-2022

Shierlaw, J., Alston, A.M., 1984. Effect of soil compaction on root growth and uptake of phosphorus. Plant and Soil 77, 15-28. 10.1007/BF02182808

Spencer, K.L., Carr, S.J., Diggens, L.M., Tempest, J.A., Morris, M.A., Harvey, G.L., 2017. The impact of pre-restoration land-use and disturbance on sediment structure, hydrology and the sediment geochemical environment in restored saltmarshes. Science of the Total Environment 587, 47-58. 10.1016/j.scitotenv.2016.11.032

Struyf, E., Dausse, A., Van Damme, S., Bal, K., Gribsholt, B., Boschker, H.T.S., Middelburg, J.J., Meire, P., 2006. Tidal marshes and biogenic silica recycling at the land-sea interface. Limnology and Oceanography 51, 838-846.

Struyf, E., Van Damme, S., Gribsholt, B., Bal, K., Beauchard, O., Middelburg, J.J., Meire, P., 2007. Phragmites australis and silica cycling in tidal wetlands. Aquatic Botany 87, 134-140. 10.1016/j.aquabot.2007.05.002

Struyf, E., Van Damme, S., Gribsholt, B., Middelburg, J.J., Meire, P., 2005. Biogenic silica in tidal freshwater marsh sediments and vegetation (Schelde estuary, Belgium). Marine Ecology Progress Series 303, 51-60. 10.3354/meps303051

Sutton-Grier, A.E., Ho, M., Richardson, C.J., 2009. Organic Amendments Improve Soil Conditions and Denitrification in a Restored Riparian Wetland. Wetlands 29, 343-352.

Temmerman, S., Govers, G., Meire, P., Wartel, S., 2003. Modelling long-term tidal marsh growth under changing tidal conditions and suspended sediment concentrations, Scheldt estuary, Belgium. Marine Geology 193, 151-169. 10.1016/S0025-3227(02)00642-4

Tempest, J.A., Harvey, G.L., Spencer, K.L., 2015. Modified sediments and subsurface hydrology in natural and recreated salt marshes and implications for delivery of ecosystem services. Hydrological Processes 29, 2346-2357. 10.1002/hyp.10368

Tovey, E.L., Pontee, N.I., Harvey, R., 2009. Managed Realignment at Hesketh Out Marsh West.

Proceedings of the Institution of Civil Engineers - Engineering Sustainability 162, 223-228. 10.1680/ensu.2009.162.4.223

Ursino, N., Silvestri, S., Marani, M., 2004. Subsurface flow and vegetation patterns in tidal environments. Water Resources Research 40. 10.1029/2003wr002702

Van Damme, S., Dehairs, F., Tackx, M., Beauchard, O., Struyf, E., Gribsholt, B., Van Cleemput, O., Meire, P., 2009. Tidal exchange between a freshwater tidal marsh and an impacted estuary: the Scheldt estuary, Belgium. Estuarine Coastal and Shelf Science 85, 197-207. 10.1016/j.ecss.2009.08.005

Van Putte, N., Meire, P., Seuntjens, P., Joris, I., Verreydt, G., Hambsch, L., Temmerman, S., 2022. Solving hindered groundwater dynamics in restored tidal marshes by creek excavation and soil amendments: A model study. Ecological Engineering 178. 10.1016/j.ecoleng.2022.106583

Van Putte, N., Temmerman, S., Verreydt, G., Seuntjens, P., Maris, T., Heyndrickx, M., Boone, M., Joris, I., Meire, P., 2020. Groundwater dynamics in a restored tidal marsh are limited by historical soil compaction. Estuarine, Coastal and Shelf Science 244. 10.1016/j.ecss.2019.02.006

Vandenbruwaene, W., Meire, P., Temmerman, S., 2012. Formation and evolution of a tidal channel network within a constructed tidal marsh. Geomorphology 151, 114-125. 10.1016/j.geomorph.2012.01.022

Verbist, K., Cornelis, W., Schiettecatte, W., Oltenfreiter, G., Meirvenne, M., Gabriels, D., 2007. The influence of a compacted plow sole on saturation excess runoff. Soil & Tillage Research 96, 292-302. 10.1016/j.still.2007.07.002

Walker, C.W., Shannon, R.D., 2006. Nitrate and Phosphate Removal Effects of Compost Amendments in Wetland Mesocosms. Transactions of the Asabe 49, 1773-1778. 10.13031/2013.22298

Waterinfo, 2022. Neerslag, droogte, getijden en overstromingen, Vlaamse Milieumaatschappij, Waterbouwkundig Laboratorium, Maritieme Dienstverlening & Kust, De Vlaamse Waterweg.

Wolf, K.L., Ahn, C., Noe, G.B., 2011. Development of Soil Properties and Nitrogen Cycling in Created Wetlands. Wetlands 31, 699-712. 10.1007/s13157-011-0185-4

Yao, S.Q., Groffman, P.M., Alewell, C., Ballantine, K., 2018. Soil amendments promote denitrification in restored wetlands. Restoration Ecology 26, 294-302. 10.1111/rec.12573

6

Synthesis and discussion

6.1 Objectives and synthesis of this thesis

Along estuaries and coasts worldwide, tidal marshes are increasingly restored to counteract the loss of biodiversity, associated with the decrease of tidal marsh area resulting from large scale land embankments for industry, agriculture and urbanization. However, when tidal marshes are restored on formerly embanked agricultural land, these newly restored tidal marshes often show an impaired delivery of ecosystem services compared to natural tidal marshes (e.g. Burden et al., 2019; Mossman et al., 2012; Spencer and Harvey, 2012; Wolters et al., 2005). The reason for this impaired delivery is still poorly understood. In this thesis, we focused on one very important ecosystem service: the contribution of restored marshes to water quality improvement as compared to natural marshes. To do so, we investigated groundwater dynamics and biogeochemical cycling in both natural and restored tidal marshes. We discovered that historical agricultural soil compaction in restored tidal marshes greatly reduced the macroporosity and hydraulic conductivity of the soil, leading to reduced groundwater dynamics as compared to natural tidal marshes (**Chapter 2**). Groundwater dynamics control the soil aeration status and the flow of nutrients. This reduction of groundwater dynamics in restored tidal marshes, therefore, strongly affects nutrient porewater concentrations and impairs the potential of restored tidal marshes to contribute to water quality improvement (**Chapter 3**). Therefore, our findings indicate the need for viable design strategies to optimize the contribution to water quality improvement in future tidal marsh restoration projects. Here, we proposed creek excavation and organic soil amendments prior to restoration as such measures. By means of a modelling study, including scenario analyses, in **Chapter 4**, we demonstrated that increasing the creek density greatly increases soil aeration and total seepage fluxes. In **Chapter 5**, the results of a large scale mesocosm experiment suggest the benefits of organic soil amendments for nutrient cycling. As such, this thesis provides new insights in the relations between soil properties, groundwater dynamics and biogeochemical cycling in restored versus natural tidal marshes and adds to the state of the art regarding optimal tidal marsh restoration. Figure 6.1 provides a schematic overview of the rationale and the main findings of this PhD thesis.
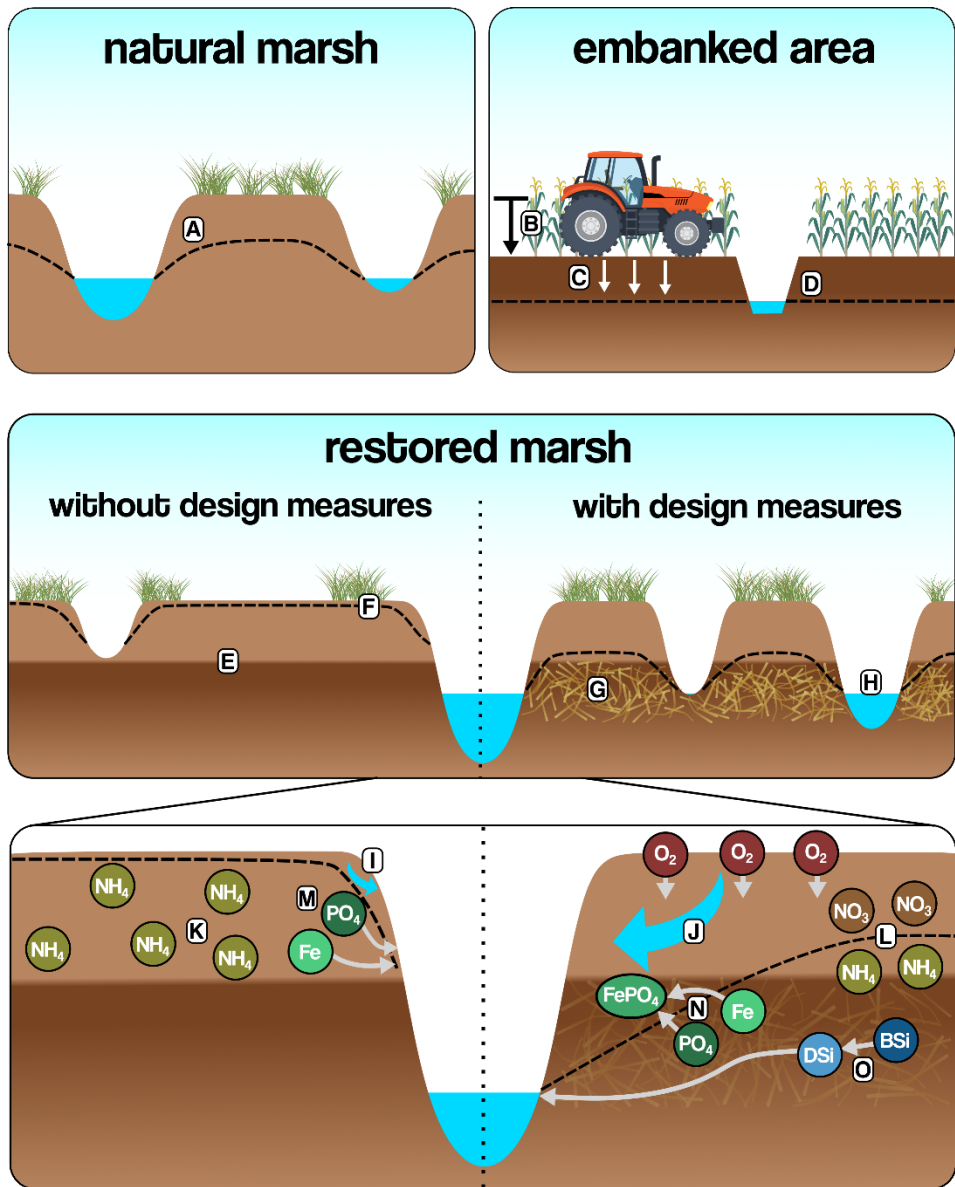
Figure 6.1: Conceptual overview of the main findings of this PhD thesis. (A): The natural marsh has a high creek density and a porous soil, leading to enhanced groundwater dynamics. (B): compaction leads to subsidence and a lower elevation. (C): The soil is compacted by the use of heavy farming equipment. (D): Artificial drainage ditches keep the groundwater permanently low, leading to mineralization of organic matter and subsequent consolidation of the soil. (E): After restoration, a layer of more porous and organic matter rich sediment accretes over time. (F): Restriction of groundwater drainage by the compacted soil and the absence of a dense creek network lead to higher average groundwater levels and reduced soil aeration. (G): Organic soil amendments increase the soil porosity and hydraulic conductivity, enhancing groundwater dynamics. (H): Creek excavation leads to a higher creek density and increased formation of a hydraulic gradient, enhancing groundwater dynamics. (I): soil aeration and seepage fluxes are limited to the zone near the creek. (J): Soil amendments and creek excavation lead to enhanced soil aeration and seepage fluxes. (K): In the always saturated zone, nitrogen is mainly present as ammonium. (L): In the well aerated zone, nitrogen is mainly present as nitrate, promoting denitrification. (M): Dissolved iron and phosphate are advectively transported towards the creek. (N): Iron is oxidized in the well aerated zone. Dissolved phosphate sorbs to iron oxyhydroxides and is trapped in the soil. (O): Biogenic silica from organic matter dissolves and is advectively transported towards creeks.

6.2 Historical soil compaction on formerly embanked agricultural land impairs subsurface hydrology after restoration.

In tidal marshes, groundwater dynamics are governed by (i) the hydraulic properties of the soil (i.e. the ease of which groundwater can flow through soil pores and the water retention capacity of the soil), (ii) the presence and density of a creek network through which groundwater can drain, (iii) the amplitude and variation of the tides and (iv) precipitation and (evapo)transpiration. In the next paragraphs, we explain how these factors affect groundwater dynamics in tidal marshes and how historical agricultural soil compaction interferes with these factors, leading to reduced groundwater dynamics in restored tidal marshes.

Tidal marsh restoration projects are mostly executed on formerly embanked land, now in agricultural use. However, centuries of agricultural land use changed the soil structure in these areas to a great extent. Excessive drainage and resulting organic matter mineralization, trampling by grazing cattle and the use of heavy equipment during the construction of the restoration site all contribute to the compaction and consolidation of the topsoil (Ballantine et al., 2012; Bantilan-Smith et al., 2009; Keshta et al., 2020)(Figure 6.1). When tidal marshes are restored in such areas, a new layer of tidally deposited sediment accretes on top of the relict compact soil. Nevertheless, the presence of this compact soil has severe implications for the developmental trajectory of newly restored tidal marshes. In Chapter 2, we compared the physical soil structure of a natural and a restored marsh using micro-CT scanning of soil cores. In the restored marsh, we compared the tidally deposited sediment with the relict agricultural soil. We found that the physical soil structure differed substantially between these two layers, whereas the texture of the relict agricultural soil and the tidally deposited soil was comparable (which is logical as they share the same origin as tidally deposited sediment). In the tidally deposited sediment, the soil is intersected by organic matter fragments and macropore (> 60 μm) networks, which are virtually absent in the relict compact layer. Macropore networks act as preferential flow channels and can increase hydraulic conductivity of the soil by several orders of magnitude, especially in otherwise lowly conductive fine-grained soils (Xiao et al., 2019; Xu et al., 2021). In that regard, we propose the idea of macropores acting as an underground extension of the creek network in tidal marshes. Although macropore networks and creek networks differ fundamentally in their geomorphologic origin and in flow resistance, they share a common function of delivering and removing water and dissolved elements to and from the marsh.

The depth of distinct soil layers (i.e. the soil stratigraphy) also plays an important role in governing groundwater dynamics in tidal marshes (Gardner, 2007). In many natural tidal marshes, the fine-grained topsoil is underlain by sandy sediment, which was deposited when the marsh was lower and experienced higher hydrodynamic forces. The presence of this sandy layer can increase seepage fluxes by an order of magnitude (Gardner, 2007). As mentioned, in restored tidal marshes, the opposite is often the case, with a more

permeable, porous topsoil of tidally deposited sediment, underlain by a compact, relict agricultural soil (Spencer and Harvey, 2012; Tempest et al., 2015). Since tidally induced groundwater level fluctuations are mostly restricted to this porous upper layer (Chapter 2), the thickness of this layer is crucial. In Chapter 4, we showed, using a numerical model, that increasing the thickness of the tidally deposited layer from 40 cm to 60 cm more than doubles the seepage volume over a spring tide – neap tide cycle. Of course, this increase depends on the hydraulic properties of both layers.

Groundwater can only drain from a tidal marsh soil when a hydraulic gradient (i.e. a difference in hydraulic head) can be established. In tidal marshes, a steep hydraulic gradient forms during ebb and low tide at the creek edges (Chapter 2, Figure 6.1), which stimulates seepage from the marsh soil into the creeks. In this way, the density of the tidal creek network controls the total seepage flux from a tidal marsh soil. Furthermore, also geomorphologic parameters such as the creek depth and bank slope affect seepage volumes (Gardner, 2005). When tidal marshes are restored on formerly embanked agricultural land, these creek networks are absent. In lower elevated parts of restored marshes, where sediment accretion is fast, creeks can develop quickly in this newly deposited sediment. In higher elevated parts, however, the shallow erosion resistant compact soil induces slower incision of creeks (Vandenbruwaene et al., 2012).

Groundwater dynamics are also inherently controlled by the tidal characteristics, especially by the tidal amplitude and the elevation of the marsh platform relative to the mean water level. In macrotidal estuaries, where the difference between high and low water is larger, a steeper subsurface hydraulic gradient can be established at low tide, inducing increased groundwater dynamics. In microtidal estuaries, groundwater dynamics are limited by smaller hydraulic gradients (Wilson and Morris, 2012). The decrease of the groundwater level during ebb and low tide starts near the creek banks and then slowly progresses further into the marsh interior (e.g. Harvey et al., 1987). As a result, the deepest drainage depth that can be reached, especially in the marsh interior, depends on the duration of the non-inundated time. In higher elevated marshes, which only flood around spring tides, this duration is longer compared to lower elevated marshes that experience a higher inundation frequency. The formerly embanked agricultural land, on which marsh restoration is mostly executed, often has a much lower elevation compared to natural tidal marshes, resulting from the lack of tidal sediment accretion, and from soil compression (Beauchard et al., 2011). When tidal marshes are restored on these areas by managed realignment (i.e. breaching the current flood defense and creating a new flood defense more land inwards), these tidal marshes experience a higher inundation frequency and attain only shallow groundwater drainage depths (Tempest et al., 2015).

Lastly, water (but not solutes) can be removed from a tidal marsh soil through evapotranspiration. Tidal marsh vegetation transpires large volumes of water through their stomata (e.g. Takahashi et al., 2014). In the marsh interior, evapotranspiration is often the main driver for groundwater removal from tidal marsh soils (Xin et al., 2017). In newly

restored tidal marshes, vegetation establishment can be hampered by soil compaction, as plant roots are unable to penetrate the compact soil (e.g. Sloey et al., 2015). As is clear from the previous paragraphs, soil compaction in formerly embanked agricultural areas impairs groundwater dynamics in newly restored tidal marshes in many ways.

6.3 Reduced groundwater dynamics negatively impact the contribution of newly restored tidal marshes to water quality improvement

Tidal marshes contribute to the improvement of the estuarine water quality (Megonigal and Neubauer, 2019; Neubauer et al., 2005). In this thesis, We focused on removal of nitrogen (N), retention of phosphorus (P) and delivery of dissolved silica (DSi). The ratio between N, P and Si in the estuarine water determines whether algal communities are composed mainly of diatom species or non-diatom species. A shift towards a non-diatom dominated community in the estuary can cause eutrophication events in the coastal zone (e.g. Struyf et al., 2007). Hence, the ratio of N, P and DSi in the estuarine water is an important factor for the estuarine ecological functioning.

Groundwater dynamics in tidal marshes affect biogeochemical cycling of N, P and DSi in two different ways. Firstly, dissolved elements follow the movement of groundwater through advective transport (Harvey and Nuttle, 1995). As such, nutrients can be exported from the marsh soil when groundwater seeps out of the creek banks, and imported into the marsh soil when surface water infiltrates the marsh platform. The mass flux of dissolved nutrients depends on the nutrient concentration and the groundwater flux. Secondly, when groundwater is removed from the marsh soil, either through seepage through creek banks or by evapotranspiration, water in larger soil pores is replaced by air containing oxygen (i.e. soil aeration). These changes in the soil aeration status determine the soil redox status (Grande et al., 2022). Together with the presence of organic matter, this redox status determines the prevailing microbially mediated biogeochemical reactions (Neubauer et al., 2005; Scott et al., 2022). A reduction in groundwater dynamics in tidal marshes restored on historically compacted soil has, therefore, also strong implications for the marsh' ability to contribute to biogeochemical cycling (Figure 6.1). From the above, it is clear that both advective transport and soil aeration, which are both mediated by tidally induced groundwater dynamics, are essential in maintaining the filter function of tidal marshes and their contribution to water quality improvement.

The removal of nitrogen from the porewater relies on coupled nitrification and denitrification processes, which take place under aerobic and anaerobic conditions, respectively (e.g. Wolf et al., 2011), indicating the need for alternating soil aeration and saturation. Where soil aeration is limited by hampered groundwater drainage, e.g. in the interior of a restored marsh, nitrification is inhibited and high concentrations of ammonium are found in the porewater (Chapter 3). In the natural marsh, total dissolved nitrogen concentrations are lowest in the marsh interior. These results support the hypothesis that N removal in restored tidal marsh soils is focused near the creeks, whereas the entire natural marsh soil contributes to N removal. However, vegetation distribution

also plays a crucial role in nitrogen removal through coupled nitrification and denitrification. Wetland plants provide a source of carbon, which is needed for denitrification, and they introduce oxygen into the soil via diffusion through their root system (Alldred and Baines, 2016).

Phosphorus is removed from the porewater by adsorption to mainly iron oxides. These iron oxides only persist in aerobic conditions, i.e. in well drained soils. At the well-drained creek banks, an 'iron curtain' develops, which traps dissolved phosphate flowing from the more anoxic marsh interior towards the creeks via advective transport (Chambers and Odum, 1990; Megonigal and Neubauer, 2019). Our results confirm this as dissolved phosphate and dissolved iron concentrations were always lower in the well aerated zone near creeks. Higher concentrations of phosphate were always found in the poorly aerated soil in the restored marsh, suggesting a reduced contribution of restored tidal marshes to P retention, since both soil aeration and advective transport are negatively impacted by reduced groundwater dynamics (Chapter 3). No correlation was found between DSi concentrations and soil aeration. Export of DSi from the marsh soil depends on the amount of BSi that is available to dissolve and on the advective transport that moves DSi towards tidal creeks (Struyf and Conley, 2009). Therefore, the export of DSi from restored tidal marshes is expected to increase over time, when BSi rich organic sediment accumulates on top of the compact agricultural soil, and the more porous structure and increased thickness of this accreted soil layer allows for increased advective transport (Chapter 4). Long term monitoring of the restored Lippenbroek site indeed showed a transition from DSi import (supposedly due to consumption by microphytobenthos) to DSi export in more recent years (Maris et al., 2021).

In conclusion, our results support the hypothesis that N removal, P retention and DSi export, and thus the contribution to water quality improvement, is limited where groundwater dynamics are hindered. However, some sites in the restored marsh did not show impaired groundwater dynamics. In the res A transect in the restored site (Chapter 3), groundwater level fluctuations persist in the marsh soil at 10 m from the creek banks, even during non-flooding tides (Chapter 3), which was never observed even in the natural marsh. Also here, we observed large amounts of water seeping out of the creek banks through macropores (presumably crab burrows) during ebb and low tides. This suggests a connection of the upper layer of tidally deposited sediment with a more sandy layer underneath the relict agricultural soil, presumably through these macropore networks. On the one hand, this observation indicates that different pre-restoration land use might lead to different degrees of soil compaction and reduction in porosity. Therefore, former agricultural land use might not always lead to reduced groundwater dynamics after restoration, implying the need for a pre-restoration assessment of soil properties and stratigraphy. On the other hand, porewater concentrations of ammonium, phosphate and iron were always lower in this well drained transect, compared to the poorly drained res B and res C transect, supporting the hypothesis of limited contribution to water quality improvement where groundwater dynamics are hindered.

6.4 Improving groundwater dynamics and nutrient cycling in newly restored tidal marshes

In Chapter 2 and Chapter 3, we discussed the inhibition of groundwater dynamics in newly restored tidal marshes by the presence of a compact soil layer and the absence of a dense creek network, preventing the establishment of a hydraulic gradient. Groundwater dynamics and biogeochemical cycling are expected to gradually improve as a layer of tidally deposited sediment accretes on top of the compact agricultural soil, and a dense creek network develops by erosive processes (Vandenbruwaene et al., 2012). These processes can take multiple decades, while a fast growing delivery of regulating ecosystem services after restoration is mostly preferred. Based on this, we hypothesized that artificial creek excavation, and application of soil amendments can amplify groundwater dynamics and jumpstart the contribution of newly restored tidal marshes to water quality improvement. To test these hypotheses, in Chapter 4 we set up a numerical, variably saturated, dual porosity (taking into account macroporosity), 2D vertical flow and transport model for a creek – marsh cross section. We then varied the number of creeks in the model domain (simulating creek excavation) and the depth of the more porous tidally deposited sediment (simulating soil amendments up to a certain depth, as amending soil with a certain amount of organic matter aims to approximate the hydraulic properties of this tidally deposited sediment). We discovered that both increasing the creek density and the thickness of the amended soil layer significantly increased the aerated proportion of the marsh soil and the total seepage volume, and decreased the residence time of solutes, leading to a higher turnover rate (Chapter 4). However, our main finding here is that especially the interaction between creek density and the thickness of the amended layer is important, meaning that increasing this thickness attains the largest effect when also the creek density is increased. Increasing the creek density increases the proportion of the marsh over which a hydraulic gradient is established at ebb and low tide. Even if the hydraulic conductivity of the soil is high (due to organic amendments), groundwater can only flow if there is a hydraulic gradient (Harvey et al., 1987).

In natural tidal marshes, creek erosion may lead to the development of wider and deeper creeks until a morphodynamic equilibrium is reached (i.e. given a certain tidal prism, as creeks widen and deepen, the bed shear stress acting on the creeks banks and bottom will decrease until a morphodynamic equilibrium between creek dimensions and tidal prism is reached (D'Alpaos et al., 2010; Lawrence et al., 2004; Vandenbruwaene et al., 2013)). In our simulations, the total cross sectional area of creeks in the model domain was kept constant to conserve this morphodynamic equilibrium, leading to more shallow and more narrow creeks as their number increased. We varied the creek density from 0.02 creeks/m to 0.1 creeks/m. The effect of adding one more creek to the domain became progressively smaller with an increasing number of creeks, especially with a larger thickness of the amended layer. Although it is beyond the results of the simulated scenarios, we speculate that, when soil amendments are applied, exceeding a certain creek density will lead to decreased seepage fluxes and advective transport, as the creeks are getting progressively

shallower. In this case, drainage of the layer of tidally deposited sediment becomes restricted by the smaller hydraulic gradients resulting from shallower creeks, rather than being restricted by the depth to the compact soil layer.

From the above, it is clear that a combination of soil amendments and creek excavation leads to increased advective flow and increased soil aeration, resulting in a faster turnover rate of porewater (Figure 6.1). Based on the results in Chapter 3, this increase in turnover rate is expected to increase the cycling of silica, as BSi dissolution is increased when DSi concentrations are lower (Huang et al., 2022). In iron rich sediments, increased soil aeration and advective flow will enhance phosphorus retention in marsh soils (Chambers and Odum, 1990; Megonigal and Neubauer, 2019). In addition, increased soil aeration likely increases nitrification rates. However, one has to be careful as excessive soil aeration increases the depth to the anaerobic zone, which might inhibit denitrification and the potential for N removal, especially in higher marshes with a very low inundation frequency (Megonigal and Neubauer, 2019).

As mentioned in Chapter 4, we assumed that amending the soil with organic matter would result in similar soil hydraulic properties as the layer of highly organic newly deposited sediment. Of course, this assumption is highly oversimplified and little is known about the effects of organic soil amendments on groundwater level fluctuations and biogeochemistry in tidal marshes. To fill this knowledge gap, we set up a large scale mesocosm experiment in Chapter 5. Three treatments (plowing, plowing and adding reed cuttings, and plowing and adding woodchips) were locally applied in a formerly embanked agricultural area with a compact subsoil. We then excavated large (1.69 m^3) soil monoliths in each of these treated plots and in one untreated control plot, which were then placed in a large mesocosm construction in the Scheldt river where they were subjected to the tides (Figure S5.1), simulating tidal marsh restoration. We observed faster groundwater drainage in the treated soil monoliths compared to the control monolith, suggesting increased porosity after the amendments. However, on soil samples taken 3 years after the start of the experiment, no significant differences in soil hydraulic properties and organic matter were found between the treated and the untreated monoliths, except for the bulk density that significantly decreased after the treatments. Since water could drain through all four sides of the monoliths, the experimental units were representative of the 'near creek zone' rather than the 'marsh interior'. Due to the impossibility to have replications of the treatments, care has to be taken when comparing results of different treatments. We found a significantly higher contribution of nitrogen removal of the amended monoliths compared to the control monoliths. However, our results are inconclusive as to whether the addition of organic material contributed to this increase.

In general, our numerical model showed that creek excavation prior to restoration can help to increase soil aeration and advective fluxes of groundwater and solutes. Although the results of the mesocosm experiment point towards a positive effect of organic matter

amendments on the contribution to water quality improvement, more research is needed to confirm this.

6.5 Design guidelines to optimize the contribution to water quality improvement in future tidal marsh restoration projects

In this paragraph, we present several viable design guidelines for future tidal marsh restoration projects to optimize the contribution to water quality improvement. This overview is based on insights gained in my PhD study and a literature review. This list is by no means complete, but it aims to help decision makers and stakeholders to restore tidal wetlands on historically compacted soil, when contribution to water quality improvement is one of the main targets.

1. **Execute a pre-restoration assessment of soil stratigraphy and soil physical properties.**

When a plan is made to restore a tidal marsh in a formerly embanked agricultural area, a study on the soil stratigraphy and the physical and hydraulic properties is essential. These properties control tidally induced groundwater level fluctuations after restoration (Gardner, 2005; Van Putte et al., 2020 (Chapter 2)). Based on this assessment, one can decide whether and which design measures are needed. If the land use history (e.g. crop rotations, pastures, tree plantations) varies throughout the area, this assessment should be done in every zone with a different land use history. One should give priority to detailed characterization of the agricultural topsoil (i.e. from the surface up to a depth of 50 cm, which is well below the depth of a possible plow pan that is usually situated at a depth of around 30 cm (e.g. Riley and Ekeberg, 1998)). This agricultural soil will be directly underneath the tidally deposited sediment and will, therefore, have most effect on the developmental trajectory of the tidal marsh. Necessary parameters include the bulk density, grain size distribution and organic matter content, and, most importantly, the saturated hydraulic conductivity and the water retention curve of the soil. The latter two are, however, difficult and time consuming to measure. If time and resources are limited, pedotransfer functions can be used to estimate the soil hydraulic properties from the bulk density, grain size distribution and organic matter content (Wang et al., 2021), although the performance of these pedotransfer functions is often limited for highly organic soils. In fine grained soils, the saturated hydraulic conductivity is mostly depending on the presence and connectivity of macropore networks (Xin et al., 2016). Therefore, special attention should be paid to the presence and abundance of macropores. When drainage ditches are present in the area, or creek excavation is planned, the soil stratigraphy should be characterized up to the depth of these ditches/creeks. Special attention should be paid to the presence of sandy layers, as these are highly permeable and can result in fast drainage of the top layers ((Gardner, 2007), Chapter 3).

2. **Creek excavation prior to restoration is essential when a creek network is absent.**

We found that increasing the density of the creek network is a very effective measure to enhance soil aeration and to increase advective groundwater fluxes (Chapter 4). Historical soil compaction slows down or prevents the natural incision of a creek network (Vandenbruwaene et al., 2013) that is crucial for both surface and subsurface drainage of the marsh. The presence of creeks enables the establishment of a hydraulic gradient at low and ebb tide, which induces porewater drainage, soil aeration and benefits nitrogen removal, phosphorus retention and advective transport of dissolved silica (Chapter 3). Furthermore, soil aeration at creek banks promotes vegetation development (Li et al., 2005). This vegetation itself can remove groundwater from the marsh soil through evapotranspiration (Xin et al., 2013) and trap sediment, increasing the sediment accretion rate (e.g. Temmerman et al., 2005). As such, the well-drained condition near creek banks induces a positive feedback loop, ultimately improving the soil hydraulic properties starting at the creek banks and spreading further into the marsh interior (Ursino et al., 2004; Xin et al., 2013).

When creek excavation is applied in restoration sites, a calculation of the morphodynamic equilibrium can be used to determine the total volume of creek excavation (D'Alpaos et al., 2010). The question then arises whether one should focus on excavating few deeper creeks, or a large number of shallower creeks. Only considering the effects on subsurface hydrology and biogeochemistry, we suggest investing in a denser network of smaller creeks to enhance soil aeration and groundwater seepage (Chapter 4). However, since tidal creek networks in natural marshes form a complex dendritic pattern with many smaller creeks connected to few larger creeks (e.g. Hughes, 2012), more research is needed to determine the optimal 3D structure of creek networks in restoration sites (Chirol et al., 2015). If highly permeable sandy soil layers occur in the first 2 m below the soil surface, it might be advisable to excavate at least some creeks to the depth of this layer, as a connection between such a permeable layer stimulates groundwater seepage, lowering the groundwater level, even in the marsh interior (Chapter 3).

3. **Apply organic soil amendments when sediment accretion rate is limited.**

In tidal marshes that are restored on a compact subsoil, groundwater level fluctuations are mostly limited to the layer of tidally deposited sediment (Chapter 2, Chapter 3 and Chapter 4). To jumpstart groundwater dynamics after restoration, organic soil amendments are proposed. The goal of these amendments is twofold. Firstly, these amendments loosen the soil and increase the porosity and hydraulic conductivity (Eusufzai and Fujii, 2012) (Chapter 5). Secondly, organic amendments increase the soil nutrient content, which is beneficial for vegetation and soil biota (Sutton-Grier et al., 2009). Soil amendments are primarily advised in restoration sites where the supply of suspended sediment is limited. In the absence of a creek network, soil amendments should be combined with creek

excavation, as creeks are necessary for the establishment of a hydraulic gradient (Chapter 4).

4. **Consider the inundation frequency when restoring tidal marshes on a low lying agricultural area.**

In Chapter 2 and Chapter 3, we showed that the depth of the variably saturated zone depends on the maximum time between tidal inundations. This time, in its turn, depends on the inundation frequency of the marsh. Formerly embanked agricultural areas typically have a low elevation (i.e. lower than the average high water level) and, therefore, experience a high inundation frequency after reintroduction of the tidal regime. As a result, these marshes are flooded almost every tidal cycle except for the lowest high waters around neap tide, which leads to waterlogged soils and prevents soil aeration. One way to reduce the inundation frequency and preserve the spring tide – neap tide variation when restoring tidal marshes on low lying formerly embanked land is the controlled reduced tide (CRT) principle, which was also applied in the restored marsh Lippenbroek studied in this thesis (Maris et al., 2007; Oosterlee et al., 2020). Here, water enters and leaves the area through separate inflow and outflow culverts. As such, the inundation frequency and the volume of water entering the area can be regulated by changing the elevation of the inlet culvert. By maintaining a lower inundation frequency, the marsh is not inundated for a longer consecutive time span around neap tide, increasing the time for groundwater drainage and evapotranspiration to remove groundwater from the soil and for oxygen to enter the soil pores. In this way, soil aeration can occur to a greater depth.

5. **Aim for fast vegetation development**

Promoting fast vegetation establishment is often the main concern in tidal marsh restoration projects (Garbutt and Wolters, 2008). Besides the well-known role wetland plants play in habitat provision (Spautz et al., 2006), storm wave attenuation and erosion protection (Schoutens et al., 2019), wetland vegetation also enhances groundwater dynamics. Wetland plants remove large volumes of water from tidal marsh soils through evapotranspiration and oxygenate the soil around their roots through aerenchyma (Sorrell and Brix, 2013). In addition, decaying plant root networks create preferential flow paths (macropores), promoting faster drainage (Xin et al., 2022). Buried plant litter is a main source of soil carbon, enhancing denitrification potential (Alldred and Baines, 2016), and the biggest source of biogenic silica, enhancing silica cycling (Struyf et al., 2005). As such, methods aiming for fast vegetation development in newly restored tidal marshes will likely also promote groundwater dynamics, and vice versa.

6.6   Insights, limitations and recommendations for future research

The insights gained in this PhD thesis have a large application potential and the proposed design measures could be applied globally where tidal marshes are restored on formerly embanked agricultural land. However, some limitations to this application potential are inevitable. While we are confident that most of our findings regarding the subsurface

hydrology apply to all tidal marsh systems (of course taking into account the local soil stratigraphy and hydraulic properties), caution is recommended when extrapolating results regarding porewater biogeochemistry to other areas. We executed our study in the freshwater (Chapter 2, Chapter 3 and Chapter 4) and brackish (Chapter 5) zone of the Scheldt estuary. However, the majority of global tidal marsh area (especially in coastal zones) is located where the flooding water is saline. In addition, many estuarine freshwater tidal marshes experience an increase in salinity due to sea level rise and decreased river discharge, increasing salt water intrusion (Li et al., 2022). There are fundamental biogeochemical differences between the soil of saltmarshes and freshwater tidal marshes (Tobias and Neubauer, 2019). Especially the concentration of sulphate (SO_4^{2-}), which is often positively correlated sea water intrusion and salinity increase, is crucial. Increased salinity can lead to the breakdown of the 'iron curtain' and can induce impaired P retention (Megonigal and Neubauer, 2019), and to N removal, as high salinity can reduce the activity of nitrifying and denitrifying microbes (Megonigal and Neubauer, 2019; Rysgaard et al., 1999). In addition, salinity alters the dissolution rate of BSi, which might affect the silica buffering capacity of a tidal marsh (Struyf et al., 2007; Yamada and D'Elia, 1984). These findings, of course, have several implications for the efficacy of the proposed design measures to improve groundwater dynamics to stimulate water quality improvement in saltmarshes versus freshwater tidal marshes.

In this PhD thesis, we focused on water quality improvement by groundwater dynamics regarding N removal, P retention and Si cycling. Nevertheless, groundwater dynamics also greatly influence soil carbon dynamics (Guimond and Tamborski, 2021). In the light of the global climate change, many recent studies focused on the ability of tidal wetlands to store carbon (e.g. Ouyang and Lee, 2020). Nevertheless, design methods to improve soil aeration by increasing the soil porosity may increase carbon mineralization and emission of CO_2 (Xiao et al., 2021). On the other hand, conditions that promote the storage of carbon (anaerobic conditions) in freshwater wetland soils lead to the emission of methane (Arias-Ortiz et al., 2021; Poffenbarger et al., 2011). These emissions are, therefore, strongly linked to groundwater level fluctuations and soil – groundwater interactions (Derby et al., 2022). In polyhaline tidal wetlands (saltmarshes), methane emission is suppressed as a result of high sulphate concentrations (Megonigal and Neubauer, 2019). Freshwater and brackish tidal marsh soils, however, can emit large amounts of methane (Poffenbarger et al., 2011). Soil aeration, water quality improvement and greenhouse gas emissions are strongly interlinked and trade-offs exist between the latter two. For example: while the application of organic soil amendments can benefit the contribution of a developing restored tidal marsh to water quality improvement, it could also increase methane emissions, as was observed in a non-tidal wetland (Scott et al., 2021).

Previously, we discussed the reduced soil aeration depth at high inundation frequencies (i.e. when soil aeration is limited by the non-inundated time around neap tide). This statement, however, needs some consideration. For marshes with a platform elevation near the mean high water level, the deepest soil aeration depth that is attained is limited

by the number of consecutive non-inundating tides around neap tide (Chapter 2). However, the highest seepage fluxes occur during spring tide, when the marsh platform is inundated every high tide (Wilson and Morris, 2012). Since advective transport of solutes increases with a higher seepage flux, also the transport of nutrients should be enhanced around spring tide. Hence, there seems to be a trade-off between soil aeration depth and advective solute transport, which are both important factors governing nutrient cycling in tidal marsh soils. Based on our results, we would expect the export of DSi to be enhanced at higher inundation frequencies (since this is mostly affected by advective transport) and the removal of N through coupled nitrification and denitrification to be enhanced at slightly lower inundation frequencies. However, as mentioned, excessive soil aeration depths can impair the potential for N removal (Megonigal and Neubauer, 2019). For the retention of P, the story is probably more complicated, as both advective transport (to transport dissolved PO_4 and dissolved Fe from the marsh interior to the creek banks) and soil aeration (to oxidize Fe, forming iron oxyhydroxides to which PO_4 can sorb). However, especially soil aeration near the creek banks is important here, which is depending less on the inundation frequency, compared to soil aeration in the marsh interior (Chapter 3). Therefore, we speculate that P retention would be enhanced at relatively higher inundation frequencies. All of these interactions, of course, also strongly depend on the hydraulic properties and stratigraphy of the soil. Based on our findings, we expect that especially in marshes where the groundwater drainage rate is limited (e.g. by the presence of a relict agricultural subsoil), a lower inundation frequency is preferred, since here only the top few centimeters are aerated in between consecutive inundations around spring tide, and longer non-inundated periods are required to attain a greater soil aeration depth (Chapter 2). On the other hand, however, a lower inundation frequency results in lower sediment accretion rates and a slower accumulation of a highly organic macroporous soil (Liu et al., 2021). In addition, the development of a tidal creek network is limited by a lower inundation frequency, and especially in an erosion resistant compact soil (Vandenbruwaene et al., 2012). As suggested, this problem can be alleviated by the execution of creek excavation and soil amendments before restoration. As is clear from this paragraph, the interplay between tidal characteristics, sedimentation rates, groundwater dynamics and nutrient cycling is very complicated.

Tidal marshes do have a significant effect on water quality in polluted estuaries (Merrill and Cornwell, 2000), but their effect might be small compared to the effect of wastewater treatment and reduction of N and P inputs in the basin. Nevertheless, tidal marshes form the last opportunity for water quality improvement (except from pelagic processes) before discharge into the ocean. In Chapter 5, we quantified the effect of soil amendments on nutrient mass balances on a small scale. However, to make any difference on water quality on the estuarine scale, soil amendments should be applied over a large area. We often found a substantial difference in the nutrient mass balance between the different soil treatments. Considering the retention of phosphate, for example, the WOOD treatment (where the soil was plowed and mixed with woodchips) resulted in more than three times

the retention of phosphate compared to the CTRL treatment (5.56 kg ha^{-1} year^{-1} vs 1.60 kg ha^{-1} year^{-1}). These values are in line with a conservative mass balance study for the restored Lippenbroek site (Maris et al., 2016). Even though the total effect on water quality improvement on the estuarine scale is small, it is non-negligible. Before the application of soil amendments in newly restored tidal marshes on a large scale, the next step would be to perform a cost benefit analysis for soil amendments. This was, however, outside the scope of this study.

In this study, field measurements and model simulations were performed on a relatively small time scale of 1 month to 1 year, ignoring changes in groundwater dynamics and nutrient fluxes resulting from an increasing marsh platform elevation due to sedimentation and subsequent changes in soil stratigraphy, marsh platform inundation frequency and vegetation composition. For future studies, we propose the coupling of our groundwater flow and transport model (Chapter 4) with a marsh sedimentation model (e.g. those presented in Fagherazzi et al. (2012)). In this way, the evolution of the contribution of restored marshes to estuarine water quality can be simulated over a longer time span. Furthermore this coupling would allow to answer relevant research questions such as how long it takes for a restored tidal marsh to be functionally equivalent to a natural tidal marsh regarding water quality improvement, and how much this time can be reduced by the application of certain design measures such as creek excavation and soil amendments.

In Chapter 2, we studied and emphasized the importance of macropore networks as preferential flow paths for groundwater and solutes. These macropores can be formed by decaying plant roots (Beven and Germann, 2013) and burrowing invertebrate species (Xin et al., 2016). Especially the presence of crab burrows greatly alters groundwater dynamics and biogeochemical cycling in tidal wetlands (Xin et al., 2009). Xiao et al. (2019) found that vertical crab burrows of fiddler crabs (*Uca* sp.) in the marsh platform enhance surface water infiltration during flooding, and drainage during ebb and low tide. In our study sites in the freshwater part of the Scheldt estuary, the invasive Chinese mitten crab (*Eriocheir sinensis*) is highly abundant and high densities of burrows (with an average size of 2 cm x 5 cm) are observed in the creek banks (rather than in the marsh platform), especially in the compact subsoil of the restored marsh. A preliminary study by De Kleyn et al. (2021) showed that up to 3 m^3 of groundwater can drain out of a single crab burrow in a restored tidal marsh during one tidal cycle. Given the high density of these burrows, they likely play a substantial role in increasing soil – groundwater interactions and nutrient cycling, especially in restored tidal marshes with a compact subsoil. Further research is needed to quantify the overall effect of crab burrows on seepage and nutrient cycling.

When studying groundwater flow and seepage in tidal marshes, fluxes, rather than groundwater heads are important. However, all field studies on groundwater dynamics, including our research in Chapter 2 and Chapter 3, depend on measurements of groundwater head in monitoring wells or piezometers. Based on these measured groundwater heads and a detailed assessment of soil hydraulic properties, the

groundwater flux can then be calculated using Darcy's law (in the saturated zone) or the Richards equation (in the variably saturated zone) (Moffett et al., 2012). However, measuring soil hydraulic properties is time consuming, a very large number of samples is required and good measurements are difficult to obtain, especially in the often highly heterogeneic soils of tidal marshes. Furthermore, when numeric models are applied to simulate soil moisture dynamics in the variably saturated zone of tidal marshes, the results of these models are difficult to evaluate with field data, as most soil moisture sensors fail to give reliable results in these systems (Xin et al., 2022). In addition, the hydraulic head in a monitoring well only equals the hydraulic head in the surrounding soil when the system is in steady state, which never really is the case in the highly dynamic system of tidal marshes. As a consequence, the measured groundwater head in the well lags behind the aquifer head (Gardner, 2009). Since groundwater head measurements are often used to calculate the groundwater flux (e.g. by means of Darcy's law), this lag may result in erroneous flux estimates. In the recent years, several methods were developed to measure the actual groundwater flux directly (e.g. Labaky et al., 2007; Verreydt et al., 2013). In a preliminary study by De Kleyn et al. (2021), we tested a new sensor developed by iFLUX, which can be inserted into monitoring wells and measures groundwater flux and direction in real time using two thermal mass flow sensors positioned perpendicular to each other. These sensors reacted rapidly to changes in flow velocity and direction and were in the same order of magnitude as calculated Darcy fluxes based on hydraulic head measurements in monitoring wells. Further research and development is essential to optimize these measuring techniques for the harsh and dynamic conditions of tidal wetlands. These newly developed methods will become an invaluable tool in ecohydrological studies and will enable easy characterization of subsurface hydrology in tidal wetlands.

Despite several limitations, we are confident that the results presented in this thesis provide new insights in the relation between subsurface hydrology and biogeochemistry in tidal wetlands, especially regarding the difference between natural and restored tidal marshes. Furthermore, the design measures that are proposed in this thesis can be used as guidelines for future marsh restoration projects to alleviate the restrictions posed by the presence of a historically compacted subsoil and to optimize the contribution to water quality improvement.

6.7   References

Alldred, M., Baines, S.B., 2016. Effects of wetland plants on denitrification rates: a meta-analysis. Ecological Applications 26, 676-685. doi.org/10.1890/14-1525

Arias-Ortiz, A., Oikawa, P.Y., Carlin, J., Masqué, P., Shahan, J., Kanneg, S., Paytan, A., Baldocchi, D.D., 2021. Tidal and Nontidal Marsh Restoration: A Trade-Off Between Carbon Sequestration, Methane Emissions, and Soil Accretion. Journal of Geophysical Research: Biogeosciences 126. 10.1029/2021JG006573

Ballantine, K., Schneider, R., Groffman, P., Lehmann, J., 2012. Soil Properties and Vegetative Development in Four Restored Freshwater Depressional Wetlands. Soil Science Society of America Journal 76, 1482-1495. 10.2136/sssaj2011.0362

Bantilan-Smith, M., Bruland, G.L., MacKenzie, R.A., Henry, A.R., Ryder, C.R., 2009. A comparison of the vegetation and soils of natural, restored, and created coastal lowland wetlands in Hawai'i. Wetlands 29, 1023-1035. 10.1672/08-127.1

Beauchard, O., Jacobs, S., Cox, T.J.S., Maris, T., Vrebos, D., Van Braeckel, A., Meire, P., 2011. A new technique for tidal habitat restoration: Evaluation of its hydrological potentials. Ecological Engineering 37, 1849-1858. 10.1016/j.ecoleng.2011.06.010

Beven, K., Germann, P., 2013. Macropores and water flow in soils revisited. Water Resources Research 49, 3071-3092. 10.1002/wrcr.20156

Burden, A., Garbutt, A., Evans, C.D., 2019. Effect of restoration on saltmarsh carbon accumulation in Eastern England. Biology Letters 15. 10.1098/rsbl.2018.0773

Chambers, R.M., Odum, W.E., 1990. Porewater Oxidation, Dissolved Phosphate and the Iron Curtain: Iron-Phosphorus Relations in Tidal Freshwater Marshes. Biogeochemistry 10, 37-52.

Chirol, C., Gallop, S., Pontee, N., Haigh, I., Thompson, C., 2015. Creek networks: natural evolution and design choices for intertidal habitat recreation, Proceedings of Sea Lines of Communication: Construction.

D'Alpaos, A., Lanzoni, S., Marani, M., Rinaldo, A., 2010. On the tidal prism - channel area relations. Journal of Geophysical Research-Earth Surface 115. 10.1029/2008jf001243

De Kleyn, T., Verreydt, G., Van Putte, N., Meire, P., 2021. "What the flux!?" - How soil-groundwater interactions and nutrient fluxes are affected by historical land use in freshwater tidal marshes. University of Antwerp (unpublished masters' dissertation).

Derby, R.K., Needelman, B.A., Roden, A.A., Megonigal, J.P., 2022. Vegetation and hydrology stratification as proxies to estimate methane emission from tidal marshes. Biogeochemistry 157, 227-243. 10.1007/s10533-021-00870-z

Eusufzai, M., Fujii, K., 2012. Effect of Organic Matter Amendment on Hydraulic and Pore Characteristics of a Clay Loam Soil. Open Journal of Soil Science 02, 372-381. 10.4236/ojss.2012.24044

Fagherazzi, S., Kirwan, M.L., Mudd, S.M., Guntenspergen, G.R., Temmerman, S., D'Alpaos, A., Van De Koppel, J., Rybczyk, J.M., Reyes, E., Craft, C., Clough, J., 2012. Numerical models of salt marsh evolution: Ecological, geomorphic, and climatic factors. Reviews of Geophysics 50. 10.1029/2011RG000359

Garbutt, A., Wolters, M., 2008. The natural regeneration of salt marsh on formerly reclaimed land. Applied Vegetation Science 11, 335-344. 10.3170/2008-7-18451

Gardner, L.R., 2005. Role of geomorphic and hydraulic parameters in governing pore water seepage from salt marsh sediments. Water Resources Research 41. 10.1029/2004wr003671

Gardner, L.R., 2007. Role of stratigraphy in governing pore water seepage from salt marsh sediments. Water Resources Research 43. 10.1029/2006wr005338

Gardner, L.R., 2009. Assessing the accuracy of monitoring wells in tidal wetlands. Water Resources Research 45. 10.1029/2008wr007626

Grande, E., Arora, B., Visser, A., Montalvo, M., Braswell, A., Seybold, E., Tatariw, C., Beheshti, K., Zimmer, M., 2022. Tidal frequencies and quasiperiodic subsurface water level variations dominate redox dynamics in a salt marsh system. Hydrological Processes 36. 10.1002/hyp.14587

Guimond, J., Tamborski, J., 2021. Salt Marsh Hydrogeology: A Review. Water 13, 543. 10.3390/w13040543

Harvey, J.W., Germann, P.F., Odum, W.E., 1987. Geomorphological Control of Subsurface Hydrology in the Creek-Bank Zone of Tidal Marshes. Estuarine Coastal and Shelf Science 25, 677-691. 10.1016/0272-7714(87)90015-1

Harvey, J.W., Nuttle, W.K., 1995. Fluxes of Water and Solute in a Coastal Wetland Sediment .2. Effect of Macropores on Solute Exchange with Surface-Water. Journal of Hydrology 164, 109-125. 10.1016/0022-1694(94)02562-P

Huang, L., Parsons, C.T., Slowinski, S., Van Cappellen, P., 2022. Amorphous silica dissolution kinetics in freshwater environments: Effects of Fe2+ and other solution compositional controls. Science of the Total Environment 851. 10.1016/j.scitotenv.2022.158239

Hughes, Z.J., 2012. Tidal Channels on Tidal Flats and Marshes, in: Davis Jr, R.A., Dalrymple, R.W. (Eds.), Principles of Tidal Sedimentology. Springer Netherlands, Dordrecht, pp. 269-300.

Keshta, A., Koop-Jakobsen, K., Titschack, J., Mueller, P., Jensen, K., Baldwin, A., Nolte, S., 2020. Ungrazed salt marsh has well connected soil pores and less dense sediment compared with grazed salt marsh: a CT scanning study. Estuarine, Coastal and Shelf Science 245. 10.1016/j.ecss.2020.106987

Labaky, W., Devlin, J.F., Gillham, R.W., 2007. Probe for measuring groundwater velocity at the centimeter scale. Environmental Science & Technology 41, 8453-8458. 10.1021/es0716047

Lawrence, D.S.L., Allen, J.R.L., Havelock, G.M., 2004. Salt Marsh Morphodynamics: An Investigation of Tidal Flows and Marsh Channel Equilibrium. Journal of Coastal Research 20, 301-316.

Li, F., Angelini, C., Byers, J.E., Craft, C., Pennings, S.C., 2022. Responses of a tidal freshwater marsh plant community to chronic and pulsed saline intrusion. Journal of Ecology 110, 1508-1524. 10.1111/1365-2745.13885

Li, H., Li, L., Lockington, D., 2005. Aeration for plant root respiration in a tidal marsh. Water Resources Research 41. 10.1029/2004WR003759

Liu, Z., Fagherazzi, S., Cui, B., 2021. Success of coastal wetlands restoration is driven by sediment availability. Communications Earth & Environment 2, 44. 10.1038/s43247-021-00117-7

Maris, T., Baeten, S., Van den Neucker, T., Meire, P., 2016. OMES rapport 2016 Intergetijdengebieden. Onderzoek naar de gevolgen van het Sigmaplan, baggeractiviteiten en havenuitbreiding in de Zeeschelde op het milieu. Ecosystem Management Research Group ECOBE, University of Antwerp, p. 153.

Maris, T., Baeten, S., Van den Neucker, T., van den Broeck, T., Meire, P., 2021. Onderzoek naar de gevolgen van het Sigmaplan, baggeractiviteiten en havenuitbreiding in de Zeeschelde op het milieu. Geïntegreerd eindverslag van het onderzoek verricht in 2020, deelrapport Intergetijdengebieden. ECOBE 021-R276. University of Antwerp, Antwerp.

Maris, T., Cox, T.J.S., Temmerman, S., De Vleeschauwer, P., Van Damme, S., De Mulder, T., Van den Bergh, E., Meire, P., 2007. Tuning the tide: creating ecological conditions for tidal marsh development in a flood control area. Hydrobiologia 588, 31-43. 10.1007/s10750-007-0650-5

Megonigal, J.P., Neubauer, S.C., 2019. Chapter 19 - Biogeochemistry of Tidal Freshwater Wetlands, in: Perillo, G.M.E., Wolanski, E., Cahoon, D.R., Hopkinson, C.S. (Eds.), Coastal Wetlands (Second Edition). Elsevier, pp. 641-683.

Merrill, J.Z., Cornwell, J.C., 2000. The Role of Oligohaline Marshes in Estuarine Nutrient Cycling, in: Weinstein, M.P., Kreeger, D.A. (Eds.), Concepts and Controversies in Tidal Marsh Ecology. Springer Netherlands, Dordrecht, pp. 425-441.

Moffett, K.B., Gorelick, S.M., McLaren, R.G., Sudicky, E.A., 2012. Salt marsh ecohydrological zonation due to heterogeneous vegetation–groundwater–surface water interactions. Water Resources Research 48. 10.1029/2011WR010874

Mossman, H.L., Davy, A.J., Grant, A., 2012. Does managed coastal realignment create saltmarshes with 'equivalent biological characteristics' to natural reference sites? Journal of Applied Ecology 49, 1446-1456. 10.1111/j.1365-2664.2012.02198.x

Neubauer, S.C., Anderson, I.C., Neikirk, B.B., 2005. Nitrogen cycling and ecosystem exchanges in a Virginia tidal freshwater marsh. Estuaries 28, 909-922. 10.1007/Bf02696019

Oosterlee, L., Cox, T.J.S., Temmerman, S., Meire, P., 2020. Effects of tidal re-introduction design on sedimentation rates in previously embanked tidal marshes.

Estuarine Coastal and Shelf Science 244. 10.1016/j.ecss.2019.106428

Ouyang, X., Lee, S.Y., 2020. Improved estimates on global carbon stock and carbon pools in tidal wetlands. Nature Communications 11, 317. 10.1038/s41467-019-14120-2

Poffenbarger, H.J., Needelman, B.A., Megonigal, J.P., 2011. Salinity Influence on Methane Emissions from Tidal Marshes. Wetlands 31, 831-842. 10.1007/s13157-011-0197-0

Riley, H., Ekeberg, E., 1998. Effects of depth and time of ploughing on yields of spring cereals and potatoes and on soil properties of a morainic loam soil. Acta Agriculturae Scandinavica, Section B — Soil & Plant Science 48, 193-200. 10.1080/09064719809362499

Rysgaard, S., Thastum, P., Dalsgaard, T., Christensen, P.B., Sloth, N.P., 1999. Effects of salinity on NH4+ adsorption capacity, nitrification, and denitrification in Danish estuarine sediments. Estuaries 22, 21-30. 10.2307/1352923

Schoutens, K., Heuner, M., Minden, V., Ostermann, T.S., Silinski, A., Belliard, J.P., Temmerman, S., 2019. How effective are tidal marshes as nature-based shoreline protection throughout seasons? Limnology and Oceanography 64, 1750-1762. 10.1002/lno.11149

Scott, B., Baldwin, A., Yarwood, S., 2021. Adding organic matter to restore wetland soils may increase methane generation and is not needed for hydric soil development.

Scott, B., Baldwin, A.H., Yarwood, S.A., 2022. Quantification of potential methane emissions associated with organic matter amendments following oxic-soil inundation. Biogeosciences 19, 1151-1164. 10.5194/bg-19-1151-2022

Sloey, T.M., Willis, J.M., Hester, M.W., 2015. Hydrologic and edaphic constraints on Schoenoplectus acutus, Schoenoplectus californicus, and Typha latifolia in tidal marsh restoration. Restoration Ecology 23, 430-438. 10.1111/rec.12212

Sorrell, B.K., Brix, H., 2013. Gas Transport and Exchange through Wetland Plant Aerenchyma, Methods in Biogeochemistry of Wetlands, pp. 177-196.

Spautz, H., Nur, N., Stralberg, D., Chan, Y., 2006. Multiple-scale habitat relationships of tidal-marsh breeding birds in the San Francisco Bay estuary. Studies in Avian Biology 32, 247.

Spencer, K.L., Harvey, G.L., 2012. Understanding system disturbance and ecosystem services in restored saltmarshes: Integrating physical and biogeochemical processes. Estuarine, Coastal and Shelf Science 106, 23-32. 10.1016/j.ecss.2012.04.020

Struyf, E., Conley, D.J., 2009. Silica: an essential nutrient in wetland biogeochemistry. Frontiers in Ecology and the Environment 7, 88-94. 10.1890/070126

Struyf, E., Temmerman, S., Meire, P., 2007. Dynamics of biogenic Si in freshwater tidal marshes: Si regeneration and retention in marsh sediments (Scheldt estuary). Biogeochemistry 82, 41-53. 10.1007/s10533-006-9051-5

Struyf, E., Van Damme, S., Gribsholt, B., Middelburg, J.J., Meire, P., 2005. Biogenic silica in tidal freshwater marsh sediments and vegetation (Schelde estuary, Belgium). Marine Ecology Progress Series 303, 51-60. 10.3354/meps303051

Sutton-Grier, A.E., Ho, M., Richardson, C.J., 2009. Organic Amendments Improve Soil Conditions and Denitrification in a Restored Riparian Wetland. Wetlands 29, 343-352.

Takahashi, H., Yamauchi, T., Colmer, T.D., Nakazono, M., 2014. Aerenchyma Formation in Plants, in: van Dongen, J.T., Licausi, F. (Eds.), Low-Oxygen Stress in Plants: Oxygen Sensing and Adaptive Responses to Hypoxia. Springer Vienna, Vienna, pp. 247-265.

Temmerman, S., Bouma, T.J., Govers, G., Wang, Z.B., De Vries, M.B., Herman, P.M.J., 2005. Impact of vegetation on flow routing and sedimentation patterns: Three-dimensional modeling for a tidal marsh. Journal of Geophysical Research: Earth Surface 110. 10.1029/2005JF000301

Tempest, J.A., Harvey, G.L., Spencer, K.L., 2015. Modified sediments and subsurface hydrology in natural and recreated salt marshes and implications for delivery of ecosystem services. Hydrological Processes 29, 2346-2357. 10.1002/hyp.10368

Tobias, C., Neubauer, S.C., 2019. Chapter 16 - Salt Marsh Biogeochemistry—An Overview, in: Perillo, G.M.E., Wolanski, E., Cahoon, D.R., Hopkinson, C.S. (Eds.), Coastal Wetlands (Second Edition). Elsevier, pp. 539-596.

Ursino, N., Silvestri, S., Marani, M., 2004. Subsurface flow and vegetation patterns

in tidal environments. Water Resources Research 40. 10.1029/2003wr002702

Van Putte, N., Temmerman, S., Verreydt, G., Seuntjens, P., Maris, T., Heyndrickx, M., Boone, M., Joris, I., Meire, P., 2020. Groundwater dynamics in a restored tidal marsh are limited by historical soil compaction. Estuarine, Coastal and Shelf Science 244. 10.1016/j.ecss.2019.02.006

Vandenbruwaene, W., Bouma, T.J., Meire, P., Temmerman, S., 2013. Bio-geomorphic effects on tidal channel evolution: impact of vegetation establishment and tidal prism change. Earth Surface Processes and Landforms 38, 122-132. 10.1002/esp.3265

Vandenbruwaene, W., Meire, P., Temmerman, S., 2012. Formation and evolution of a tidal channel network within a constructed tidal marsh. Geomorphology 151, 114-125. 10.1016/j.geomorph.2012.01.022

Verreydt, G., Annable, M.D., Kaskassian, S., Van Keer, I., Bronders, J., Diels, L., Vanderauwera, P., 2013. Field demonstration and evaluation of the Passive Flux Meter on a CAH groundwater plume. Environmental Science and Pollution Research 20, 4621-4634. 10.1007/s11356-012-1417-8

Wang, M., Liu, H., Lennartz, B., 2021. Small-scale spatial variability of hydro-physical properties of natural and degraded peat soils. Geoderma 399. 10.1016/j.geoderma.2021.115123

Wilson, A.M., Morris, J.T., 2012. The influence of tidal forcing on groundwater flow and nutrient exchange in a salt marsh-dominated estuary. Biogeochemistry 108, 27-38. 10.1007/s10533-010-9570-y

Wolf, K.L., Ahn, C., Noe, G.B., 2011. Development of Soil Properties and Nitrogen Cycling in Created Wetlands. Wetlands 31, 699-712. 10.1007/s13157-011-0185-4

Wolters, M., Garbutt, A., Bakker, J.P., 2005. Salt-marsh restoration: evaluating the success of de-embankments in north-west Europe. Biological Conservation 123, 249-268. 10.1016/j.biocon.2004.11.013

Xiao, K., Wilson, A.M., Li, H., Ryan, C., 2019. Crab burrows as preferential flow conduits for groundwater flow and transport in salt marshes: A modeling study. Advances in Water Resources 132. 10.1016/j.advwatres.2019.103408

Xiao, K., Wilson, A.M., Li, H., Santos, I.R., Tamborski, J., Smith, E., Lang, S.Q., Zheng, C., Luo, X., Lu, M., Correa, R.E., 2021. Large CO2 release and tidal flushing in salt marsh crab burrows reduce the potential for blue carbon sequestration. Limnology and Oceanography 66, 14-29. 10.1002/lno.11582

Xin, P., Jin, G.Q., Li, L., Barry, D.A., 2009. Effects of crab burrows on pore water flows in salt marshes. Advances in Water Resources 32, 439-449. 10.1016/j.advwatres.2008.12.008

Xin, P., Kong, J., Li, L., Barry, D.A., 2013. Modelling of groundwater-vegetation interactions in a tidal marsh. Advances in Water Resources 57, 52-68. 10.1016/j.advwatres.2013.04.005

Xin, P., Wilson, A., Shen, C., Ge, Z., Moffett, K.B., Santos, I.R., Chen, X., Xu, X., Yau, Y.Y.Y., Moore, W., Li, L., Barry, D.A., 2022. Surface Water and Groundwater Interactions in Salt Marshes and Their Impact on Plant Ecology and Coastal Biogeochemistry. Reviews of Geophysics 60. 10.1029/2021RG000740

Xin, P., Yu, X.Y., Lu, C.H., Li, L., 2016. Effects of macro-pores on water flow in coastal subsurface drainage systems. Advances in Water Resources 87, 56-67. 10.1016/j.advwatres.2015.11.007

Xin, P., Zhou, T.Z., Lu, C.H., Shen, C.J., Zhang, C.M., D'Alpaos, A., Li, L., 2017. Combined effects of tides, evaporation and rainfall on the soil conditions in an intertidal creek-marsh system. Advances in Water Resources 103, 1-15. 10.1016/j.advwatres.2017.02.014

Xu, X., Xin, P., Zhou, T., Xiao, K., 2021. Effect of macropores on pore-water flow and soil conditions in salt marshes subject to evaporation and tides. Estuarine, Coastal and Shelf Science. 10.1016/j.ecss.2021.107558

Yamada, S.S., D'Elia, C., 1984. Silicic acid regeneration from estuarine sediment cores. Marine Ecology-progress Series 18, 113-118. 10.3354/meps018113

7

Supplementary information

Photo by Tim van den Broeck

S3. Supplementary information Chapter 3

Supplement S3.1: Methods for the chemical analysis of soil samples.

Soil samples were taken with a gouge auger. A subsample of every sample was fully dried at 70 °C. To analyze the BSi content in the soil samples, three subsamples of 30 mg dried soil material were incubated in 25 mL 0.5 M NaOH at 80 °C for 3 h, 4 h and 5 h, respectively. Samples were then filtered and the extracted Si was analyzed via colorimetry on a segmented flow analyzer (SAN++, Skalar, Breda, The Netherlands). Soil N and C concentrations were analyzed through combustion using a CNS-analyzer (Flash 2000, Thermo Fisher Scientific, Waltham, USA). The total P content was measured on a fresh (non-dried) subsample. After digestion of the sediment with H_2SO_4-salicylic acid-H_2O_2 and selenium, the P concentration was analyzed via colorimetry.

Table S3.1: Spearman correlation between the respective element concentration and the soil saturation index (SSI). negative ρ values indicate a negative correlation. Ns = not significant.

solute	p	ρ	significance
Fe	< 0.001	0.44	***
PO$_4$	< 0.001	0.43	***
Mn	< 0.001	0.33	***
NH$_4$	< 0.001	0.32	***
Ca	< 0.001	0.16	***
Cl	< 0.001	0.16	***
Na	< 0.001	0.16	***
K	< 0.001	-0.11	***
SO$_4$	< 0.001	-0.21	***
NO$_3$	< 0.001	-0.21	***
Zn	< 0.001	-0.24	***
Si	0.439	0.02	Ns
Mg	0.570	0.02	Ns
NO$_2$	0.291	-0.03	Ns
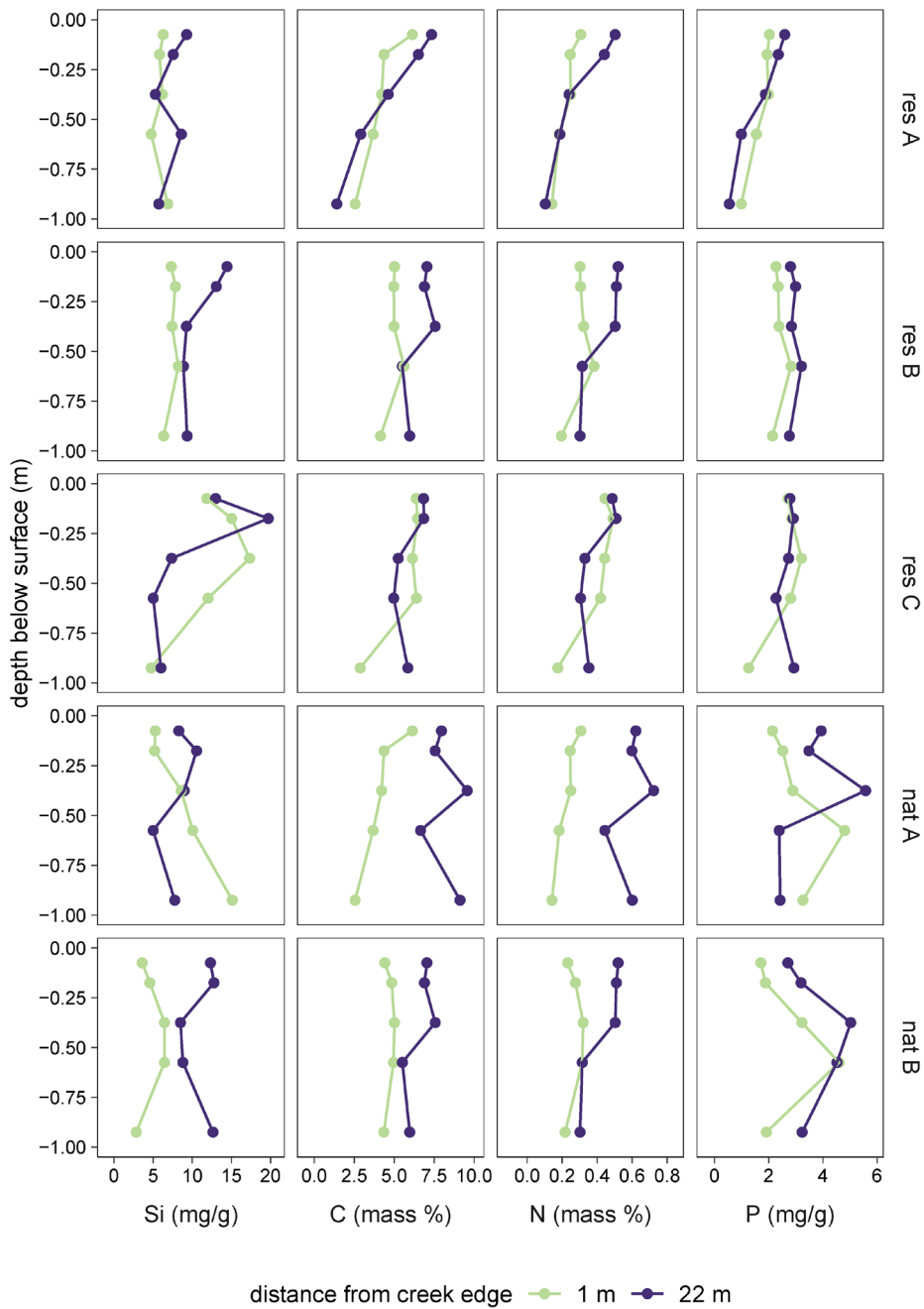
Figure S3.1: Soil Si, C, N and P concentration as a function of depth below the soil surface in the restored marsh (res) and the natural marsh (nat).
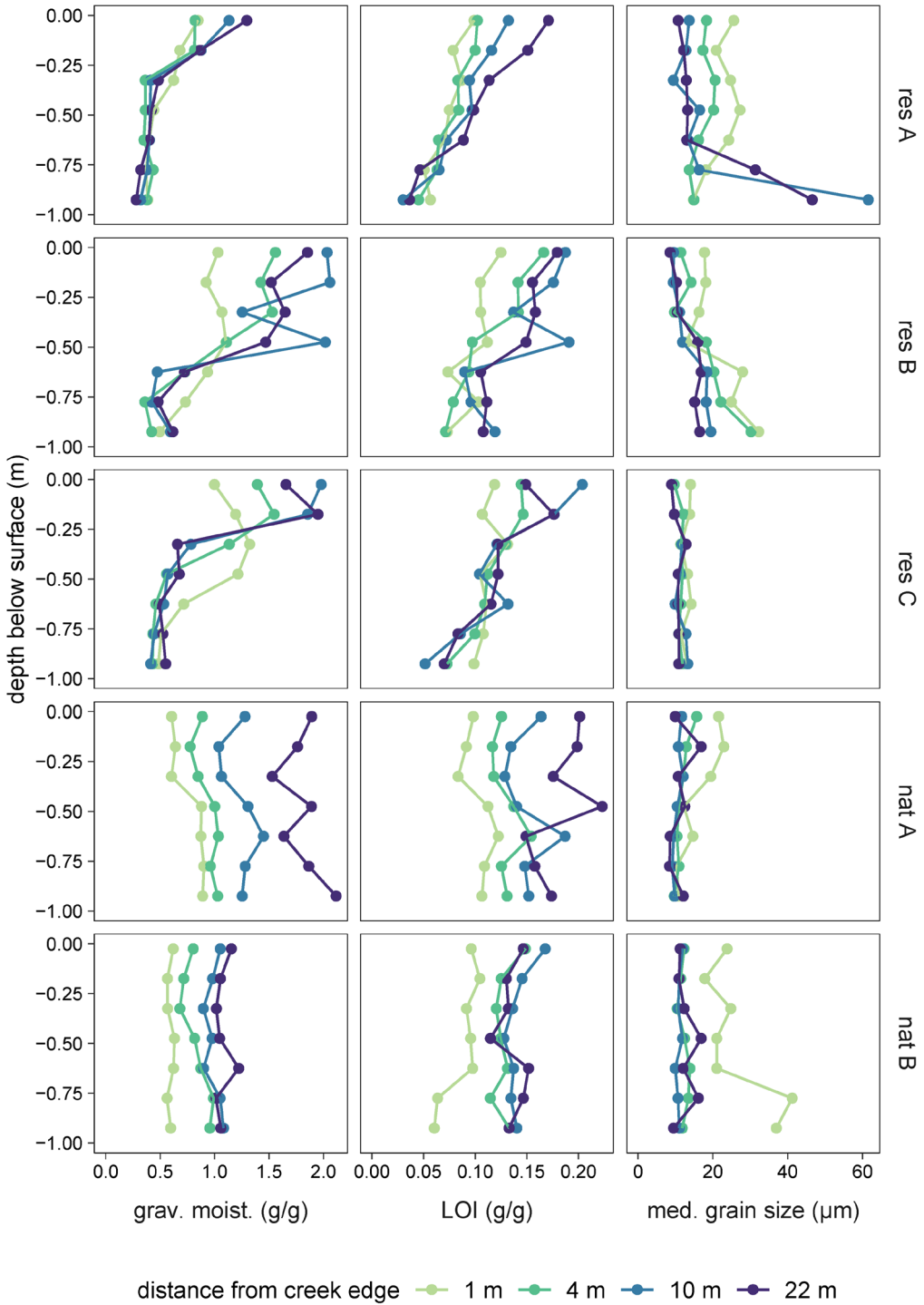
Figure S3.2: Soil properties as a function of depth below the soil surface in the restored marsh (res) and the natural marsh (nat).
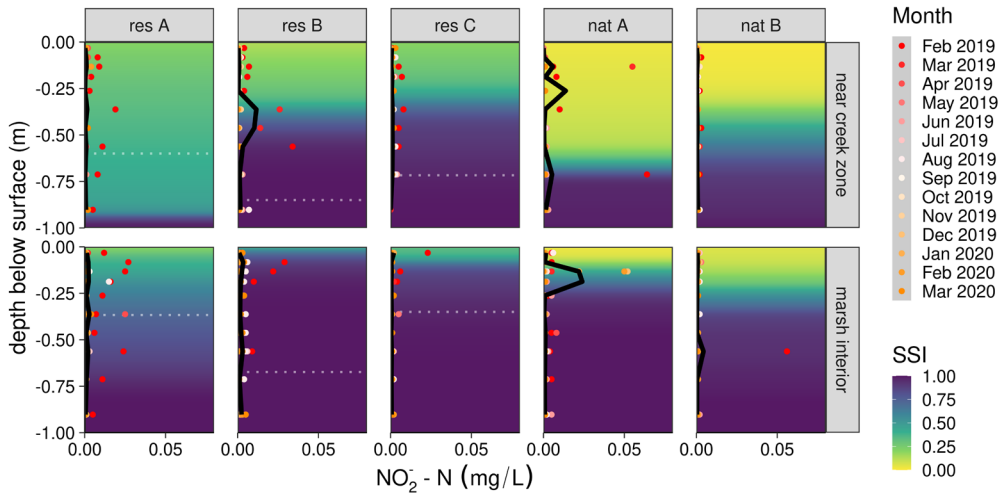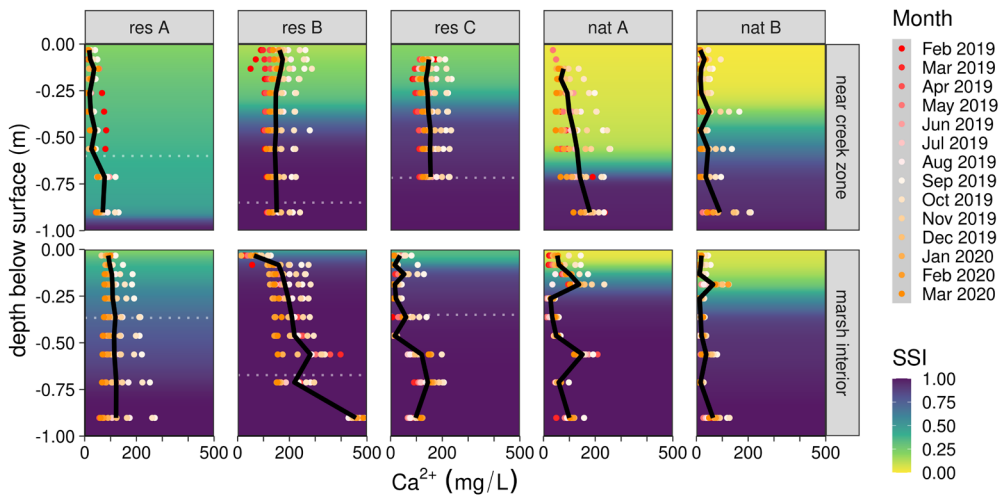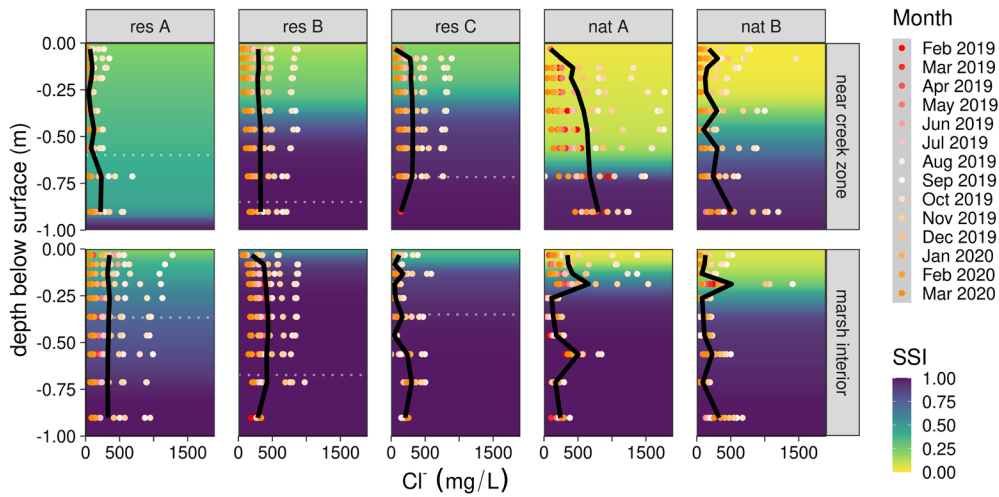
Figure S3.3: Porewater concentrations of nitrite. Bullets indicate the individual monthly results and the black line represents the mean concentration. Background colors indicate the soil saturation index (SSI). Grey dotted lines represent the transition between the tidally deposited sediment layer and the underlying compact relict soil in the restored marsh. Near creek zone and marsh interior are 1 m and 22 m from the creek edge, respectively.
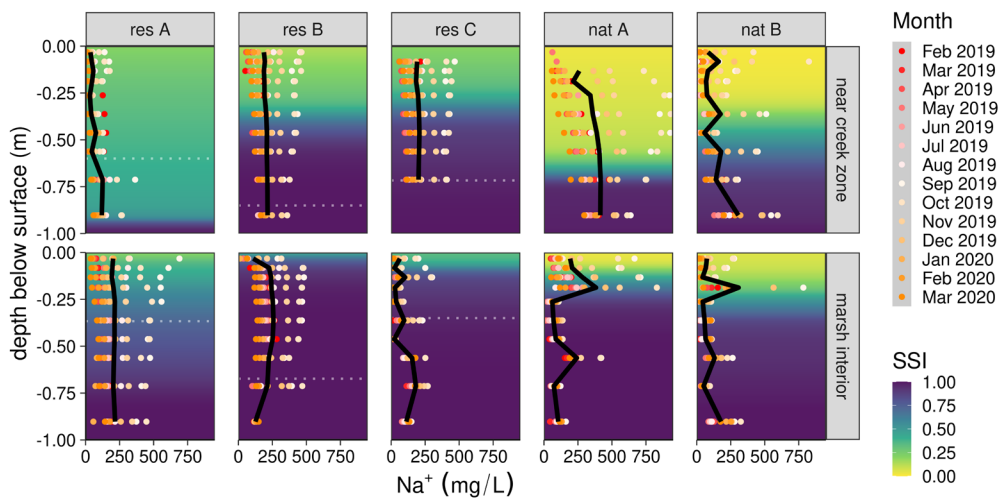

Figure S3.4: Porewater concentrations of calcium. Bullets indicate the individual monthly results and the black line represents the mean concentration. Background colors indicate the soil saturation index (SSI). Grey dotted lines represent the transition between the tidally deposited sediment layer and the underlying compact relict soil in the restored marsh. Near creek zone and marsh interior are 1 m and 22 m from the creek edge, respectively.
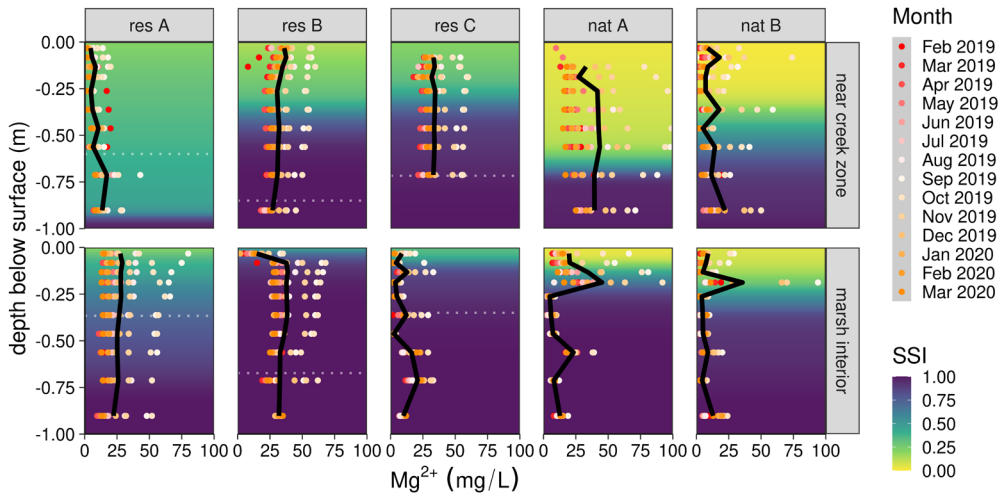
Figure S3.5: Porewater concentrations of chloride. Bullets indicate the individual monthly results and the black line represents the mean concentration. Background colors indicate the soil saturation index (SSI). Grey dotted lines represent the transition between the tidally deposited sediment layer and the underlying compact relict soil in the restored marsh. Near creek zone and marsh interior are 1 m and 22 m from the creek edge, respectively.
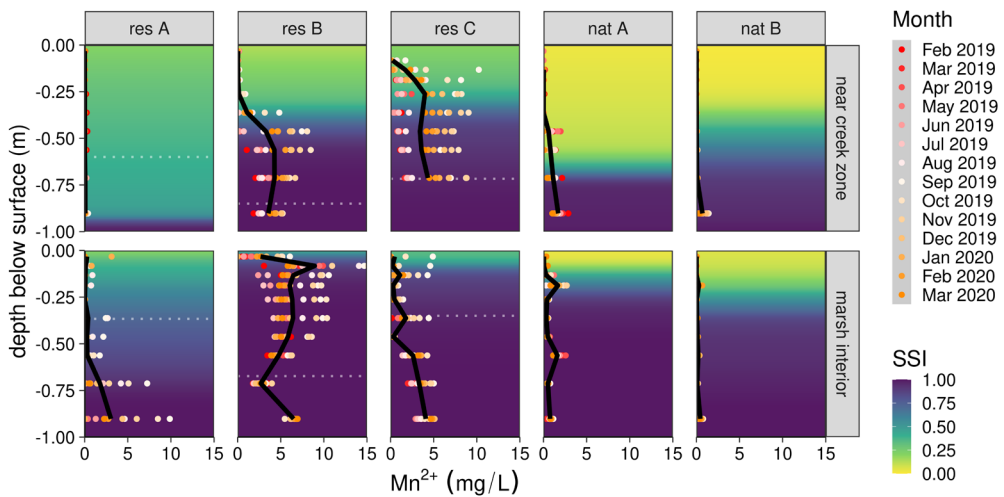

Figure S3.6: Porewater concentrations of sodium. Bullets indicate the individual monthly results and the black line represents the mean concentration. Background colors indicate the soil saturation index (SSI). Grey dotted lines represent the transition between the tidally deposited sediment layer and the underlying compact relict soil in the restored marsh. Near creek zone and marsh interior are 1 m and 22 m from the creek edge, respectively.
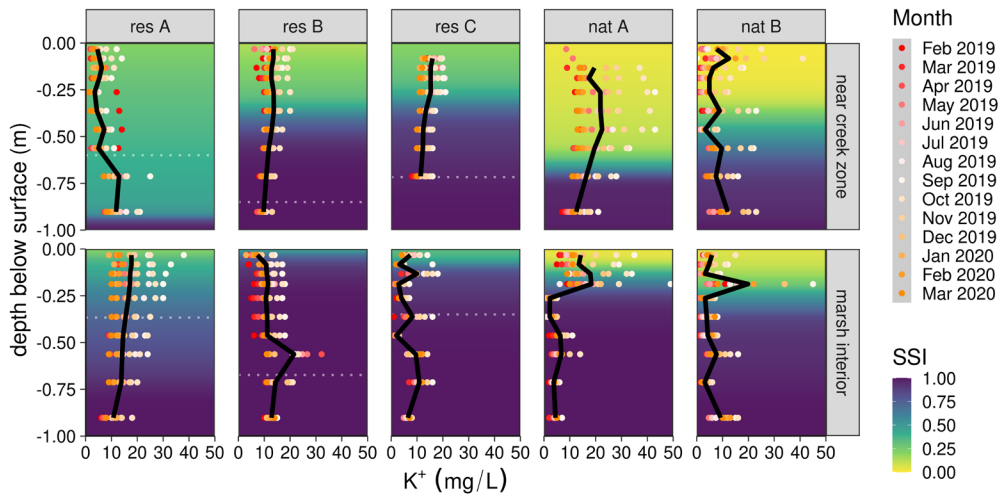
Figure S3.7: Porewater concentrations of magnesium. Bullets indicate the individual monthly results and the black line represents the mean concentration. Background colors indicate the soil saturation index (SSI). Grey dotted lines represent the transition between the tidally deposited sediment layer and the underlying compact relict soil in the restored marsh. Near creek zone and marsh interior are 1 m and 22 m from the creek edge, respectively.

Figure S3.8: Porewater concentrations of manganese. Bullets indicate the individual monthly results and the black line represents the mean concentration. Background colors indicate the soil saturation index (SSI). Grey dotted lines represent the transition between the tidally deposited sediment layer and the underlying compact relict soil in the restored marsh. Near creek zone and marsh interior are 1 m and 22 m from the creek edge, respectively.
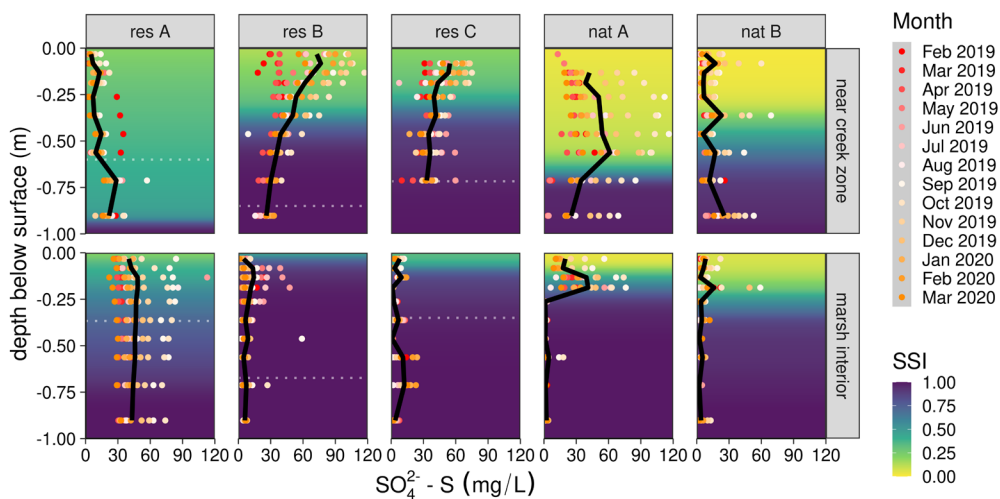
Figure S3.9: Porewater concentrations of potassium. Bullets indicate the individual monthly results and the black line represents the mean concentration. Background colors indicate the soil saturation index (SSI). Grey dotted lines represent the transition between the tidally deposited sediment layer and the underlying compact relict soil in the restored marsh. Near creek zone and marsh interior are 1 m and 22 m from the creek edge, respectively.

Figure S3.10: Porewater concentrations of sulphate. Bullets indicate the individual monthly results and the black line represents the mean concentration. Background colors indicate the soil saturation index (SSI). Grey dotted lines represent the transition between the tidally deposited sediment layer and the underlying compact relict soil in the restored marsh. Near creek zone and marsh interior are 1 m and 22 m from the creek edge, respectively.
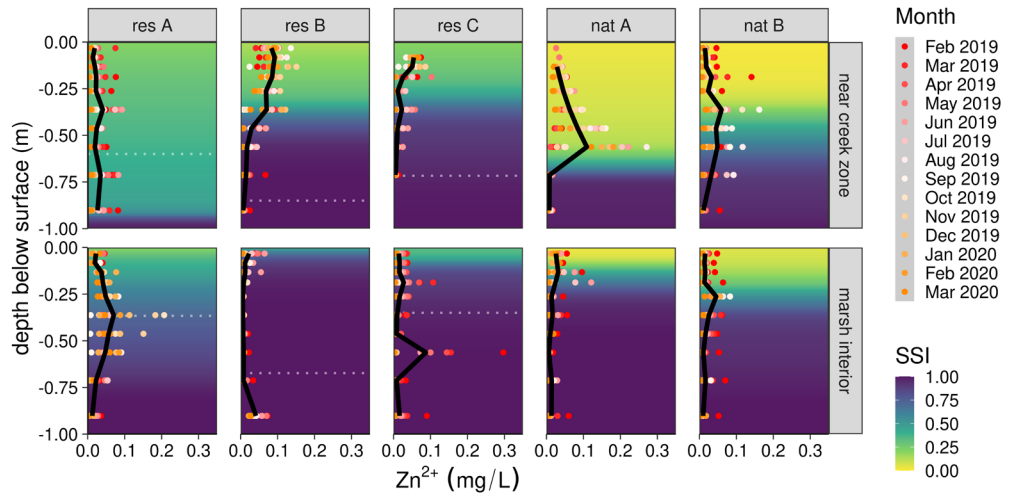
Figure S3.11: Porewater concentrations of zinc. Bullets indicate the individual monthly results and the black line represents the mean concentration. Background colors indicate the soil saturation index (SSI). Grey dotted lines represent the transition between the tidally deposited sediment layer and the underlying compact relict soil in the restored marsh. Near creek zone and marsh interior are 1 m and 22 m from the creek edge, respectively.

S4. Supplementary information Chapter 4

Supplement S4.1: Sensitivity analysis for the numerical groundwater flow and transport model.

The hydraulic conductivity (K_s) has the most profound effect on all simulated variables (Figure S4.1a, d, j, g). In the field study, we found that K_s ranges several orders of magnitude in the newly deposited sediment (Figure 4.3). A good estimate of the saturated hydraulic conductivity is therefore essential to accurately simulate the subsurface hydrology. In our study, we calibrated the K_s to obtain the best ME values for the pressure heads. The K_s value that lead to the best simulated pressure heads ($3.50 \cdot 10^{-5}$ m/s) was well within the range of the field measured K_s values (Figure 4.3).

The α value is positively correlated with the cumulative seepage flux, but negatively correlated with the drainage depth (Figure S4.1b, k). The α value is inversely related to the air entry value (the minimum applied suction at which the soil starts to desaturate). Therefore, a smaller α value indicates a higher air entry value, which means that a higher suction needs to be applied for a similar volume of drainage. Hence the deeper groundwater drainage levels at a lower α value.

The model performance increased when switching to a dual porosity model based on water mass transfer (Equation 4.6). As the water mass transfer coefficient (ω) was unknown, we ran several model simulations with different ω values to calibrate the model. Model runs with a smaller ω value (i.e. less transfer between the mobile and immobile regions) show a faster initial drainage compared to model runs with a higher ω value (i.e. more transfer between the two regions). As a result, the spring tide drainage depth increases with a decreasing ω value. During neap tide drainage, the final drainage depth is not affected by the ω value, as the fast initial drainage slows down when the groundwater level approximates the compact soil layer. A larger ω value leads to higher seepage fluxes and a faster solute exchange (Figure S4.1c, i).

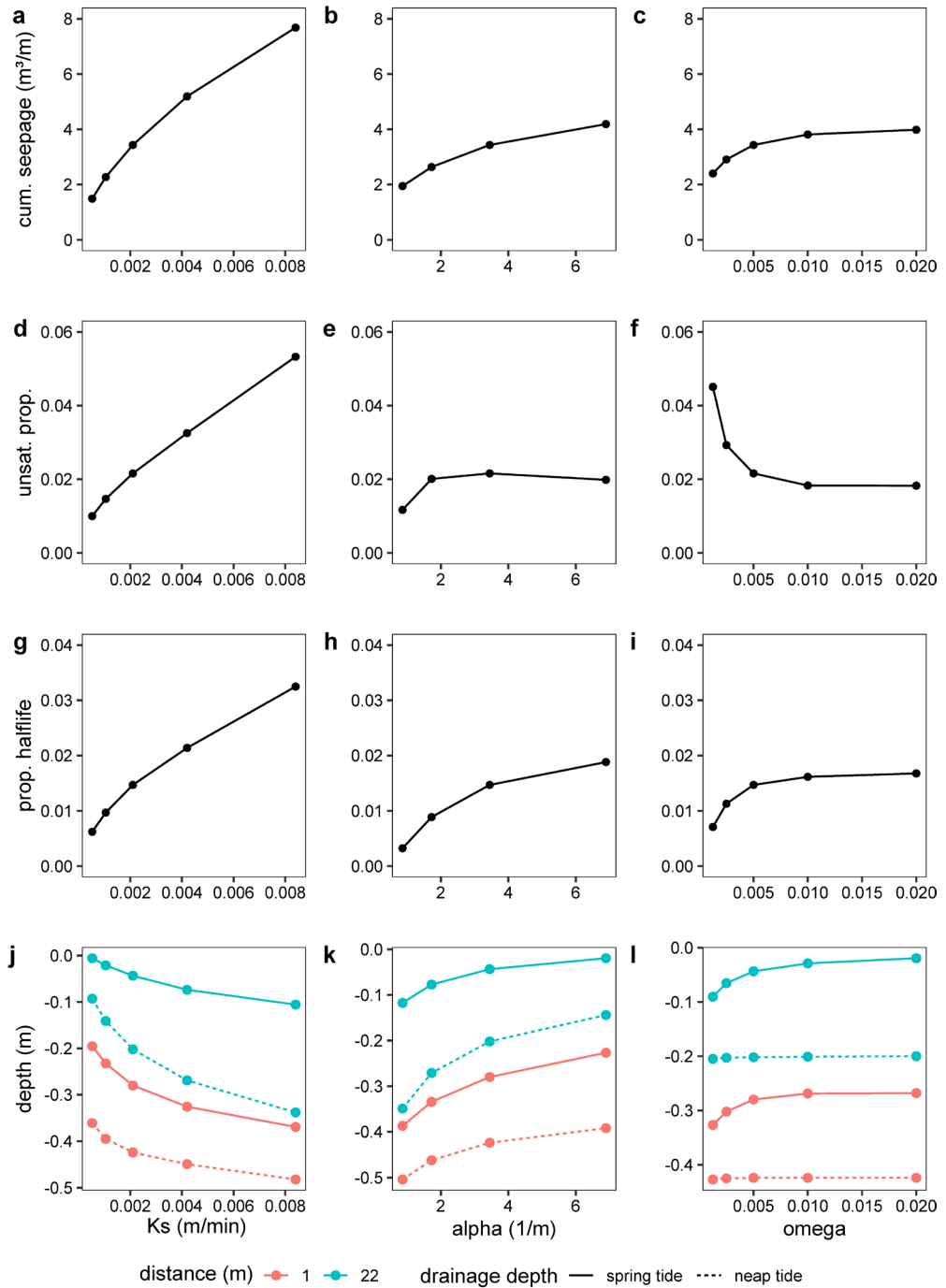Figure S4.1: Sensitivity to the hydraulic conductivity (Ks) (a, d, g, j), the α value (b, e, h, k), the mass transfer coefficient (ω) (c, f, i, l) of (a, b, c) the cumulative seepage flux, (d, e, f) the proportion of the domain in which the soil moisture content drops below 0.5 during the modeled time span, (g, h, i) the proportion of the domain in which at least 50 % of the solute mass is removed during the modeled timespan, (j, k, l) the spring tide drainage depth (solid line) and neap tide drainage depth (dashed line) in the near creek zone (red line) and the marsh interior (blue line).

S5. Supplementary information Chapter 5

Supplement S5.1: Methods and results of the soil chemical and physical parameters before application of the treatments.

Before the application of the treatments, we determined the grain size distribution with a Mastersizer 2000 (Malvern Panalytical Ltd.) based on laser diffraction after treatment with HCl and H_2O_2 to remove organic matter. Sediment particles were classified following the scale of Wentworth (1922) and Udden (1914). The particle size distribution was analyzed after application of the soil treatments, as this parameter is not expected to be affected by the treatments. The distribution of particle size follows a similar pattern across all plots, with an increasing fraction of sand and a decreasing fraction of silt deeper in the soil profile (Figure S5.2). In the REED plot, sand accounts for the largest fraction at a depth of 0.75 m.

In addition, we measured the concentrations of extractable N and P on the samples taken before the application of the treatments using 1-M KCl for N and ammonium acetate EDTA for P. Following centrifugation, the concentration of N (NO_3, NO_2 and NH_4) and P (PO_4) was determined by colorimetry (see main text).

Soil nutrient concentrations were compared between the plots before the application of the treatments to verify the assumption that soil nutrient contents did not differ between plots at the start of the experiment. Both the NH_4 concentration ($p = 0.52$) and PO_4 concentration ($p = 0.20$) did not significantly differ between the plots (Figure S5.3). Concerning the concentration of NO_3, there is a significant difference between the PLOW and the REED treatment ($p = 0.01$), and between the CTRL and the REED treatment ($p = 0.01$). However, in both cases, the difference was only 0.63 mg/kg.

Supplement S5.2: Methods and results of the soil hydraulic properties after start of the experiment.

To determine the long-term effect of the soil amendments on the soil hydraulic properties, the undisturbed soil samples taken after 29 months were used to assess the saturated hydraulic conductivity (K_s) and the soil water retention curve (SWRC) of the soil. K_s was measured using either the constant head method (highly conductive samples) or the falling head method (lowly conductive samples). The SWRC was constructed by determining the volumetric water content of the soil samples after applying suctions of -0.1, -0.3, -0.5, -0.7 and -1.0 m with a laboratory sandbox, and suctions of -3.40, -10.20 and -153.00 m with ceramic pressure plates.

The soil hydraulic properties 29 months after the start of the experiment are shown in Figure S5.4. At that time, approximately 20 cm of sediment has been deposited on top of the amended soil. Soil samples between 3 cm and 8 cm depth are taken in this deposited soil layer. This layer has the highest volumetric water content at saturation (i.e. the highest porosity). The layer of 32 – 37 cm depth corresponds to the soil layer that was subject to the treatments, which were applied up to a depth of approximately 30 cm. The soil water retention curve reveals a slightly higher porosity in the treated soil compared to the CTRL

monolith. At a depth of 65 – 70 cm, which is below the depth of the treatments, the soil water retention curve follows a similar pattern in all monoliths. The curve is steep, which means that a large suction needs to be applied for a decrease in volumetric soil water content. We found no evidence of a significant difference of saturated hydraulic conductivity between the treatments, which might be due to the small sample size.
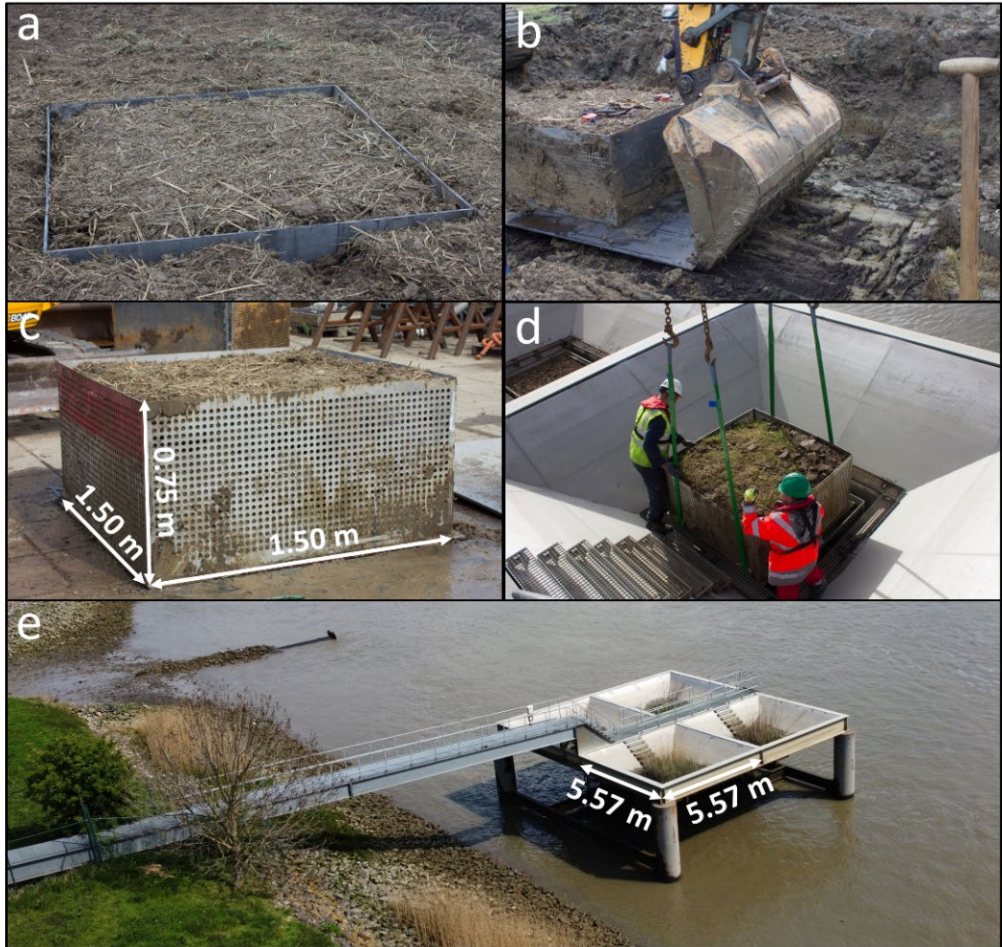

Figure S5.1: Overview picture of the steps taken to perform the experiment. (a): inserting steel containers of 1.50 m by 1.50 m surface area and 0.75 m depth into the four soil excavation zones (Figure 5.1) (b): inserting and welding a baseplate under the soil monoliths (c): transferring the monoliths to stainless steel containers with perforated side walls (d): placing the monoliths in the mesocosm set-up (e): overview of the mesocosm set-up.
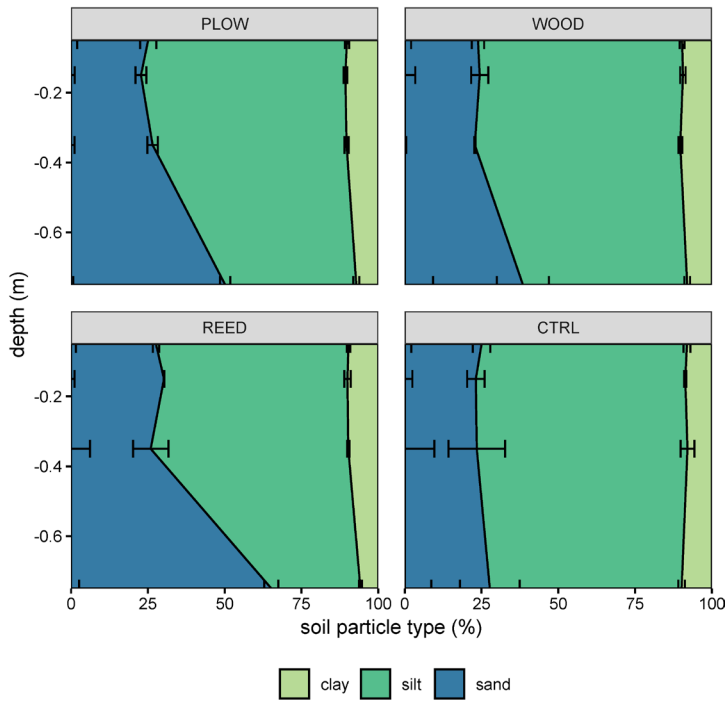
Figure S5.2: Volumetric grain size distribution in the four plots after application of the treatments. Error bars denote the standard deviation.
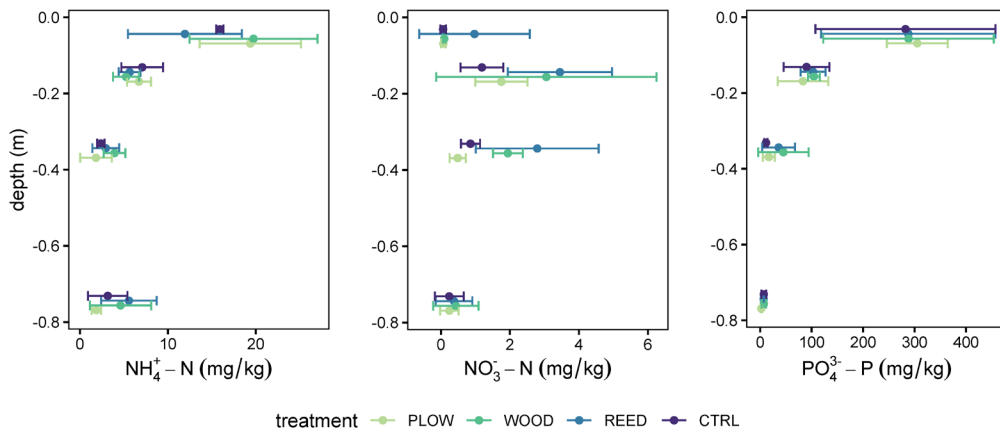

Figure S5.3: Comparison of soil nutrient properties at the selected plots before application of the treatments. Colors represent the future treatment on the respective plot. Error bars indicate the standard deviation (n = 3). Points and error bars are slightly shifted along the y-axis to avoid overlap.
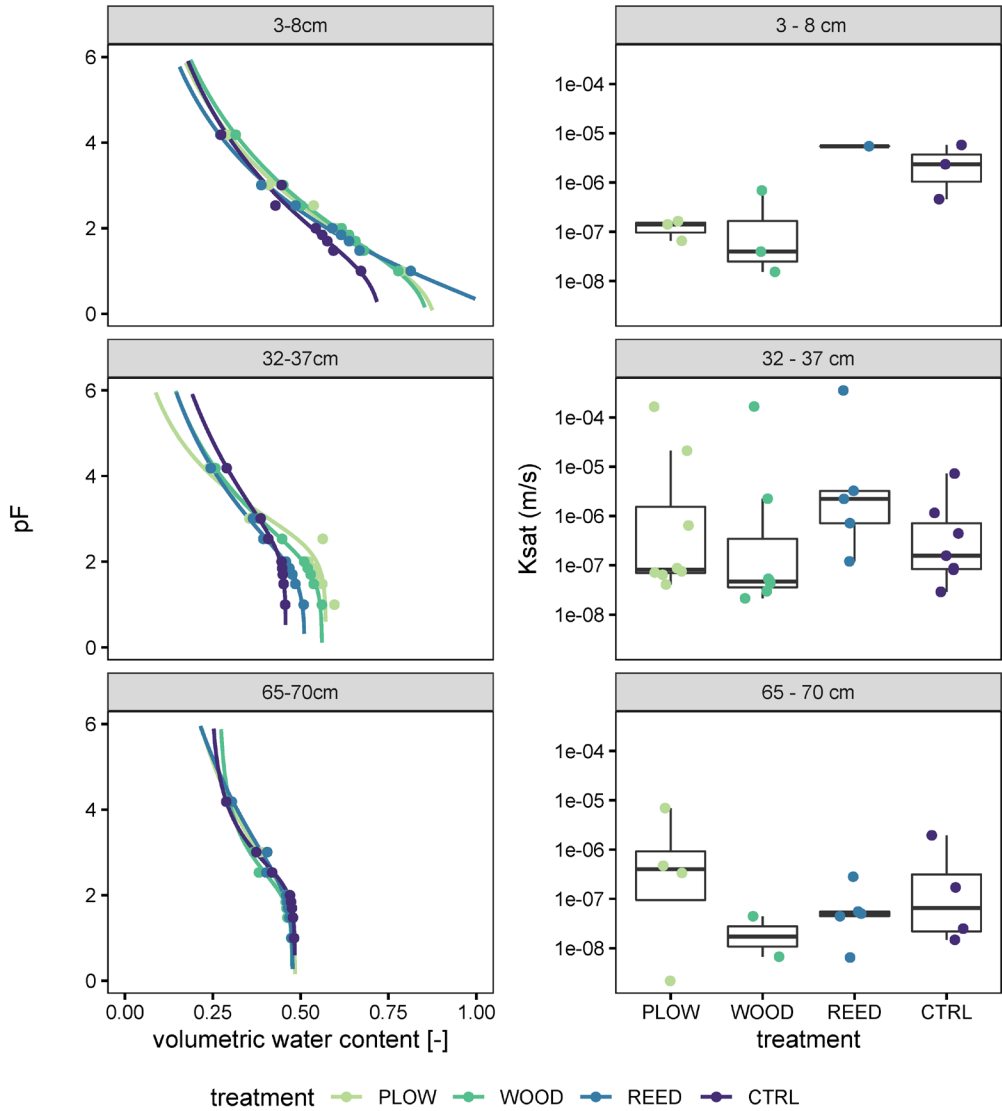
Figure S5.4: (a): soil water retention curves for the different treatments. Points indicate the mean measured volumetric soil water content for an applied suction. Lines represent the fitted retention curve using the van Genuchten – Mualem model (van Genuchten, 1980) (b): saturated hydraulic conductivity of the soil in the four treatments. Points are slightly shifted along the x-axis to avoid overlap. Note the log scale on the y-axis.
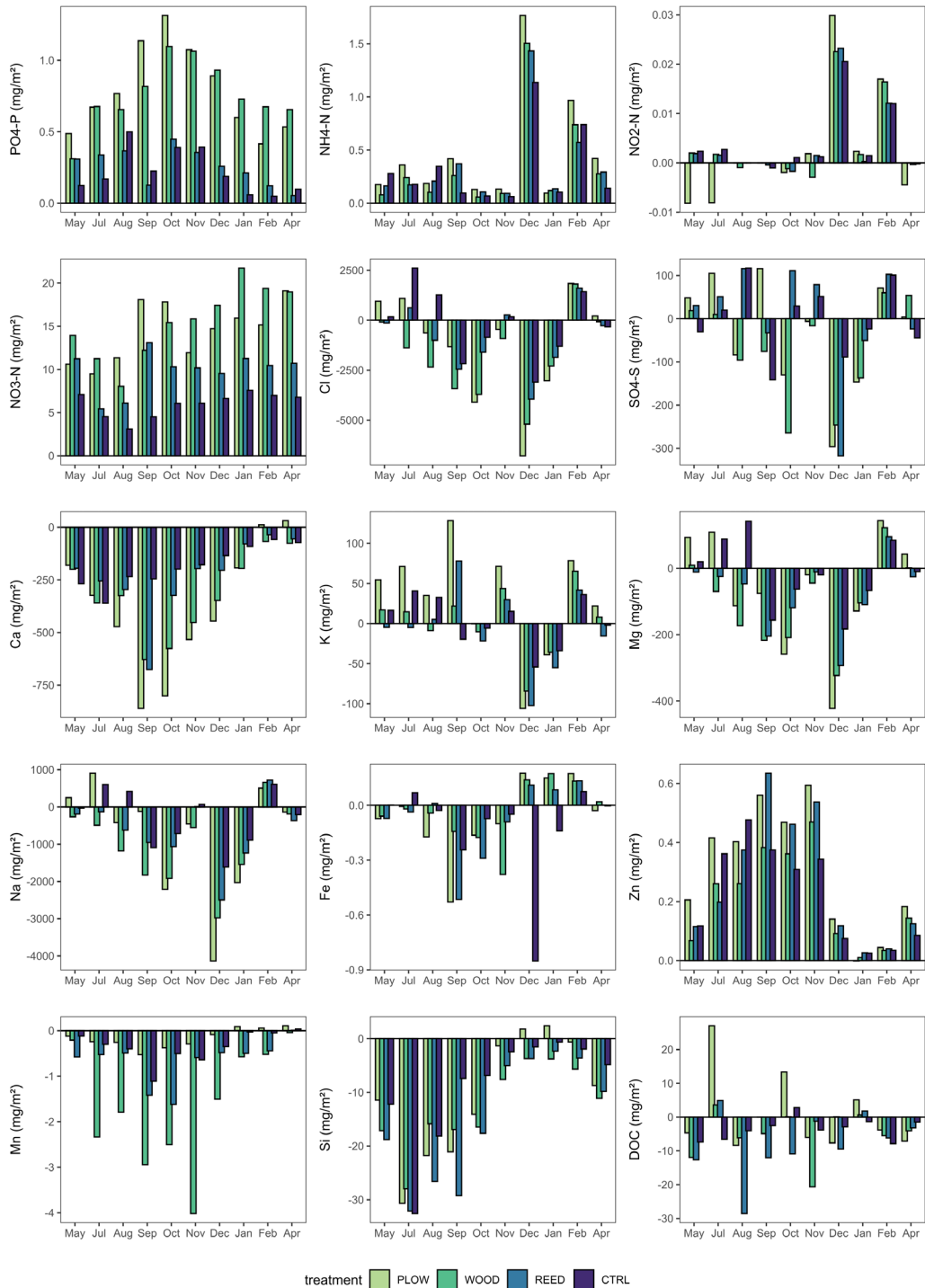
Figure S5.5: Mass balance per unit of area for all measured elements. A positive mass balance indicates a net import of the respective element into the soil. Data from May 2019 to April 2020.

Table S5.1: properties of the samples taken for chemical analyses and the respective laboratory method. CFA: continuous flow analysis, ICP: inductively coupled plasma analysis, DOC: dissolved organic carbon.

	vial 1	vial 2	vial 3
volume	30 mL	30 mL	10 mL
pre-treatment	3.0 mL H_2SO_4 (69 %)	1.5 mL HNO_3 (69 %)	none
laboratory method	CFA	ICP°	CFA
measured parameters	NH_4, NO_2, NO_3, Cl	PO_4, SO_4, Ca, K, Mg, Na, Fe, Zn, Mn, Si	DOC

Table S5.2: Comparison of the spring tide drainage depth between the treated soils and the CTRL monolith.

	Difference [m]	Lower CI [m]	Upper CI [m]	p
PLOW - CTRL	-0.47	-0.47	-0.47	<0.001
REED - CTRL	-0.17	-0.18	-0.17	<0.001
WOOD - CTRL	-0.11	-0.11	-0.10	<0.001

Table S5.3: comparison of the mass balance between the treated soils and the CTRL monolith.

nutrient	comparison	lower 0.95 CI [mg/m^2]	difference [mg/m^2]	upper 0.95 CI [mg/m^2]	p-value
TDIN	CTRL-PLOW	5.48	8.63	11.77	<0.001
	CTRL-WOOD	6.37	9.52	12.67	<0.001
	CTRL-REED	0.78	3.93	7.08	0.010
	spring-autumn	-3.36	-0.14	3.07	0.999
	winter-summer	-8.04	-4.83	-1.61	0.002
PO4	CTRL-PLOW	0.39	0.57	0.75	<0.001
	CTRL-WOOD	0.36	0.54	0.73	<0.001
	CTRL-REED	-0.14	0.04	0.22	0.937
	spring-autumn	0.19	0.38	0.57	<0.001
	winter-summer	-0.01	0.18	0.37	0.065
DSi	CTRL-PLOW	-8.63	-1.70	5.23	0.910
	CTRL-WOOD	-10.69	-3.76	3.17	0.467
	CTRL-REED	-12.96	-6.03	0.90	0.107
	spring-autumn	-1.86	5.22	12.29	0.211
	winter-summer	-28.42	-21.35	-14.27	<0.001

Table S5.4: vegetation evolution in the four soil monoliths.

treatment	start	Year 1		Year 2		Year 3	
PLOW	No vegetation	*Agrostis stolonifera*	85%	*Aster tripolium*	40%	*Aster tripolium*	20%
		Lolium perenne	5%			*Vaucheria* sp.	5%
		Rumex × pratensis	3%				
WOOD	No vegetation	*Agrostis stolonifera*	80%	*Bolboschoenus maritimus*	70%	*Bolboschoenus maritimus*	40%
REED	No vegetation	*Agrostis stolonifera*	40%	*Vaucheria* sp.	25%	*Aster tripolium*	5%
		Lolium perenne	3%	*Aster tripolium*	5%		
CTRL	*Agrostis stolonifera*	55%	*Agrostis stolonifera*	100%	*Elytrigia repens*	5%	*Elytrigia repens*	5%
				Atriplex prostrata	5%	*Phragmites australis*	5%
				Vaucheria sp.	5%		

7.1   References

Udden, J.A., 1914. Mechanical composition of clastic sediments. Geological Society of America Bulletin 25, 655-744.

van Genuchten, M.T., 1980. A Closed-form Equation for Predicting the Hydraulic Conductivity of Unsaturated Soils. Soil Sci Soc Am J 44, 892-898.

Wentworth, C.K., 1922. A scale of grade and class terms for clastic sediments. The Journal of Geology 30, 377-392.